AN INVESTIGATION INTO THE LONGITUDINAL ROLLING OF TUBES THROUGH TWO GROOVED ROLLS.

by

Abdel-Rahman Mohamed Said Abdel-Haleem

(A.S.Haleem)

B.Sc.(Mech.Eng.)

Submitted in fulfilment of the requirements of the Degree of Doctor of Philosophy.

February 1978

The University of Aston in Birmingham

Department of Mechanical Engineering

Supervisor: Dr. I.M.Cole

Advisor : Professor D.H.Sansome

SUMMARY

Summary

This work is an investigation of the process of the longitudinal rolling of tubes through two grooved rolls with the aim of contributing to the full understanding of the mechanics of the process in order to increase its efficiency. The tubes which were unsupported internally, were rolled through an oval groove.

Two types of operation were examined, viz, sinking, where no external tensions were applied to the tube, and stretch-reducing where front and back tensions were applied in different proportions.

Lead tubes were rolled under dry rolling conditions to simulate the hot rolling of steel. Two types of passes were used, viz., rolling round tubes through the oval groove (R-O pass), and rolling the resulting oval tubes through the oval groove (O-O pass) with the major axes of the two ovals at right angles to each other. Recordings were made of all the loads, velocities, dimensions and pressure distribution. To achieve this, tests were carried out on a fully equipped 2-high roll stand based on an old milling machine. Devices were also designed for the application of the front and back tensions.

A novel design of the pressure measuring pin loadcells was developed incorporating new features which simplified its use and increased its reliability. The four loadcells in the shape of cantilevers were fixed to one block, thus making the removal and refitting of the assembly for inspection relatively simple.

A new theoretical approach to the problem based on the strain energy principle has been presented and compared with existing equilibrium approaches and the test results.

The question of presence and shape of a neutral zone on the surface of contact has been studied in some detail and a new idea put forward. Also the extent and effect of the pre-contact plastic zone, i.e, free zone, on other process parameters,e.g., arc of contact and pressure peak has been examined and verified with specially devised tests.

The variation of the wall thickness of the tube has been studied in the light of the experimental test results and the available theoretical treatments.

A general survey of recently available literature, together with surveys covering specific aspects of the problem have also been carried out.

Key Words

Tube-rolling

Pin-loadcells

Pressure-distribution

Stretch-reducing

Energy Method

CONTENTS

NOTATION

A	Cross-sectional area of tube at the entry plane.
a	Cross-sectional area of tube at the exit plane .
A_c	Area of contact between tube and roll .
b	Width of groove.
d	Outside tube diameter (mean value) .
d_g	Groove diameter.
d_i	Internal diameter of tube (mean value).
d_m	Mean diameter of tube (mean value).
e	Eccentricity
e_g	Eccentricity of the groove.
e_i	Roll spring.
h_g	Height of groove.
L	Length of the arc of contact.
L_g	Calculated length of arc of contact(from geometrical considerations).
L_m	Measured length of arc of contact corrected only for finite width of pin.
L_m^*	Measured length of arc of contact corrected for the finite width of the pin and also for torque sharing.
m	Shear factor.
N	Rotational speed of the rolls.
P	The roll separating force (RSF).
p	Roll pressure.
p_h	Roll pressure due only to homogeneous deformation.
p_m	Mean roll pressure.
r	Reduction in area %.
R_e	Effective roll radius.

R_f Radius of the arc of the free zone.

r_g Radius of groove.

R_m Mean radius of the roll.

R_r Radius of the roll at the root of the groove.

R_s Radius of the roll at the shroud.

R_θ Radius of the roll at a point on the groove making angle θ with vertical.

r_o Radius of tube at entry.

r_1 Radius of tube at exit.

S Surface area of the tube in the deformation zone(area of application of p_h) .

t Wall thickness of the tube.

U Tube velocity in the direction of rolling.

v Tangential roll velocity.

V Volume of tube in deformation zone.

v_h Horizontal component of roll velocity.

v_r Relative velocity between the tube and rolls.

$\dot{V}$ Volume rolled per unit time.

W Work of deformation per unit volume.

W_e Work of external forces per unit volume.

W_i Internal work of deformation per unit volume.

W_t Total work of deformation per unit volume.

$\dot{W}$ Rate of doing work.

$\dot{W}_f$ Rate of doing work against friction.

Greek symbols:-

γ Torque sharing factor.

δ Mean draft.

δ_r Draft at root of groove.

δ_t Change in wall thickness of tube (mean value).

δ_{tr} Change in wall thickness of tube at root of groove.

$\epsilon_{\ell,r,\theta}$ Logarithmic strain in the axial, radial, and tangential directions respectively.

$\bar{\epsilon}_m$ Generalised strain.

$\bar{\epsilon}_A$ Apparent strain.

$\bar{\epsilon}_f$ Frictional strain.

θ Groove angle.

θ_c Groove angle of contact.

θ_e Effective groove angle.

θ_m Maximum groove angle.

$\theta_{1,2,3 \text{ or } 4}$ Groove angles made by pins 1,2 ,3 or 4 of the pin loadcells.

μ Coefficient of friction.

$\bar{\sigma}_Y$ Yield stress in uniaxial compression(mean value).

τ Shear stress.

ϕ Angle of contact at any point on surface of contact.

ϕ_m Maximum angle of contact(i.e.,angle of contact at entry plane).

ω Angular velocity of the roll.

Subscripts

Unless otherwise specified:

o Entry plane condition.

1 Exit plane condition.

r At root of the groove, or relative.

f Frictional.

h Homogeneous.

m Mean, or Measured.

i	Internal.
e	External or
	Effective
θ	At groove angle θ
1,2,...	Pin loadcell number.

N.B.

Other symbols, mainly from outside sources, used in this text, are defined as they appear.

I

INTRODUCTION

In the manufacture of seamless tubes, the longitudinal rolling of the tube through two or more grooved rolls in one of its forms represents an important part of the process. The three forms of longitudinal rolling are as follows:-

1) mandrel rolling where a mandrel is inserted inside the tube to provide internal support while the tube is being rolled between the rolls.
2) tube sinking in which the inside of the tube is unsupported,
3) stretch-reducing which is similar to tube sinking except that tensions are applied to the front and back of the tube to reduce the loads and increase the deformation.

These three forms of longitudinal tube rolling are normally carried out in a series of stands called a continuous mill.

In a typical manufacturing process for seamless tubes the steel used for the process is continuously cast and then made into round billets in a billet mill. These billets are then heated to rolling temperature and by piercing them over a plug in a piercing mill, converted to hollow blooms. These hollow blooms are then rolled over a long mandrel in the mandrel mill. The sizes of the tubes produced so far in the manufacturing process are limited to a few diameters. In order to increase the range of diameters produced the tubes are then passed in the next stage through a stretch-reducing mill.

This example illustrates a characteristic feature of many tube manufacturing process in that the tube goes through

several processing stages.

In the Assel elongating process a sinking mill is usually installed with the elongator. This process is apparently used for the production of medium-and heavy-wall tubes. In such a sinking mill and also in the stretch-reducing mill the successive stands are normally disposed at 90° to each other. This arrangement is important since the shapeof the groove in each stand produces an oval tube. Therefore in order to produce the desired circular tube shape the major axes of the ovals of the tube and the groove must be at right-angles to each other due to the stand disposition. The major tube axis from the width of any pass enters into and is reduced to the height of the next pass. This then becomes its minor axis which is formed into the width of the subsequent pass.

One of the main problems with the tube sinking process is the increase in wall thickness which takes place as a result of reducing its diameter. As the reduction in diameter increases so does the variation in the wall thickness. In addition, as a result of sinking the tube in one stand, wall thickening is not uniform around the section of the tube, being greater on two diametral planes corresponding to the pass width Therefore, as the reduction in diameter is increased, the variation in the mean wall thickness along the tube increases and is accompanied by the tendency of the tube bore to become square. For these reasons the total permissible reduction in diameter in a sinking mill is restricted.

In a stretch-reducing mill the tube is subjected to interstand tension which is created by adjusting the speeds of

the successive stands. The roll speed in any stand is adjusted so that the tangential velocity of the roll is greater than the velocity of the tube coming out of the preceding stand. This results in the creation of tension in the tube. Consequently wall thickening produced by the rolling forces alone (i.e, as in sinking) is reduced. Although the stretch reducing process can reduce or eliminate wall thickening, it has its inherent problem known as the thickened ends. As the tube ends are not subjected to the full effect of interstand tensions, they are therefore thicker than the rest of the tube. This problem of wasted ends is partly overcome by keeping the distance between the stands of the mill to a minimum.

From an analytical view point the process of tube sinking or stretch-reducing is complex. From the attempts that have been made to formulate a mathematical model of the process, three have resulted in the three theories now existing. These theories are all of Russian origin and are based on the equilibrium method of analysis. This method involves the consideration of the equilibrium of forces acting on an element of the tube in the deformation zone together with a yield criterion. The resulting differential equations are then solved for the appropriate end conditions. These theories, however, proved unsuccessful in predicting the roll pressure according to the experimental results of Cole (1) as will be discussed in chapter (VI) of this work. For this reason it was felt at the onset of this investigation that a different theoretical approach should be attempted and the strain energy method was thought feasible in conformity with the recommendations

of (1). Hence the development of a new theoretical approach to the problem was one of the objectives of this work.

The question of friction between the tube and the rolls has also been dealt with in a different manner to that used in the Russian theories. The use of the constant friction factor concept instead of the Coulomb type of friction is believed to be more applicable to the actual process of hot rolling of steel tubes in which sticking can take place on the surface of contact, as well as to the simulation process of rolling lead tubes in which sticking does not take place. When sticking occurs on the surface of contact the assumption of a sliding friction , of the Coulomb type for instance, is no longer valid.

Due to the importance of the variation in the wall thickness of the tube particularly for the sinking process as shown before, a study of this parameter was required.

The deformation of the tube between the rolls is an important factor affecting the produced tubes as well as the rolling loads and justified studying in some detail. The phenomenon of the pre-contact plastic deformation i.e, the free zone, and its effect on the calculated length of the arc of contact, observed experimentally, were aspects of the tube deformation which required further analysis.

In order to obtain an accurate comparison between the deformation stresses developed in the tube rolling process and the corresponding theoretical values, it was necessary to study the distribution of contact stresses at various points on the surface of contact. This knowledge was also

important for the assessment of the nature of deformation. Information gained from the pressure distribution curves can be used in studying the significance of other parameters and their influence on the process, e.g. arc of contact, neutral zone and the free zone. In this regard the available test data were not sufficient and the need for a further study in this field was present from the start of this investigation. Therefore, one of the objectives of this work was to improve the technique of measuring the pressure distribution and the method of calibration in order to provide reliable results.

The presence and shape of the neutral zone in flat rolling is well defined. The neutral zone is the zone at which the frictional forces change direction and the relative velocity between the metal and rolls is zero. In tube rolling however, the situation is more complex and the question of presence and shape of the neubral zone needed clarification and was therefore included as part of this study.

The experimental test data on the rolling of oval tubes through oval grooves is scarce despite the fact that this type of pass is the more common one in sinking or stretch-reducing mills in practice. The tendency of investigators to roll round tubes in round or oval passes was basically to simplify the analysis. It was felt necessary to provide data on the rolling of oval tubes in oval grooves for the purpose of the present and any future investigation.

II

LITERATURE SURVEY

The work of Cole[1] at the University of Aston in Birmingham, of which the present investigation is an extension, is a comprehensive study of the tube rolling process. Cole notes at the start of his review of published work on longitudinal rolling of tubes that publications concerning these processes were very far to seek and that there was very little emanating from the English language sources while most of the published work was of Russian or German origin. To some extent this statement is still valid to date and since the publication of his work the number of new publications of direct relevance to these processes is small. An experimental two-roll stand was constructed for tests on lead tubes of 44.5 mm (1.75 in.) outside diameter and 6.4 mm (0.25 in.) wall thickness. The groove shape was circular and the rolls came from one of the finishing stands of a production mill. By varying the size of the gap between the two rolls, Cole was able to effect a change in the reduction of area per pass. Because of non-circularity, the cross-sectional area was obtained by weighing specific lengths of tube and knowledge of the density of lead. The dimensions of the deformed tube were measured with reference to the point on the surface of the tube corresponding to the root of the groove. This method has the disadvantage of not taking into account the transverse variations in the dimensions of the tube after rolling. However, the author's main interest was the measurement of the change in wall thickness as a result of rolling on the assumption that the change in one plane is

representative of the total change in wall thickness. A comparison was made between the experimental change in wall thickness and that predicted by formulae suggested by Gun [40] and Gulyaev,et al [50]. The comparison showed that the two formulae overestimated the change in wall thickness with that of Gun's exceeding the measured value by over 100% . Poor correlation was also found between the measured roll pressure and that predicted by theories [32], [33] and [34]. The measured value of the pressure on the rolls was of the order of 17.00 N/mm^2 while those predicted by the three formulae were in the region of 6.0 N/mm^2. It is worth noting here that Cole used PVC discs on the surface of the roll to cover the pin tips and prevent the back extrusion of lead into the annular clearance between the pin and its bush. Tests were carried out in the present work, and are reported later, to study the effect of using these discs on the measured pressure. These tests have shown that the presence of these discs increases the measured pressure by amounts which depend on the thickness of the disc and its size relative to the size of the pin. The increase however was not such that it would make the correlation above significantly better. These theories [32], [33] and [34], will be further examined in chapter (VI) of this work.

Four pin loadcells were used for measuring the pressure distribution round the groove and along the arc of contact. The pins were made of Silver Steel and had diameters of a nominal 1.27 mm. depending on fitting.

The bodies of the loadcells were made of Araldite since it has a high Poisson's ratio and the loads involved were low. Four strain gauges were bonded to the body of each loadcell. Each loadcell was individually fitted in a hole drilled in the roll for that purpose. The angles of the pins being 0, 30, 60 and 80 degrees. The calibration of the pin loadcells suffered from response hysteresis under decreasing load which could not be overcome. This problem limited the usage of the pin loadcells results for analytical purposes. The pressure distribution curves however showed a pressure peak close to the entry plane, a phenomenon which has been observed in the present investigation. Good correlation was found to exist between the measured roll separating force and that calculated by the summation of pressure distribution curves round the groove.

The arc of contact was assumed to be of the same length for every position round the groove. This assumption was based on observations of a tube which was covered with a white emulsion paint and then rolled. The tube was stopped in the gap and the surface was examined. No mention was made of any deformation of the tube prior to its contact with the roll (the free zone). Cole concludes from his study of the pressure distribution curves that the position of the neutral plane is very different from the flat rolling situation being near the entry plane for tube rolling and near the mid-position between entry and exit planes in flat rolling. Tests in the present investigation confirm the difference between flat

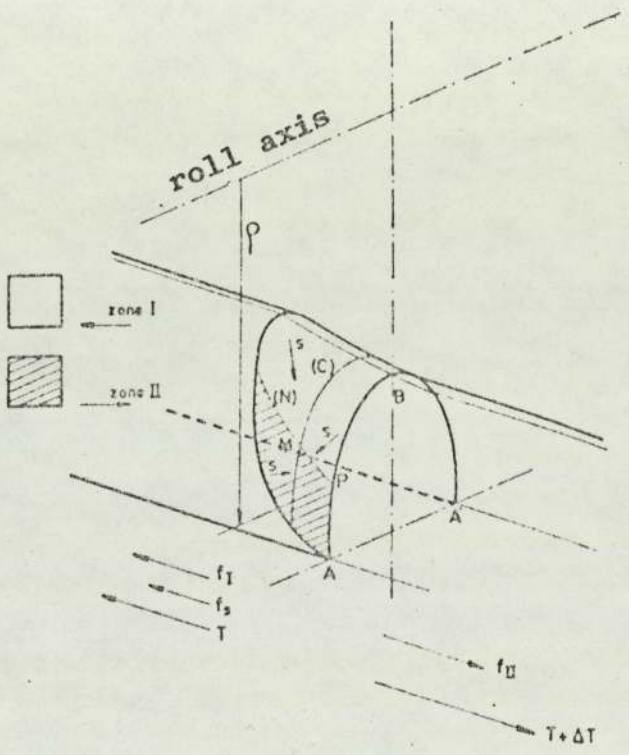

Fig. (1)

Extent of deformation

according to Fazan

rolling and tube rolling in this respect but indicate that the position of the neutral plane varies round the groove and could be near the exit plane, for certain positions on the groove surface. This point is discussed in detail in chapter(VIII)of the present work.

Cole's work includes a comprehensive study of literature on different aspects of the problems of tube sinking, stretch reducing, and mandrel rolling. Particular attention was paid to the review of the methods of measurement of contact stresses.

The experimental results of Cole's investigation as well as certain other aspects of the problem studied in his work will be further discussed in the relevant sections.

Of particular interest is a paper by Fazan et al [2], 1967 in which he discusses some aspects of the tube rolling problem being investigated in the present work. He acknowledges that the position of the neutral point varies with the groove angle, due to the variation of roll radius. He suggests that line (N), on figure (2) of his paper reproduced here as fig. (1) , represents the locus of the point of no-slip on the surface of the tube in the deformation zone. His definition of the roll radius is the distance from the centre of the roll to the point of no-slip at the plane of exit. In this connection the author shows that a knowledge of the exit velocity of the tube would be important. It had been established in the present work that measurement of tube velocities is very useful with regard to the question of the neutral point. The author suggests that as an approximation, line

(N) divides the surface of contact into two equal zones, i.e., zone I = zone II in figure (1).

On the question of wall thickness variation during rolling the author takes the view held by (15), (20) that the thickness remains unchanged if the stretch factor is equal to 0.5 (the stretch factor is the ratio of axial stress in the tube to the yield strength of its material.) He also concludes that a change in wall thickness and diameter between stands takes place as a result of the tension in the tube. This conclusion was founded upon the fact that certain rolling schedules which entail large reductions in thickness would not be attainable by a series of passes under tension in the absence of inter-stand deformation and also upon confirmation by laboratory experiments. The method suggested for calculating the change in wall thickness however carries within itself a weakness as a result of not knowing how to calculate the deformation by tension between the stands.

The theoretical treatments presented in the paper were based on the equations suggested by Neumann and Hanke (20) and included the following assumptions:-

1- deformation is symmetrical round the tube axis,
2- the directions of the principal stresses are radial, tangential (hoop), and longitudinal,
3- von Mises yield criterion applies,
4- radial stress varies linearly across the tube thickness,
5- the thickness of the tube remains unchanged,
6- the frictional stress is equal to μs where s is

the normal pressure and μ the coefficient of friction.

7- for the hot rolling of steel at 900-950 ^{o}C, μ takes a value between 0.35 and 0.40.

It has also been assumed that the radial stress follows a linear distribution across the thickness of the tube with the external pressure equal to twice the mean radial stress across the section. After developing the basic plasticity equations as applied to the tube forming problem, the author then used these equations to calculate the variation in tension during the passage of the tube through a stand and the tube deformation between the stands referred to earlier. In deciding on the value of the coefficient of friction of 0.35-0.40 the author suggests that the mean pressure of the rolls on the tube is only in the order of 4.9 N/mm^2 for the rolling of steel at 900-950 ^{o}C apparently with tensions applied. The remainder of the paper is concerned mainly with the stretch reducing process and the determination and adjusting of the speed of the stands with emphasis on the usefulness of measuring the tube velocity. An example is given of how this is done during an experimental simulation of the stretch reducing process.

A report on the operation of a continuous tube-rolling mill by Neuhoff, et al was published in 1970 (3). The report started by describing the continuous tube rolling process in which a mandrel is used inside the tube in a mill normally constructed of 7 or 9 stands consisting of an arrangement of two-roll stands offset at 90^{o} to each other. The authors then reviewed the difficulties

encountered in the operation of the mill, namely: the deviations in wall thickness in the area of the acceleration of the mandrel at the entry of the rolling material and its exit, and the loads on the tool and its service life. The first problem, that of uneven flow of material, was said to be caused by the change of speed of the mandrel, thus the rear stands, because of the increase in mandrel speed created by them, pull more rolling material into the front stands.

The authors suggested the following measures to counteract the appearance of wall thickness and diameter changes along the length of the tube:

1- minimum possible coefficient of friction between mandrel and tube.

2- maximum possible reduction per pass in the first stands.

3- controlled variations in the speed of the rolls against the change of mandrel speed.

The authors studied the rolling forces and the loads, on the mandrel with a view to determining the limitations of the process.

Tselikov et al (4) published a study of the development of the continuous rolling of tubes in the USSR in 1970.

A section of an article by Blazynski (1970) on the recent developments in seamless steel tube-making was devoted to the longitudinal tube rolling process. For the sinking mill a reduction in diameter of between 3 and 5% was said to be the practice. The advantages of the three-roll system over the two-roll system were discussed,

including an increase in diameter reduction per stand to about 14%. Since this article was mainly a review, no attempt was made on the part of its author to offer solutions to the problems mentioned or to discuss in any detail the theoretical treatments of the longitudinal tube rolling process. On the analytical side, the equations developed by Kirichenko[34] for the prediction of the pressure on the rolls were presented and were said to be of particular interest since they include the effect of ovality.

In a paper by Gulyaev et al[5] published in 1971, a study of the dimensions of oval passes was made with a view to determining their optimum degree of ovalization. The study was partly theoretical and partly empirical. By solving the variation equation for media with linear strengthening of the material for the case of tube rolling without mandrel, a width coefficient was obtained This was a function of the thickness to diameter ratio, tension in the tube, and the coefficient of friction between the rolls and the tube. The equation contained constants which were not commented upon. By analysing the equation for the width coefficient for two-roll passes with small coefficient of friction the authors stated that wider passes were required to avoid overfilling of the groove. Calculated coefficients and experiment showed good agreement. Graphs were presented showing the variation of the minimum value of "spread parameter" as a function of tension and thickness/diameter ratio and also the dependence of the minimum value of the parameter

used for determining the width to height coefficient on these variables. On the bases of the proposed method of determining the dimensions of oval passes, a new pass design was developed and tested on a 22 stand mill. It was claimed that as a result of using the newly developed pass design the final transererse wall-thickness variation of the tubes was reduced from 17-20% to 12-15% . It was also claimed that a considerable improvment in the internal surface quality of the tubes was obtained.

Two important points were mentioned in passing these were (i) : that the actual deformation zone is much larger than the geometrical zone and consists of a pre-zone and the true geometrical zone,

(ii) that the ratio between the actual area of contact of the tube with the roll and the theoretical one, determined by integration was between 0.85 and 0.90 it was not clear however how these values were obtained. Tests in the present work have shown that the ratio between the actual arc of contact and the geometrical arc of contact was around 0.7.

In a paper by Vatkin et al [6] published in 1971, the effect of metal strengthening on the distribution of longitudinal stresses in the deformation zone during the reduction of tubes was established. The equilibrium of forces acting on an element in the deformation zone was considered and the resulting differential equation solved giving an expression for the longitudinal stress in both entry and exit zones. The wall-thickness was assumed unchanged within a stand and the external contour of the

deformation zone was assumed to have the shape of a right circle in any transverse section i.e. the stresses in the cross section of the tube were uniform. A Coulomb type of friction was assumed. A yield criterion of the type $\sigma_r + \sigma_t = 1.15\,\sigma_3$, implying a plane strain condition, was used. An analysis was then presented of the effect of the coefficient of friction and of different stress relationships generated under the action of external axial forces, on the distribution of longitudinal stresses. Expressions for the limit stresses at entry and exit were deduced. The effect of tensions on the positions of the neutral plane was explained in detail.

Vashkin et al [7] published a paper in 1971 dealing with the evaluation of specific pressure of metal on the rolls in tube rolling on a mandrel. The equilibrium method was used to calculate the contact pressure in both the reduction and compression zones without allowing for the reciprocal influence of the two zones on each other. A discontinuity was obtained in the value of the specific pressure between the two zones which was not observed experimentally. When allowance was made for the supporting force created by the reduction zone, the value of the pressure on the compression zone was much higher than the experimental value. A value for the supporting force of one half of that created by the reduction zone was therefore used. A parabolic law was assumed for the pressure distribution over the width of the pass giving a maximum value at the apex of the pass. The mean pressure was compared with three test results on hot steel, (see Fig.(2) on page

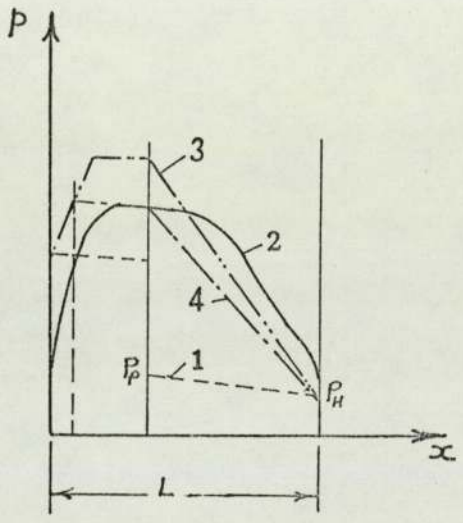

Fig. (2)

Specific pressure in deformation zone according to ref. (7), calculated:-

1-by calculation, without allowing for the reciprocal influence of the zones;

2-experimental;

3-allowing for supporting force $\sigma_{x.p}$ from reduction zone;

4-allowing for supporting force $\sigma_{x.p}/2$

17) and the agreement was good. Hence the authors concluded that their formulae could be recommended for engineering calculations.

Some of the symbols in the article were not explained and are not clear. Tests in the present work have shown the maximum value of the pressure to occur away from the root of the groove. The good agreement obtained can not be fully justified since only three test results were apparently used for the comparisons.

In a publication on research at works laboratories and Institutes at the Urals Scientific Research Institute for Tube Industry (8) in 1971, two articles relating to tube rolling were included. The first of these was by Blinov and Lomachenko concerned with the development of a technology for the reduction of tubes in four-roll stands with two driven rolls. It was stated that theoretical analysis of the reduction process in the four-roll pass showed that four-roll stands with two driven rolls have significant advantages over the two-and four-roll stands in use at the present time. Stability of the tubes in the four-roll pass was said to be 25 to 40% higher than in the three-roll pass enabling tubes with high d/t ratio to be rolled. It is difficult to determine what was meant by stability of the tube or how it was measured. Since the paper was only an outline of research activities no details were included and a proper assessment of the analysis could not therefore be made.

The second article was by Matveev, et al and was concerned with a polarization-optical (presumably photo

elastic) investigation of the stress and deformation state in tube production. Model optically-sensitive materials, used in the study of stresses and deformations by the polarization-optical method, were studied. It was stated that a method was developed for determining the contact stresses in a round or oval pass under conditions of plane simulation (presumably plane strain).
The effect of the shape of the pass and the degree of filling on the character and magnitude of the contact stresses was established. As in the previous article no further details were presented.

Vater [9] published a paper in 1971 in which he considered the effect of flow conditions on the force and work requirements and also on the material flow in plastic deformation. He showed that in a flow hypothesis of the kind $\sigma_1 - \sigma_3 = c\, K_f$ where the value of c lies between 1.0 and 1.15 , the value of c has a significant influence on the deformation ratios obtained from the flow diagrams. The correct value of c can be obtained from test results and practical observations. The effect of c on the structure of the deformation ratios as well as on the force and energy required was discussed. Flow diagrams for different c values are presented to demonstrate its effect.

A Polish paper by Jelomek [10] in 1971, also dealt with flow diagrams and the stretch factor. The variation of the stretch factor Z with the number of stands in a mill is shown diagrammatically.

Okamoto [11] published a paper in 1971 in which he introduced the deformation factor as a means of calculating

the stresses in three dimensional deformation problems. From the condition of volume constancy he defines the deformation factor as : $\gamma = 0.5 + \frac{\phi_\theta}{\phi_\ell}$ where ϕ_θ and ϕ_ℓ are the logarithmic strains. He then considers the stress-strain relationships in conjunction with the vonMises yield criterion to calculate the principal stresses in terms of the deformation factor. In applying these analyses to tube deformations he suggests the use of a mean deformations factor (γ_m) to cater for the variation of stress and strain across the wall of the tube. This is defined in terms of the deformation factor as:

$$\gamma = \frac{r_a \cdot r_b}{r^2} \cdot \gamma_m$$

where r_a and r_b are the inside and outside radii of the tube and r is the radius corresponding to γ. The author then suggests an approximate theory using the mean deformation factor in which the stresses across the tube wall are assumed equal to those at the geometrical mean radius. Having made this assumption he obtains equations for the stresses in the tube for two cases: when the outside pressure and axial tensile stresses act on the tube but the inside stress is zero i.e, case of tube sinking, and when the inside pressure and axial tensile stress act on atube but the outside pressure is zero. This approximate theory was applied to the case of mandrel rolling of tubes where there are usually two zones, a reduction zone and a compression zone. According to his procedure, therefore the outside pressure on the tube in the reduction zone, which

is similar to tube rolling without a mandrel, can be calculated as follows:

1) $\gamma = 0.5 + \frac{\Phi_a}{\Phi_e}$

2) $\sigma_r = \frac{1}{\sqrt{3}} \left(2\gamma / \sqrt{\gamma^2 + 0.75} \right) K_f \ln \left(\frac{r_a}{r_b} \right)$

where k_f is defined as the mean yield stress of the material, σ_r outside pressure on tube.

Although the equations presented for this application are the same as those developed in his approximate theory, the author does not use the mean deformation factor which is part of his theory. As can be seen from the above expression friction has not been taken into account or even discussed in the paper.

In another paper (12) Okamoto applies the same principle to the case of mandrel rolling. His aim was to determine the conditions for overfilling and underfilling of the groove. Friction was not taken into account on the assumption that the forward slip regions are balanced with the backward slip regions of outside and inside of the tube.

The expression suggested by Okamoto for the stress in terms of the yield stress and the strain could readily be compared with that presented by Neumann and Hanke in 1955 (20).

Potapkin, et al (13) published a paper in 1972 in which they study the effect of external zones on distribution of specific pressures in the hot rolling of flats.

Although the paper does not deal with the tube rolling process the phenomenon observed is similar to that of the free zone in tube rolling and which is studied in section (4) of chapter (VIII) of this work. The conclusions drawn are significant.

The authors indicate that experimental investigations show that for a stock of $L/h < 1$ (where L is the length of arc of contact and h is the height of stock), the curves of specific pressure have a peak close to the entry plane. The occurrence of pressure peaks is dependent, among other things, on the L/h ratio. The authors state that due to the inaccuracies resulting from using large pin diameters in relation to the length of arc of contact when measuring the pressure distribution, reliability of the experimental results of previous workers is questionable. In order to eliminate these inaccuracies rolls of 1500 mm diameter were used in conjunction with the loadcells shown in fig.(3). A ball was placed on top of the pressure transmitting pin and protruded above the roll surface by 0.1 mm. Experiments showed that ball projections of between 50 μm-200 μm had no influence on the pressure curves. These limits are much higher than those found in the present work and in (25), (26), and present investigation. However the conditions here are different mainly due to the use of this type of loadcell and the difference in the limits could be partly attributed to that. The pressure curves presented in the paper, and reproduced in fig(4), show the effect of L/h ratio on the occurrence of pressure peaks.

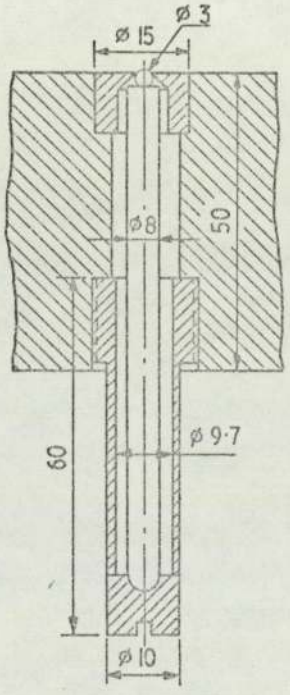

Fig. (3) TENSION DYNAMOMETER

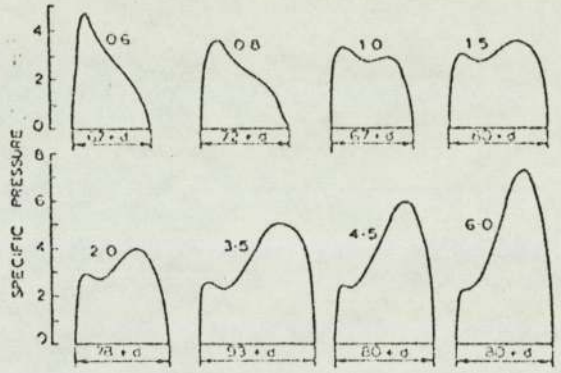

Fig.(4) Experimental curves of specific pressures. Numbers on curves = ratio l/h_{av}.

The authors explain the peak close to the entry plane for $L/h < 0.8$ as being the result of the supporting action of metal flow. They also conclude that when rolling thick stock ($L/h < 0.8$) the external friction is found to have only a weak effect on the stress state in the deformation zone in comparison with the effect of external zones. With an increase in the ratio L/h the effect of external friction increases while that of external zones diminishes.

It is worth noting that for their tests the authors used lead specimens on roughened rolls.

Proctor and Jubb [14] published a paper in 1973 in which they discussed some aspects of the stretch reducing process with particular reference to the stretch reducing Mill at the Weldless Steel Tube Co. The authors show that the equation developed by Neumann and Hanke [20] which relates the longitudinal stress in the tube to its yield strength and the radial and tangential strains, could be used as a basis for the calculation of roll speeds and for selecting the appropriate size of the parent tube to be produced from the primary mill to give the minimum finished size. This equation takes the form:

$$X_{\ell m} = \frac{\sigma_1}{K_f} = \frac{\frac{\psi_r}{\psi_t}(2 - E_m) + (1 - 2E_m)}{\frac{\psi_r}{\psi_t}(1 - E_m) - e(E_m - 1)}$$

where:

$X_{\ell m}$: is the stretch factor

σ_1 : longitudinal stress

K_f : tensile yield strength

ψ_r & ψ_t :radial and tangential strains

E_m :is the average thickness to mean diameter ratio of the tube.

The problem of polygonization of the tube bore, which is more pronounced for thick tubes and high diameter reductions, was said to be influenced by the stretch factor and the roll pass design. It was shown that a roll groove design which minimizes the differences in contact length across the groove inhibits the formation of polygonization.

The authors avoid the problem of calculating the position of the neutral point in calculating the roll speeds by assuming that it occurs at the root of the groove in all stands. The resulting inaccuracies of the speed calculation are overcome by facilitating additional speed control known as the stretch vernier. The problem of end thickening which increases with the amount of stretch in the mill, diameter reduction, and the increase in distance between stands, could be overcome by varying the roll speeds during rolling. This could by accomplished by the use of separate drives for each stand with electronic speed control. The article was concluded by discussing the various process measurement techniques used at Weldless to control the quality of the tubes produced.

Gulyaev and Ivshin [15] published a paper in 1973 in which they review the then existing formulae for calculating the change in wall thickness during tube reduction . They also develop a formula which they claim to be structurally simpler, more accurate, and applicable over the full range of wall thicknesses, reductions and tensions.

Their analysis is based on the calculation of the displacements of the tube outer and inner surfaces. They present a comparison between experimental results and the predictions of the various formulae.

These formulae, however, will be discussed and reviewed in the section of chapter (VI) dealing with the wall thickness variation in tube rolling.

Experiments on the rolling of lead and on the determination of its yield strength were carried out by Tamano, et al[16] and Shida[17] in Japan. Tamano used the results of Shida's work on lead to obtain an expression for the yield stress of pure lead in plane compression (k) in the form :

$$K = 1.35 \exp.\left(\frac{370}{T+273}\right) \epsilon_p^{0.23} \lambda_p^{0.07}$$

where:

T temperature ^{o}C

ϵ_p and λ_p are the two dimensional strain and strain-rate (s^{-1}) respectively.

Tamano suggests that for the rolling of lead sheets under dry conditions, the coefficient of friction has a value of 0.26. This value was obtained from comparing the experimental roll force with the theoretically calculated values in which the coefficient of friction was varied by applying various lubricants.

Gulyaev et al[18] studied the transverse variation in the wall thickness of the tube during reduction in two-and three-roll mills, in a paper published in 1974. After analysing the existing method of investigating this

phenomenon, the authors conclude that the statistical methods normally used were not valid in many cases due to experimental difficulties. In their method the transverse wall thickness variations are made up of two components :

i) eccentric and,

ii) induced by rolling.

The authors suggest that the function of wall thickness variation in the transverse section of the tube can be presented in the form of a complex cyclic function with periods equal to the tube perimeter. This function includes an harmonic component with a period equal to the tube perimeter and a set of higher frequency fluctuations. From test measurements and analysis it was found that the eccentric component, and also harmonic fluctuations of the second and fourth orders, predominate on the two-roll mill, and third and sixth orders on the three-roll reducing mill.

Lomachenko, et al[19] published a paper in 1973 in which they present the result of an experimental investigation carried out at Urals Tube Research Institute on the determination of transverse wall thickness variations when hot reducing in two-and four-roll stands. The four-roll stand had only two driven rolls subtending an angle of 120°. The authors found that the transverse wall thickness variation for the four-roll stand with a reduction of 3-7% two to three times less than for the two-roll stand. The results show that the character of the variation is approximately the same when reducing tubes with d_o/t_o equal to 18 - 16.6 in the two-roll stand and with d_o/t_o = 7.7 to

7.2 in the four-roll stand. Amongst their conclusions is that the metal consumption in a mill could be reduced by replacing the two-roll stands by four-roll stands with two driven rolls.

III

THE EXPERIMENTAL SET UP

(III-1) The Experimental Roll Stand:

The reconditioned and modified milling machine (type Herbert 23p) used for the previous investigation (1) was used in the present work to provide the drive and a rigid stable base for the roll stand. Further extensive modifications were carried out in order that the rig would suit the purposes of this investigation. These modifications included:

1- The use of a pair of double helical gears to transmit the motion from the top to the bottom shaft smoothly and without vibrations.

It had been noticed in the previous investigation that the vibrations from the previously used spur gears had superposed a cyclic variation on the UV traces similar in nature to the shape of the gear teeth. Therefore to eliminate such interference helical gears were used.

2- A removable top roll: for purposes of calibrating the pin loadcells in-situ. Hence the top shaft was made of two parts :
one part was fixed and carried the driving gear, and the other carried the roll and was thus readily movable. The two parts were connected together by a cylindrical coupling used also as the torquemeter. The fixed part of the shaft was part of the original milling machine arbor and was driven by the machine gears.

3- A two-part bottom roll shaft: in order to alter

the gap setting without changing the centre distance between the double helical gears . The fixed part carried the driven gear and the unrestrained part carried the roll. A special flexible coupling was used to connect the two parts of the shaft and to provide axial adjustment for the unrestrained part of the bottom roll shaft. Thus changing the gap setting between the two rolls was achieved by moving the bottom roll shaft vertically as required. The freedom of movement of the unrestrained bottom shaft, in the vertical direction, permitted the measurment of the roll separating force by specially designed loadcells.

4- Special Roll Supports: the roll supports and bearings were designed to provide rigidity and allow the removal of the top roll and the measurment of the roll separating force.

5- Modified Rolls: the rolls were modified to suit the requirements of pin loadcell assembly and the groove shape.

6- A new tube tensioning unit: the methods of applying back and front tension were either modified as in the case of the front tension or entirely redesigned and remade as in the case of the back tension.

7- New instrumentation ; the loadcells, torquemeters and other measuring equipment were redesigned except for the two tension loadcells which were re-used.

8- An additional flexible coupling was included

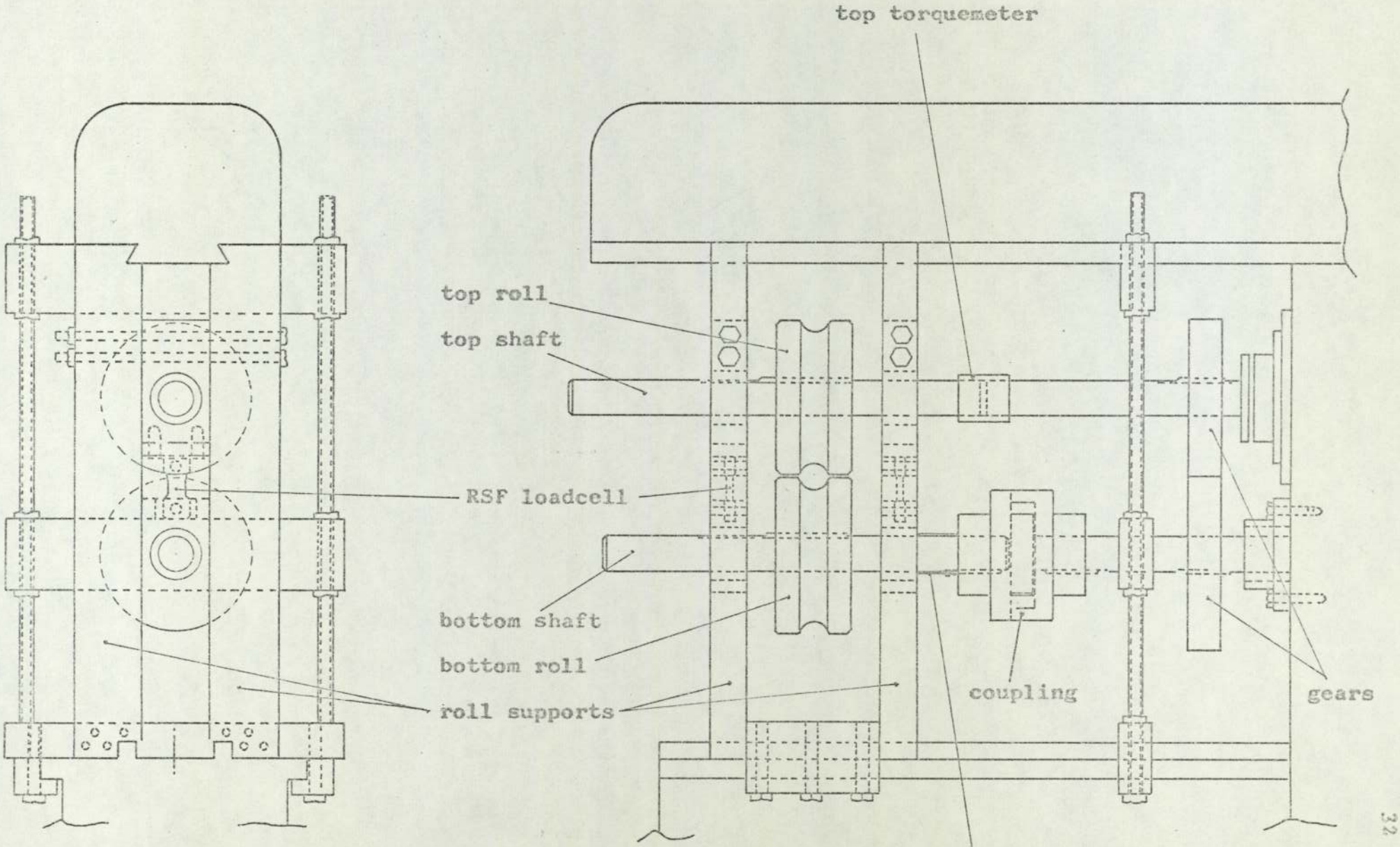
top torquemeter
top roll
top shaft
RSF loadcell
bottom shaft
bottom roll
roll supports
coupling
gears
bottom torquemeter

Fig.(5)

Photo. (1)

General View of the Roll Stand

with one of the Supports Removed.

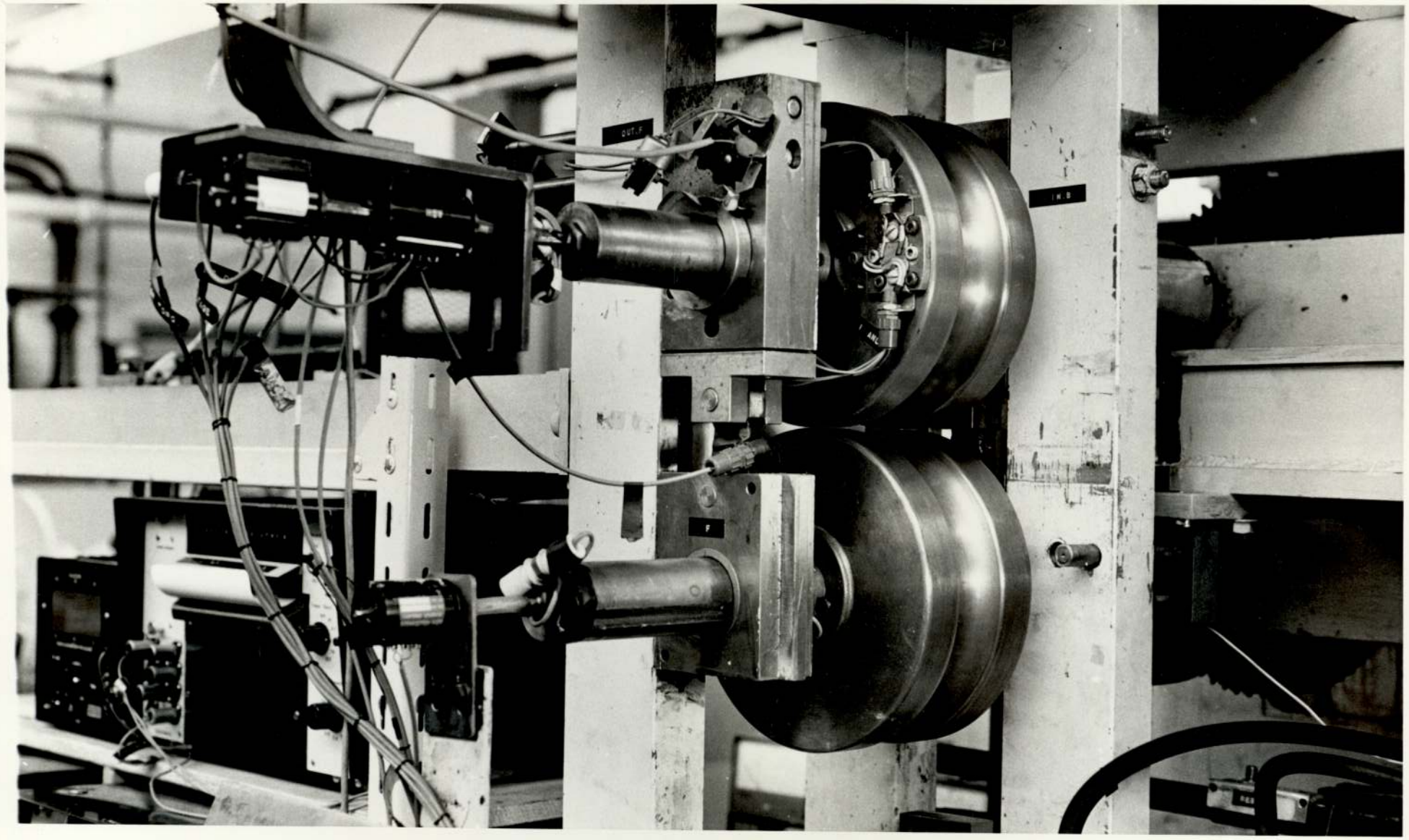
OUT.F
IN.B

between the motor and the machine to eliminate vibrations and their transmission to the traces.

A general view of the experimental roll stand is shown in fig. (5) and photo. (1) in which one of the roll supports was removed.

The flexible coupling used on the bottom shaft was chosen after an extensive study of the literature on the available types of couplings. The requirements were those of compactness constant speed and spatial adjustment. The type shown in fig. (6) known as the American coupling , was selected since the specification indicated it to be the most eligible. However, when the coupling was used it resulted in a cyclic fluctuation of the recorded loadcell traces.The fluctuations were sometimes of the same order as the recorded loads and therefore were unacceptable. Even under no-load running condition the traces suffered from the fluctuations. Different lubricants were tried on the interface between the floating disc and the flanges in order to reduce the frictional forces which had been found to be responsible for the fluctuations. Even so, the improvement was not significant and other ways of minimizing the effects were sought. Consequently the design of the coupling had to be modified as follows:

a- the floating disc was redesigned as shown in fig. (7) . The new disc consisted of two square plates with ball bearings fitted between them at the corners. It was hoped that by replacing the

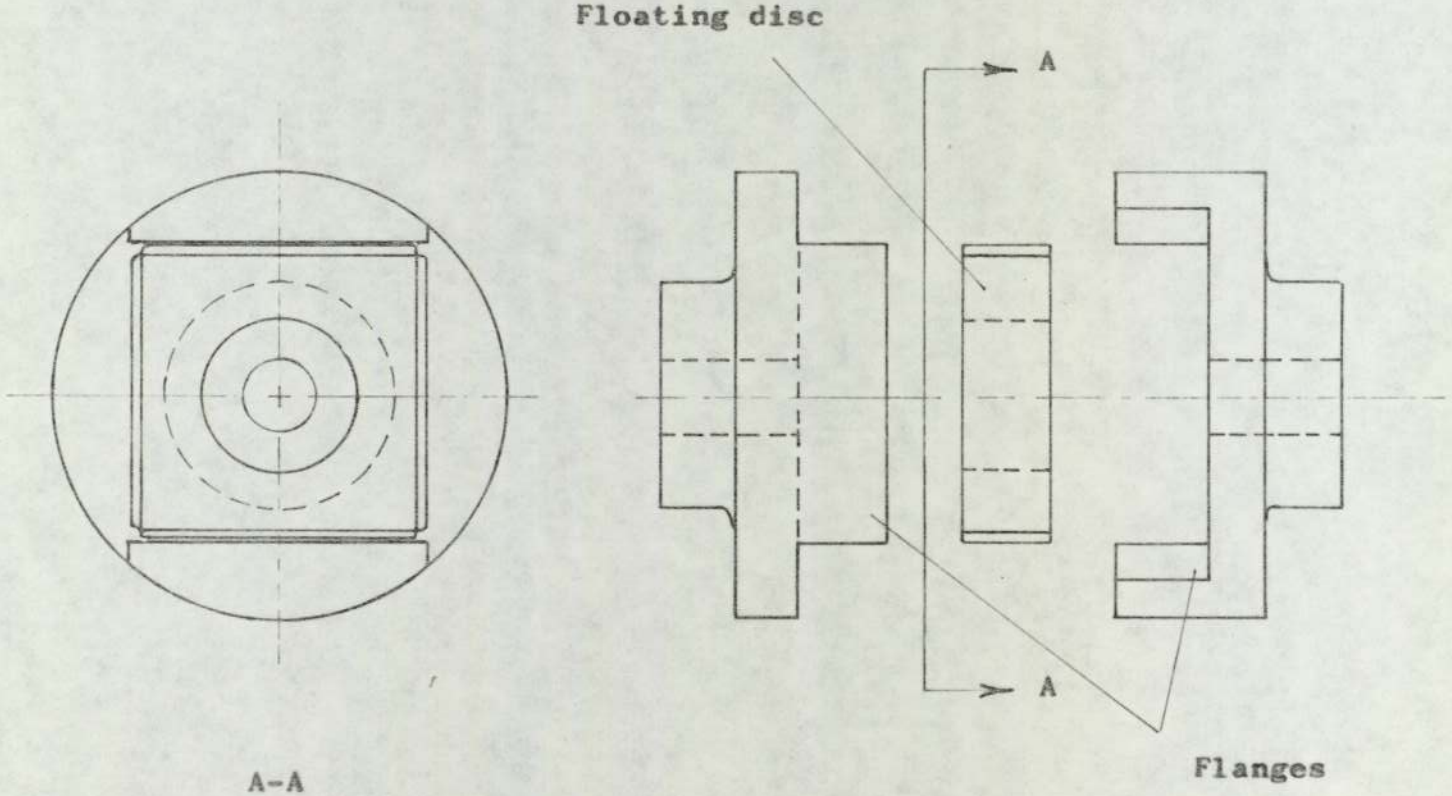

Fig. (6)

The Coupling

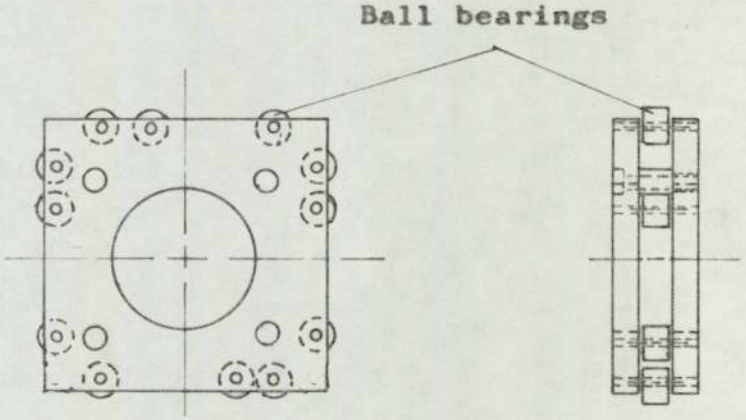

Fig. (7)

Modified Floating Disc for

The Coupling

brass strips with these ball bearings the frictional forces would be greatly reduced.

b- the faces of the two flanges in contact with the floating disc were lined with hard steel liners. These liners were heat treated and after grinding were fitted in position.

After reassembling the coupling and fitting it in position some tubes were rolled and no fluctuations that could be attributed to the coupling were found. Therefore this modified coupling was used throughout the trials and has proved continually successful.

(III-2) Methods of Applying Tensions

(III-2-1) The Back Tension Device

After an extensive study of the literature on the techniques used for applying back tension to the rolled strip, bar, or tube, the use of a braking system was believed to be more suitable for this application than that previously employed . The friction between a moving friction pad pressed against a stationary surface provided the required braking effect. Consequently variation of the amount of tension was made by varying the pressure on the pads.

Preliminary tests had shown that in order to be able to roll a sufficient length of tube to achieve steady state rolling conditions without the end of the tube

bending under its own weight, the tube had to be guided. Bending of the tube resulted in the torque on the two shafts not being equally shared and made measuring of the length of the arc of contact more difficult. Guiding of the tube ends was required for sinking as well as for stretch reducing.

With this in mind the system shown in photograph (2) was chosen.

To ensure that the value of the applied back tension was maintained at a constant level with small variations in the tube velocity and in the surface condition on the interface between the pads and the surface of the channel, some tests were carried out for this purpose. A one metre long steel bar of 25mm x 5mm dimensions (cross section),having a surface finish similar to that of the channel sides,was fixed to the stationary chuck of a lathe and was kept in a horizontal position. An automobile disc brake unit with manual pressure adjustment was fixed on the saddle of the lathe. With the bar between the friction pads under pressure, the saddle was engaged and moved along the bar at various speeds. Drops of oil and water were put on the surface of the bar from time to time. The bar was fixed to the chuck through a loadcell which was connected to a UV recorder and the tension in the bar was thus recorded.

This investigation shewed that small variations in the speed and the frictional conditions did not have a significant effect on the braking force produced

Photo. (2)

The Roll Stand With the Front

and Back Tension Devices.

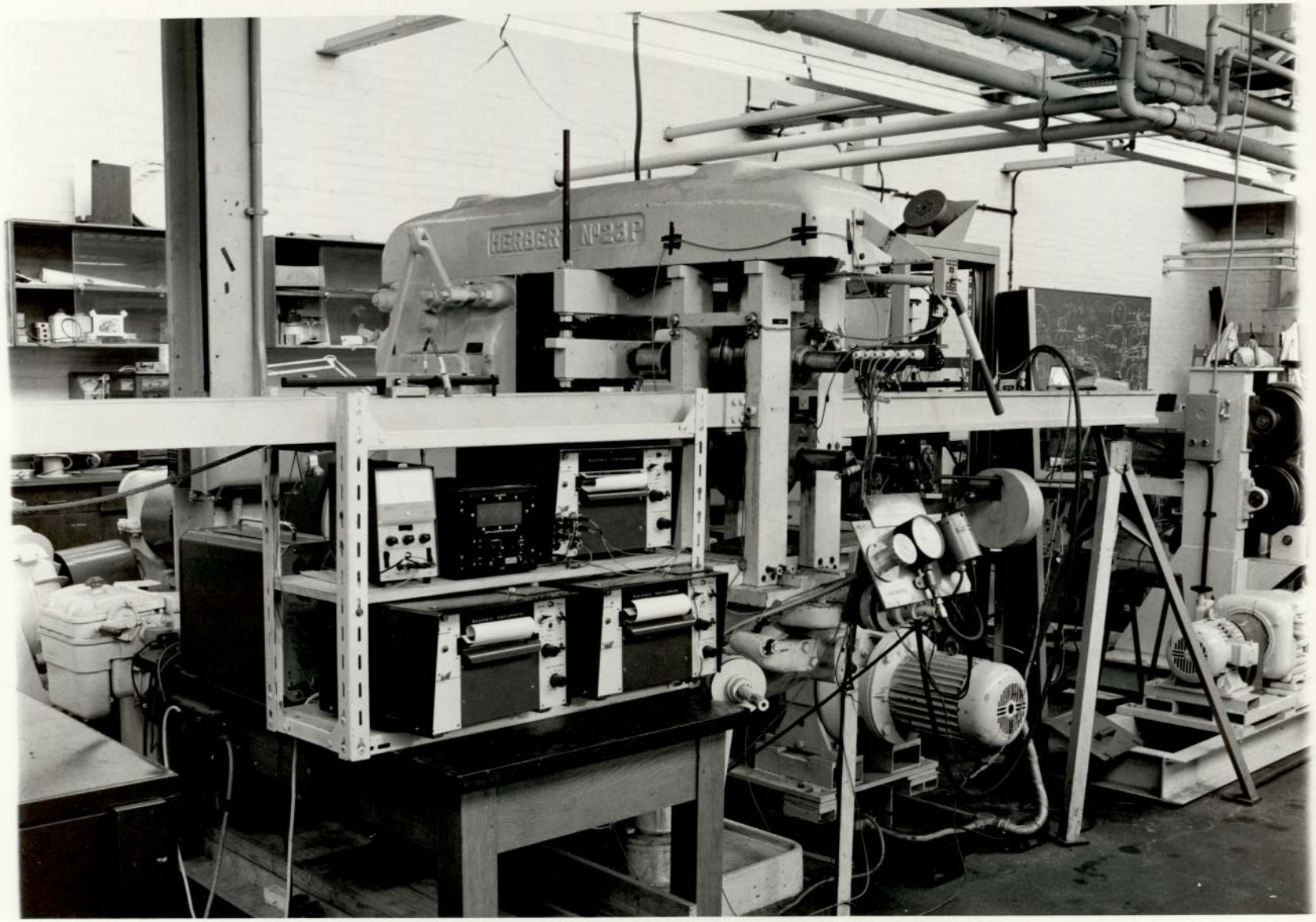
HERBERT No 23P

in the bar. Accordingly, the design shown in photo. (2) was made.

The two sides of a rolled channel section provided the stationary surfaces against which the two friction pads were pressed. The channel was carried on the two front vertical supports in fig. (5) at one end and a tripod with height adjustment at the other. The channel was made horizontal by the use of a spirit level and adjusting the screw rod on the tripod.

The carriage carried an automobile brake cylinder with two pistons to which the friction pad holders were fixed. The carriage had four wheels and ran along the channel in a guide. The pressure on the pistons was provided by an arrangement similar to that used in a road vehicle except that the piston of the master cylinder was acted upon by a pivoted L-shaped bar carrying a weight . To vary the pressure on the piston, the weight was appropriately positioned on the bar thus changing the leverage ratio and hence the force on the piston. An electric motor was used to drive a screwed rod which ran through the weight consequentially adjusting its position. A pressure gauge connected into the brake fluid line gave an indication of the pressure on the pads. The gauge was later calibrated to indicate, conveniently but approximately, the resulting tension in the tube. The pressure and hence the tension were remotely controlled.

Arrangements were made so that the force on the

master cylinder piston could be released and therefore no braking effect took place. The carriage could then be used to guide the end of the tube for the sinking process.

(III-2-2) The Front Tension Device (photo. 3)

In a stretch-reducing mill, the interstand tension is produced by the difference in the speeds between the stands, with the inlet speed requirement of a stand being higher than the output speed from the previous stand. The magnitude of the tension in the tube between two stands is altered by altering the relative speed between the stands.

The same concept has been adopted in this investigation. An electric motor, photo.(3) with a variable speed gearbox had a drum fixed to the output shaft of the gearbox. The drum had a helical slot machined on the surface round its periphery. One end of a wire-rope was attached to a point on the outer surface of the drum at the start of the slot and the front of the tube was attached to the other end of the rope. By driving the drum so that its peripheral velocity was slightly higher than the exit velocity of the tube from the roll stand, tension in the tube was created. By varying the speed of the drum the amount of tension in the tube was controlled.

To provide guidance for the front of the tube an

Photo. (3)

Front Tension Device

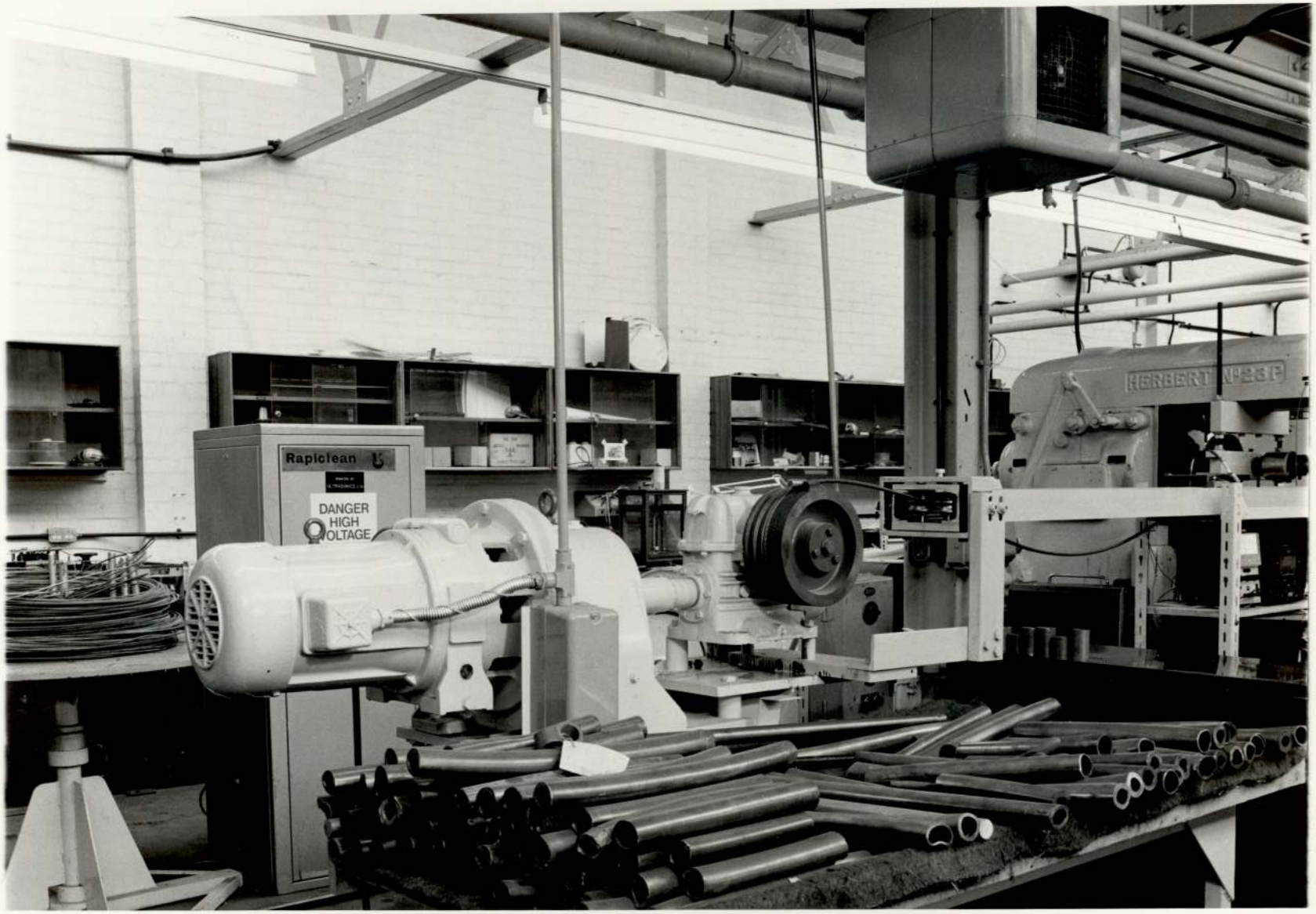
Rapiclean
DANGER
HIGH
VOLTAGE
HERBERT

arrangement similar to that for the back of the tube was adopted. Two C-shaped sections provided a guide for the carriage. The tube end was attached to the carriage through the front tension loadcell. On the opposite side of the carriage was attached one end of the wire rope from the front tension drum. To ensure the axial alignment of the applied tension a guiding arrangement for the rope was made at the end of channel near the front tension drum. Two small rollers with semi-circular grooves were fitted with their axes in the vertical direction as shown in photo.(3). This arrangement prevented the lateral movement of the rope due to the helical groove on the drum. The gap between the two rollers was somewhat bigger than the diameter of the wire rope passing through it.

The settings on the speed control knob were calibrated to indicate approximately the magnitude of the front tension for initial setting purposes.

The controls of the back and front tensions were conveniently situated on the control box photo.(3) in front of the roll stand.

The front tension channel was fixed to the two outlet side vertical supports at one end and to the mount of the motor, i.e. the foundation at the other end with facility for height adjustment.

The front tension and back tension channels were set in line with the centre of the groove before the tests commenced.

(III-3) Measuring Equipment:

(III -3-1) Roll Separating Force(RSF) Loadcells:

The movable (i.e. unrestrained) part of the bottom shaft of the roll stand was attached to the top shaft through the two RSF loadcells as shown in fig.(5). The two bearing blocks of the movable part of the shaft were designed so that they could slide vertically, guided by the slots in the supports, photo.(1) . The design of the loadcell itself can be seen in fig. (8) . Eight foil strain gauges were mounted on the two faces of the loadcell and were connected into a bridge. The material of the loadcell was steel type EN 26 heat treated to condition(V) according to standard specifications. A view of the loadcells can also be seen by reference to photograph (1).

(III-3-2) Torque

It was important to measure the rolling torque on both shafts since any variation in torque sharing between the two rolls would indicate a variation in conditions at the roll surface. For example measurement of the length of arc of contact which was of great importance, could only be made from the pin loadcell traces and in order that the measured arc of contact can represent the mean value, it must be corrected using the knowledge of the torque sharing factor.

The torque on the top shaft was measured by means

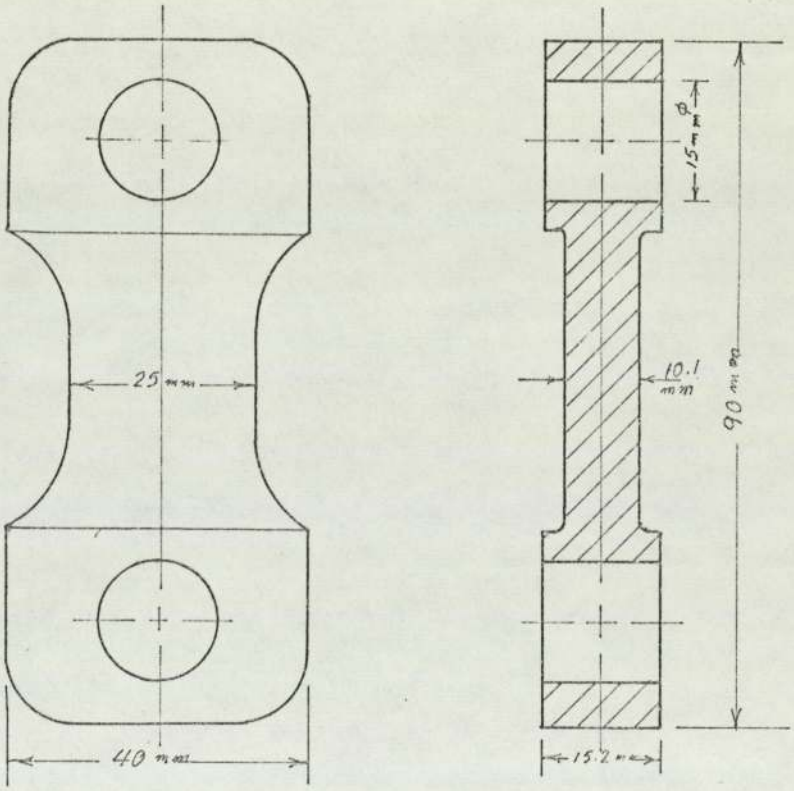

Fig.(8)

RSF loadcell

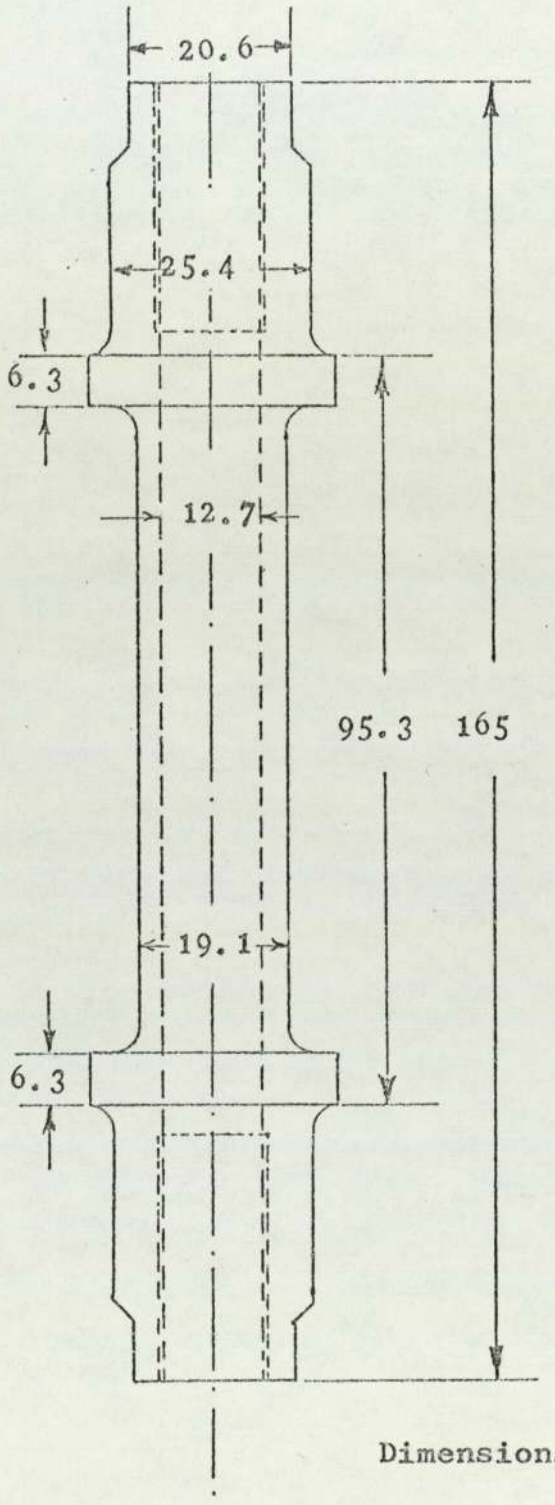

Fig. (9)

Tension loadcell

of four standard 45 torque gauges mounted on the collar (see fig.(5)) , which connects the two parts of the top shaft . The gauges were connected in a bridge circuit and the leads from the torquemeter followed the path described in the section on instrumentation.

Similarly, the torque on the bottom shaft was measured by means of four standard 45° electrical resistance torque gauges but mounted directly on the shaft itself in the position shown in fig. (5) . Both torquemeters were protected against outside damage.

(III-3-3) Tensions:

Two tension loadcells used in the previous investigation (1) were checked and when found to be in good working order used to measure the back and front tensions The design of these loadcells can be seen in fig. (9). Each loadcell carried eight strain gauges and was compensated both for temperature and bending.

One end of the back tension loadcell was fixed to the inlet channel carriage and its other end was connected to the tube holder. Similarly, the front tension loadcell was fixed to the exit-side channel carriage and carried the exit-side tube holder.

(III-3-4) Velocities:

In the first series of tests, i.e. free sinking where the ends of the tube were not guided, the tube was not

straight because it was free to bend under its weight or because of the variation in frictional conditions at the interface between the tube and the rolls. Therefore, in these circumstances measurement of tube velocity was not easy. A number of methods was considered (e.g. light-activated switches, magnetic switches . ... etc.) but all proved unsuitable because of the unguided movement of the tube ends.

To overcome this difficulty, the method finally adopted comprised a string, with a clamp on one end and a weight on the other, driving a cam which activated two microswitches. The cam was fixed to a small pulley which was driven by the string. The weight on the free end of the string provided tension to prevent it from slipping over the pulley . When the string was clamped to the moving tube end the cam activated the switches which in turn triggered an electronic timer. The tube velocity was calculated from the time recorded and the fixed distance on the cam. The arrangement is shown in fig. (10) .

In the second series of tests, where the ends of the tube were guided, the velocity measurement was simpler. A light-activated switch was fixed to each of the two carriages - which were attached to either end of the tube - and moved axially with it. Two small light sources at a known distance from each other (381mm) were fixed to the sides of the inlet and exit channels. As the switch passed the lights it produced signals which were recorded on the UV recorder traces with time signals also recorded for reference.

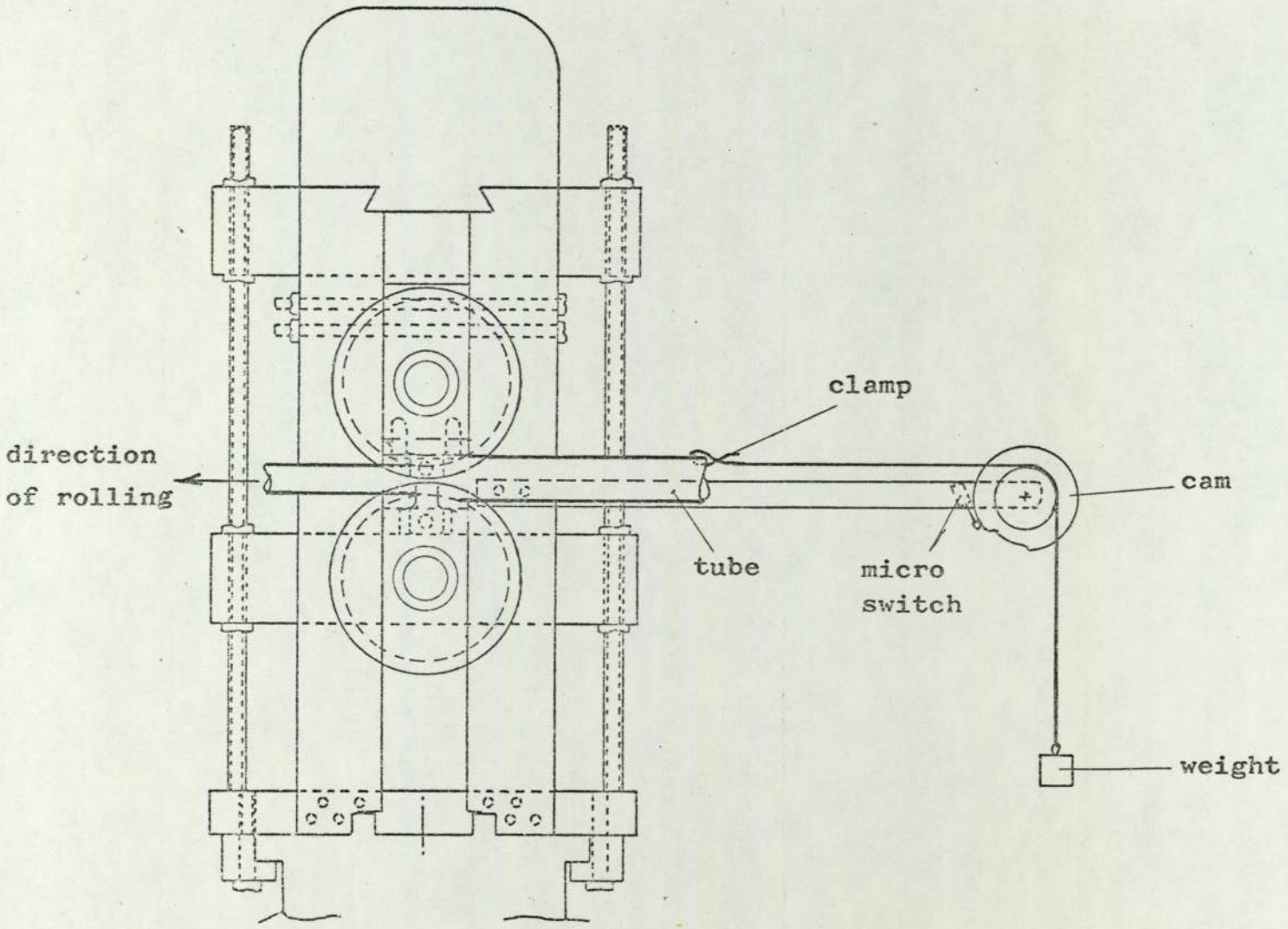

Fig. (10)

Measurement of tube velocity

(III-4) Tube & Roll size

(III-4-1) Tube size

The only comprehensive study of the tube rolling process readily available in English is that by Cole[1] also carried out at the University of Aston in Birmingham. In his investigation, Cole used lead tubes of nominal outside diameter of 1.75 inch (44.5mm) and wall thickness 0.25inch(6.3mm).

His test results and conclusions were used to provide a background against which the plan of the present investigation was conceived. To make good use of his experimental work and to provide a firm basis for comparison of results, the size of tube used in Cole's work was included amongst the sizes to be used for the present investigation.

Two factors influenced the choice of tube sizes, firstly the need to study the effect of diameter to thickness ratio (d/t) and secondly,the desire to be able to obtain different pass reductions without having to alter the gap. To fulfil these two requirements it was decided to use tubes having the same nominal outside diameter but of various d/t ratios. The three selected d/t ratios were 4.7 , 7 and 14 for tubes of nominal outside diameter of 44.5mm. Thus for a certain gap setting three different reductions in area per pass were achieved. Two independent variables could be studied in this way: the first is the effect of d/t ratio on the process parameters(i.e. area of contact, rolling loads and torque, reduction per pass etc.) and the second is the effect of varying the adjustment of the

gap between the rolls on the shape of the tube as well as on the other process parameters. In addition to these two variables, others could be studied also e.g. effect of d/t on wall thickness variation and on the pressure distribution curves, which were of particular interest.

The lead tubes were supplied in lengths of 1.5 m in the as-extruded form. They were carefully packed in wooden boxes to avoid distortion and surface damage during transit and consequently the tubes were usable without the need for any preparatory treatment.

(III-4-2) Test Specimens:

In order to produce reliable and reproducible results it was important that steady state conditions prevailed during the recording of the various parameters. To achieve this a sufficient length of tube was rolled before recordings were made. This eliminated the possible variation of roll speed from no-load to full-load condition and ensured that frictional conditions were those assumed to exist between the rolls and the tube. Unless a sufficient length of tube were rolled the recordings were unrepresentative. Also, all factors contributing to each set of readings were recorded. Another reason for requiring steady state conditions was that all the theoretical studies assumed steady state conditions.

Handling long lengths of pure lead tubes and maintaining them straight was difficult. Therefore the need to roll a length sufficient to ensure that reliable data was collected conflicted with the need to roll short straight tubes.

With a bent tube torque sharing between the two rolls was disturbed due to the change in the area of contact between the tube and rolls. Some preliminary tests were carried out to establish a compromise.

These tests showed that a minimum length of about 380 mm was necessary to ensure reproducibility of the results. Therefore it was decided that for the first series of tests, i.e., free sinking, the length of the specimen should be 450 mm with the recordings being made half way through the length. For guided sinking and when tensions were applied the specimen length was increased to 700 mm and 1.5 m respectively.

To determine the minimum specimen length for steady state rolling, a number of specimens of different lengths were cut from the same tube and rolled under identical conditions. The pressure distribution curves, roll-separating force, roll torques, and areas of contact were compared. When allowance was made for non-homogeneity of wall thickness and friction conditions, it was found that the reproducibility improved little for specimen lengths of over 380 mm and therefore this length was considered to be the minimum permissible. However for the free sinking trials it was necessary following a similar comparison of parameters to increase this length by between 15 and 20%.

The specimen length for the guided sinking trials was increased by the attachments to the leading and trailing ends. Similarly, for the stretch-reducing trials a further increase in specimen length was required to allow for

the build up of tension in the tube before the recordings could be made. However, in these trials instantaneous readings were made for increasing values of tensions.

(III-4-3) Roll size and material:

The two rolls were manufactured in the University workshops. The material was steel type EN 24 which has the chemical and physical properties listed in Appendix (A). No heat treatment was necessary since the roll stresses were relatively low and the number of trials was limited.

The size of the rolls was made similar to that used in industry for similar sizes of rolled tubes. The other limiting factor was the special design of the pin loadcell assembly which necessitated an increase in the roll diameter to enable the assembly to be accommodated.

The diameter of the roll at the root of the groove was 189.2 mm and that at the shroud was 226.9 mm.

The groove shape fig.(11), was of the single radius oval pass design [21] since it is relatively simple for the analysis of the deformation zone and also it is not uncommen in practice. The groove had a slight relief near the corners. The groove radius (r_g) was 23.39 mm while its depth at the root (h_g) was 18.9 mm. Thus the groove eccentricity (e_g) was 4.5 mm.

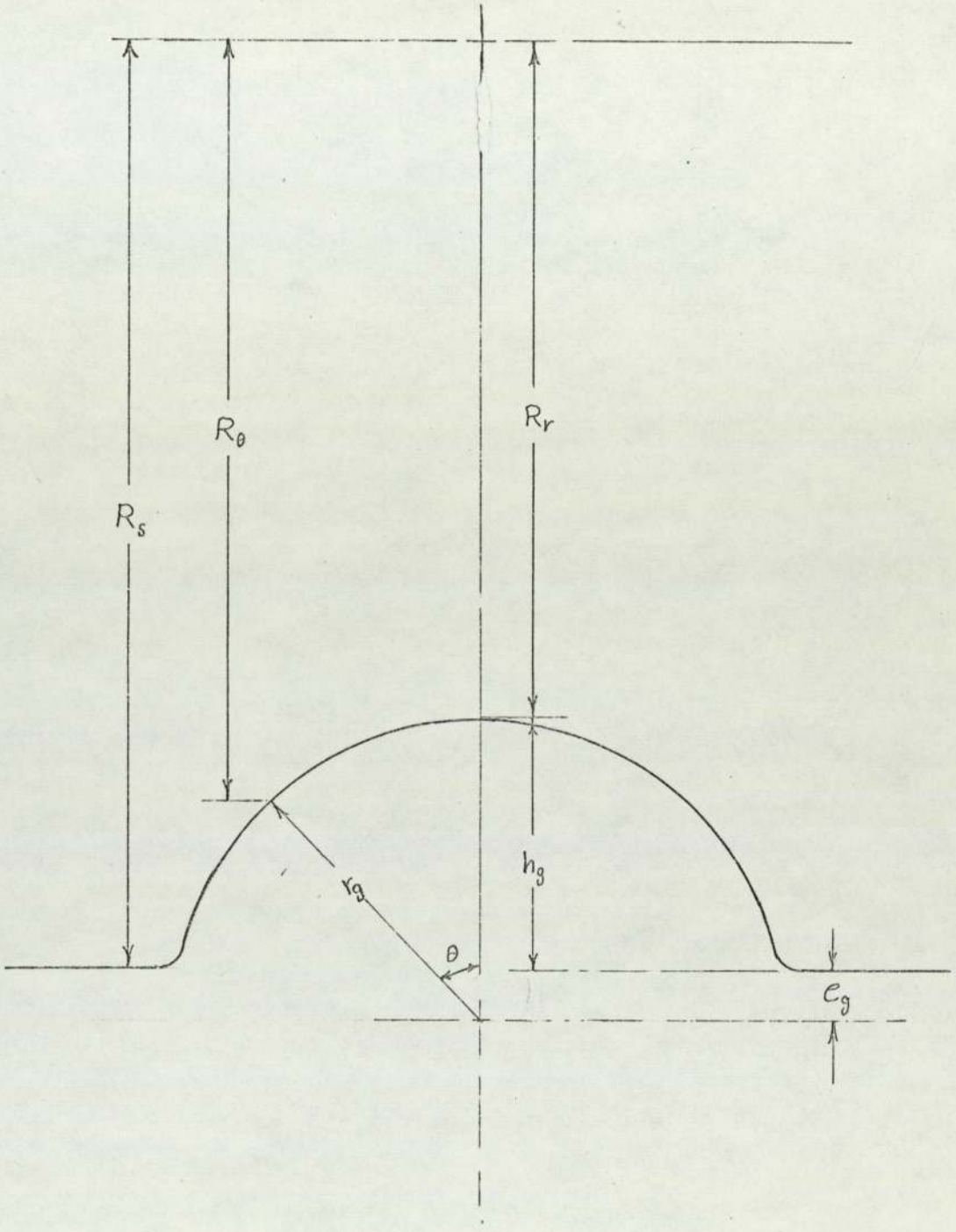

Fig.(11)

Geometry of groove

(III-5) Instrumentation

Transmitting the voltage supply to the bridges of the various loadcells and the signals from these bridges to the recording instruments was the first step towards obtaining permanent recordings of the rolling loads.

The two roll-separating force loadcells and the loadcells for front and back tension presented no problem since the connections were simply made by using screened cables.

However complications arose when the loadcells rotated with the rolls as was the case of the pin loadcells and the two torquemeters. The bottom shaft carried only one torqumeter in the position shown in fig.(5) . The four-lead screened wire from the torquemeter passed the back bearing through the keyway, then the roll through a hole drilled axially in it for this purpose, and finally thruogh a central hole in the shaft which ran from its free end to a point between the roll and the front bearing. A slip ring was axially attached to the end of the shaft through a flexible tubing-which permitted small misalignments. Screened wires were used between the slip rings unit and the instrument table.

Connections to the top shaft, however, were more complicated since the four pin loadcells and the top roll torquemeter had all to be accommodated. This meant that if each of the bridges was supplied separately, a group of five four-lead screened wires had to be taken through a central hole in the shaft to the slip rings unit at the end of it. Preliminary tests on the pin loadcells had shown that the required sensitivity of

their bridges was approximately the same and therefore it was possible to use one value of supply voltage for them. This meant that the size of the group of wires which passed through the hole in the shaft could be reduced by using five twin-lead screened wires for the pin loadcells and onefour-lead wire for the torquemeter. The torquemeter cable followed a path similar to that of the bottom torquemeter. The wires from the pin load-cell assembly needed only to pass through the central hole to the free end of the shaft. A combination of two slip ring units had to be used since the largest unit avaliable could not accommodate 14 leads. The two units were coupled together by drilling a small central hole through the spindle of the large one allowing the wires to the coupled unit to pass through it. The combined unit was fixed to the body of the rig and attached to the top shaft with a flexible tubing, screened wires were again used between the slip ring units and the instrument table,photo.(1).

Voltage Supply

The bridges were supplied by four stablised dc suppliers. The values of the dc voltages for the various bridges are listed in table (B1) Appendix(B) . The stability of dc voltages was checked during the tests with a digital voltmeter. The dc power source supplying current to the top torquemeter was integral with the amplifier used with the bridge.

Bridge Balancing

This was achieved by the use of balancing resistors in the form of potentiometers connected as shown in fig.(12).

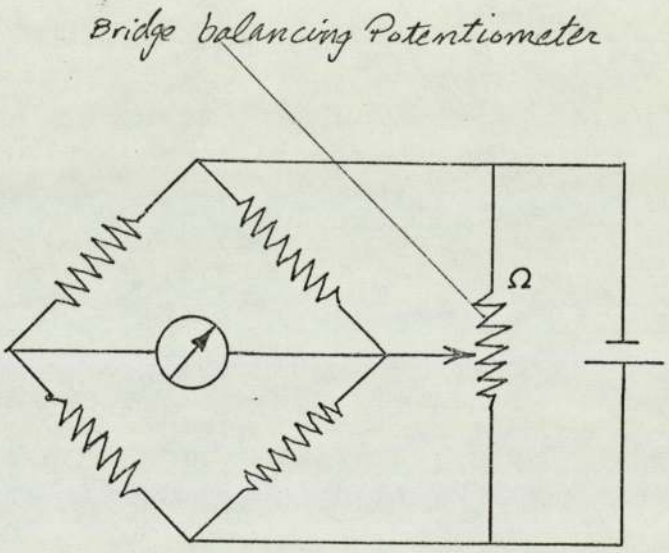

Fig. (12)

Bridge balancing was kept under constant observation and any drift rectified.

Signal Amplification

The signals from the torquemeters were not large enough, even with the use of the most sensitive galvanometers available and the maximum permissible voltage, to provide an adequate deflection of the galvanometers. Therefore two dc amplifiers were used to amplify the signals.

Recording of the signals

The final stage in measuring load or torque was the recording of the signals produced by the different loadcells when under load. Ultra violet(UV) recorders seemed ideal and the type selected was made by Southern instruments. During the sinking tests, two UV recorders, with ten channels each, were used. The four pin loadcells signals were put separately on one chart. The paper recording the signals from the pin loadcells ran only during the passage of the pins on the tube. The speed of this paper was set high to give accurately measurable traces as the angle of contact was only small. The second recorder dealt with the two torquemeters and the two roll separating force loadcells and operated at a relatively low speed since the recordings were made for the whole length of the testpiece.

Table(B1) Appendix(B) shows the values of the natural frequencies for the various galvanometers used in conjunction with the various bridges. A view of most of the instruments mentioned above is shown in photograph (2).

A cam on the top shaft actuated two microswitches

during the passage of the pins over the tube. The first of these controlled the UV recorder which recorded the pin loadcell signals while the second provided event marks on the recording paper of the second UV recorder. These marks were made during the passage of the pins over the surface of the tube and were used as datum lines.

(III-6) Calibration

Wherever possible, direct calibration of loadcells was carried out in situ. Where there were doubts about the accuracy or reproducibility of one method, an additional method was employed or the technique was altered and the results compared. As in the case of the pin loadcells three methods of applying loads were employed in order to eliminate any uncertainty.

Because of the importance of calibrations all loadcells were calibrated immediately before testing started and recalibrated after testing was finished. Also, during calibrations, the constant voltage supply to the loadcells was checked and adjustments were made when necessary.

Calibration of the Torquemeters

After fitting the top and bottom torquemeters to their respective shafts as shown in photo. (4), each was calibrated by applying the load in the form of dead weights to the end of a 900 mm long arm which was fixed to the shaft. The gears of the milling machine were engaged, and therefore locked, to prevent the shafts from rotating during calibration. The lever was fitted to the free end of

Photo. (4)

Positions of Torquemeters

and Coupling.

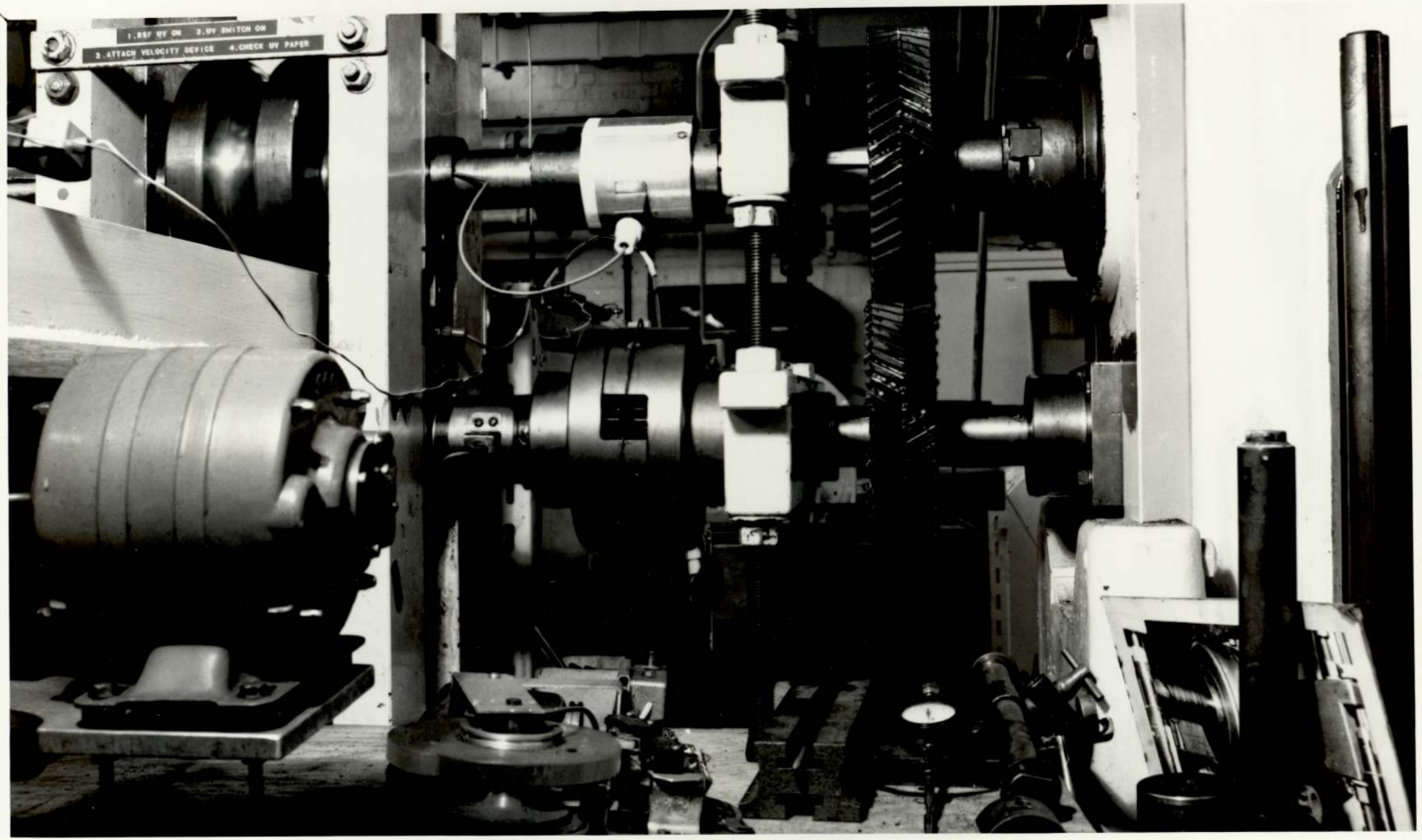
1. RSF UV ON 2. UV SWITCH ON
3. ATTACH VELOCITY DEVICE 4. CHECK UV PAPER

the shaft in a horizontal position to apply a torque in the same direction as that occurring in a test. The lever, which was marked in mm, carried a hook and was fitted with a carriage on rollers, this allowed it to move smoothly along the arm. To counter balance the weight of the lever arm, another arm of the same weight was fitted to the shaft in the same horizontal plane as the first lever arm but pointing in the opposite direction. A weight was attached to the hook and moved along the lever arm with readings recorded at intervals of 150 mm. Torquemeter readings were recorded during both increasing and decreasing values of torque.

Torquemeter Calibration Results

Figs.(13) and (14) show the calibration curves for the top and bottom torquemeters respectively. It can be seen from fig.(13) that generally the calibration curve is a straight line except at the lower end where it appears to exhibit some hysteresis. The predicted working torque for each roll was in the region of 70-140 N.m which is in the linear part of the curve and unlikely to be affected by any change of shape that might result from any corrections introduced. Nevertheless, attempts were made to minimise these effects by eliminating the causes of the non-linearity. It was believed that the reason for this behaviour, besides the friction in the bearings, was the possible misalignment between the two parts of the top shaft. The influence of friction in the bearings and possible misalignment may have been more significant at low torques where their contribution to the small signal from the

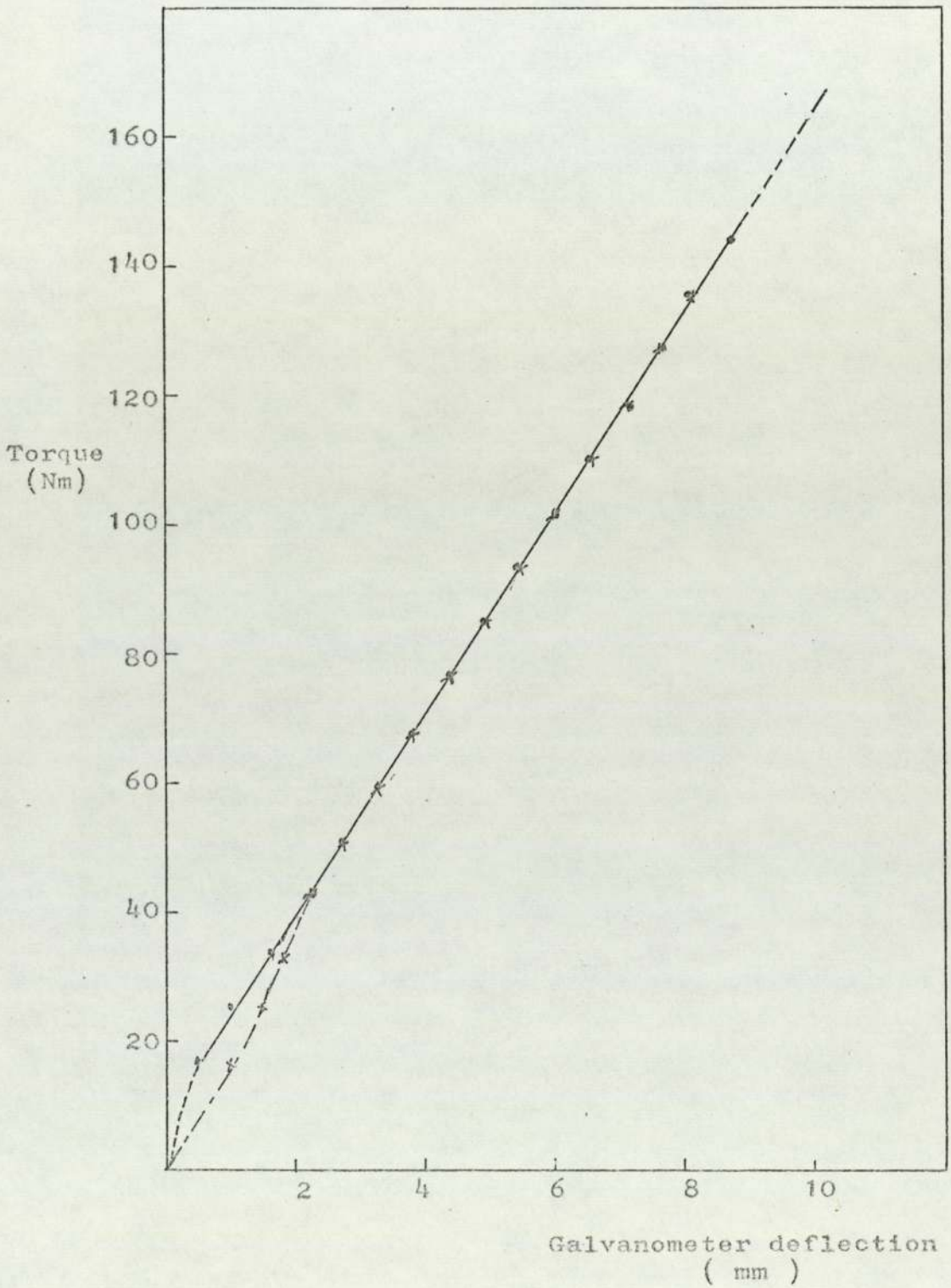

Fig.(13)

Calibration of Top Shaft Torquemeter

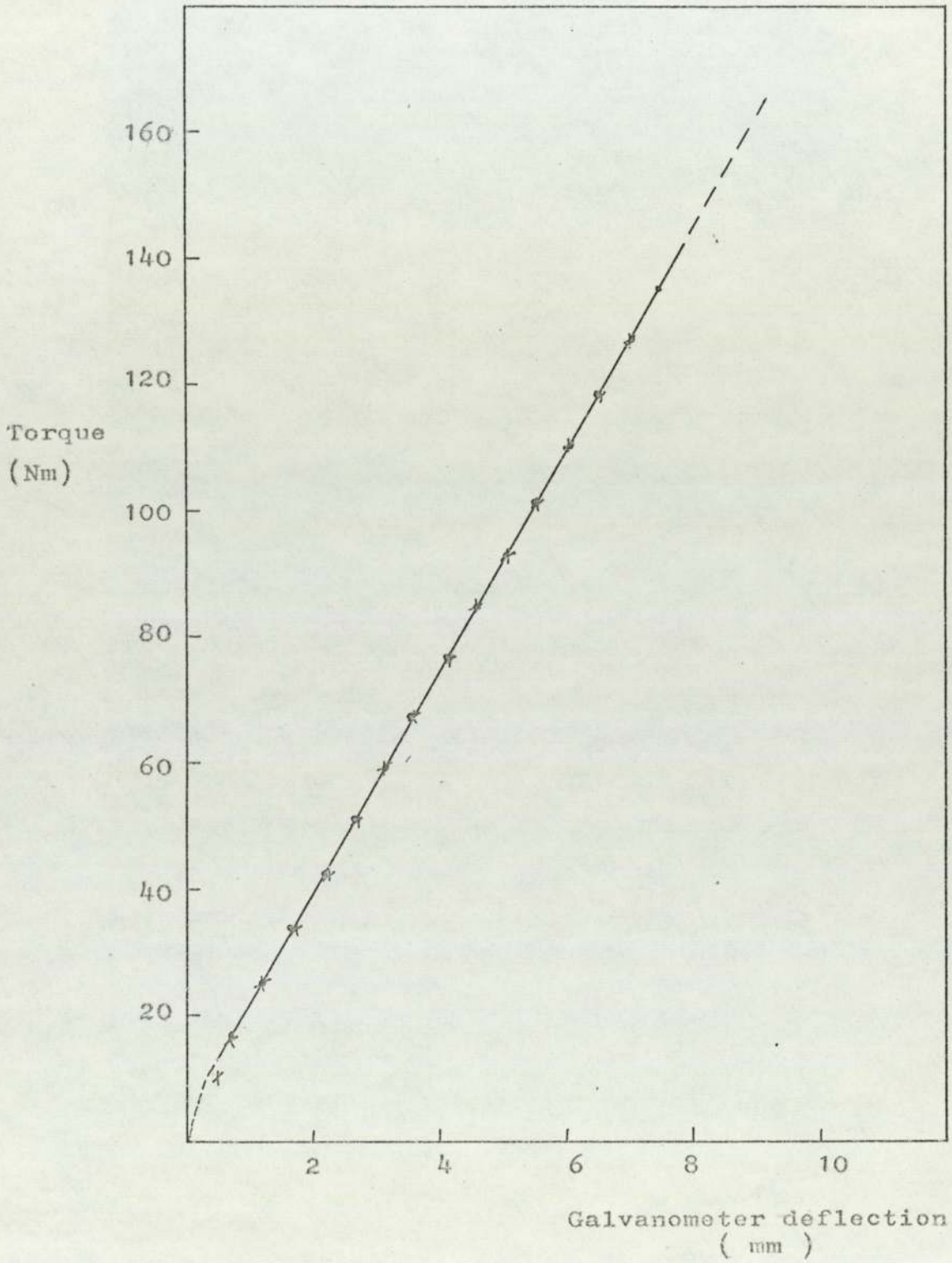

Fig.(14)

Calibration of Bottom Shaft Torquemeter

torquemeter was proportionately high . To reduce the effect of possible misalignment on the torque readings, the two top bearing blocks were loosened slightly. This resulted in some improvement and was adopted throughout the tests.

For the bottom torquemeter, it can be seen from fig. (14) that the extent of the non-linearity at the lower end of the curve was less than for the top torquemeter, fig.(13) and was not accompanied by hysteresis. This amount of non-linearity could not be reduced as the two bearing blocks were not fixed to the supports, even so the actual torques were hardly influenced by any of non-linearity at the lower end of the curve.

Calibration of the Roll Separating Force(RSF) Loadcells

It is always preferable to calibrate the loadcells in situ thus taking into account all the factors that might influence the performance of a loadcell. These factors include the method of fixing, wiring, and any friction that could obstruct the free movement of the loadcell. Failure to simulate any or all of these factors in the method of calibration used, calls for an in situ calibration or some correction.

The RSF loadcells, were always subjected to a tensile force and the movement of the loadcells, resulting from extension under load, was very small. Also the end fixing of the loadcells was easily reproduced in a test machine and the same leads were used for calibrations and tests. Therefore, due to the difficulty involved in trying to apply loads to the loadcells for calibration purposes in situ and the capability of simulating accurately the

actual conditions on a testing machine, the two RSF loadcells were calibrated on a tensile testing machine.

A 2000 lbf (8.9kN) Denison testing machine was used. The two loadcells were both attached to the arms of the machine in series. Thus the same load was applied to both loadcells simultaneously. A maximum load of 2000 lbf (8.9kN) was believed to cover all the working loads expected for various rolling conditions. A step of 200 lbf (890 N) was chosen and the loadcells readings were recorded for each loading step both on the increasing and decreasing side of the load. A warming up period of approximately two hours was allowed before calibration started.

Results of RSF loadcells Calibrations

Fig.(15) and (16) show the calibration curves for the front and back loadcells respectively. It can be seen from the figures that the calibration curves for both loadcells exhibit no hysteresis or zero drift. The recalibration of the loadcells after the test series was finished confirmed this. The gradients of the calibration curves were as follows:

Front loadcell	76.25	N/mm
Back loadcell	73.12	N/mm

Calibration of the Front and Back Tension Loadcells

The calibration method employed was similar to that described for the calibration of the RSF loadcells. The question of simulating the actual working conditions in the calibration method used was readily solved by the fact that loading under actual conditions was identical with that in the testing machine. This resulted from the

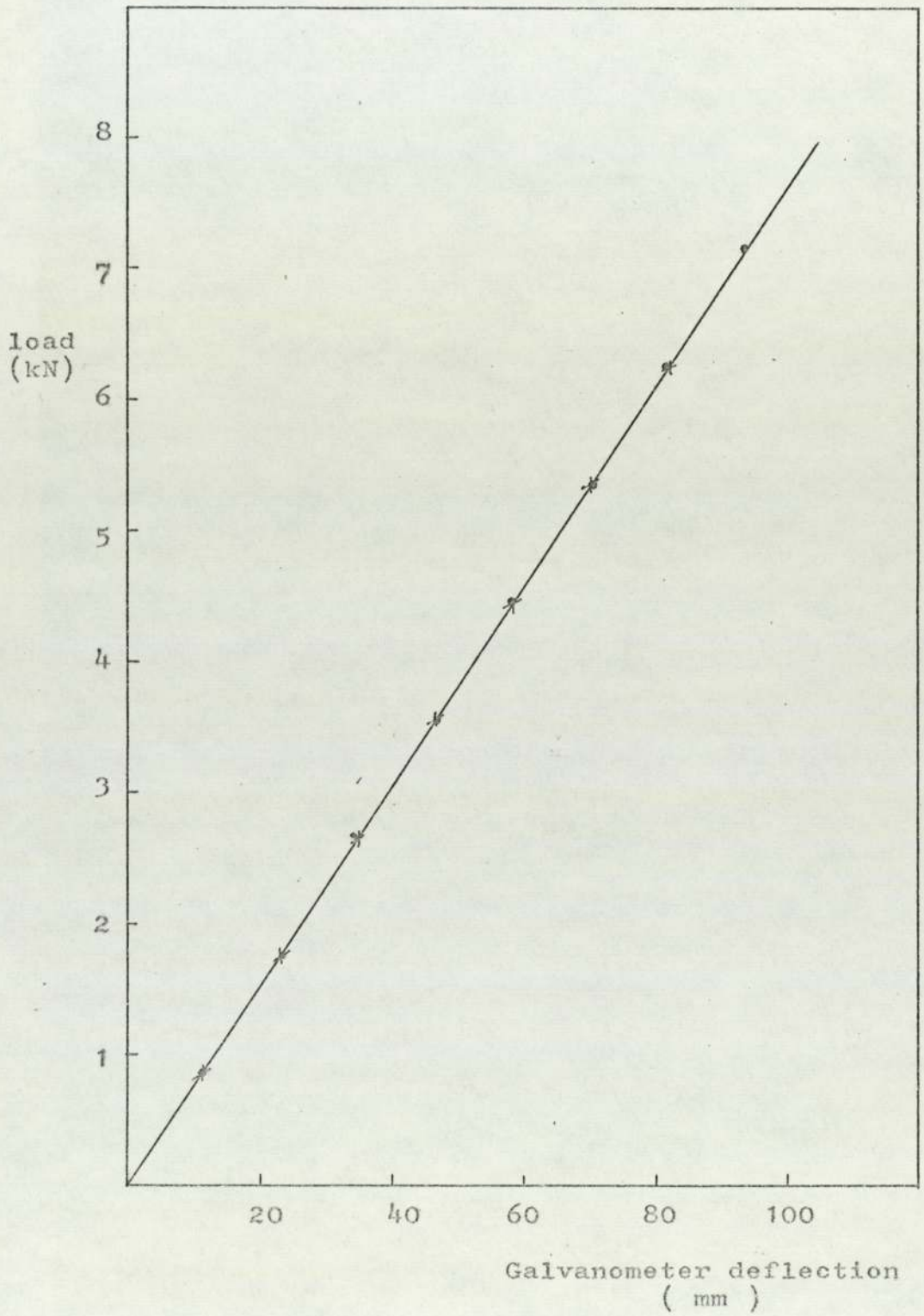

Fig.(15)

Calibration of Front RSF loadcell

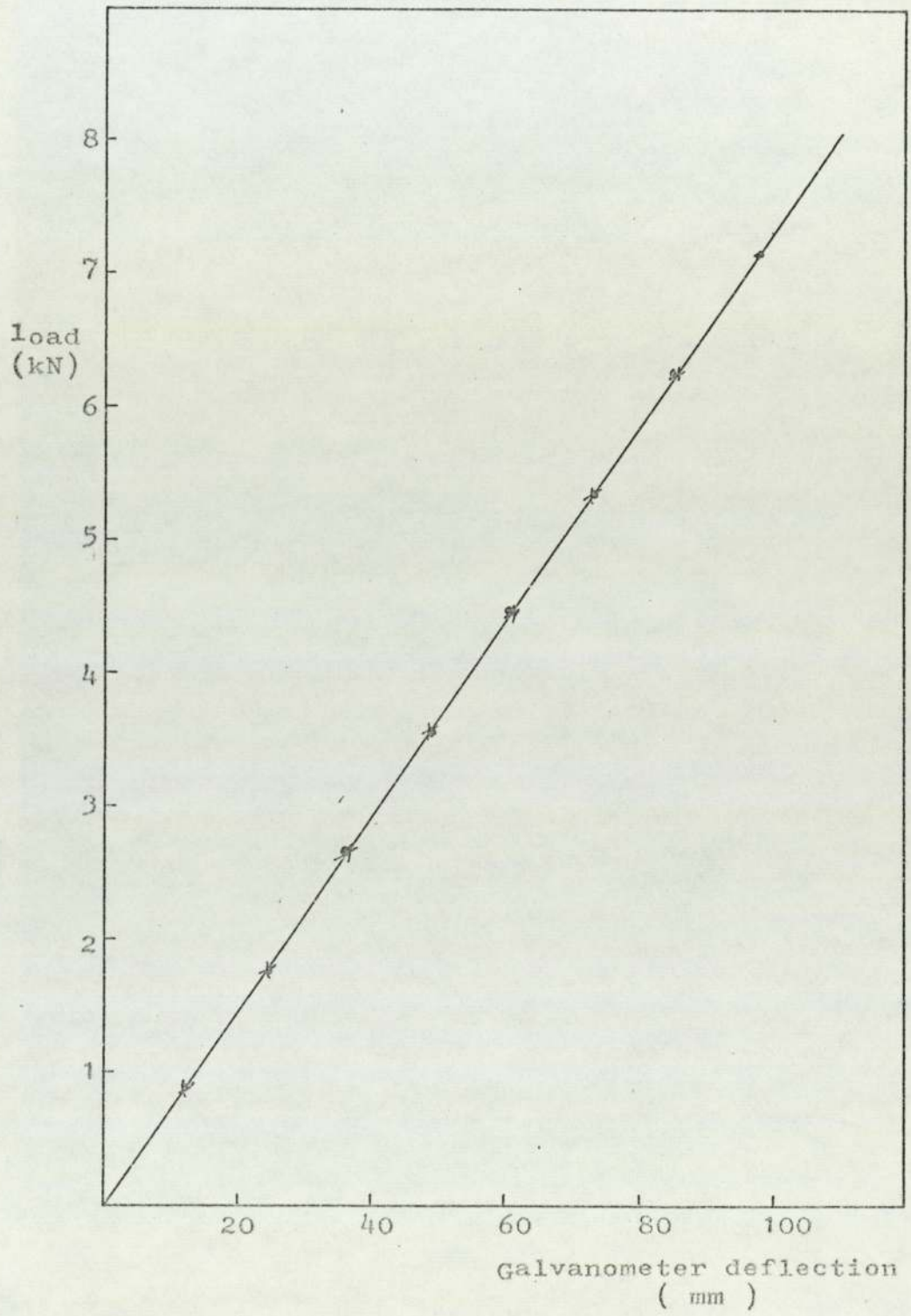

Fig.(16)

Calibration of Back RSF loadcell

fact that the tension loadcells were subjected to tensile forces with no friction or fixing problems. The only missing factor was that of the effect of the weight of the tube in producing bending stresses in the loadcells. But since the loadcells were compensated for bending, and this was checked, this problem did not arise.

Therefore, the tensile testing machine used for calibrating the RSF loadcells was used to calibrate the tension loadcells. A load step of 100 lbf (445N) was chosen and a maximum load of 1600 lbf (7.1 kN) was applied. Readings were recorded for each step, both on the increasing and decreasing side of the load.

Results of Tension Loadcell Calibration

Figs.(17) and (18) show the calibration curves obtained for the front and back tension loadcells respectively. As can be seen from the figures the calibration curves for both loadcells were excellent, exhibiting no hysteresis, zero drift or non-linearity.

The gradients were:

Front tension loadcell	85.30	N/mm
Back tension loadcell	80.87	N/mm

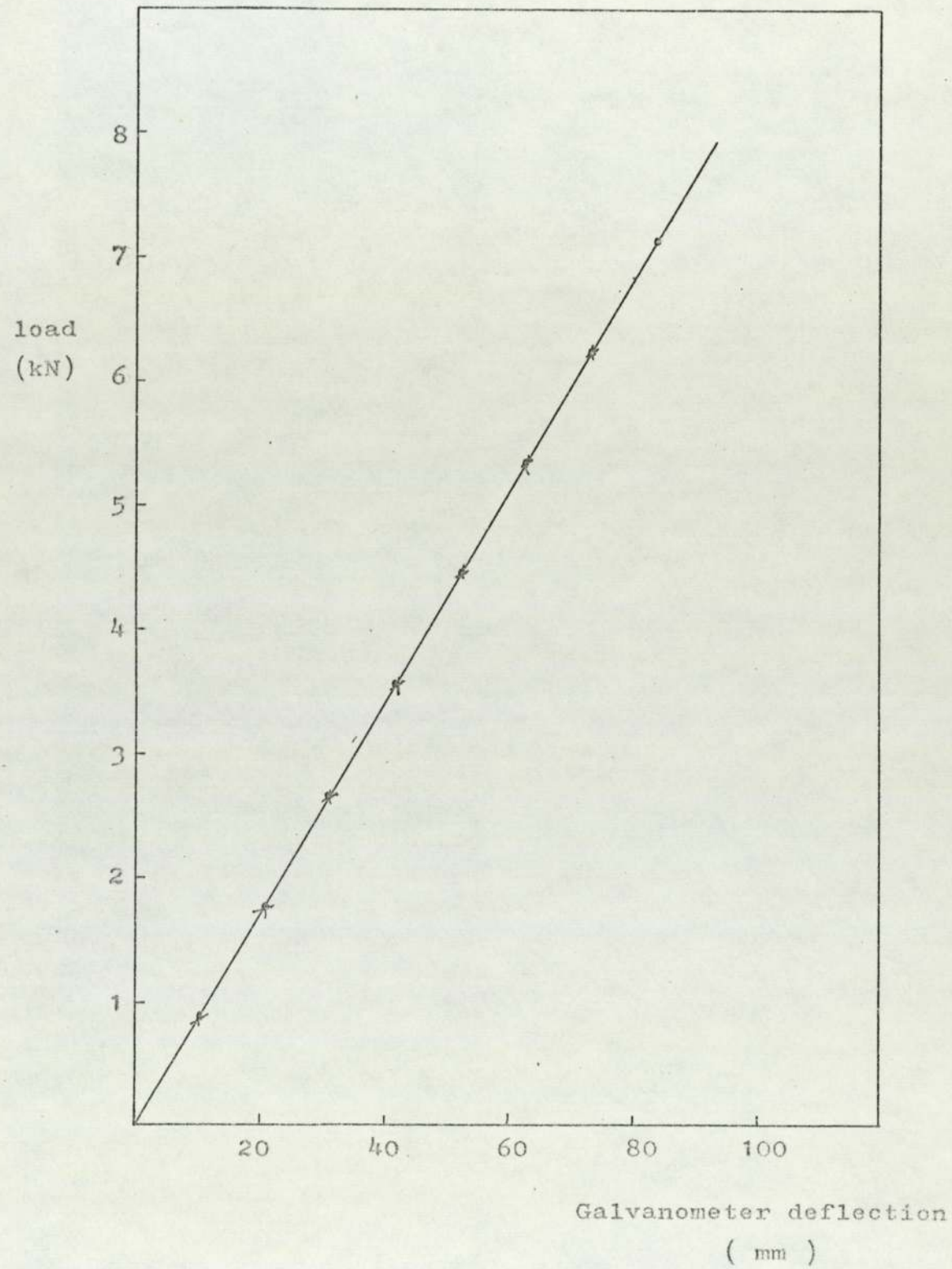

Fig. (17)
Calibration of Front Tension loadcell

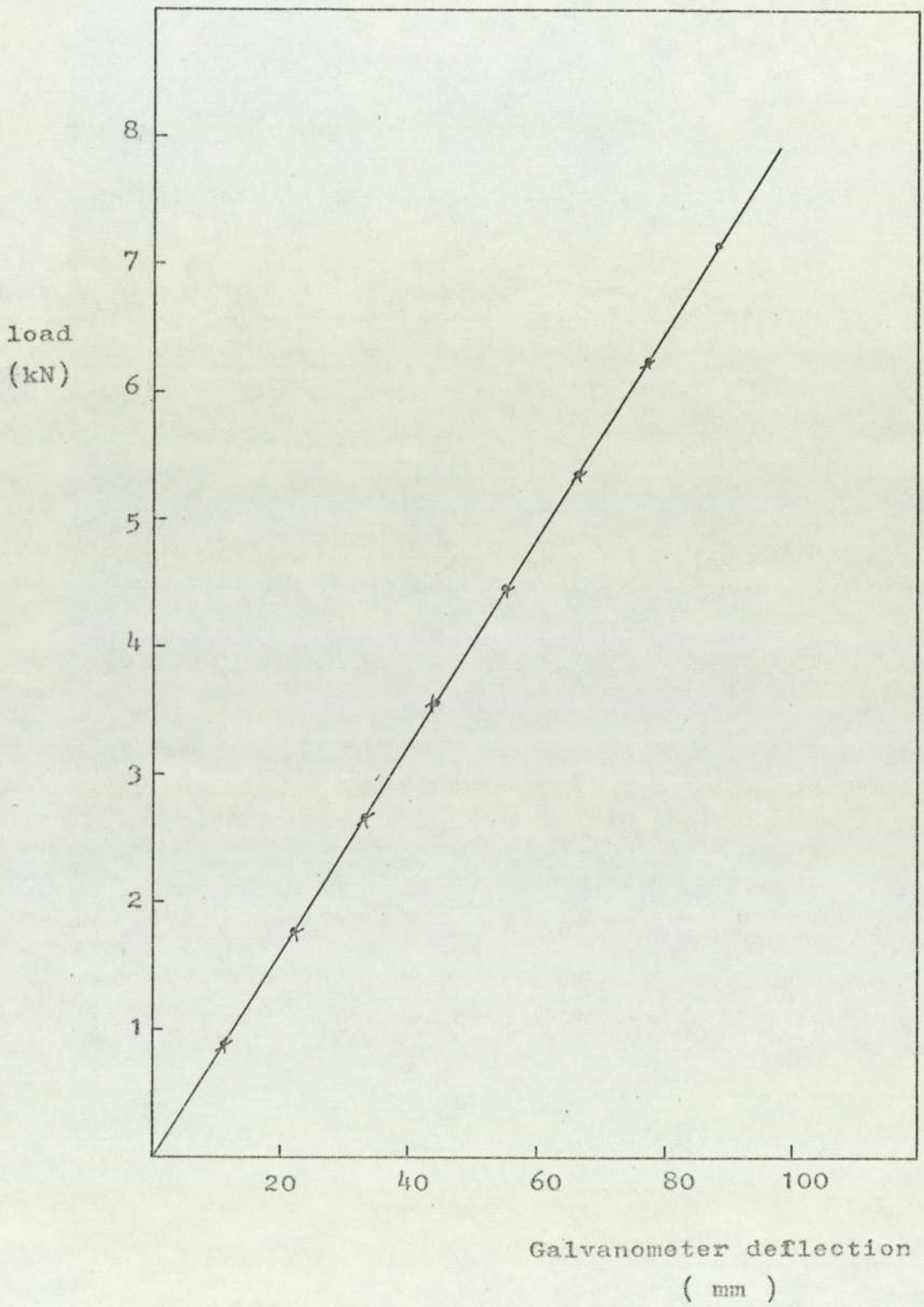

Fig.(18)

Calibration of Back Tension loadcell

IV

EXPERIMENTAL PROCEDURE

The Experimental Procedure

Since rolling in the actual process is carried out under dry conditions, rolling in the simulation process was also carried out under similar conditons. To achieve this, the tubes and rolls were thoroughly cleaned and degreased before each test by the use of trichloroethylene. The surfaces of the tube and rolls were clean and dry consistantly before each test.

Due to the uncertainty about homogeneity of the wall thickness of the tubes and the influence this would have on the rolling loads, and the pressure distribution in particular, the testing procedure was designed to cope with this situation. Attempts were made to eliminate the non-homogeneity of wall thickness(e.g. by drawing the tubes on a mandrel) but these had not proved satisfactory. Therefore each test was repeated and the average of all the measurements was taken.

Thus for each test set up from the first series of tests three test specimens , normaly cut from the same tube, were rolled and the averages of the three sets of measured parameters taken to represent this set up. In the second series of tests however where the specimen length was long enough to permit three sets of recordings to be made there was no need to repeat the tests.

In presenting these results, however, the three sets of results were included since in some cases there were some differences between the three sets representing one test condition making it possible for these individual sets to be considered separately and the difference discussed.

A warm up period of about two hours was allowed before testing started. Prior to each testing session the balance of the loadcells bridges was checked and when necessary rectified. Also the voltage supply for all loadcells was checked by the use of a digital voltmeter before and during each test.

The roll speed was 1.590RPM

To affect the reduction of area per pass, different roll gap settings were used in conjunction with the three wall thicknesses to give different reductions. However it was found that some of these combinations had overlapped and the number of pass reductions obtainable was smaller.

Test Phases:

One feature of the present work was the rolling of oval tubes through an oval groove, an aspect of the tube rolling process which had not been fully investigated before. The oval tubes were produced by rolling round sections through an oval groove. Results of the Oval-to-Oval passes should be useful in any future analysis which might involve such passes. It is a fact that in an actual reducing mill most of the passes are of the oval-to-oval type.

At first the plan was to divide the testing into two phases sinking and stretch reducing. But due to the difficulties encountered in measuring tube velocities for the sinking phase, as mentioned in section (III-3-4), and the need to obtain accurate velocity measurements, the plan was altered. These alterations were the result of preliminary tests. Accordingly testing was divided into the following three phases:

Phase 1: Free sinking

This was the original sinking phase. In this series of tests the tube ends were unguided i.e., free. Each test representing a certain set of conditions was repeated three times for the reasons given earlier in this section.

The specimen length was 450 mm, 15-20% above the minimum necassary to ensure steady state rolling conditions.

The passes rolled were:

i- Round-to-Oval pass (R-O): where the original circular tube was rolled through the oval groove producing an oval tube.

ii- Oval-to-Oval pass (O-O): where the oval tubes produced by the R-O passes were rolled again through the oval groove with the major axes of the two ovals at right angles to each other similar to the actual process.

However, the results of these oval-to-oval passes were not satisfactory in terms of measured loads due to the tendency of the tube to rotate about its axis. Difficulty was encountered in trying to stop the rotation of the tube without guiding it.

Phase II: Guided Sinking

Guiding the two ends of the tube made it possible to measure the tube velocities more accurately. By attaching the two ends of the tube to the carriages of the inlet side and exit side channels the movement of the tube was restricted to an axial movement.

The test pieces were 1.5 m long allowing the pin

loadcells to contact the tube surface three times giving three sets of recordings for assumedly identical conditions.

As the tube was long enough for the steady state conditions to be reached, especially for the second and third sets of results, comparison was made between these results and the results of similar tests from the free sinking stage. This comparison showed that, within acceptable limits, the results of the corresponding tests from phases I and II were identical. This was a further proof that steady state conditions had prevailed in the free sinking trials. It also showed that guiding the ends of the tube did not affect the measured quantities while simplifying measurement of tube velocities.

Tests were carried out, as in the case of free sinking, under dry conditions. A similar procedure to that followed in phase I and described earlier in this section for cleaning and degreasing the tubes and rolls was employed.

Reduction of area per pass was affected in the same way as in phase I.

Further to simplifying the measurement of tube velocities this method produced straight lengths of tubes which were easy to handle and were rolled again in oval-to-oval passes. The problem encountered in the free sinking stage of the rotation of the tube in the oval-to-oval passes did not occur because the tube ends were guided. Hence the results of the O-O passes were more reliable.

Phase III: Stretch Reducing:

This phase is similar to phase II except that front

and back tensions were applied to the tube in varying combinations.

Measurement of cross-sectional area of the tube:-

To determine the percentage reduction of area per pass, it was necessary to measure the cross-sectional area of the tube before and after rolling.

Several methods were considered including the direct measurement of the area by the use of a planimeter with a sheet of transparant perspex on the cross-section to be measured. Other methods included the measurement of the X and Y co-ordinates of points on the outer and inner surfaces and feeding these coordinates into the computer to calculate the area between two curves using a suitable approximation e.g, Simpson's. The method employed by (1) which consisted of weighing a certain length of the tube and calculating its cross-sectional area from knowledge of the density of the material was also considered. This method involved difficult preparations of the specimens and provided information on the cross-sectional area only.

The method adopted consisted of the following procedure:

a- photographing the cross-section of the specimen,

b- projecting the image on a screen where it could be traced and measured.

There were some doubts about this method regarding the distortion caused to the image by the lens and also by the streching of the film material due to the heat produced during the projection period. Tests were carried out on a number of specimens which had been measured

directly by the use of the planimeter and by weighing. Measurements were compared and the photographic method proved to be highly accurate. This was due to the use of high quality equipment with high resolution lenses and also to the procedure followed in positioning the specimen and using sectional paper as a scale indicator. By enlarging the image nearly ten times the actual size, errors of measurement were decreased. Since most of the optical distortion of the lens occurs near the edges and away from the centre of the image, the specimen was positioned in the middle of the view finder ensuring that the axes of the lens and the specimen coincided. A hole was cut in a sheet of sectional paper which was fixed to a piece of thin glass resting horizontally on the specimen cross-section. The scale factor was taken from the squares on the paper and had therefore included any amount of distortion that might have occured.

Linear measurements of the transverse variation of the wall thickness were also made for a number of specimens for comparison with the mean value.

By measuring the area of the outside and inside ovals of the cross-section, a mean value for the outside and inside diameters of the tube was calculated, hence the mean wall thickness. These values were believed to be more representative of the true dimensions of the tube than those made with reference to a particular point on the surface. This is because they take into account the transverse variation of the diameter and wall thickness of the tube since the shape of the cross-

section was not a true circle.

Thus this method of measurement enabled measurement of the cross-sectional area of the specimen and also the tube dimensions at the position corresponding to the root of the groove.

Maximum groove angle of contact:- (θ_c)

If complete filling of the groove takes place, as was the case in the majority of Round-to-Oval passes, then the maximum groove angle of contact (θ_c) is equal to the maximum groove angle (θ_m),

i.e. $\theta_c = \theta_m$

However, for large gap settings and also for all Oval-to-Oval passes complete filling did not occur and θ_c was less than θ_m as can be seen from fig.(19):

The spread of metal in the groove was discussed by Gulyaev et al[5] in a paper published in 1971. The expression they present for calculating the spread index $\Delta b/\Delta h$, where Δb is the absolute draft at the root of the groove, is a complex one. It contains a large number of constants and depends on nearly all of the geometrical parameters of the rolls, groove and tube. However they present the solution for the hot rolling of tubes graphically as a function of the tension (Z) and wall thickness to diameter ratio (which is shown on the fig.20 with the coefficient of friction in the brackets). The three groups of curves are for two-roll grooves (A), three roll grooves (5) and four-roll grooves (B). This graph

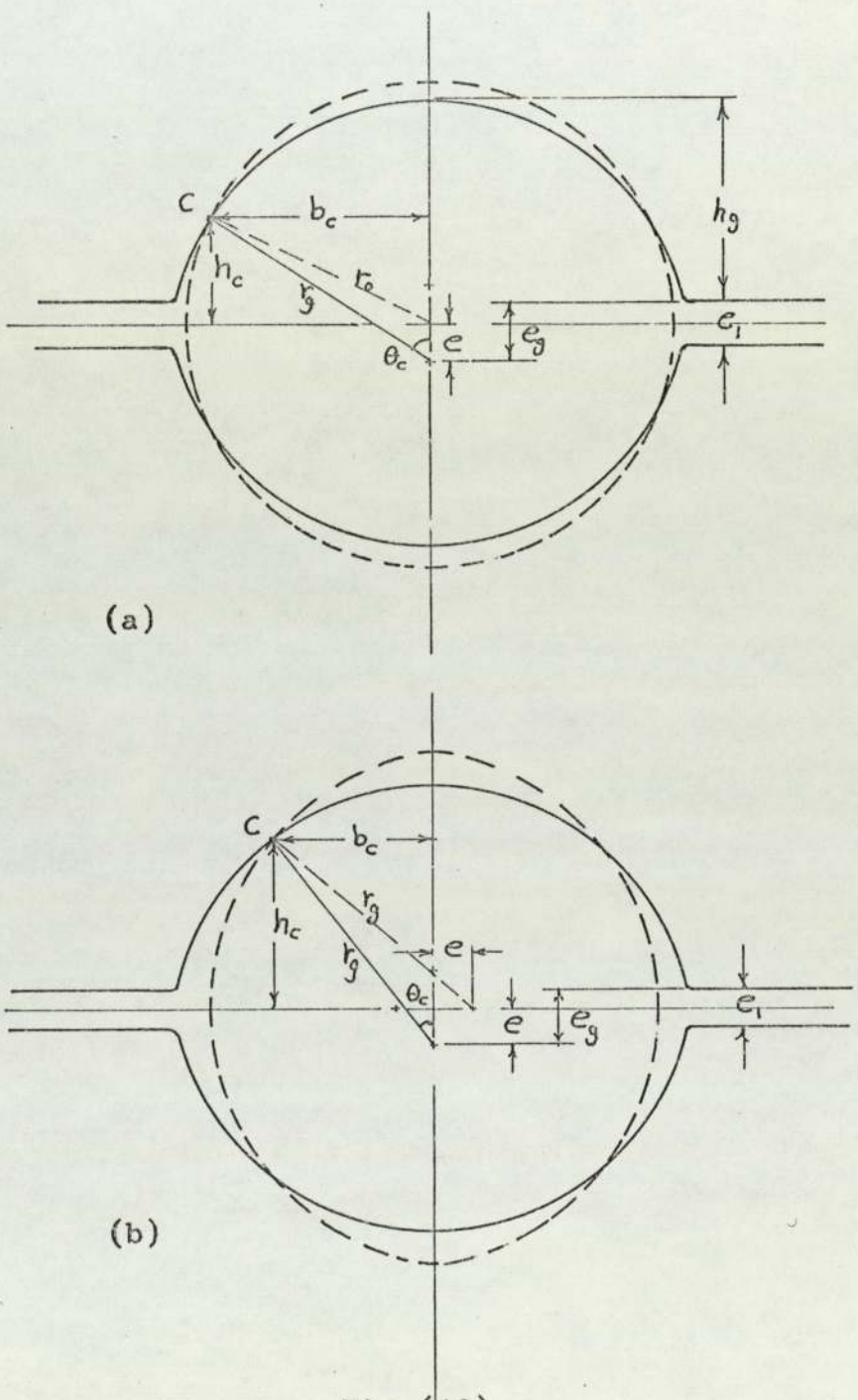

Fig. (19)

Maximum groove angle of contact

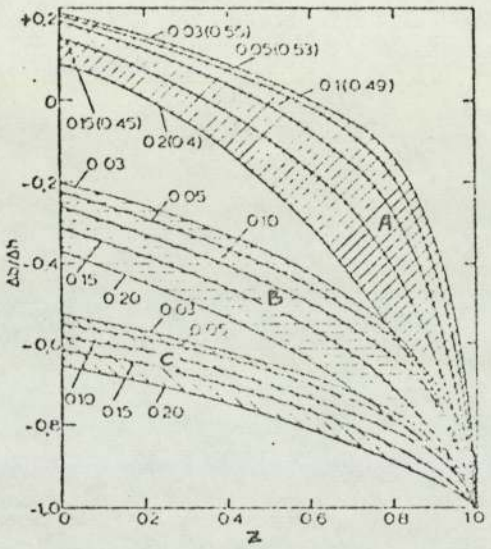

Fig. (20) Variation of minimum value of spread parameter as a function of tension z and thickness/diameter ratio of tubes t/d (numbers on curves; brackets are given coefficients of friction μ) for two-roll (A), three-roll (B), and four-roll (C) passes

is reproduced here as fig.(20). It can be seen from this figure that for Z = 0 (i.e., sinking) and t_o/d_o ratios between 0.03 and 0.1 the value of $\Delta b/\Delta h$ for two roll grooves is approximately 0.2.

It is therefore reasonable to assume that for small reductions, as is the case in the present investigation, metal spread can be neglected. The maximum draft obtained in the tests with respect to the root of the groove δ_r was 6.70 mm as can be seen from table (VII.2) of the test results. Hence 0.2 δ_r will be equal to 1.34 mm, i.e. b_c in fig.(19) would be increased by 0.67 mm. This amount represents about 3% of b_c for the Round-Oval pass, fig. (19-a) and about 6% for the Oval-Oval pass, fig.(19-b). Thus for determining the maximum groove angle of contact θ_c fig.(19) point c has been assumed to represent the extent of the surface of contact around the groove.

For Round-Oval passes with initial tube outside diameter d_o and from geometrical consideration of fig. (19-a) we obtain:

$$\cos \theta_c = \frac{1}{2r_g e} \left(r_g^2 - \frac{d_o^2}{4} - e^2 \right) \ldots\ldots (IV.1)$$

where:-

$$e = e_g - \frac{e_1}{2}$$

e_g is the eccentricity of the groove which is equal to the difference between the groove radius r_g and the groove depth h_g .

For oval tubes produced by rolling round tubes through the same gap setting as is required for the Oval-Oval pass , fig.(19-b) we obtain :-

$$\cos\theta_c = \frac{\sqrt{1 + 4\left(\left(\frac{r_g}{e}\right)^2 - 1\right)} - 1}{2r_g/e} \qquad \ldots\ldots\ldots\ldots (IV.2)$$

The following values of θ_c were calculated for d_o = 44 mm from equations (IV.1) and (IV.2) above for various gap settings:

Gap setting	Round-Oval	Oval-Oval
I	$\theta_c = 78^\circ$	27°
II	75°	25°
III	71°	23°

The above values of θ_c have been used for calculating the area of contact. However since these values are for nominal diameter, other values for different values of d_o will be calculated separately.

Yield Stress of Lead

A similar method to that used by Cole[1] to obtain the true stress-strain curve for the lead was employed here, i.e, by plane strain compression indentation testing. The lead specimens were in the form of strips 50 mm wide by 5 mm thick prepared from flattened parts of unrolled tube. They were fine machined. The indenting tools were 9.0 mm wide.

Following the same procedure used by Cole the true stress-strain curve was obtained. The curve was the same as that obtained by Cole, fig.(21).

It was found possible to express the mean yield stress ($\bar{\sigma}_y$) in terms of the generalised strain for the uniaxial condition relevant to tube sinking as

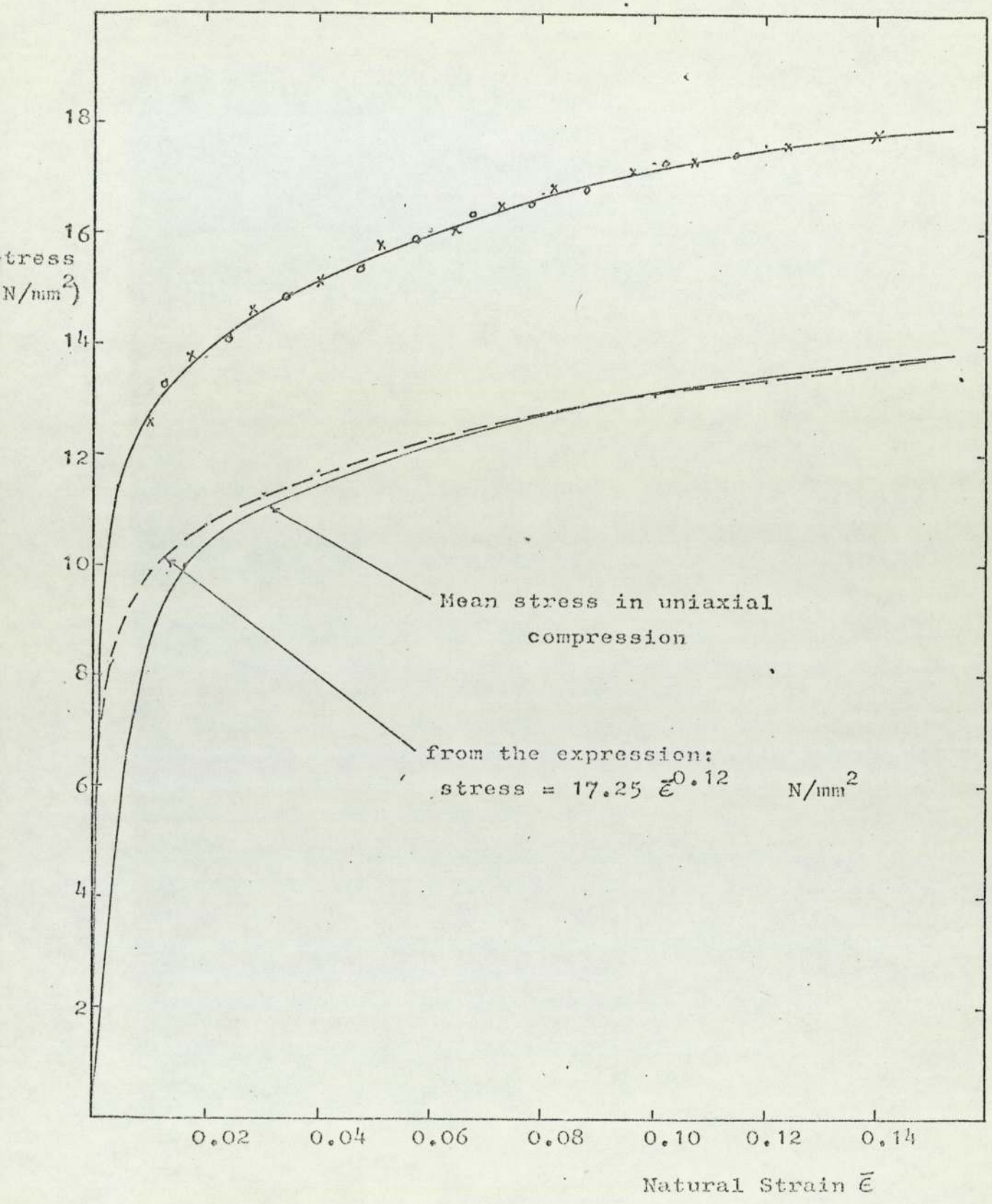

Fig.(21)

True Stress-Strain Curve for Lead in

Plane Compression

follows (shown as the dotted curve in fig.(21))

$$\overline{\sigma_f} = 17.25\ \bar{\epsilon}^{0.12} \quad N/mm^2 \qquad \ldots\ldots\ldots (IV.3)$$

The mean value of the stress was obtained from the true stress-strain curve for different values of $\bar{\epsilon}$. This mean value was thenconverted to the uniaxial condition by multiplying it by $\sqrt{3/2}$ (1) .

The expression for the generalised strain, $\bar{\epsilon}_m$, is, (1):-

$$\bar{\epsilon}_m = \sqrt{\frac{2}{3}}\ \sqrt{\epsilon_l^2 + \epsilon_r^2 + \epsilon_0^2} \qquad \ldots\ldots\ldots (IV.4)$$

where

$$\epsilon_1 = \ln \frac{A_o}{A_1} \quad ,$$

$$\epsilon_r = \ln \frac{t_o}{t_1} \quad ,$$

$$\epsilon_0 = \ln \frac{d_o - t_o}{d_1 - t_1}$$

V

MEASUREMENT OF PRESSURE DISTRIBUTION

Pressure Distribution

(V-1) Introduction:-

In order to obtain an accurate comparison between the deformation stresses developed in a metal-forming process and the corresponding theoretical values, it is necessary to study the distribution of contact stresses at various points on the tool surfaces. This knowledge is also important for the accurate assessment of the nature of deformation during the metal-forming processes and in particular the rolling process. Information gained from the pressure distribution curves is valuable in studying the significance of other parameters and their influence on the process, e.g.arc of contact, neutral zone and the free zone.

The usefulness and importance of the measurement of contact stresses were realised in flat rolling long ago and work on the problem of measuring these stresses started as early as 1929 when Huber [22] attempted to measure the pressure exerted by the deforming material on the roll by measuring the total force separating the two rolls and the area of contact. He was only able to estimate the mean pressure.

The idea of using a pressure-transmitting pin protruding through the roll surface and acting against a transducer was employed first by Siebel in 1933 [23]. In spite of the inherent problems of this method, developments have proved it to be most useful for recording the pressure distribution in metal forming processes such as rolling and it can be relied upon to yield

meaningful data. These problems which are applicable to any technique employing a pressure-transmitting pin may be summarised as:-

a) the back extrusion of work piece material into the annular clearance between the pin and the bearing surface which guides the free axial and/or radial movement of the pin. The presence of such extruded material inhibits the free movement of the pin hence affecting its performance.

b) the effect that the presence of the pin has on the state of stress being recorded. This effect can be minimized by reducing the diameter of the pin.

The special requirements of metal deformation problems have resulted in a variety of pin loadcell designs and many designs, together with explanations on the means employed to overcome the problems, have been reported.

A comprehensive review of most of the published work on the problem of measurement of contact stresses can be found in reference [1].

However some works which were of particular importance to the present investigation since they involved aspects of the problem which were being studied in this work will be reviewed.

(V-2) Previous Work:-

Siebel and Lueg [23] were among the first workers in this field who used the pin loadcell technique for measuring the pressure distribution in the case of flat rolling. The design consisted of a pressure-transmitting pin which fitted accurately into a cylindrical hole, one

end of it was flush with the roll face while its other end pressed upon a piezoelectric crystal placed inside the roll. The use of a 2 x 2 mm square section pin presented them with the main difficulty since the correction needed was large because the arc of contact was of the order of 8 or 9 mm.

This type of transducer was given some consideration during the present work because it is relatively sensitive and small in size and could be accommodated inside the roll more easily especially in the case of multi-pin designs. Preliminary tests however have shown it to be more sensitive to temperature variations than other types, e.g. straingauges . The load-deflection curves for the piezo-electric transducer exhibited an unacceptable degree of nonlinearity in the range of loads expected in the rolling tests of the present work.

The next major work was that of Orowan [24] in 1950 and 1952 where a photoelastic dynamometer was used. Orowan retained the idea of a pressure-transmitting pin but with modifications aimed at avoiding the difficulties encountered by Siebel and Lueg. The sensing device was changed to eliminate the slip-rings, increase the sensitivity , reduce the inertia and avoid the electronic problems. To reduce the effect of the presence of the pin on the state of stress being measured, a 0.7 mm diameter tungsten pin was used which was equivalent, so far as the recorded curve was concerned, to a square pin of about 0.5 mm width as compared with the 2 mm wide pin used by Siebel and Lueg. An interesting part of the work of Smith [25] et al,

in 1952 was devoted to the study of the effect of the protrusion and recession of the recording pin on the shape, magnitude, and general characteristics of the observed pressure distribution curves. It was noticed during their experiments that the pin always protruded slightly above the roll surface when in contact with the stock, and penetrated it. The depth of penetration was determined by observing the surface of the rolled strip under a microscope focusing first on the strip surface and then on the bottom of the pin impression. Fully annealed copper strips, 2 mm thick x 40 mm wide, were used and the measurements of pressure distribution were made for different pin protrusions with a constant reduction and with the condition of each experiment kept constant. The results were given for the recorded pressure distribution when the pin projected by amounts from 0.150 mm to -0.172 mm, fig.(22). It was found that for pin protrusions of up to 25 μm the error in the maximum stress recorded was less than 3% , while the increase in the area under the curve was less than 6%. It was also found that the pin protrusion had some effect on the shape of the pressure distribution curves but again for protrusions of up to 25 μm the shape of the curves were not appreciably different from those which would be obtained with a perfectly flush pin. They concluded, therefore, that small amounts of pin protrusions did not invalidate their results.

The work of Parish [26] which was published in 1955 is of a similar nature to that of Smith [25], et al.

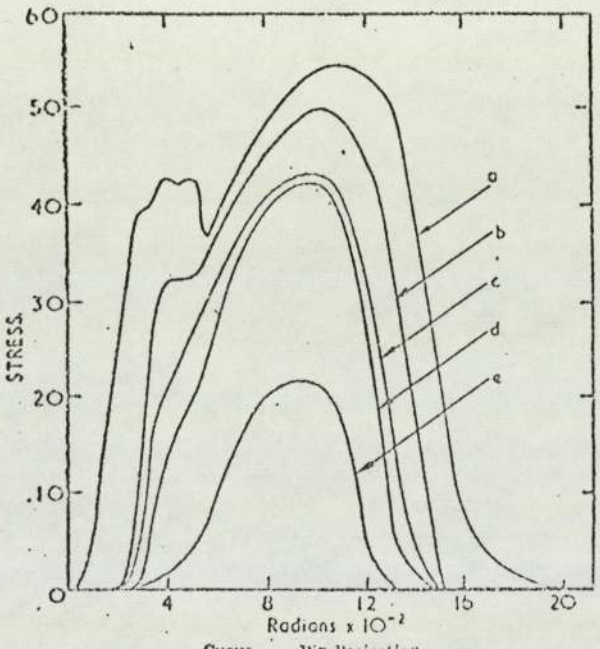

Curve	Pin Projection
a	0·150 mm.
b	0·052 mm.
c	0·026 mm.
d	0·000 mm.
e	— 0·172 mm.

Fig. 22 -Recorded pressure distribution curves for varying pin projections

A pressure transmitting pin of a rectangular section 0.79 mm (1/32 in.) in the direction of rolling by 12.7 mm ($\frac{1}{2}$ in.) wide in the direction of the roll axis was used together with a photo-electric transducer . Parish studied the effect of pin protrusion and recession under load on the pressure distribution curves. He showed that the relationships between the peak pressures and the pin heights were linear, and that the effect of pin protrusion on both the base length of the curve and its general shape was negligible for small pin projections. He then worked out corrections for pin protrusion and pin depression under load due to difference of compressibility between the roll and the pin, the latter being less stiff than the former. A comprehensive study was carried out by Palme and MacGregor [27] at the Massachusetts Institute of Technology in an attempt to measure the coefficient of friction in the contact zone during the rolling of Aluminium, Copper and Steel bars.

The technique they employed for this purpose was that of a pressure-transmitting pin with a strain gauge type transducer.

The measuring device was inserted into a diametral hole which was made in the upper roll of a two high rolling mill. It consisted of a square shank cantilever loadcell with small round end of 2.35 mm (0.0925 in.) dia. which projected centrally through a 2.54 mm (0.10 in.) dia. hole in the roll surface and was flush with it.

Three pairs of SR-4 wire strain gauges were mounted on the sides of the element so that one pair measured the

radial displacement while the other two measured the two lateral deflections of the pin in two perpendicular directions for measuring shear stresses. To allow for the pin tip to deflect laterally, a minimum radial clearance of about 0.095 mm (0.00375 in.) had to be used. This in fact presented them with a problem and was, indeed, the cause of the failure of their attempts to measure the frictional stresses. As soon as the leading edge of the pin tip entered the arc of contact, rolled material was extruded into the gap between the pin and the hole. This gave false readings for the shear stresses at the entry side of the arc of contact and prevented the pin from deflecting laterally in opposite direction as it passed the neutral point. The basic design was modified in an attempt to overcome this problem. Steel washers were used to overlap the annular clearance between the pin and the hole without obstructing the functioning of the measuring device. The idea did not achieve its objectives and the shear stress measurements had to be abandoned after further unsuccessful attempts. The same problem existed with the normal pressure measurements but on a smaller scale.

The results of the work of Smith, et al,[25] on the effect of pin protrusions on the pressure distribution curves were used to show that their results were not invalidated by the amounts of pin protrusions that occurred, since these did not exceed 76 μm(0.003 in.) (about 3% of the pin dia.).

In the work of Muzalevskii and Grishkov [28] in 1959 the same idea for measuring the shear stresses was used, i.e. by measuring the lateral deflections of the pin end, although a different element design was employed.

A minimum clearance of 41 μm (0.0016 in.) between the pin and the hole was believed to be adequate to allow a detectable lateral deflection. To overcome the problem of back extrusion, compressed air was fed into the interior cavity of the insert to act as a cleaning system by blowing the rolled material fragments out of the annular clearance. No results were presented in the paper.

Of direct relevance to the present investigation is Cole's [1] approach to the measurement of radial pressure in tube rolling since this is one aspect of the present work. He measured the distribution of pressure not only along the arc of contact but also around the periphery of the tube. This meant that one measuring element was not enough. Four elements were placed inside the roll around the groove, fig.(23), one at the root of the groove and three at 30°, 60° and 80° from the centre of the groove. Because of size limitations, Araldite, having a high poisson's ratio, had to be used for making the bodies of the loadcells, fig.(24). The pins were made from Silver Steel and were a nominal 1.27 mm (0.050 in.) dia. They had enlarged ends and were bonded to the loadcell bodies. Four small strain gauges were bonded to the body of each loadcell. Phosphor bronze bushes were press fitted into the cavities and the pins protruded through them to the surface of the roll groove. The problem of back extrusion was overcome by simply

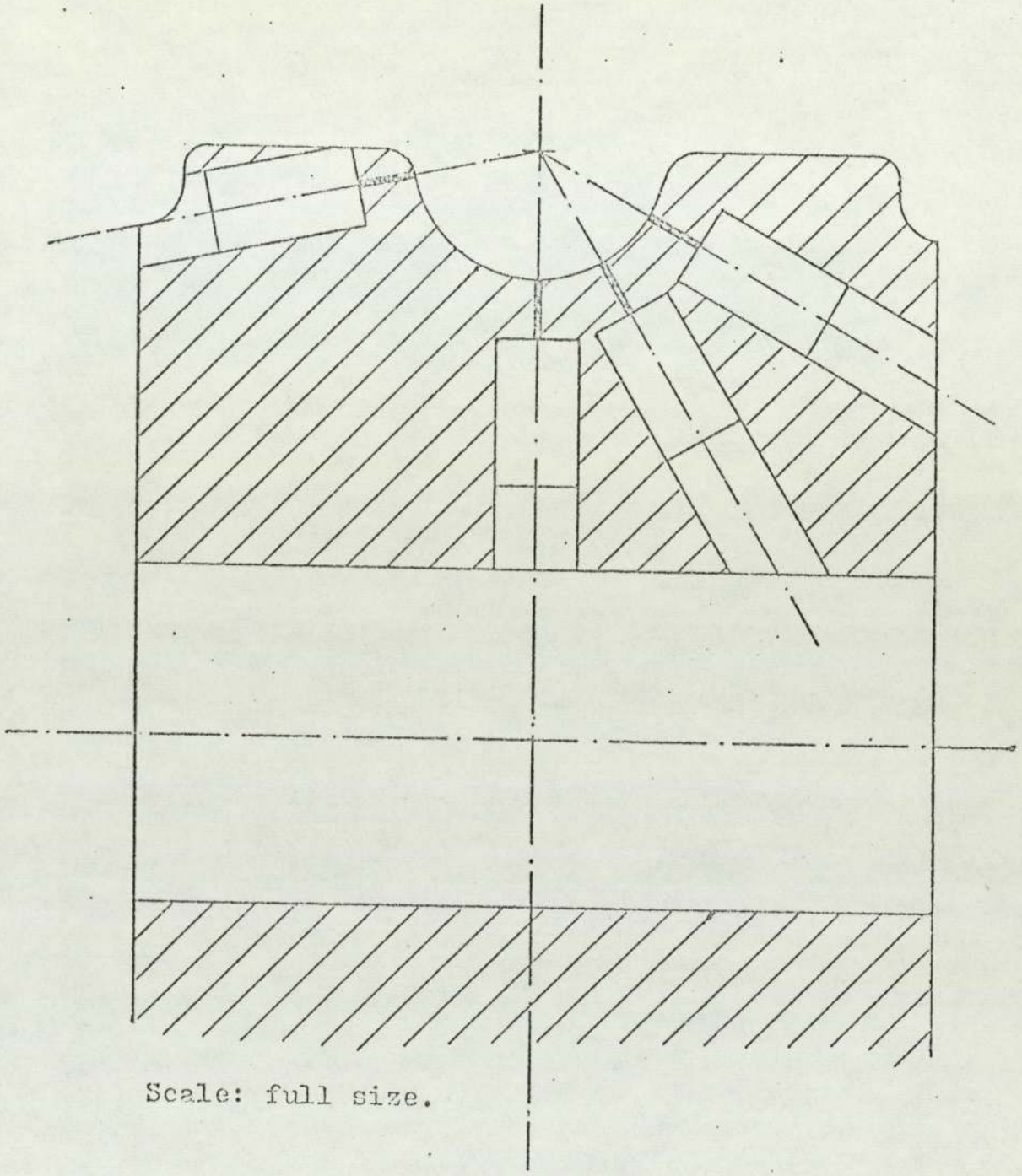

Fig. (23)

Disposition of pin loadcells in the roll groove in Cole's work

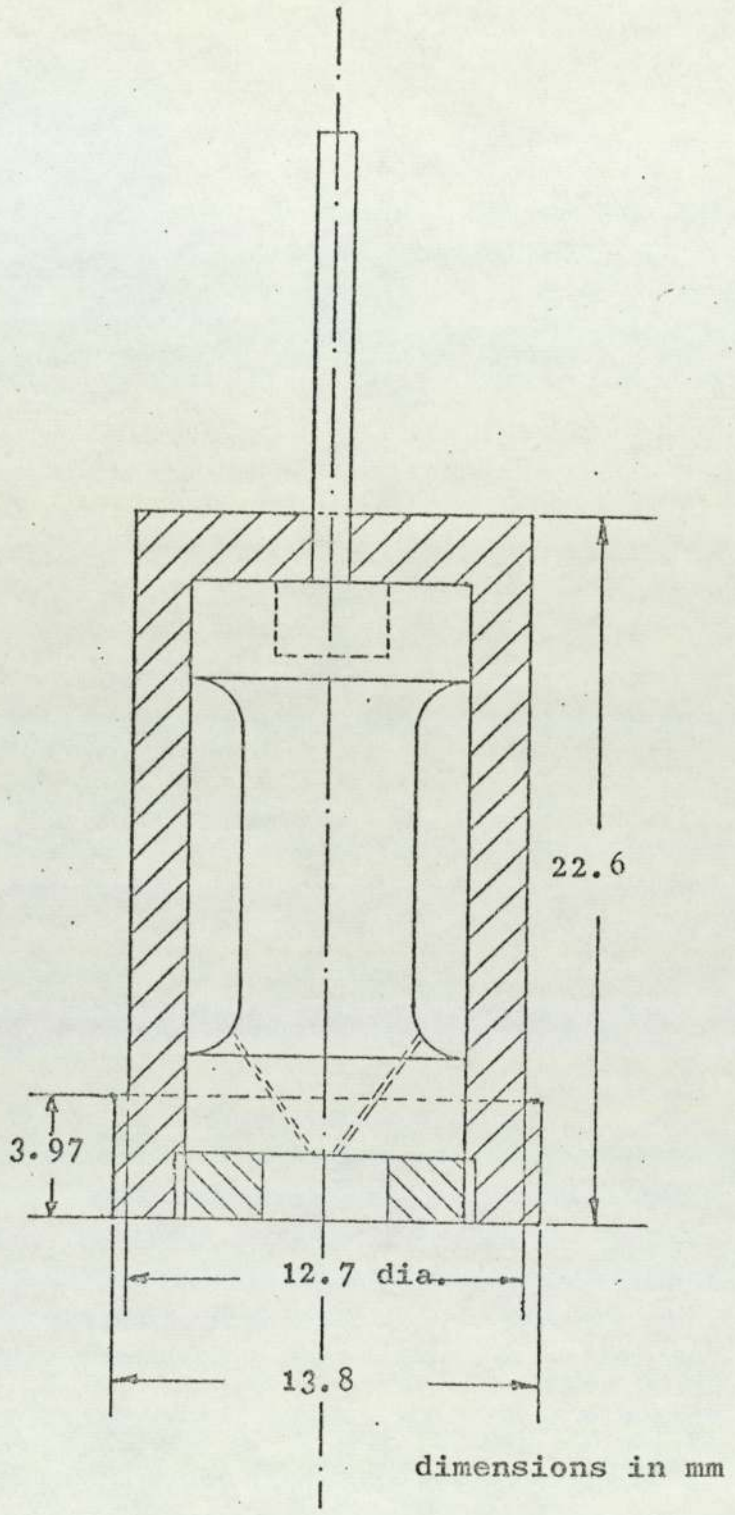

Fig. (24)

Pin Loadcell as used

by Cole.

covering the pin and its bush with a disc of PVC self-adhesive strip. The effect of the presence of such discs and their thicknesses was found to be negligible after successive calibrations with and without the presence of a disc showed that there was no detectable effect. It was therefore concluded that the technique could be used with certainty. However, the second difficulty, that of response hysteresis under decreasing load, was not overcome. This meant that only the load-increasing part of the curves could be used. It was stated that because of the random nature of the results, it was difficult to assess the way in which the radial pressure was distributed round the groove. Because of the simplicity of Cole's method of overcoming one of the main inherent problems of the pin loadcell technique, it has been investigated further and is reported in chapter (VIII).

(V-3) Design:

The idea of a pressure-transmitting pin was employed after extensive study of the possible methods.

The design used in the present work was developed to investigate some of the phenomena occurring in the tube rolling process for which the mechanics of deformation have been particularly obscure. The factors which have led to the design finally adopted were:

a) the contact stresses were low because a soft material was rolled. This necessitated the use of highly sensitive transducers.

b) the need to employ more than one loadcell, due to the variation of the contact stresses round the

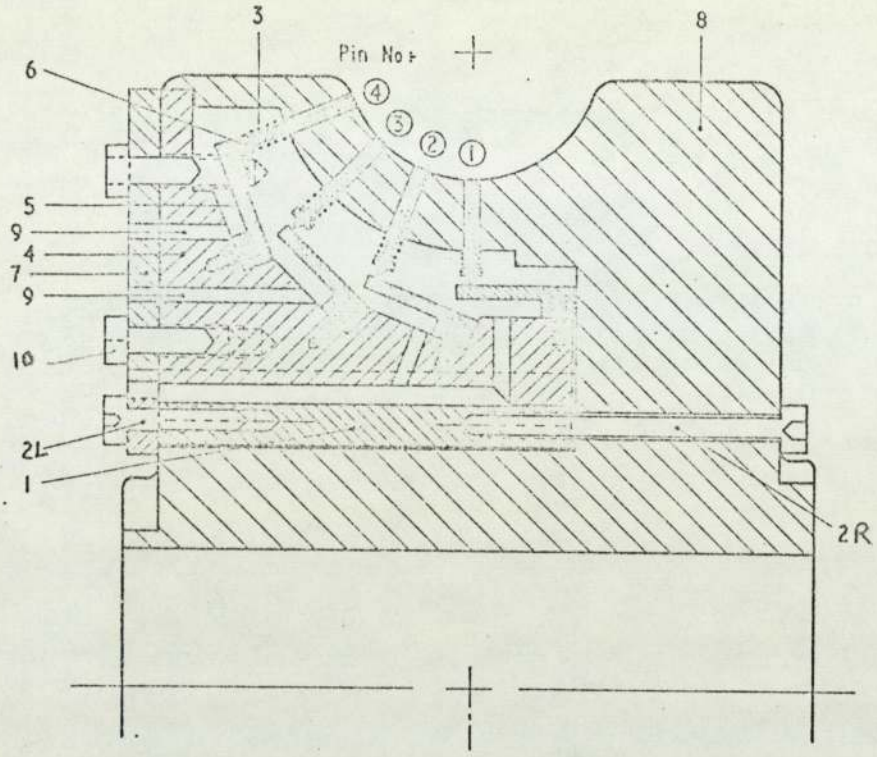

a) Assembly

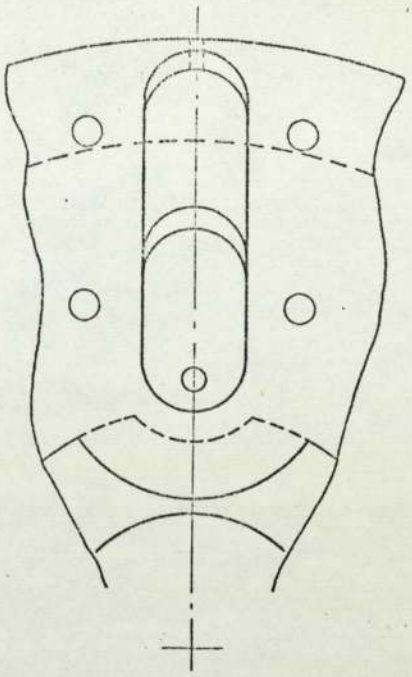

b) Slot in the Roll

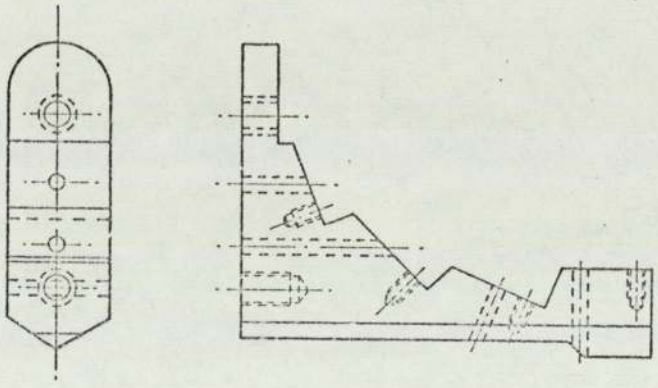

c) Main Block

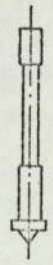

e) Pressure Transmitting Pin

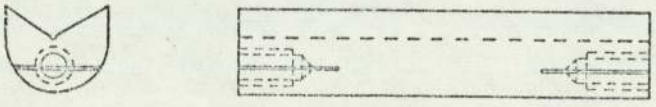

d) Supporting Block

FIG(25)

PIN LOAD CELLS ASSEMBLY

Photo. (5)

Pin Loadcell Assembly Withdrawn from the Slot in the Roll.

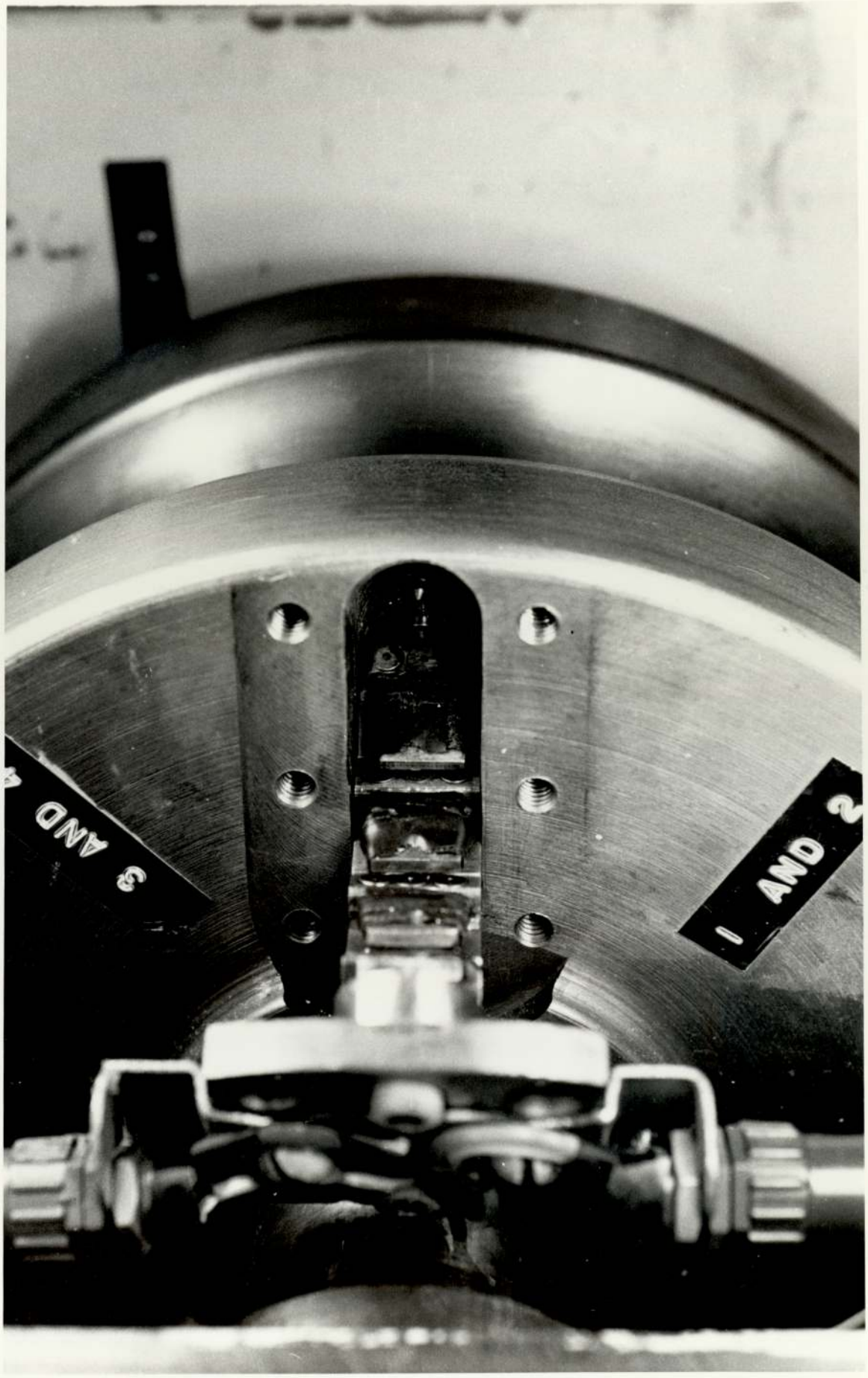
3 AND
1 AND 2

groove. In flat rolling one pin loadcell may suffice for the measurement of the radial pressure but in tube rolling the deformation and the forces are known to vary round the groove and therefore it was important to use more than one loadcell.

c) the necessity of removing the loadcells from the roll in order to investigate the presence of extruded metal on the surfaces of the pins without disturbing the calibration.

This was believed to be an important factor in determining the reliability of the results and was therefore investigated in the present work.

These factors, together with the need for simplicity of design, have resulted in the choice of the assembly shown in photograph(5) and outlined in fig.(25) .

The technique employed utilised four pressure-transmitting pins located radially in the roll at planes making 0^{o}, 22.5^{o}, 45^{o} and 67.5^{o} with the root of the groove, see fig.(25) .

Following the study of several designs of pin loadcells and much preliminary experimental work, the forces exerted on the pin by the tube were transmitted to a cantilever type transducer, fig. (25) . Calculations have shown that a cantilever of dimensions $(2.5 \times 12 \times 15)$ mm would give the required amount of deflection under the expected load without being too flexible in relation to the roll. This has meant that a surface area of (12×15) mm on each face of the cantilever was available for mounting the strain gauges. With gauges of 1 mm active length it

was possible to mount four gauges on each face giving, when connected in a bridge circuit, high bridge outputs from small cantilever deflections. This was particularly important in the present work since the pressures on the pins were low. Tests on a model loadcell have shown that the galvanometer deflections under the expected range of loads were sufficient for accurate measurements to be made from the curves.

In previous investigations [1], [51] on tube rolling a separate assembly for each loadcell was used. This while facilitating the separate adjustment and setting of each individual loadcell , makes it difficult to remove the loadcells and inspect them for back-extruded metal without having to remove the roll. Because of the difficulties encountered by Palme and MacGregor[27] due to the presence of back-extruded metal in the annular clearance between the pin and the orifice and the doubt this has cast over the validity of their results, it was thought important to facilitate the easy removal of the assembly for checking. Therefore the transducer assembly for the four loadcells was made as one unit. The block(4) fig.(25) was shaped so that when the cantilevers(5) were fixed to it as shown, the angles they made with the vertical were 0^{o}, 22.5^{o}, 45^{o} and 67.5^{o} which corresponded to the angles made by the four pins (6). The main difficulty expected from this type of system was that adjustment of the heights of the pins could only be made for the whole system or for a group of pins at a time and not for a single pin. To overcome this difficulty adjustment of the heights of the pins with respect to the

surface of the roll was made by the action of the two tapered bolts (2) and the split ends of the supporting block(1). By turning either or both of these bolts, together with the adjustment of the tightness of the fixing bolts (10) it was found possible to arrive at a combination whereby one pin could be adjusted in height without disturbing the setting of the other pins significantly. This was one of the reasons that tests were carried out to investigate the effect of pin protrusion or recession with respect to the roll surface on the recorded pressures. These tests showed that pin protrusions of up to 25 μm did not affect the results significantly in conformation with the findings of Smith [25] et al and Parish [26].

The initial setting was made by grinding the pins to be flush with the surface of the roll and then they were adjusted by turning bolts (2) fig. (25) clockwise so that the pins protruded above the surface of the roll by amounts not exceeding the 25 μm limit. There was no difficulty in readjusting the pin heights after removing the assembly for inspection. After refitting the assembly the heights of the pins were checked and/or adjusted to within the limits mentioned above.

In order to accommodate temporarily any back-extruded fragments of metal, the pin was designed with a relief as shown in fig. (25) providing an enlarged clearance between the pin and the orifice where the burr could be accommodated without disturbing the performance of the pin loadcell.

The main block (4) fitted into a slot made in the side of the top roll for that purpose, fig.(25) and photograph (5). The radial cylindrical holes for the pins were drilled and bored. After machining, the pins were heat treated and ground and were fitted into the corresponding orifices individually to give free axial movement with the minimum of clearance. The pins were ground flush with the surface of the roll after the whole assembly had been fitted in position and the fixing plate fig.(25) bolted to the side of the roll.

The pins were not fixed to the cantilevers for two reasons:-

a) with a fixed pin, as the cantilever deflects under load the tip of the pin will tend to move tangentially and rest against the wall of the orifice. This may result in additional stresses on the cantilever and thus affects the recordings. It may also increase the friction between the pin and the orifice hence affecting its performance adversely.

b) a floating pin ensures that only the radial component of the contact stresses is transferred to the cantilever and recorded.

Small springs (3) were used to keep the pins in contact with the cantilevers. Since the pins were not fixed to the cantilevers, relative movement between the pins and the cantilevers was possible, but as this was of a very small order, because the measured pressures were low, it was believed that neither the performance of the pins nor the cantilevers was affected. Calibration of the

pin loadcells in situ has shown that the relative movement had no effect on the performance of the loadcells.

Leads from the strain gauge bridges on the cantilevers were brought out through holes (9) drilled in the main block (4).

The material of the pins and cantilevers was steel type En 24 as used for the rolls.

Removal of the whole assembly was carried out by unscrewing bolt (2R) and loosening bolt (2L) to allow the withdrawal of the supporting block. The bolts fixing the plate (7) to the roll were undone and before withdrawing the assembly, the main block(4) was lowered first as far down as it would go and then withdrawn to avoid damaging the strain gauges when the pins retracted under the action of the springs. The pins were withdrawn individually from inside the slot.

When grinding the pins to be flush with the surface of the roll, compressed air was used to prevent the metal burr, resulting from the grinding operations, from entering the clearance between the pin and the orifice. Nevertheless, when the assembly was removed for the first time for checking , the rim on the pin tip, also resulting from the grinding operations, restricted the movement of the pins in the holes. This point has not been discussed before in any publication on the subject. However, it could not be established whether the presence of the metal burr and the rim on the pin tip as a result of the grinding operations had any significant effect on the pin loadcell performance under load since no recordings

were made at this stage. It is believed that calibration of the loadcells in situ after the grinding operations should show this effect, at least partly, as non-linearity of the caibration curves, especially under decreasing load, and probably also as zero drift. In most cases however the grinding operations were carried out after calibrations took place thus leaving this effect unchecked.

(V-4) Pin loadcell Calibration :-

Before describing the method of calibration used in this work, a review of some of the methods used by other investigators which relate directly to the present investigation will be made. The method used by Orowan, et al, [24] in 1950 for the calibration of the photoelastic dynamometer, and in 1952 by Smith, et al [25] involved the application of force directly on to the pin through the action of a weight on a lever arm as shown in fig. (26) A tungsten pin was attached to the lever arm and was centred accurately on the pin under calibration. The pin in the roll was protruding approximately 1 mm from the roll surface and, when the calibration was completed, the pin was ground until its end was flush with the surface of the roll. This method, and all others in which a pin is used to transmit the force from a lever arm or dead weights to the measuring pin, will be called the pin-to-pin method. A review of most of the published work on contact stress measurement [1] showed that a pin-to-pin method of calibration similar to that adopted by Orowan [24] was employed by most investigators. In most cases the pin loadcells were calibrated in situ and were ground flush

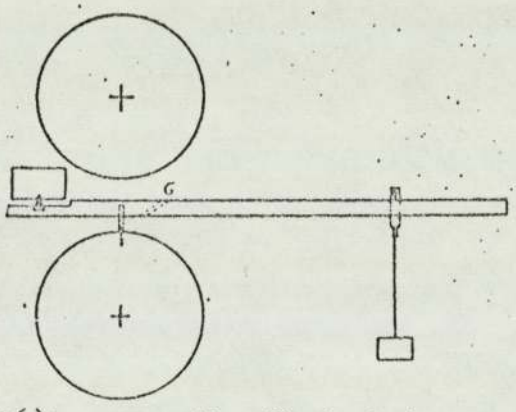

(24), (25)

Fig. (26) Apparatus used for calibrating the dynamometer

with the surface after calibration. But in a few cases they were calibrated out of position, then inserted in their cavities and finally ground flush with the surface.

In a brief paper by Osadchii and Gleiberg in 1959[29] the measuing devices(diaphragm and direct-action carbon pick-ups) were apparently calibrated on a 4.9 kN (500 kg) press before and after operation and a calibrational accuracy of 5 per cent was reported. This is significant since calibration was carried out before and after testing thus reducing the element of doubt on the reliability of the results. It was not clear, however, whether the measuring devices were calibrated in or out of position. More attention was paid to the calibration problem in the work of Frisch[30] in 1955 on the measurement of cylinder wall pressure during the extrusion of commercially pure lead, where the calibration of the pressure gauges was carried out on three different steps, i.e. dead-weight calibration, calibration using a rubber billet under no-flow conditions,and calibration using lead billet under no-flow conditions. In the first method, fig.(27),force was directly applied to the measuring pin by the use of dead weights, i.e., a pin-to-pin technique. This gave a linear calibration curve. In the second method, a rubber billet was placed in the extrusion container while a solid plate was used to close the die opening and for the application of compression. This method too gave linear response and calibration curves which were the same as those obtained from the pin-to-pin method. An interesting third method

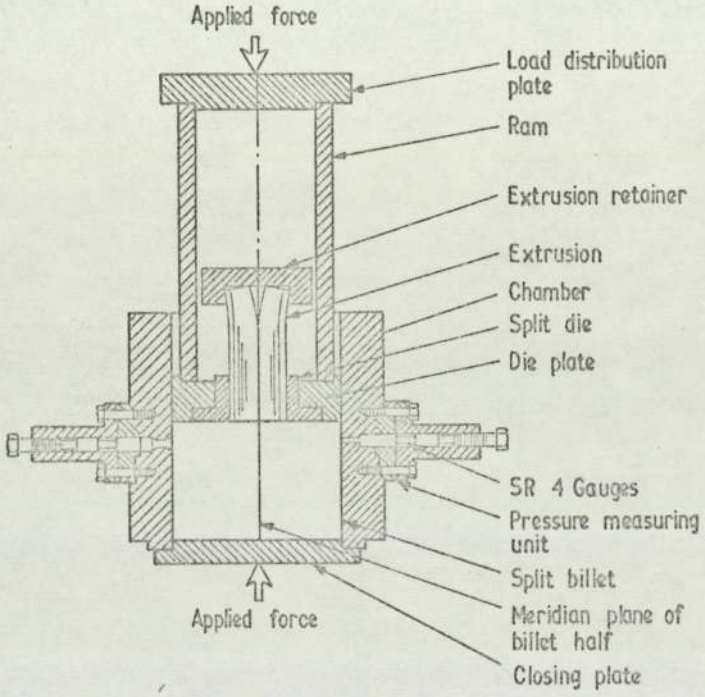

Fig. (27)

SECTIONAL VIEW OF INDIRECT EXTRUSION APPARATUS AND SR-4 PRESSURE

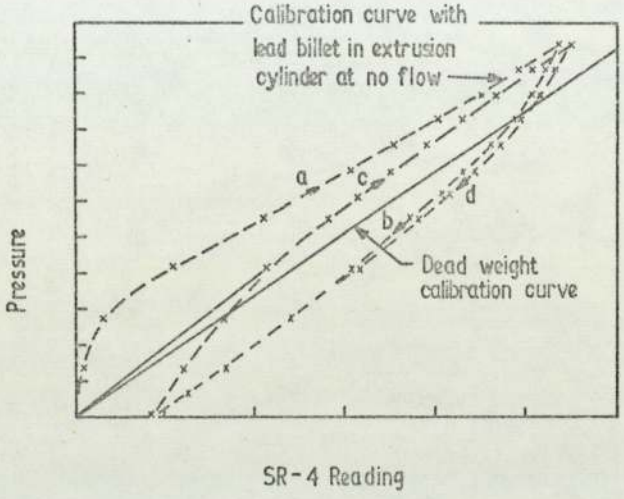

a) MEAN-PRESSURE CALIBRATION CURVE

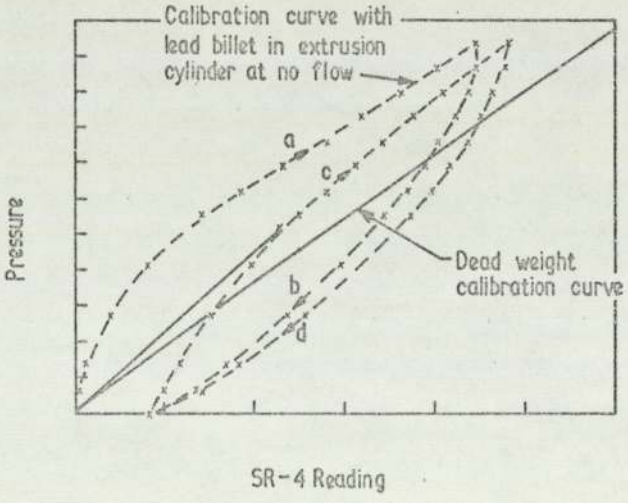

b) MEAN-PRESSURE CALIBRATION CURVE

Fig. (28)

of calibration was employed to ensure the fidelity of the measuring elements. This was the calibration under simulation of the process being investigated. A lead billet was subjected to compressive loads in the same way as the rubber billet, i.e, under no-flow conditions. It was found, as can be seen from curve (a) fig. (28) that the gauge did not respond immediately but that a considerable load had to be applied before the curve became parallel to the dead weight calibration curve. Furthermore, when decreasing the load the curve (b) neither coincided with curve (a) nor did it return to the intial zero reading. Continued loading and unloading produced pressures along curves (c) and (d) respectively. Frisch's explanation for this was that the pressure gauges would not respond until the metal in the cylinder reached a critical stress. It was assumed that a plug of lead was extruded in to the pin hole, as the billet expanded under load, and hence prevented the measuring pin from returning to its initial position upon unloading. The reason that the curves obtained from subsequent loading and unloading were not the same as those representing the initial loading and unloading condition was said to be the increase in the lead plug diameter as well as its length as the lead billet expanded under the effct of the compressive loads.

Reference to the calibration curves of Frisch and to his explanation for the difference in shape between the calibration curves under simulation of the process and those obtained by the dead-weight method shows that the

effect of pin recession, either initially or under load, contributed to the resulting distortion of the calibration curves.

Noritsyn, Glovin and Bazyk (1964) [31] in their investigation of the forging process envisaged that the worked material flows over and in to the indenting pin orifice as illustrated in fig.(29) and as discussed by Cole [1] . The method used by Cole [1] during his investigation of tube rolling was a pin-to-pin method. A proving ring was used fig.(30) with a dial gauge attached to it across the diameter with facilities for setting the device to the required angle to give an axial force on the pin loadcell. The device was pre-calibrated by dead-weights.

In the present investigation a model pin loadcell was used to investigate the response of the loadcell under different conditions. The pin loadcell was assembled as illustrated in fig.(31). The pin-guiding block was made from the same steel used for making the rolls and had its top face machined to a surface finish similar to that of the roll sufface. The pin hole was also identical in size and internal surface finish to the pin holes in the roll. Dead-weights were applied on the disc. A reference response curve was produced by loading the pin directly, i.e. using a pin-to-pin method. This is curve (a) fig.(32) to (34).

Tests were then carried out to check the response of the loadcell under conditions similar to those in tube rolling. In an attempt to reprøoduce these conditions a lead disc 1.5 mm thick by 9 mm in diameter was positioned

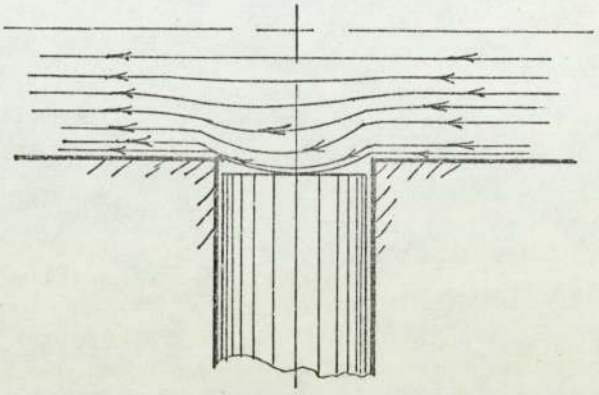

Fig. (29)

Flow of metal into orifice

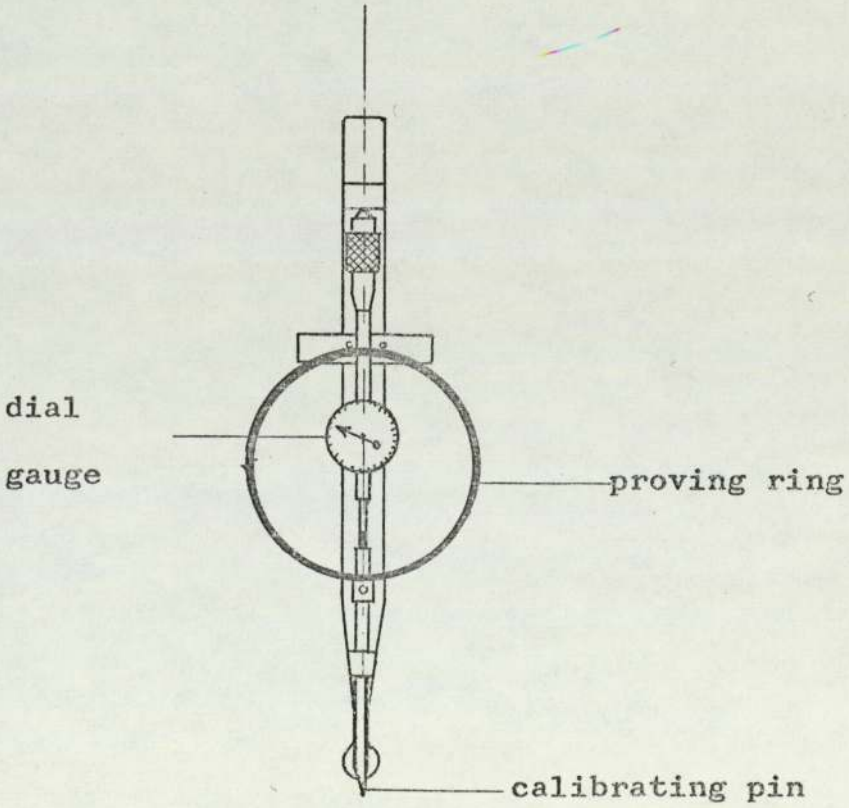

Fig. (30)

Proving Ring

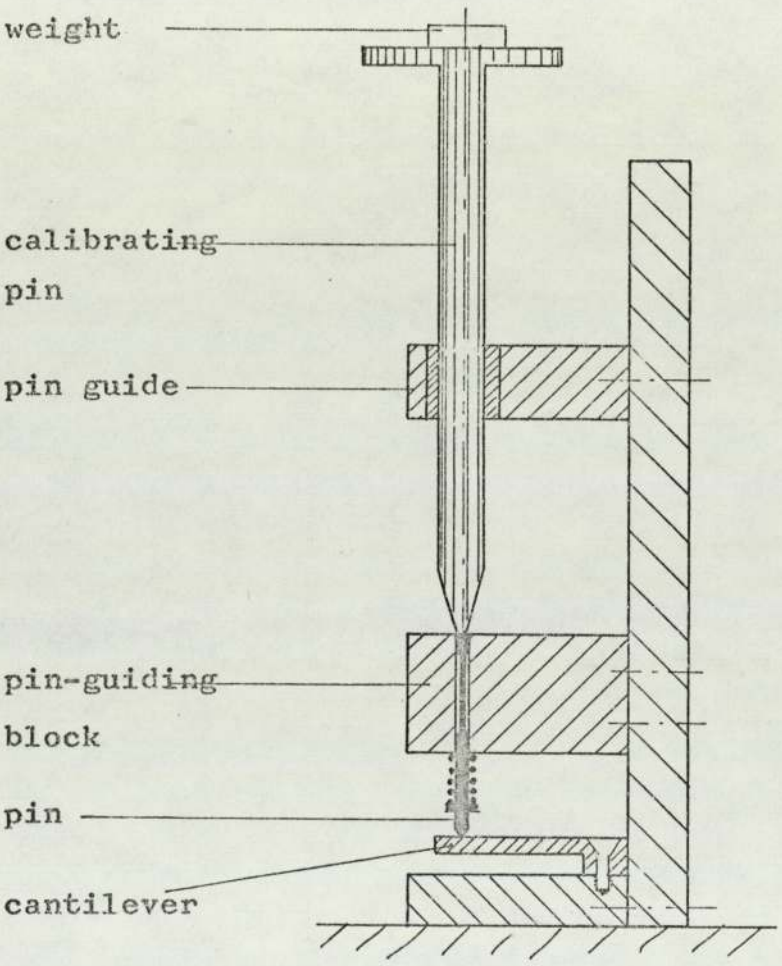
weight
calibrating
pin
pin guide
pin-guiding
block
pin
cantilever

Fig. (31)

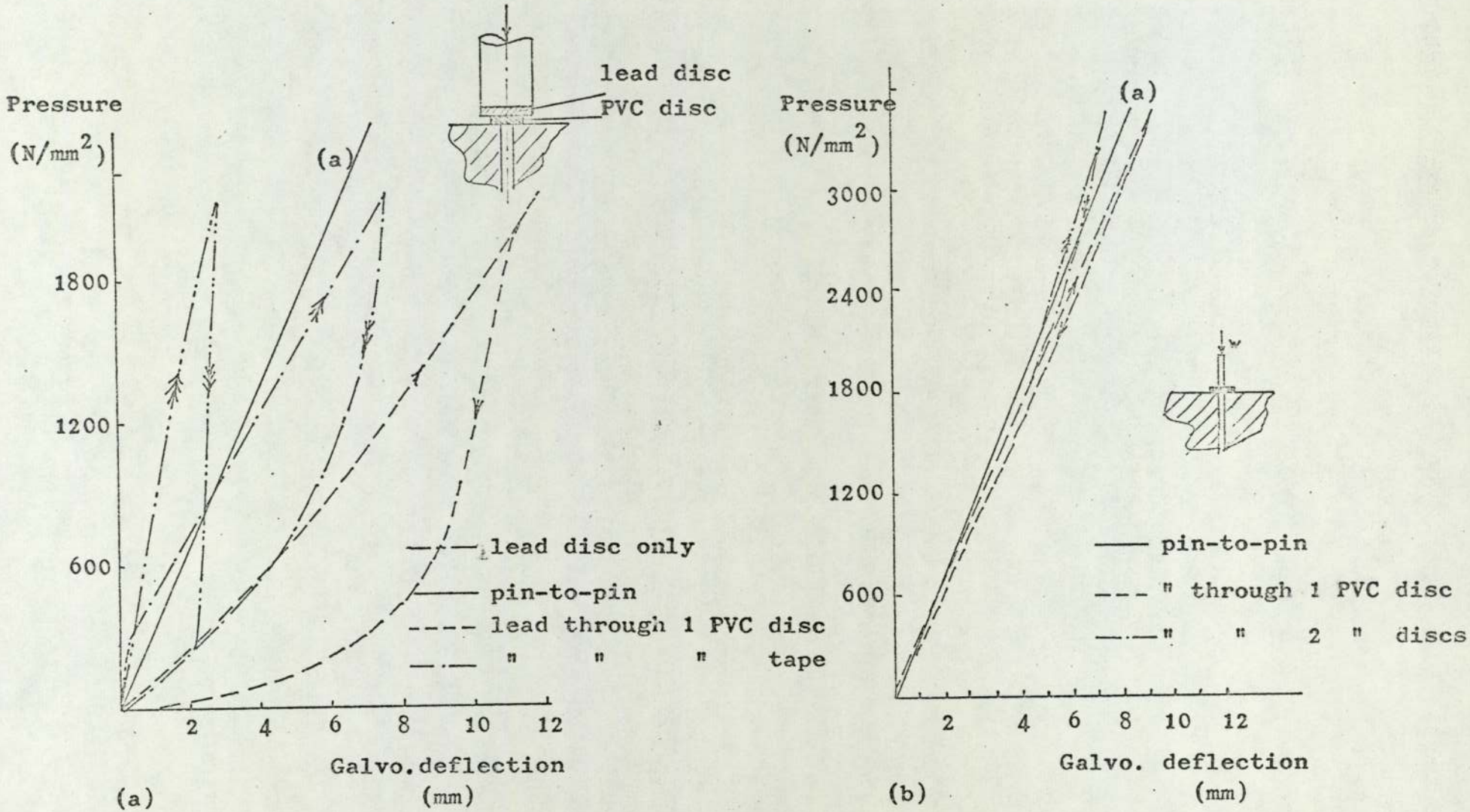
Pressure
(N/mm²)
1800
1200
600
(a)
lead disc
PVC disc
lead disc only
pin-to-pin
lead through 1 PVC disc
" " " tape
2
4
6
8
10
12
Galvo. deflection
(mm)
(a)
Pressure
(N/mm²)
3000
2400
1800
1200
600
(a)
pin-to-pin
" through 1 PVC disc
" " 2 " discs
2
4
6
8
10
12
Galvo. deflection
(mm)
(b)

Fig. (32)

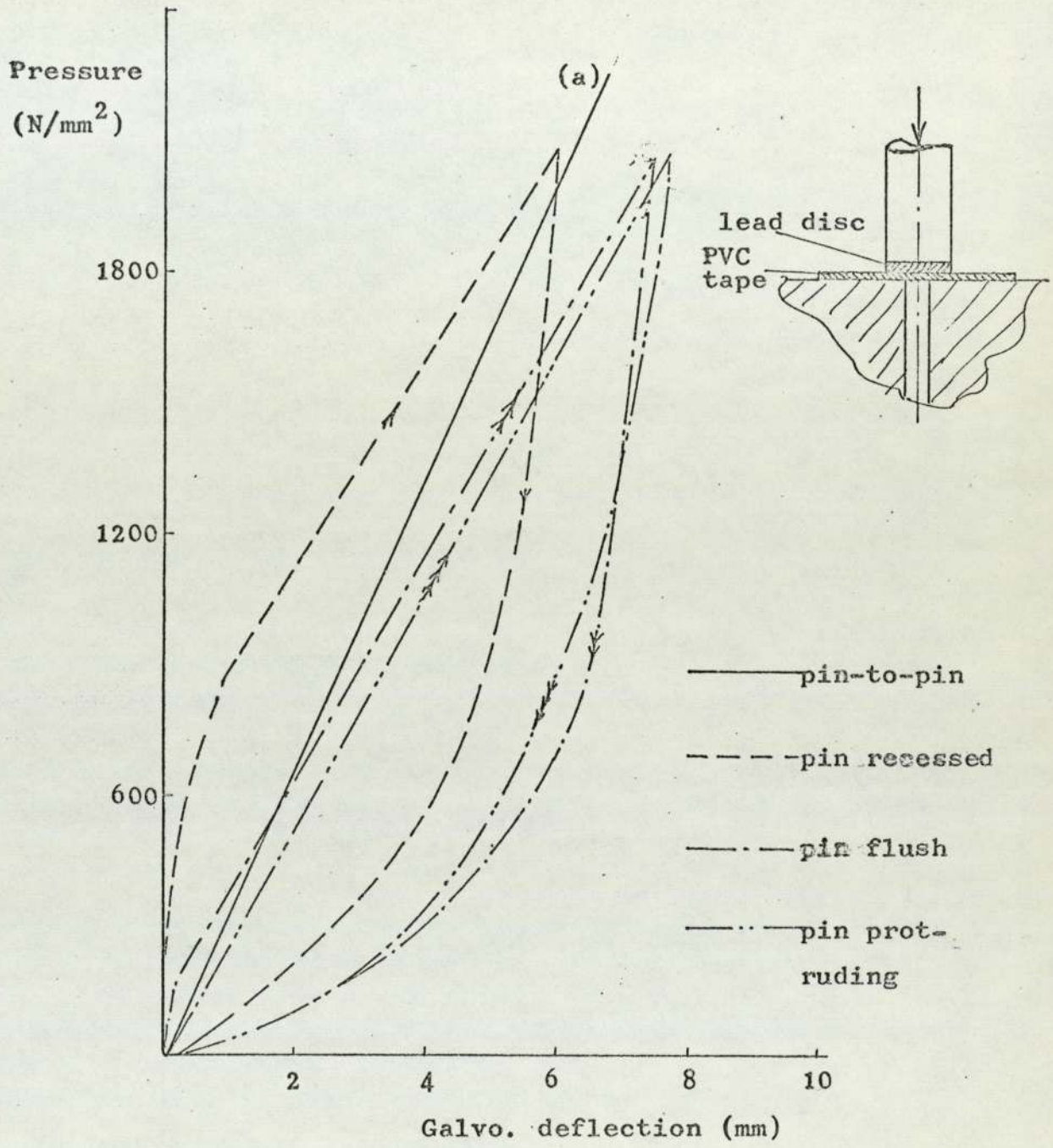
Pressure
(N/mm²)
(a)
1800
1200
600
2
4
6
8
10
Galvo. deflection (mm)
lead disc
PVC
tape
pin-to-pin
pin recessed
pin flush
pin prot-
ruding

Fig. (33)

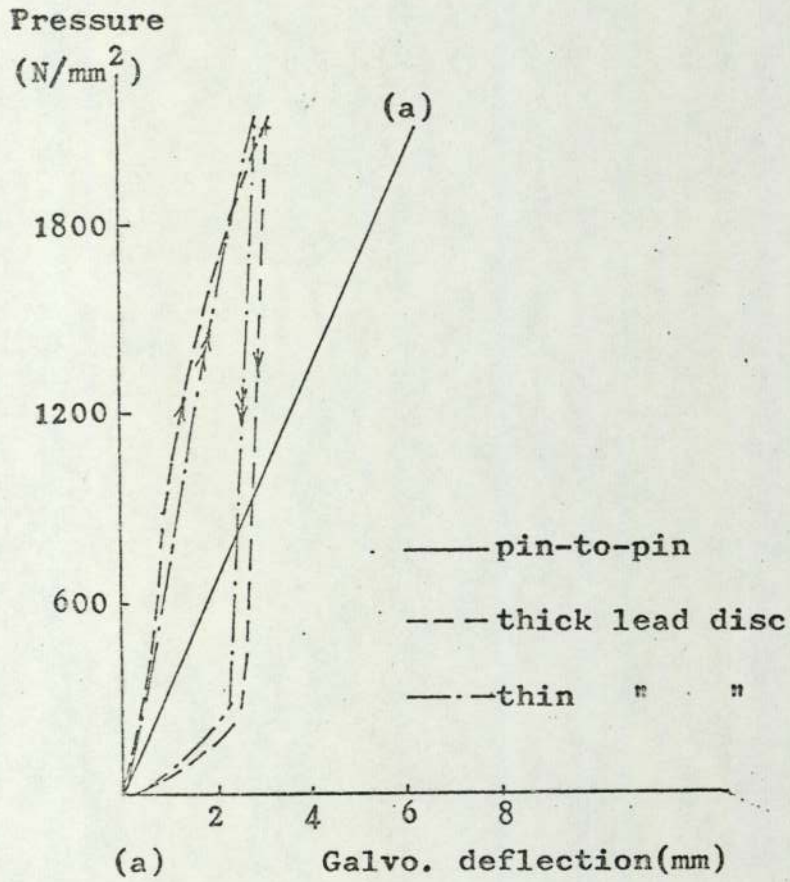
Pressure
(N/mm^2)
(a)
1800
1200
600
pin-to-pin
thick lead disc
thin " "
2
4
6
8
(a)
Galvo. deflection(mm)

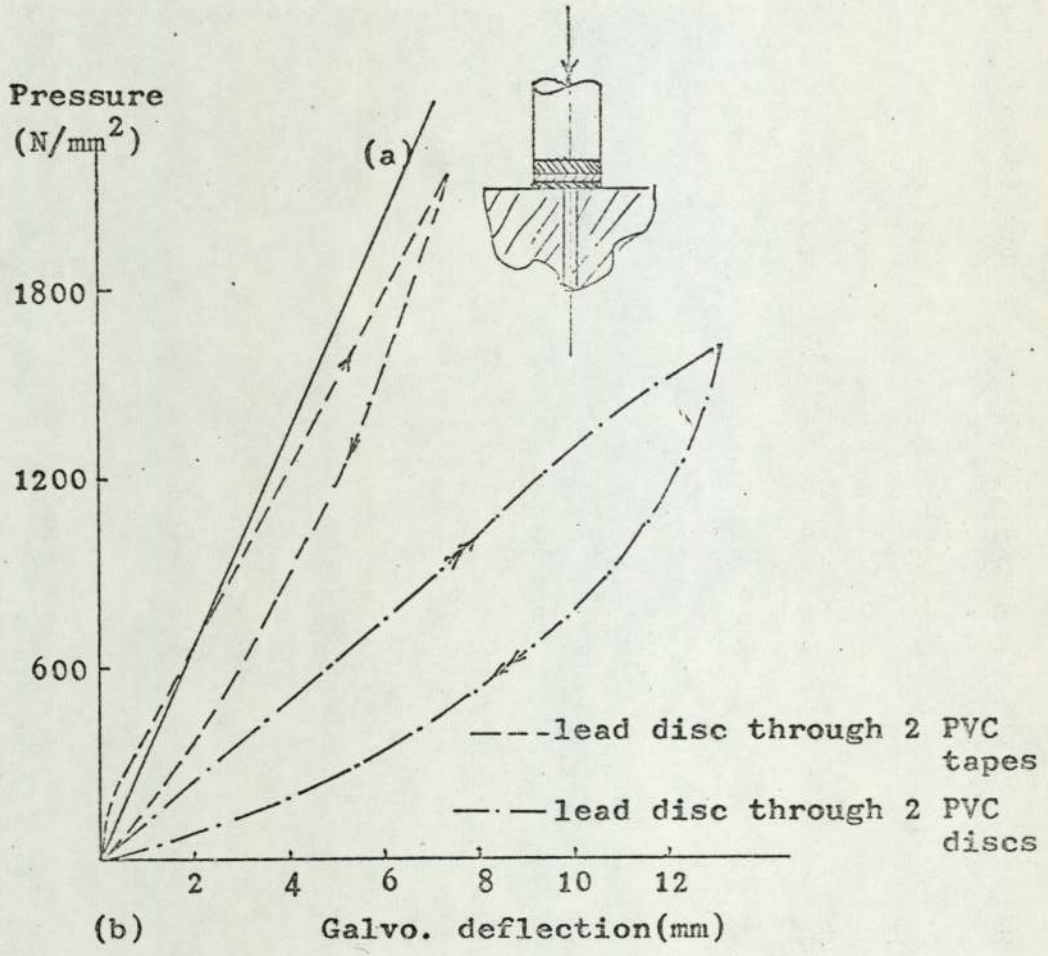
Pressure
(N/mm^2)
(a)
1800
1200
600
lead disc through 2 PVC tapes
lead disc through 2 PVC discs
2
4
6
8
10
12
(b)
Galvo. deflection(mm)

Fig. (34)

between the loading rod and the pin end as shown in fig. (32a). This test was repeated for three positions for the pin end with respect to the surface of contact, i.e, pin recessed, pin flush and pin protruding, but with a PVC tape under the lead discs as shown in fig. (33). The PVC tape was used because it was found to give the nearest response to that of the pin-to-pin calibration. The effect of using lead discs of different thicknesses is shown in fig. (34-a). Fig. (32-b) shows that with a pin-to-pin method of calibration, the effect of using PVC discs cannot be established.

With the pin recessed below the surface of contact, a small rod of lead was formed on the surface of the disc and the response was almost zero until the length of this rod was equal to the amount of recession, i.e., when it touched the pin. The response was improved when the pin was flush with the surface and further improved for a protruding pin.

It can therefore be concluded, according to these tests, that a recessed pin yields an incorrect representation of the contact stresses and that a protruding pin is more advantageous and gives results which are more representative of the state of stress being recorded providing that the amount of protrusion is limited.

The method of calibration employed in this work utilized the use of a pin-to-pin technique and dead weights. The arrangement is shown in fig. (35). The top roll was removed from the rig together with the removable part of the shaft with slip rings and wiring still connected. The roll was fixed to a pivot (o) with locking facility. The shaft and roll could be rotated in a vertical

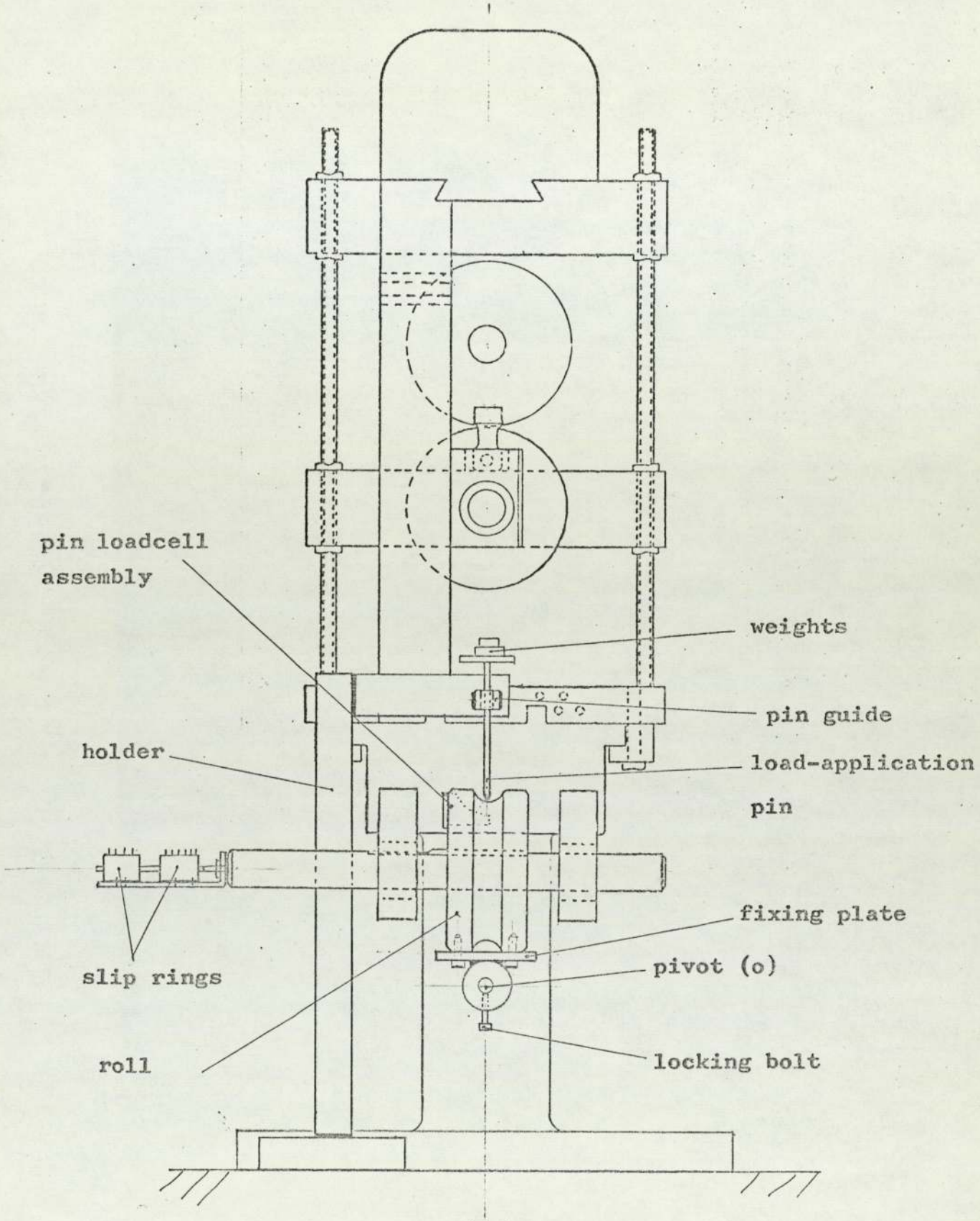

Fig. (35)

Calibration of pin loadcells

plane about the pivot.

A spirit level with angle indicator was used to locate each pin vertically where the load was applied through the loading pin. The calibration curves for the four loadcells are shown in fig. (36) to (39) . They showed no hystresis or zero drift of any significance. Calibration was carried out before testing started and after it was finished. The calibration of the pin load cells was also checked frequently using the proving ring arrangement used in Cole's work [1] . The two calibration methods gave almost identical results.

The gradients for the four pin loadcells are:-

Pin 1	0.181	$N/mm^2/mm$
Pin 2	0.173	$N/mm^2/mm$
Pin 3	0.200	$N/mm^2/mm$
Pin 4	0.212	$N/mm^2/mm$

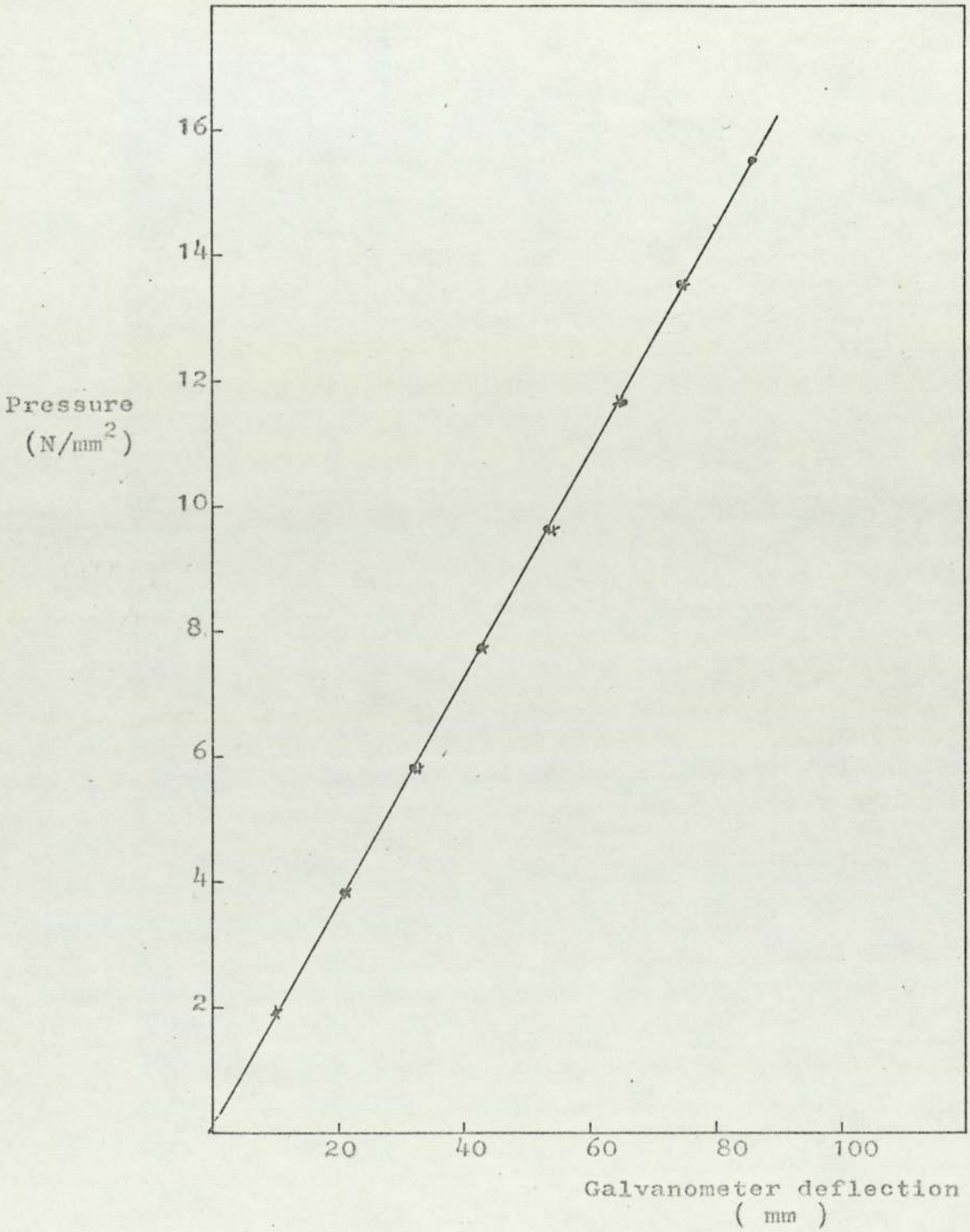

Fig. (36)

Calibration of Pin loadcell number 1 (0^{o})

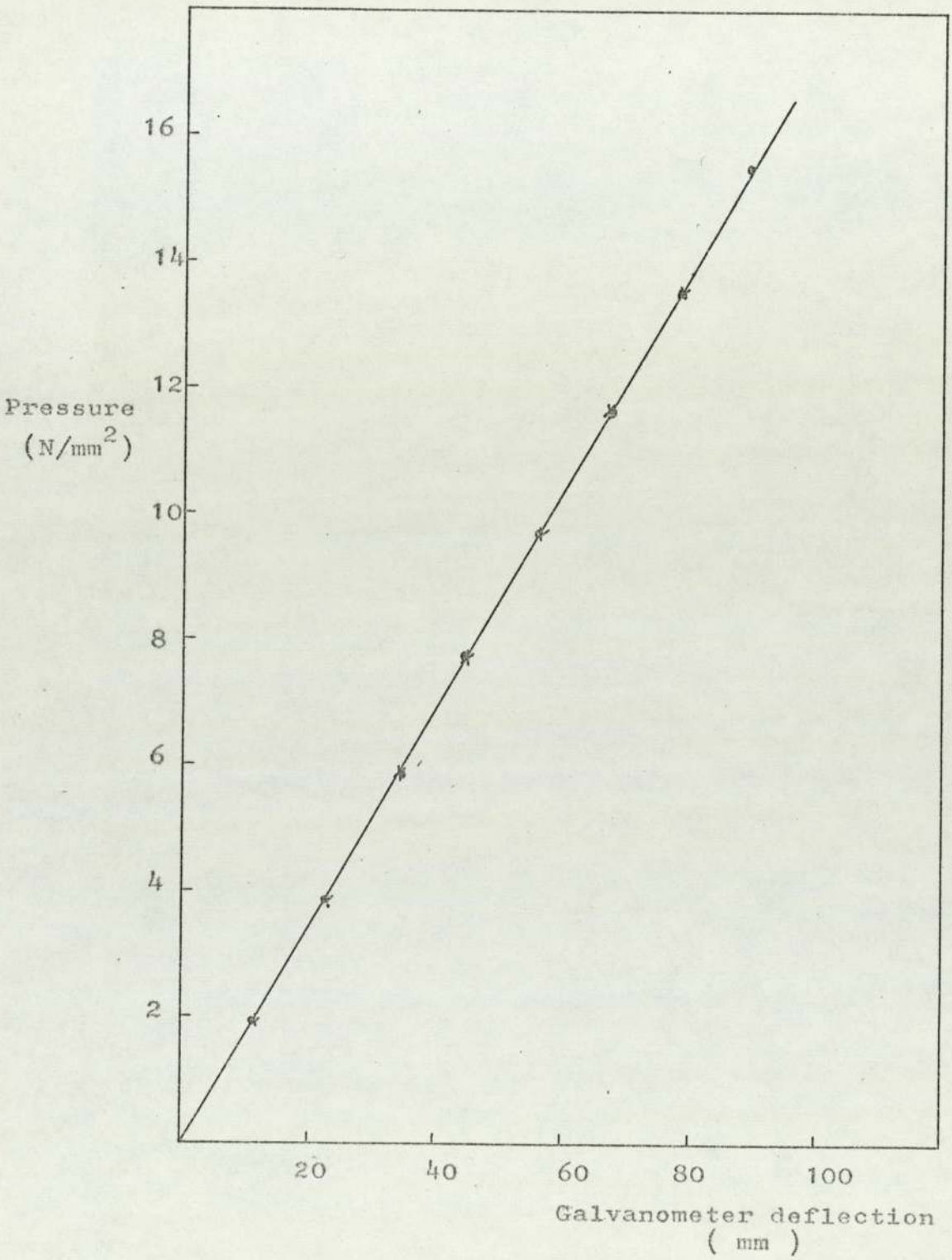

Fig.(37)

Calibration of Pin loadcell number 2 (22.5°)

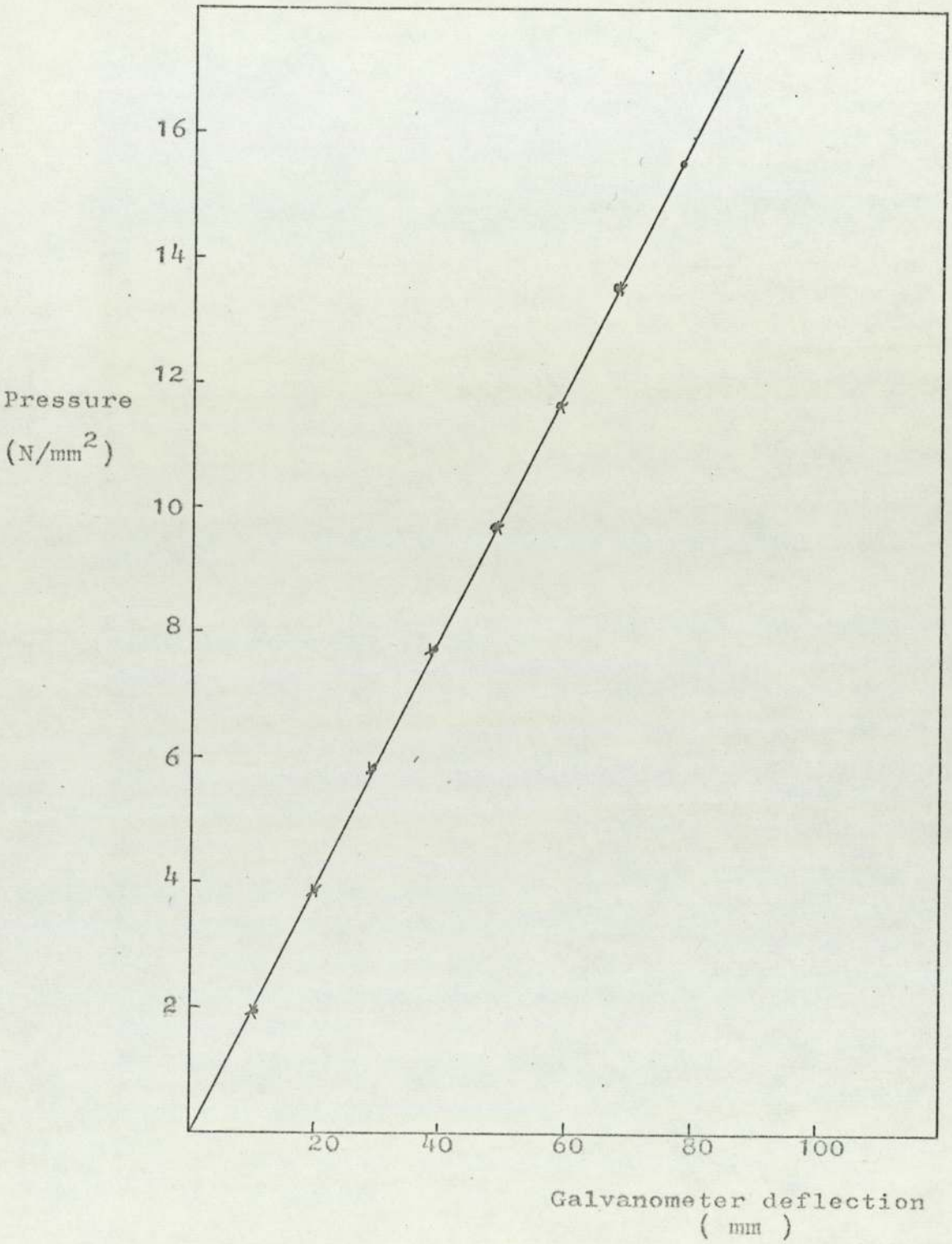

Fig.(38)

Calibration of Pin loadcell number 3 (45^{o})

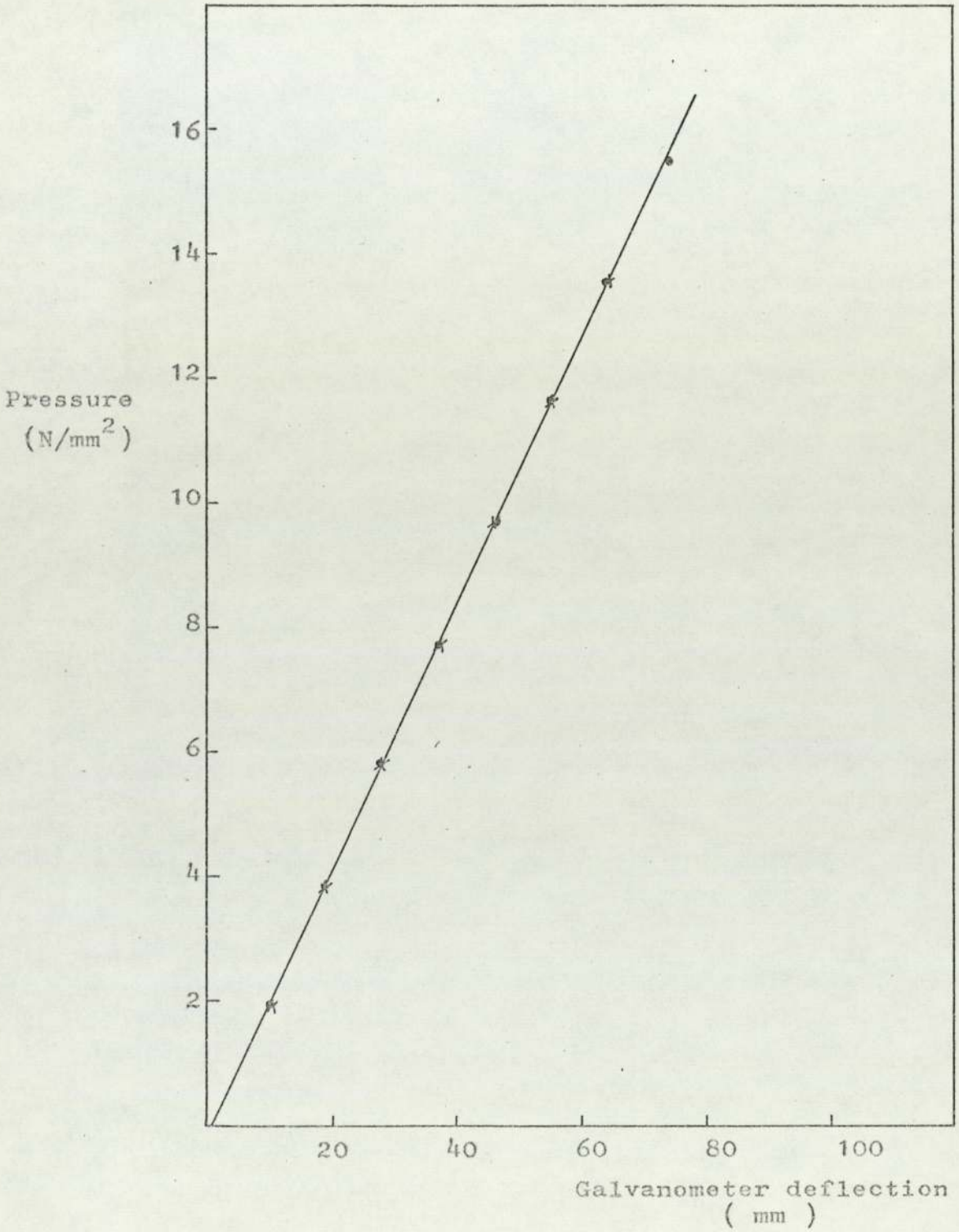

Fig. (39)

Calibration of Pin loadcell unmber 4 (67.5°)

VI

THEORETICAL ANALYSIS OF THE PROBLEM

(VI-1) Determination of Roll Pressure:

Existing theories:

Since the publication of Cole's work in 1969 no new theories relating directly to tube rolling have been put forward. For comparison purposes the theories put forward by Shveikin and Gun (1958) , Vatkin (1954) and Kirichenko (1964) will be discussed. For a full review of these theories reference should be made to Cole's work [1] .

(VI-1.1) Shveikin and Gun [32] (1958):

Basing their analysis on the theory of axially symmetric shells, Shveikin and Gun put forward a simple theory for the prediction of roll pressure. Friction between the tube and the rolls was neglected and the arc of contact was replaced by a chord, see fig. (40).

For tube sinking, the final equation takes the form:

$$p = \sigma_y \left(\frac{t_o}{d_{om}} + \frac{t_1}{d_{1m}} \right) \qquad \text{(VI.1)}$$

The authors compare the predictions of equation (VI.1) with the test results of Vatkin [33] on steel tubes. Generally, this equation overestimates the roll pressure but the agreement presented was acceptable. However in his commentary on this comparison Cole [1] makes the point that the values of the yield stress of steel used in equation (VI.1), (294 N/mm^2 for cold rolling and 58.8 N/mm^2 for hot rolling) are not correct. He shows that these values are a serious underestimate. Therefore the agreement which Shveikin & Gun obtained must be questionable.

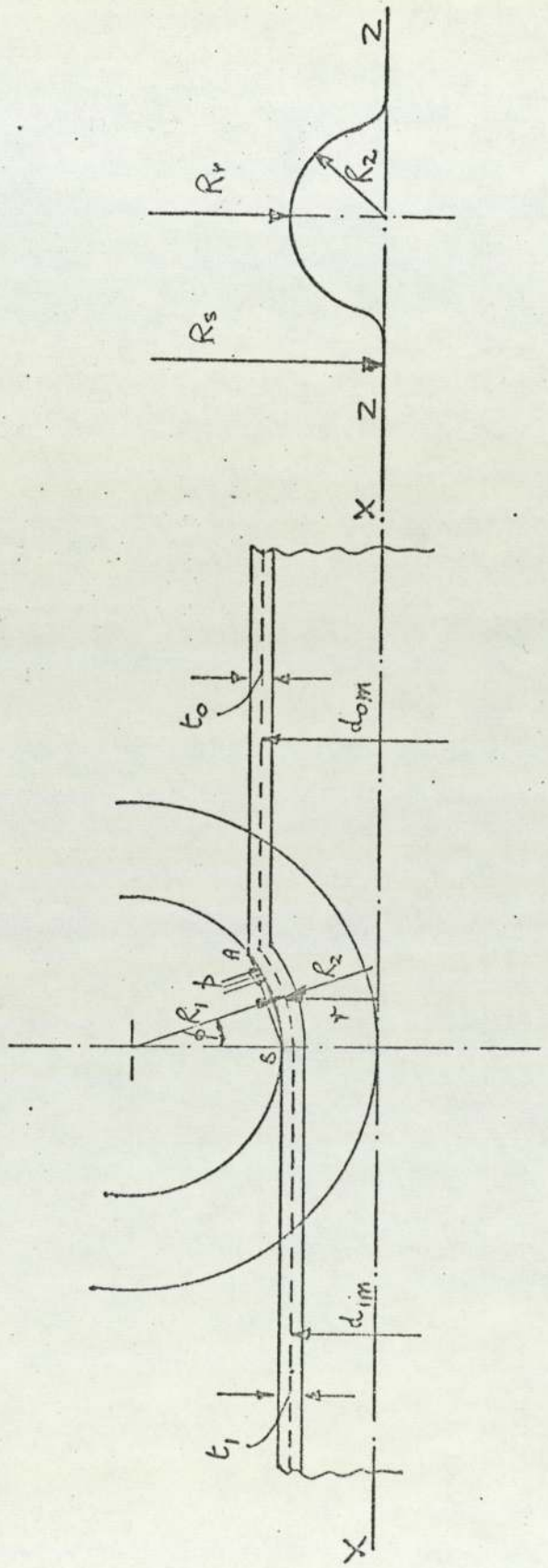

Fig. (40)

(VI-1.2) Vatkin[33], (1954), see fig. (41):

Vatkin used the equilibrium approach to develop the differential equations. He considered the equilibrium of forces acting on an element of tube in the deformation zone. The main assumptions which Vatkin made were:

1) No change of wall thickness i.e. $t_o = t_1$

2) The principal stresses are:-

   i) the compressive longitudinal stress σ_x

   ii) the radial compressive stress on the outer surface of the tube σ_r

   iii) the circumferential stress σ_θ .

3) the yield criterion was :

$$\sigma_x - \sigma_\theta = 1.15 \ \sigma_y$$

4) the relationship between σ_r and σ_θ was obtained by considering the equilibrium of a semi-circular section of the tube thus giving:

$$\sigma_\theta = \sigma_r \cdot \frac{d_g}{2t} \qquad \text{at any section.}$$

5) the arc of contact is approximated to a chord and has the same length for all positions round the groove.

6) A dry type of friction exists between the tube and the rolls, of the kind:

$$\tau = \mu p \qquad \text{at any section.}$$

After arriving at two equations giving the pressure distribution for the entry and exit zones in the form:

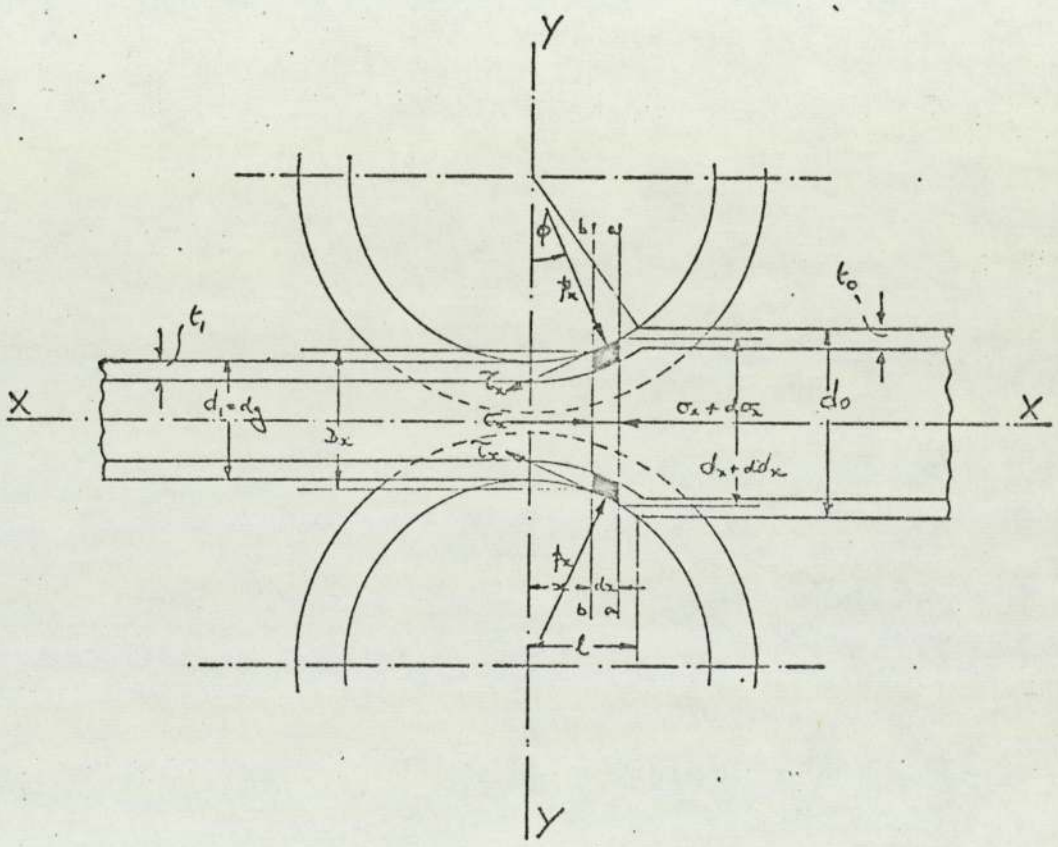
Y
X
X
Y
t_1
t_0
$d_1 = d_y$
D_x
d_0
$\sigma_x + d\sigma_x$
$d_x + dd_x$
τ_{xy}
τ_x
τ_x
ϕ
ϕ_x
ϕ_x
b
a
d_x
b
a
l

Fig. (41)

$$p_x = -k^* Q_1 \left(\left(\frac{1}{Q} - 1\right) \left(\frac{d_o + d_{1i}}{d_x + d_{1i}} \right)^{1/Q} - 1 \right)$$

.....(VI.2)

for the entry zone and

$$p_x = -k^* Q_1 \left(\left(\frac{1}{Q_1} + 1\right) \left(\frac{d_x + d_{1i}}{d_1 + d_{1i}} \right)^{1/Q_1} - 1 \right)$$

.....(VI.3)

for the exit zone , he then gives the equation for the average roll pressure in the form:

$$p_{av} = \frac{k^* Q}{\delta} \left\{ \left[(d_o + d_{1i}) - \frac{(d_o + d_{1i})^{1/Q}}{(d_1 + d_{1i})^{\frac{1}{Q}} - 1} \right] - \delta \right\}$$

.....(VI.4)

in which

$$k^* = 1.15 \sigma_y \cdot \frac{2t}{d_g}$$

$$1/Q = \mu \frac{4L}{\delta} - 1 \quad , \text{ and } \quad d_{1i} = d_1 - 2t_i$$

Vatkin then compares the predictions of the above equation with his experimental results [33] referred to earlier in this section. For the cold rolling of steel tubes Vatkin used a coefficient of friction $\mu = 0.25$ and a yield stress value $\sigma_x = 294$ N/mm^2 (30 kgf/mm^2), which Cole [1] has shown to be a serious underestimate. The predicted values of the roll pressure p_{av} were higher than the experimental values. This Vatkin attributed to a large coefficent of friction μ. However Cole disputed this reason in the light of the underestimated value of the yield stress used in the calculations.

Vatkin's records of the roll pressure showed a peak at a point between the middle of the deformation zone and

the exit plane. It was noted that the deviation of the position of the peak(i.e. neutral plane) from the middle was small.

Results of tests carried out in the present investigation have shown that the position of the neutral plane is a function of the groove angle θ and that depending on the value of θ the position of the neutral plane moves towards the exit or entry planes.

(VI-1.3) Kirichenko[34], (1964):

Kirichenko's approach is similar to that of Vatkin[33] in so far as it is an equilibrium approach. The main assumptions being similar to those of Vatkin i.e. the shear stress due to friction $\tau = \mu p$, the arc of contact is approximated to a chord, no change in wall thickness during rolling, the principal stresses are σ_r, σ_θ and σ_x as in Vatkin's theory and the yield criterion being of the type:

$$\sigma_x - \sigma_\theta = k\sigma_y$$ although k was not defined.

However, Kirichenko considered the general case of an oval tube being rolled in an oval groove as shown in fig.(42).

The relationship between σ_θ and p differed from that of Vatkin and was obtained by resolving the forces in the radial direction as in fig.(43). This relationship took the form:-

$$p = \frac{2\sigma_\theta t}{(\cos\phi + \mu \sin\phi\cos\theta)\, d_x}$$

as opposed to Vatkin's

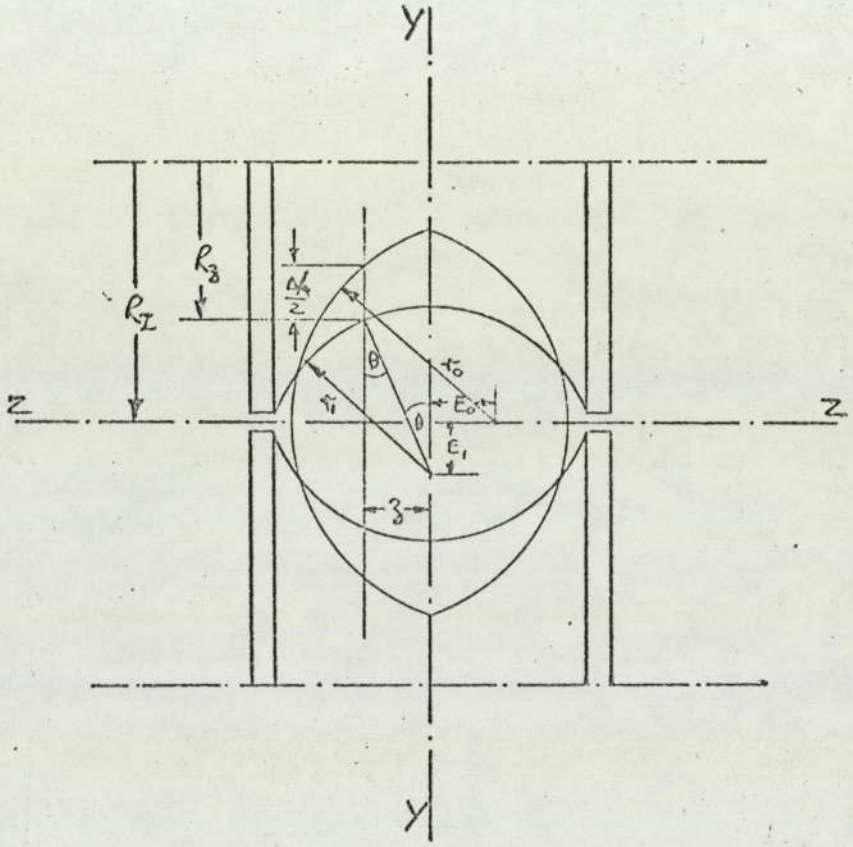

Fig. (42)

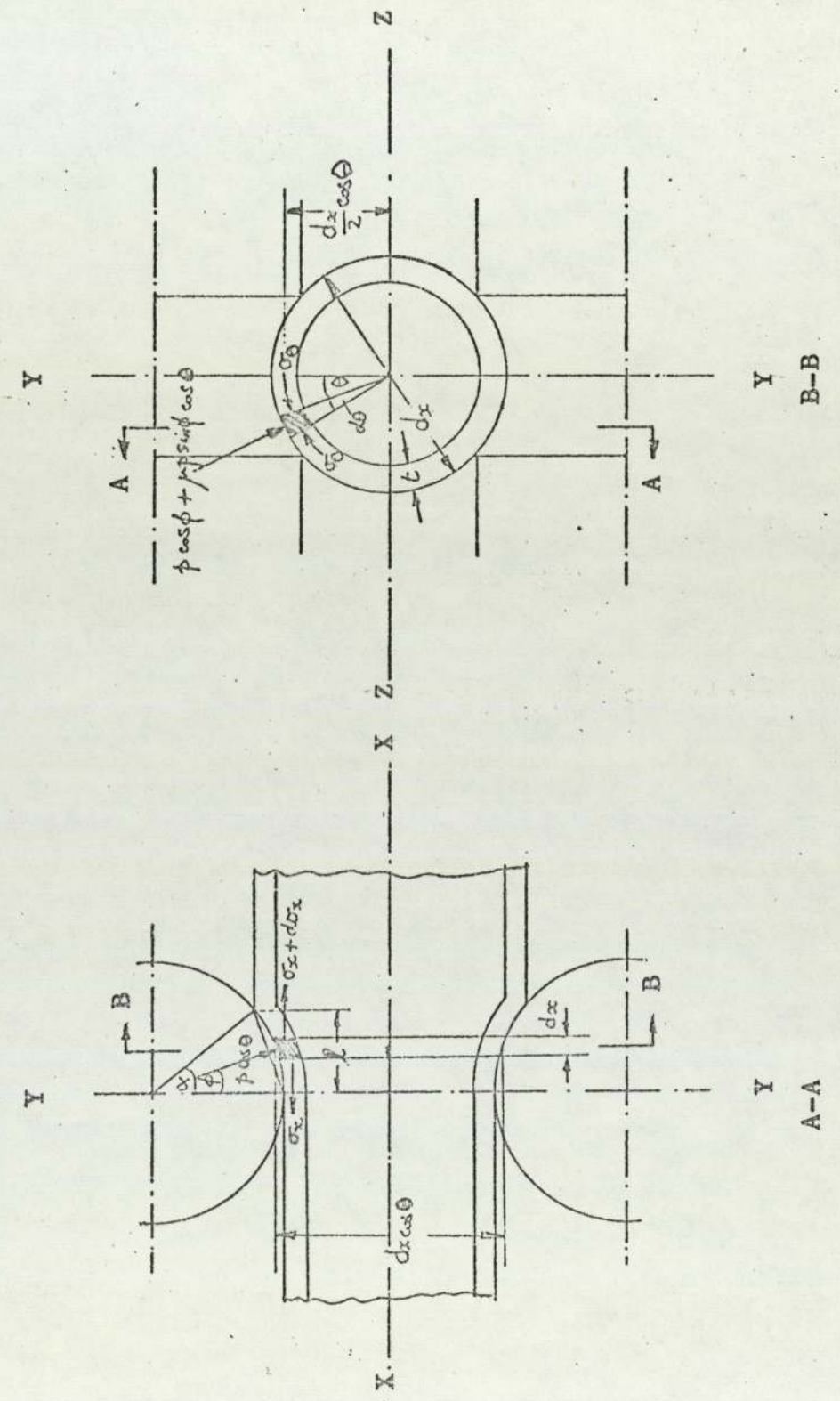

Fig. (43)

$$p = \frac{2\sigma_\theta t}{d_g}$$

in which the friction contribution was not considered.

Kirichenko presents two equations for the calculation of the arc of contact (L) and angle of contact (ϕ) when rolling an oval tube in an oval groove, based on geometrical consideration of figs.(42) and (43).

These equations are:

$$L = \left[R_z^2 - (R_z - \frac{\Delta h}{2})^2 \right]^{1/2}$$

$$= \left[(R_I + E_1 - \sqrt{r_1^2 - z^2})^2 - (R_I - \sqrt{r_o^2 - (E_o + z)^2})^2 \right]^{1/2} \quad \ldots\ldots\ldots\ldots (VI.6)$$

and

$$\tan\phi = \frac{\Delta h}{2L} = \frac{\sqrt{r_o^2 - (E_o + z)^2} - \sqrt{r_1^2 - z^2} + E_1}{\left[(R_I + E_1 - \sqrt{r_1^2 - z^2})^2 - (R_I - \sqrt{r_o^2 - (E_o + z)^2} \right]^{1/2}} \quad \ldots\ldots\ldots\ldots (VI.7)$$

After solving the differential equations resulting from consideration of the equilibrium of forces acting on an element in the inlet zone, Kirichenko presents two formulae for determining the pressure distribution in the deformation zone.

These take the form for the sinking process,

$$p' = \left[kt/(r_1 + x \tan\phi \cos\theta - t/2) (\cos\phi + \mu \sin\phi \cos\theta) \right] x$$

$$\left[\frac{1}{1+A} + \left(\frac{r_1 + L \tan\phi \cos\theta - t/2}{r_1 + x \tan\phi \cos\theta - t/2} \right)^{1+A} \cdot \frac{A}{1+A} \right] \ldots (VI.8)$$

for the inlet zone.

and

$$p'' = \left[kt/(r_1 + x\tan\phi\cos\theta - t/2)(\cos\phi - \mu\sin\phi\cos\theta) \right] \times \left[-\frac{1}{B-1} + \left(\frac{r_1 + x\tan\phi\cos\theta - t/2}{r_1 - t/2} \right)^{B-1} \cdot \left(\frac{B}{B-1} \right) \right]$$

.....(VI.9)

for the outlet zone.

where

$$A = \frac{\cos\theta(\mu - \cos\theta\tan\phi)}{\sin\phi(\mu\tan\phi\cos\theta + 1)}$$

and

$$B = \frac{\cos\theta(\mu + \tan\phi\cos\theta)}{\sin\phi(1 - \mu\tan\phi\cos\theta)}$$

Cole [1] commented that for A to take the necessary positive value μ must be greater than $\tan\phi$. He also found that Kirichenko's equation for calculating the angle of contact gave a considerable overestimate.

Kirichenko presents no experimental results to support his theory but presents graphs showing the variation of roll pressure along the arc of contact fig.(44).

In another publication [35] Kirichenko developed an equation for the calculation of the rolling torque for the longitudinal rolling of bars and tubes. He considers the friction forces as being the only forces responsible for the rolling torque. By reference to figs.(45)and (46) and due consideration for the direction of the frictional drag, the equation for the rolling torque T was written in the form:

$$T = m \int_{z_1}^{z_2} \left[\int_{\gamma}^{\alpha} \tau R_z \cdot R_z \, d\phi - \int_{o}^{\gamma} \tau R_z \cdot R_z \, d\phi \right] \frac{dz}{\cos\theta}$$

.....(VI.10)

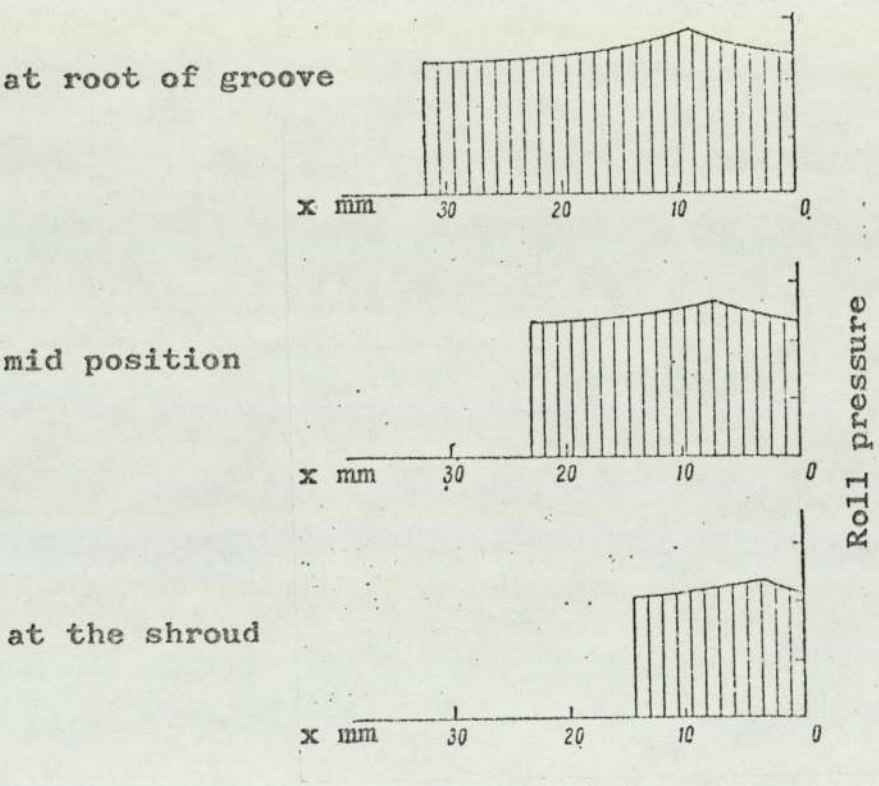
at root of groove
x mm
30
20
10
0
mid position
x mm
30
20
10
0
at the shroud
x mm
30
20
10
0
Roll pressure

Fig. (44)

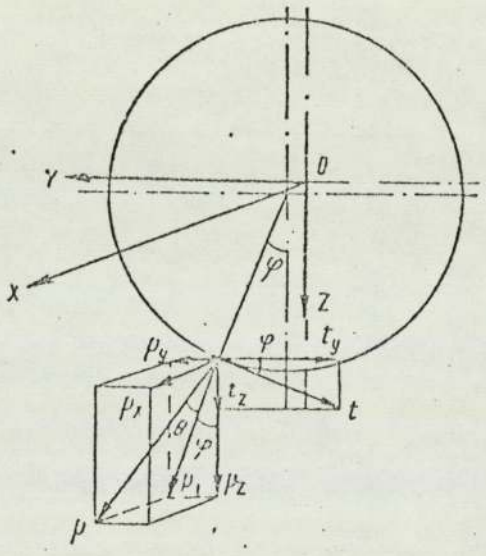

Fig. (45)

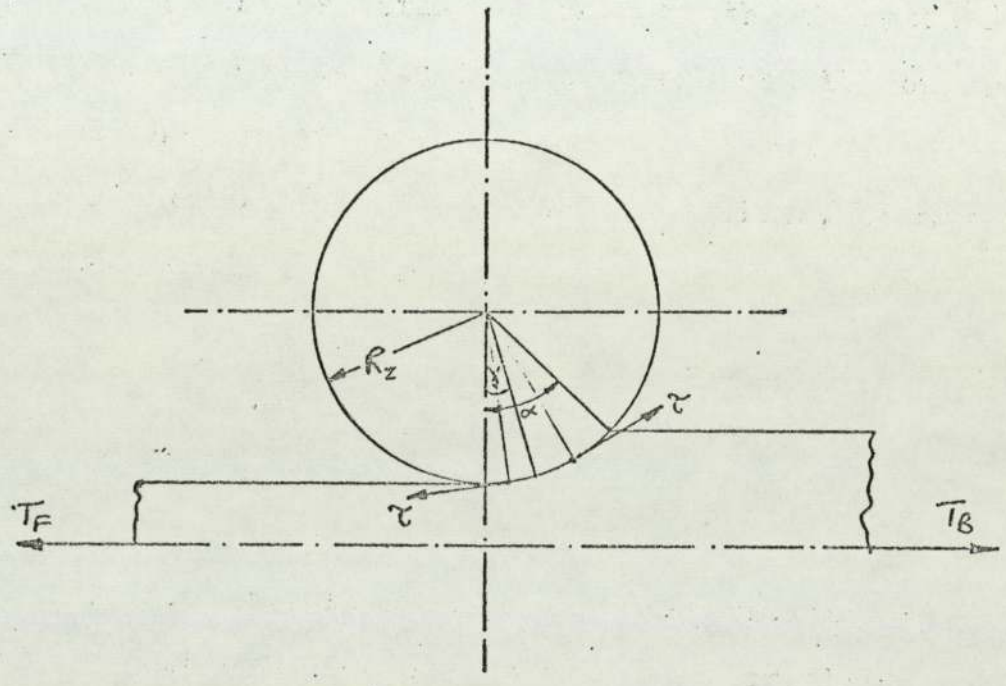

Fig. (46)

in which m is the number of rolls per stand and γ is the neutral angle.

By assuming a Coulomb tybe of friction:

$$\tau = \mu p$$

and a uniformally distributed normal pressure p on the contact surface he integrates the above equation to give:

$$T = m \mu p R_{av} \left(A_{tot.} - 2 A_{out} \right) \quad \ldots\ldots\ldots (VI.11)$$

where

R_{av} is the mean roll radius in the deformation zone.

A_{tot} is the total contact area.

A_{out} is the area of the exit zone.

For the determination of R_{av}, Kirichenko proposes the use of the expression:

$$R_{av} = \frac{1}{2}\left(\text{Roll diameter} - \frac{\text{area of groove}}{\text{width of groove}} \right) \quad \ldots\ldots (VI.12)$$

The final form of the expression for determining the rolling torque is given as a function of the horizontal and vertical projections of the area of contact, i.e, A_H and A_V respectively.

$$T = m \, P_V \, R_{av} \, \frac{A_V}{A_H} \quad \ldots\ldots\ldots\ldots\ldots\ldots (VI.13)$$

in which P_V is the roll separating force expressed as:

$$P_V = p. \, A_H \quad \ldots\ldots\ldots\ldots\ldots\ldots (VI.14)$$

Once again no experimental evidence was presented but Kirichenko states that the correlation between the

calculated values of the rolling torque and those found in tests for the rolling of tubes in grooves was good giving an error of less than 10 per cent.

(VI-1.4) Cole's Work[1] (1969):

Cole did not present any theoretical treatment of the problem but examined the three theories mentioned before and made comparison between their predictions and his test measurements. He found that the three theories gave very poor, if any, correlation with the test results for the sinking process. The three theories underestimated the value of the roll pressure.

Although Cole's results of the pressure distributions were higher than they should be due to the use of PVC discs to cover the tips of the pressure-transmitting pins, as was found from the present work, the difference between the calculated values from the theories and the test results was still large.

It has been found during the present investigation that the use of PVC discs on the tips of the pin loadcells of the size used by Cole, i.e. 6.4 mm in diameter, has caused the recorded pressure to be some 22% higher than without the discs as shown in fig.(52) on page(189).

The mean measured value of roll pressure which Cole used to compare with the theoretical predictions was:

$$p_m = 16.82 \text{ N/mm}^2$$

and if we apply a reduction factor of 0.78 to this value to eliminate the effect of using the PVC discs we get:

$p_m = 13.12 \text{ N/mm}^2$

Against this value of p_m, the following were the various theoretical predictions:

Shveikin & Gun (formula (VI.1))

$p_G = 5.19 \text{ N/mm}^2$

Vatkin (formula (VI.4))

$p_V = 5.72 \text{ N/mm}^2$

Kirichenko (formula (VI.8))

$p_K = 5.05 \text{ N/mm}^2$

The coefficient of friction used for Vatkin's and Kirichenko's formulae was 0.25. Kirichenko's prediction is for a point mid-way through the arc of contact ($\phi = 10^\circ$) at the root of the groove ($\theta = 0^\circ$).

Even with the reduced value of p_m the correlation is still very poor. The three theories seem to give similar results.

(VI-1.5) The theory

It was clear from the start of the present investigation that a new approach to the problem of predicting the rolling loads was required since the equilibrium approach used by Shveikin and Gun[32], Vatkin[33] and Kirichenko[34] has proved unsatisfactory by comparison with the test results of Cole[1] as shown earlier.

The shortcomings of the equilibruim approach as employed by [32], [33] and [34] have been discussed in reference [1] and are discussed further below:

1) It is necessary in this approach to use a yield criterion. The type used by the three workers was Tresca's in the modified form $\sigma_1 - \sigma_3 = \beta \sigma_y$ where B takes values between 1.00 and 1.15. The value of B was not defined by Kirichenko while it was given the value of 1.00 by Shveikin and Gun. and 1.15 by Vatkin. The latter case implies deformation in plane strain which Cole[1] states to be unacceptable for sinking. It is more accurate to apply the vonMises yield criterion in the case of tube sinking as shown in [1], [52]. Sachs suggests that the use of this criterion involves considerable calculations and for this reason it is sufficiently accurate to give B the value of 1.1 in the modified Tresca criterion.

2) To apply a yield criterion, the directions of principal stresses must be defined. In the case of the three theories dealing with tube rolling[32],

(33) and (34) the directions of the principal stresses are assumed to be:- longitudinal, tangential(hoop), and radial. While this system of principal stresses is acceptable in cold forming where the friction forces are low and hence the shear stress contribution is small, its application to hot forming processes with high friction forces must be questionable. With sticking friction, as is believed to be the case with the hot rolling process, then the yield criterion with this system of principal stresses cannot be used (1).

The above two points are inherent features of any equilibrium approach and represent fundamental assumptions which determine the accuracy of a particular theory. Together with other assumptions, mainly concerning friction, they are believed to be the reason for the lack of correlation found in Cole's work.

A new approach for the theoretical treatment of the tube rolling process was therefore sought and the strain energy method was believed to represent a reasonable alternative approach.

The first drawback of this method is that it only gives the average roll pressure and does not therefore provide information on the distribution of the pressure round the groove or along the arc of contact. However although knowledge of the pressure distribution is useful in understanding the mechanics of the process, as will be seen in the discussion of results, it is sufficient for practical applications to determine the average pressure.

In this method the work done per unit volume of rolled tube , in the case of sinking , is assumed to be made up of the

following components:-

1) Work of homogeneous deformation W_h needed to change the shape of the tube.

2) Work done against friction W_f .

3) Redundant work W_r .

The first component represents the minimum possible work required to achieve the desired reduction. It would be the work required if the tube could be extended in tension without necking. The second component represents the work done against friction at the tube-roll interface. The third component is the redundant work needed to shear the tube material as it passes into and out of the deformation zone due to the change of direction which the tube material suffers. This component increases as the draft, and hence the reduction of area, increases. But since, for rolling, the ability of the rolls to draw in the material is limited to the maximum possible angle of bite, the maximum angle of contact and reduction per pass are also limited. In addition to that, the conditions of overfilling of the groove and marking of the surface of the tube are other limiting factors to the maximum possible angles of contact and reductions in tube rolling. However in other forming processes e.g. extrusion and drawing, the die angle can be large and the contribution of the redundant work to the total work done can be significant. In the present case this component will be neglected due to the small reductions associated with tube rolling in two grooved rolls.

The total work of deformation per unit volume is equal to the area under the true stress-strain curve, fig. (47) for the

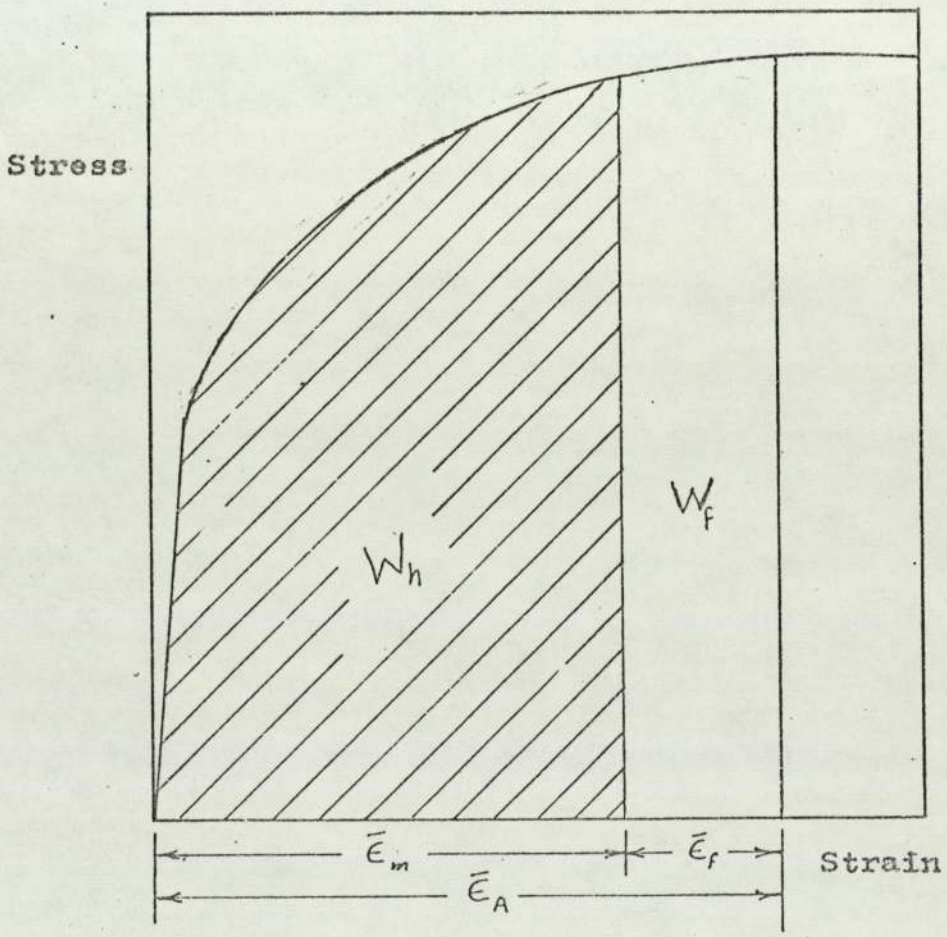

Fig.(47)

Work of Deformation

appropriate total strain $\bar{\epsilon}_A$. This area is made up of two parts (36):-

1) the first part corresponds to the work of homogeneous deformation W_h for which the strain is equal to $\bar{\epsilon}_m$, the generalised strain.
2) the second part corresponds to the work done against friction for which the frictional strain is $\bar{\epsilon}_f$.

Assuming that the contributions of the two components are additive we have

$$W_t = W_h + W_f \qquad \text{.....(VI.15)}$$

This assumption is a basic assumption in the strain energy approach and corresponds to that of the directions of principal stresses and yield criterion in the equilibrium approach. It implies that the friction contribution is superimposed on the work of homogeneous deformation and that the state of stresses is not affected by the presence of friction. The validity of this assumption therefore increases the lower the value of the friction contribution.

By employing the apparent strain concept and the above assumption we have :

$$\bar{\epsilon}_A = \bar{\epsilon}_m + \bar{\epsilon}_f \qquad \text{.....(VI.16)}$$

Hence the total work of deformation W_t is equal to the integral of the true stress-strain curve between the limits of zero strain and $\bar{\epsilon}_A$, which is the total area under the curve as in fig. (47).

By calculating the two components of the total work of deformation separately, it is possible to determine W_t .

1) Work of homogeneous deformation W_h :-

The area under the true stress-strain curve fig.(47) for the generalised strain $\bar{\epsilon}_m$ is the internal work of homogeneous deformation W_{hi} and is calculated as follows :-

$$W_{hi} = \int_0^{\bar{\epsilon}_m} \sigma_y \, d\epsilon \qquad \ldots\ldots\ldots (VI.17)$$

The integration could be simplified by taking an average value of the yield stress before and after rolling.

$$W_{hi} = \bar{\sigma_y} \, \bar{\epsilon}_m \qquad \ldots\ldots\ldots (VI.18)$$

To calculate the external work of homogeneous deformation, W_{he}, which would be that required if the tube could be extended in tension without necking, the process of rolling the tube will be approximated to that of a tube under an external uniform pressure sufficient to cause plastic deformation and produce the same final tube dimensions, fig. (48).

In this case the increment of plastic work dW_{he} will be equal to :

$$dW_{he} = p_h \cdot S \cdot dr \qquad \ldots\ldots\ldots\ldots (VI.19)$$

Where p_h is the uniform pressure for homogeneous deformation,

S is the surface area of application of p_h

$= 4L \cdot r_g \theta_c$

putting $L = R_r \Phi_m$ in tube rolling

then $S = 4 R_r \Phi_m r_g \theta_c \qquad \ldots\ldots\ldots\ldots (VI.20)$

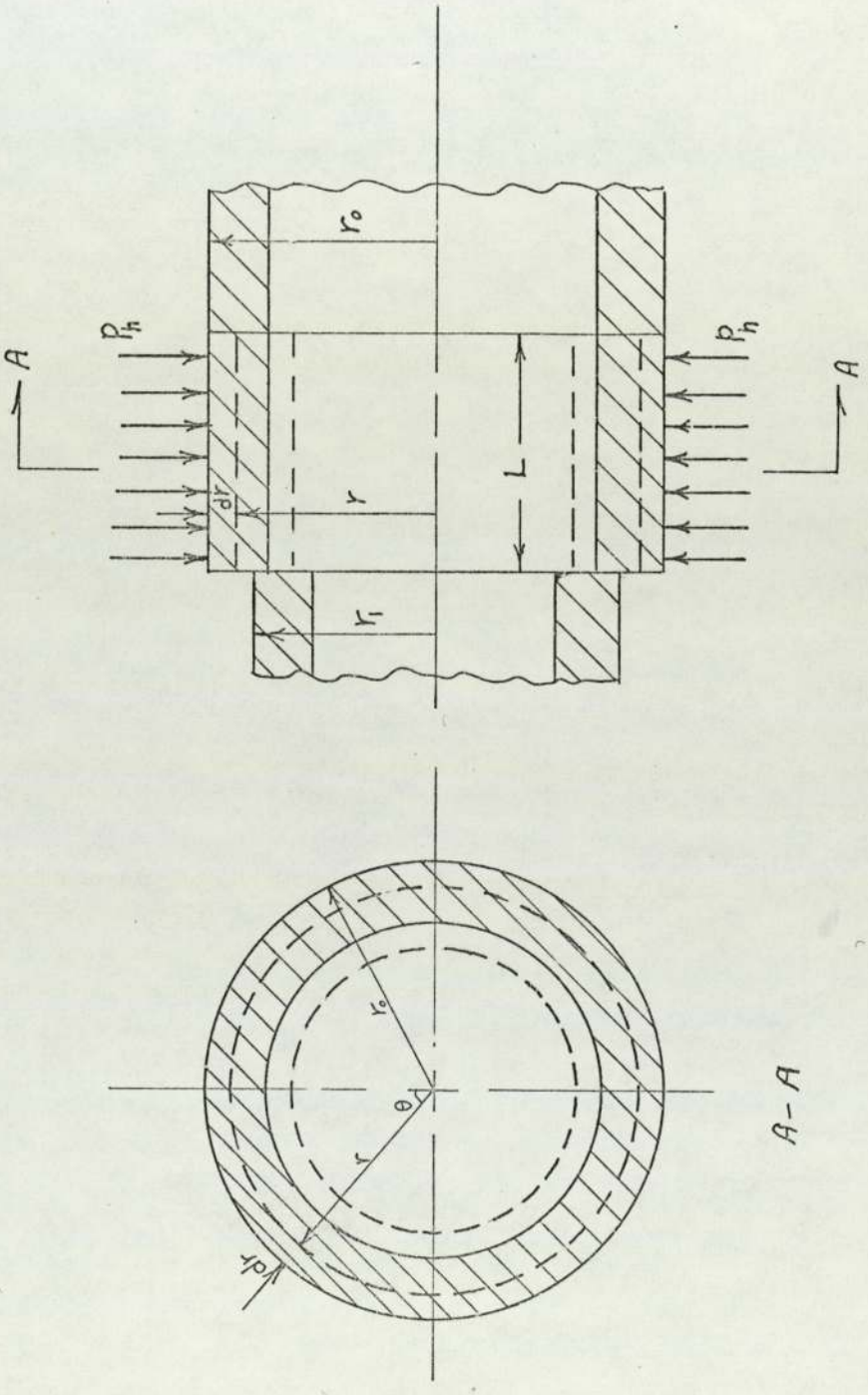

Fig. (48)

dr is the change in the tube radius as a result of the increment of plastic deformation.

Therefore

$$dW_{he} = 4\, p_h\, R_r\, \Phi_m\, r_g\, \theta_c \cdot dr$$

and

$$W_{he} = \int_{r_o}^{r_1} 4\, p_h\, R_r\, \Phi_m\, r_g\, \theta_c \cdot dr \qquad \ldots\ldots\ldots (VI.21)$$

but since p_h is assumed constant then

$$W_{he} = 4\, p_h\, R_r\, \Phi_m\, r_g\, \theta_c \int dr$$

$$= 4\, p_h\, R_r \Phi_m\, r_g\, \theta_c\, (r_o - r_1) \qquad \ldots\ldots\ldots (VI.22)$$

but $\delta = d_o - d_1 = 2(r_o - r_1)$

$$W_{he} = 2\, p_h\, R_r \Phi_m\, r_g\, \theta_c\, \delta \qquad \ldots\ldots\ldots (VI.23)$$

Hence, the work of homogeneous deformation per unit volume will be :-

$$W_{he}/\text{vol.} = \frac{W_{he}}{V} \qquad \ldots\ldots\ldots (VI.24)$$

where

$$V = A_o \cdot U_o \cdot \frac{\Phi_m}{\omega} \qquad \ldots\ldots\ldots (VI.25)$$

and putting $U_o = \omega R_r$ we have

$$V = A_o\, R_r \Phi_m \qquad \ldots\ldots\ldots (VI.26)$$

from equations (VI.24) and (VI.26):

$$W_{he}/\text{vol.} = \frac{2p_h\, R_r \Phi_m\, r_g\, \theta_c\, \delta}{A_o\, R_r \Phi_m}$$

$$W_{he}/vol = \frac{2\, p_h\, r_g\, \theta_c}{A_o} \qquad \ldots\ldots\ldots\ldots (VI.27)$$

Assuming no energy losses we can equate the work per unit volume of internal forces to that of the external forces, i.e.,

$$W_{hi} = W_{he} \qquad \ldots\ldots\ldots\ldots (VI.28)$$

$$\bar{\sigma}_y\, \bar{\epsilon}_m = \frac{2\, p_h\, r_g\, \theta_c\, \delta}{A_o} \qquad \ldots\ldots\ldots\ldots (VI.29)$$

from which we obtain :-

$$p_h = \frac{\bar{\sigma}_y\, \bar{\epsilon}_m\, A_o}{2\, r_g\, \theta_c} \qquad \ldots\ldots\ldots\ldots (VI.30)$$

This equation gives the part of the roll pressure associated with homogeneous deformation. To obtain the total mean roll pressure the contribution of friction must be considered.

2) Work done against friction W_f

The mechanics of friction are complex and determination of the exact functional relationship between the frictional shear stress τ and the other variables is difficult [37]. There are two main types of friction for forming without lubrication. The first and more commonly used type is the Coulomb friction in which the tangential stress is proportional to the pressure p between the two bodies, in the form:

$$\tau = \mu p \qquad \ldots\ldots\ldots \text{(VI.31)}$$

the coefficient of friction μ is usually assumed to be constant for a particular set of conditions.

The second type is the constant shear stress type in which τ is related to the shear yield stress of the material being deformed and is assumed constant irrespective of the pressure.

Thus $$\tau = m \frac{\sigma_Y}{\sqrt{3}} \qquad \ldots\ldots\ldots\ldots \text{(VI.32)}$$

in the constant shear type of friction.

The friction factor m is taken as constant for a particular set of conditions. In the absence of friction, m = 0 . The maximum value that m can take is 1.0 since the maximum shear a material can stand according to von Mises yield criterion is $\frac{\sigma_Y}{\sqrt{3}}$

Avitzur [37] showed that with the assumption of constant friction factor, the computations of friction losses are easier.

In the hot rolling of steel it is now accepted that sticking friction prevails over the whole or part of the

surface of contact between the rolls and the rolled material, i.e, $\tau = \frac{\sigma_Y}{\sqrt{3}}$ for complete sticking.

Cole [1] states that under these conditions the assumption of Coulomb friction is not valid, as suggested originally by Orowan in 1943. A combination of sliding friction and sticking, with $\tau = \frac{\sigma_Y}{\sqrt{3}}$, has been shown to exist in the hot forming of metals.

The material rolled in the present work was pure lead in simulation of the hot rolling of steel. Although a sticking friction may occur in the latter process preliminary tests have shown this not to be the case for the rolling of lead. Bland & Ford's approximate method [38] of determing the friction stresses by applying an increasing back tension to the tube until it stops and measurement of the resulting forces and torque was used. These tests showed that the friction stress was less than the shear yield stress of lead.

In this analysis the constant shear stress concept has been adapted in the form:

$$\tau = m \frac{\sigma_Y}{\sqrt{3}} \qquad \ldots\ldots\ldots \text{(VI.32)}$$

This concept permits the application of this theory to the hot rolling of steel where sticking can be assumed by giving the friction factor m the value of 1.0 .

As will be seen in the discussion of results the surface of contact between the tube and groove can be divided into three zones with respect to the groove angle θ , see fig. (63-a) on page (219);

Zone I: between $\theta = 0^{o}$ and $\theta = \theta_{eo}$ in which the tube is always faster than the roll and therefore corresponds to the exit zone in flat rolling .

Zone II: between $\theta = \theta_{eo}$ and $\theta = \theta_{e1}$. This zone corresponds to the whole of the deformation zone in flat rolling with two equal entry and exit zones.

Zone III: between $\theta = \theta_{e1}$ and $\theta = \theta_{c}$, the maximum angle of contact. In this zone the rolls are always faster than the tube and it therefore corresponds to the entry zone in flat rolling.

In the light of the test results, it is possible to d vide the surface of contact into two equal zones with respect to the groove angle θ . As shown in fig.(49) the first zone corresponds to the exit side of the deformation zone in flat rolling and has the limits

$$\theta = 0 \qquad \text{to } \theta = \theta_{n}$$

where $\theta_{n} = \theta_{c}/2$ as a first approximation.

The second zone is bounded by θ_{n} and θ_{c} and corresponds to the entry zone in flat rolling.

As in the case of the work of homogeneous deformation, the work per unit volume of the internal forces to overcome friction W_{fi} is equal to the part of the area under the true stress-strain curve associated with friction as shown in fig.(47); i.e,

$$W_{fi} = \int_{\bar{\epsilon}_{m}}^{\bar{\epsilon}_{A}} \sigma_{\bar{y}} \, d\epsilon \qquad \text{.....(VI.33)}$$

Again taking a mean value of the yield stress $\sigma_{\bar{y}}$ we obtain

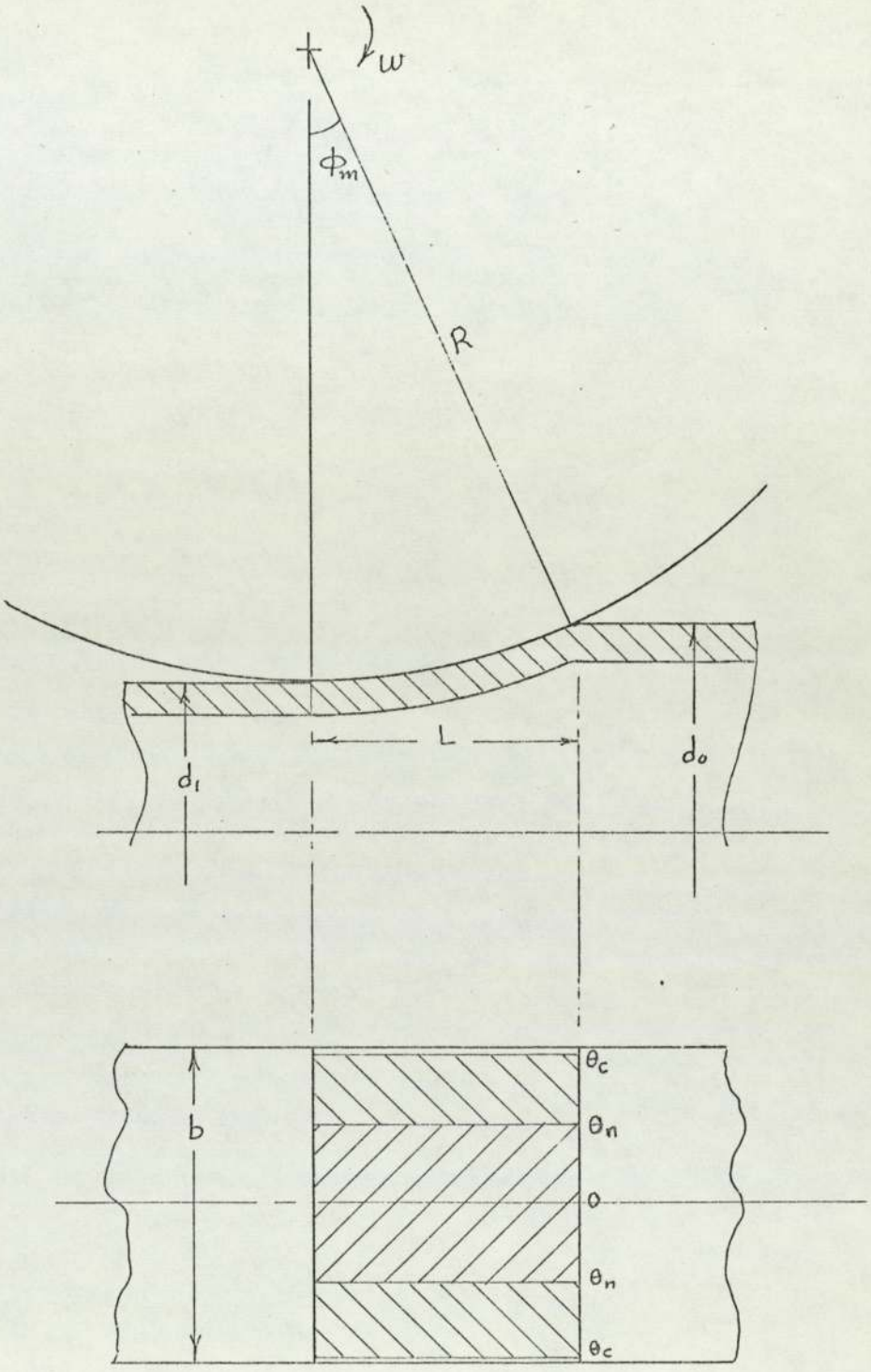

fig. (49)

$$W_{fi} = \bar{\sigma}_y (\bar{\epsilon}_A - \bar{\epsilon}_m) \qquad \text{(VI.35)}$$

but from equation (VI.16):

$$\bar{\epsilon}_A = \bar{\epsilon}_m + \bar{\epsilon}_f$$

$$W_{fi} = \bar{\sigma}_y \bar{\epsilon}_f \qquad \text{(VI.35)}$$

The next step is to determine the work of external friction forces.

If U is the tube velocity at any point on the surface of contact, making the angle ϕ with the line connecting the centres of the two rolls, then it will be assumed constant across the vertical plane passing through this point. Furthermore the variation of U with the angle of contact ϕ is assumed to be linear as shown in fig.(63-b). This makes it possible to write U in terms of ϕ and U_o, the tube velocity at entry, as follows:

$$U = U_o \left[1 + r\left(1 - \frac{\phi}{\phi_m}\right)\right] \qquad \text{(VI.36)}$$

The tangential roll velocity v is equal to $R_\theta \cdot \omega$

where $R_\theta = R_r + r_g (1 - \cos\theta)$ (VI.37)

from the geometry of fig.(11), page (51).

$$\therefore \quad V = \omega \left[R_r + r_g (1 - \cos\theta)\right] \qquad \text{(VI.38)}$$

The relative velocity between the tube and the rolls v_r is therefore:

$$v_r = V - U$$

$$= \omega \left[R_r + r_g (1 - \cos\theta)\right] - U_o \left[1 + r\left(1 - \frac{\phi}{\phi_m}\right)\right] \quad \text{(VI.39)}$$

It is clear that v_r will be negative in the first zone(1)

and positive in the second zone (2).

The rate of friction work in zone (1) is :

$$\dot{W}_{fe1} = 4 \int_s \tau \, v_r \, ds \qquad \ldots\ldots\ldots\ldots (VI.40)$$

but $\quad ds = R_r \, d\Phi \cdot r_g \, d\theta$

$$\therefore \dot{W}_{fe1} = 4 \int_0^{\Phi_m} \int_0^{\theta_n} \tau \, v_r \, R_r \, r_g \, d\Phi \, d\theta \qquad \ldots\ldots\ldots (VI.41)$$

$$= 4 \int_0^{\Phi_m} \int_0^{\theta_n} \frac{m_1 \bar{\sigma}_y}{\sqrt{3}} R_r \, r_g \left\{ \omega \left[R_r + r_g (1 - \cos\theta) \right] - U_o \left[1 + r \left(1 - \frac{\Phi}{\Phi_m} \right) \right] \right\} d\Phi \, d\theta \qquad \ldots (VI.42)$$

where m_1 is the constant friction factor in zone (1) .

After integrating and rearranging we get:

$$\dot{W}_{fe1} = \frac{4}{\sqrt{3}} m_1 \bar{\sigma}_y R_r \, r_g \, \Phi_m \, \theta_n \left[\omega \left(R_r + r_g \left(1 - \frac{\sin\theta_n}{\theta_n} \right) \right) - U_o \left(1 + \frac{r}{2} \right) \right] \qquad \ldots\ldots (VI.43)$$

putting $\quad \theta_n = \theta_c / 2$

$$\dot{W}_{fe1} = \frac{2}{\sqrt{3}} m_1 \bar{\sigma}_y R_r \, r_g \, \Phi_m \, \theta_c \left[\omega \left(R_r + r_g \left(1 - \frac{2 \sin\theta_c/2}{\theta_c} \right) \right) - U_o \left(1 + \frac{r}{2} \right) \right] \qquad \ldots\ldots\ldots (VI.44)$$

Similarly for the second zone (2) with

$$\tau = m_2 \frac{\bar{\sigma}_y}{\sqrt{3}}$$

where m_2 is the constat friction factor in zone (2) :

$$\dot{W}_{fe2} = \frac{2}{\sqrt{3}} m_2 \bar{\sigma}_y R_r \, r_g \, \Phi_m \, \theta_c \left[\omega \left[R_r + r_g \left(1 - \frac{2}{\theta_c} \left(\sin\theta_c - \sin\frac{\theta_c}{2} \right) \right) \right] - U_o \left(1 + \frac{r}{2} \right) \right] \qquad \ldots\ldots\ldots\ldots (VI.45)$$

The volume rolled per unit time is

$$\dot{V} = A_o \, U_o \qquad \ldots\ldots\ldots\ldots (VI.46)$$

putting $\quad U_o = \omega R_r$

$$\dot{V} = A_o \, R_r \, \omega \qquad \ldots\ldots\ldots\ldots (VI.47)$$

Now, the work per unit volume W_{fe} can be calculated as follows:

$$W_{fe} = \frac{\dot{W}_{fe}}{\dot{V}} = \frac{\dot{W}_{fe}}{A_o R_r \omega}$$

hence from equation (VI.44):

$$W_{fe1} = \frac{2}{\sqrt{3}} \frac{m_1 \bar{\sigma}_y r_g \phi_m \theta_c}{A_o} \left[\left(R_r + r_g \left(1 - \frac{2 \sin \theta_c/2}{\theta_c} \right) \right) - \frac{U_o}{\omega} \left(1 + \frac{r}{2} \right) \right] \quad \ldots\ldots\ldots\ldots (VI.48)$$

and from equation (VI.45):

$$W_{fe2} = \frac{2}{\sqrt{3}} \frac{m_2 \bar{\sigma}_y r_g \phi_m \theta_c}{A_o} \left[R_r + r_g \left(1 - \frac{2}{\theta_c} \left(\sin \theta_c - \sin \frac{\theta_c}{2} \right) \right) - \frac{U_o}{\omega} \left(1 + \frac{r}{2} \right) \right] \quad \ldots\ldots (VI.49)$$

Therefore the total work of the external friction forces W_{fe} per unit volume is :

$$W_{fe} = W_{fe1} + W_{fe2} \quad \ldots\ldots\ldots\ldots\ldots\ldots (VI.50)$$

and from equations (VI.48), (VI.49), and (VI.50) we get:-

$$W_{fe} = \frac{2}{\sqrt{3}} \frac{\bar{\sigma}_y r_g \phi_m \theta_c}{A_o} \left\{ m_1 \left[R_r + r_g \left(1 - \frac{2 \sin \theta_c/2}{\theta_c} \right) - \frac{U_o}{\omega} \left(1 + \frac{r}{2} \right) \right] + m_2 \left[R_r + r_g \left(1 - \frac{2}{\theta_c} \left(\sin \theta_c - \sin \frac{\theta_c}{2} \right) \right) - \frac{U_o}{\omega} \left(1 + \frac{r}{2} \right) \right] \right\} \quad \ldots\ldots\ldots\ldots (VI.51)$$

After rearranging and putting $U_o = \omega R_r$ equation (VI.51) reduces to:

$$W_{fe} = \frac{2}{\sqrt{3}} \frac{\bar{\sigma}_y r_g^2 \phi_m \theta_c m_2}{A_o} \left[\left(1 + \frac{m_1}{m_2} \right) \left(1 - \frac{r R_r}{2 r_g} \right) - \frac{2}{\theta_c} \left(\sin \theta_c - \sin \frac{\theta_c}{2} \left(1 - \frac{m_1}{m_2} \right) \right) \right] \quad \ldots\ldots (VI.52)$$

Assuming no energy losses :

$$W_{fe} = W_{fi} \quad \ldots\ldots\ldots\ldots\ldots\ldots\ldots\ldots (VI.53)$$

From equations (VI.35), and (VI.53), the frictional strain $\bar{\epsilon}_f$ is:

$$\bar{\epsilon}_f = \frac{2}{\sqrt{3}} \frac{r_g^2 \phi_m \theta_c m_2}{A_0} \left[\left(1 + \frac{m_1}{m_2}\right)\left(1 - \frac{r R_r}{2 r_g}\right) - \frac{2}{\theta_c}\left(\sin\theta_c - \sin\frac{\theta_c}{2}\left(1 - \frac{m_1}{m_2}\right)\right)\right]$$

.....(VI.54)

in the above equation, ϕ_m can be replaced by $\overset{*}{L}_m / R_r$.

Under normal rolling conditions, the frictional stress, which is assumed here to be independent of the roll pressure is likely to be the same. Therefore, the ratio m_1/m_2 will be equal to 1.0. However, since it is known that a combination of sticking and sliding friction can exist in hot rolling, it is possible to simulate this situation by giving the ratio m_1/m_2 a value other than 1.0. This would be sufficient if the frictional stress in one zone is constant but is different from that in the other zone.

The value of the shear factor itself m, if set to zero, would result in a lower bound solution where it represents the frictionless condition. When m is set at 1.0, i.e., condition of complete sticking, the resulting solution is an upper bound solution. The value of the actual roll pressure should, idealy, lie between these two limits. Avitzur [37] suggests that for actual manufacturing processes, the value of the shear factor m is usually less than 1.0 . However, if sticking does take place, as is believed to be the case in hot rolling, then the value of m would be equal to or approach 1.0.

Total Mean Roll Pressure p_m :

From equation (VI.16) the apparent strain $\bar{\epsilon}_A$ is:

$$\bar{\epsilon}_A = \bar{\epsilon}_m + \bar{\epsilon}_f$$

and $$p_m = p_h \cdot (\bar{\epsilon}_A / \bar{\epsilon}_m)$$

$$= p_h \cdot (1 + \bar{\epsilon}_f / \bar{\epsilon}_m) \qquad \text{.....(VI.55)}$$

(VI-2) Wall Thickness Variation

Previous Work:

In this section some of the published formulae for the prediction of wall-thickness variation during tube rolling will be reviewed. In section (VIII-13) of chapter(VIII), comparison will be made between test results and these theoretical predictions. This review is based on a paper by Gulyaev and Ivshin [15] in 1973.

(VI-2.1) Gun, et al

In 1958 Shveikin and Gun [39], using the theory of axially symmetric shells, worked out a formula which took the form:

$$\frac{t_o}{t_1} = \left(\frac{d_1}{d_o}\right)^{0.3} \qquad \text{(VI.56)}$$

And in 1968 Gun [40] published a new formula which he said was more accurate than the previous one [39].
The new formula took the form:

$$\frac{\delta t_i}{\delta d_i} = \frac{\lambda - a}{(1+a)} \cdot \frac{t_i - 1}{d_i - 1} \qquad \text{(VI.57)}$$

where

$\delta t_i = t_i - t_{i-1}$ is the change in wall thickness

$\delta d_i = d_{i-1} - d_i$ is the change in tube diameter.

$\lambda = 1 - 2(t_{i-1}/d_{i-1})$

$a = 3\lambda^2(1 - \gamma\sqrt{1+3\lambda^4(1-\gamma^2)}/(1-3\lambda^4\gamma^2)$

$\gamma = \frac{\sigma_x}{\sigma_y}$ coefficent of plastic tension

$= 0$ for sinking

$a = 3\lambda^2$ in the case of sinking

(VI-2.2) Shevchenko & Yurgelenas:[41] (1959)

This equation applies to stretch-reducing as well as to sinking. It includes a correction factor suggested by Gulyaev. When rearranged and reduced to the sinking form, the equation can be written in the form:

$$\frac{\delta t_i}{\delta d_i} = \frac{t_{i-1}}{d_{i-1}} \cdot \frac{\phi_i}{m_i} \frac{(1-2T_i)}{(T_i-2)} \left[1 + \frac{\phi_i}{2} \cdot \frac{1-2T_i}{T_i-2}\right] \quad \text{(VI-58)}$$

where $\phi_i = \ln \frac{d_i - t_{i-1}}{d_{i-1} - t_{i-1}}$; $T_i = \left(\frac{t_{i-1}}{d_{i-1}} + \frac{t_{i-1}}{d_i}\right)^K$

k is Gulyaev's correction factor

$= 1.57$ for two-roll mill

m_i = per-centage reduction of diameter

(VI-2.3) Kolmogorov [42] (1963)

This formula is recommended for thin-walled tubes:

$$\frac{\delta t_i}{\delta d_i} = \frac{1}{2} \frac{t_{i-1}}{d_{i-1}} \left(1 - \frac{3\gamma_i}{\sqrt{4-\gamma_i^2}}\right) \quad \text{(VI.59)}$$

where γ_i is the coefficient of plastic tension

$= 0$ for sinking

Therefore the formula takes the simple form:

$$\frac{\delta t_i}{\delta d_i} = \frac{1}{2}\,(t_{i-1}/d_{i-1}) \qquad \text{for sinking} \qquad \text{(VI.60)}$$

(VI-2.4) Anisiforov, et al [43] (1970)

The formula of Anisiforov was published in the form:

$$\delta t_i = t_{i-1}\, B\, \ln(d_i - t_{i-1}/d_{i-1} - t_{i-1}) \qquad \text{(VI.61)}$$

where:

$$B = \frac{1 - 2z_i - \alpha_i}{2 - z_i + \alpha_i} \qquad \alpha_i = n' n'' \frac{t_{i-1}}{d_{i-1}}$$

n', n'' are coefficients for the influence of friction and the free zone deformation on the value of the specific pressure (the authors recommended using $n' n'' = 1.3$)

with $z_i = 0$ for sinking

$$B = \frac{1 - \alpha_i}{2 + \alpha_i} \qquad \& \qquad \alpha_i = 1.3\,\frac{t_{i-1}}{d_{i-1}}$$

(VI-2.5) Shveikin and Ivshin [44] (1965)

Their formula has the form:

$$\frac{\delta t_i}{\delta d_i} = \frac{t_{i-1}}{d_{i-1}} \frac{1 - a(1 - t_{i-1}/d_{i-1})}{1 - 2\,t_{i-1}/d_{i-1}} \qquad \text{(VI.62)}$$

where for sinking

$$a = 0.5 + \frac{t_{i-1}}{d_{i-1}}\left(1 + 5.7\,\frac{t_{i-1}}{d_{i-1}}\right) - 0.3\,\mu\,\frac{L_i}{d_{i-1}}$$

μ is the coefficient of friction

L_i is the length of the arc of contact.

(VI-2.6) Gulyaev and Ivshin [15] (1973)

In their analysis, Gulyaev and Ivshin extend the Lyame-Gadolin [45] formula for the compression of thick-walled tubes to the conditions of tube rolling. Where a tube is axially loaded, the Lyame-Gadolin formula for the radial displacement of any point of a cross-section of the tube being deformed has the form:

$$u_r = -\frac{p r_H^2}{E(r_H^2 - r_B^2)}(1-\gamma)r + (1+\gamma)\frac{r_B}{r} - \frac{\gamma}{E}\sigma_z r \qquad \text{(VI.03)}$$

where

γ is Poisson's ratio
= 0.5

E modulus of elasticity of the tube material,

r_H & r_B outside and inside radii of the tube respectively,

p specific pressure on the outer surface of the tube which they determine from consideration of the equilibrium conditions of a half-cylinder.

As the change in wall-thickness is equal to the difference between the displacements of the outer surface of the tube and its inner surface, substitution of $r = r_g$ in Lyame-Gadolin equation produces the following equation for the change in wall-thickness:

$$\frac{\delta t_i}{\delta d_i} = C\,\frac{t_{i-1}}{d_{i-1}} \qquad \text{(VI.04)}$$

where

$$C = \frac{2\left[1 - 3\left(\frac{t_{i-1}}{d_{i-1}}\right) - 2Z_i\left(1 - 2\,\frac{t_{i-1}}{d_{i-1}}\right)\right]}{(1-Z_i)\left[1 + 3\left(1 - 2\,\frac{t_{i-1}}{d_{i-1}}\right)\right] + 2Z_i\left(1 - \frac{t_{i-1}}{d_{i-1}}\right)}$$

substitution of $z_i = 0$ for sinking gives:

$$C = \frac{2\left(1 - 3\frac{t_{i-1}}{d_{i-1}}\right)}{1+3\left(1-2\frac{t_{i-1}}{d_{i-1}}\right)^2}$$

Gulyaev and Ivshin present a chart for the calculation of coefficient C for different values of z and t/d ratios.

They claim that their new formula (VI.64) is simpler and more accurate than other existing formulae. They also claim that it covers a wider range of thickness to diameter ratios.

Comparison between Kolmogorov's expression (VI.59) and equation (VI.64) shows that Kolmogorov has given the coefficient C the value 0.5 for all values of t/d ratio. However reference to the expression for C suggested by Guylaev for the case of sinking, or to the chart, shows that for t/d ratios of between zero, and 0.15, the value of C varies between 0.5 and 0.445. As the ratio t/d increases, the deviation of C from the 0.5 figure increases according to Guylaev's expression until C takes the value of -0.7 for t/d = 0.45 It could be said therefore that for t/d of up to 0.15, i.e, for relatively thin tubes, the Kolmogorov approximation holds good in accordance with Gulyaev's work. It remains to be seen however whether they agree with the test results of the present work.

A graphical comparison between the above formulae is shown in fig. (50).

(VI-2.1) Cole [1] (1909)

Cole does not present a solution to the problem of predicting wall-thickness variation himself but shows that by comparison with test data Gun's first [39] and Yurgelenas's formulae overestimate the value of $\delta t/\delta d$. The final tube dimensions were made at points corresponding to the root of the groove. For the t_o/d_o ratio used throughout Cole's tests, which was 0.1422, most of these formulae give values of $\delta t/\delta d$ of about 0.072 (from $\delta t/\delta d$ - t_o/d_o curves in Gulyaev's paper[15]). The ratio $\delta t/\delta d$ calculated from Cole's tables of results varies between 0.321 to 0.0199 for reductions of area of 3.9% and 11.0% respectively.

(VI-2.8)

The method used for measuring the average change in wall thickness which was outlined in chapter(IV) involved the measurement of the areas made by the outer and inner contours of the cross section of the tube. The diameters of the equivalent outer and inner circles were then calculated. The wall thickness was calculated as one half the difference in diameters.

The method proposed here is based on the average change in wall thickness and the condition of constancy of volume rate.

From volume rate constancy we have:

$$A_o U_o = A_1 U_1 \qquad \text{.....(VI.65)}$$

putting $$A_o = t_o (d_o - t_o) \qquad \text{.....(VI.66)}$$

and $$A_1 = t_1 (d_1 - t_1) \qquad \text{.....(VI.67)}$$

we get

$$t_o(d_o - t_o) U_o = t_1(d_1 - t_1) U_1 \qquad \text{.....(VI.68)}$$

The error resulting from replacing d_1-t_1 by d_1-t_o in the value of d_1 is less than 1% for the small changes in the wall thickness normally resulting in one stand.

Therefore from equation (VI.68) above:

$$t_1 = \frac{(d_o/t_o - 1)t_o}{(d_1/t_o - 1)} \cdot \frac{U_o}{U_1}$$

But $U_o/U_1 = 1 - r$

$$t_1 = \frac{(d_o/t_o - 1)\, t_o}{(d_1/t_1 - 1)} \cdot (1 - r) \qquad \text{.....(VI.69)}$$

And

$$\delta_t = t_1 - t_o = t_o\left[(1-r)\,\frac{(\frac{d_o}{t_o} - 1)}{(\frac{d_1}{t_o} - 1)} - 1\right] \qquad \text{.....(VI.70)}$$

Therefore :

$$\frac{\delta_t}{\delta} = \frac{t_o}{\delta}\left[(1-r)\frac{\left(\frac{d_o}{t_o} - 1\right)}{\left(\frac{d_1}{t_o} - 1\right)} - 1\right] \qquad \text{(VI.71)}$$

This equation can only be used for relatively thin tubes ($d_o/t_o > 5.0$) since it does not predict the drop in δ_t/δ for $d_o/t_o < 5.00$ shown in fig. (50) (from reference [15]), and also observed experimentally.

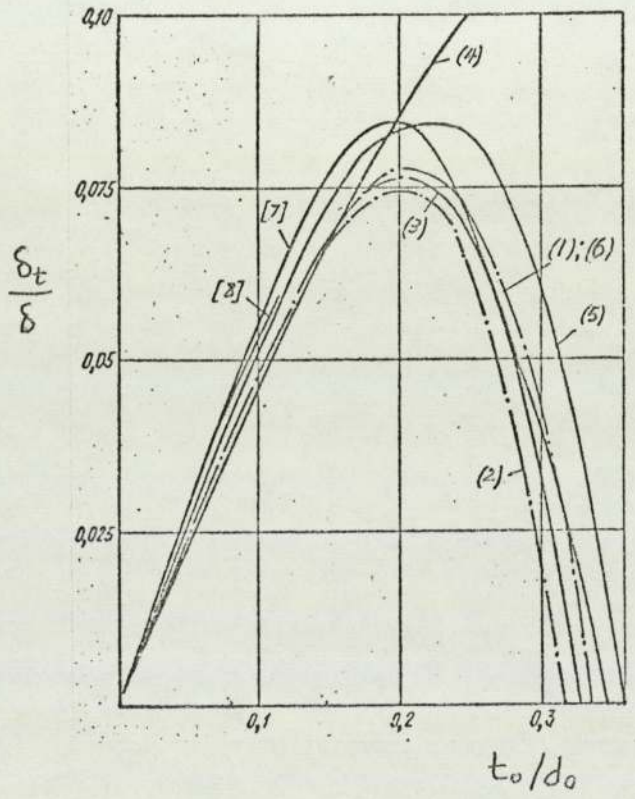

Fig. (50)

Variation in Wall Thickness for Rolling without Tension with a diameter Reduction of 5%(ref. 15) as calculated by:-

(1) Gun, 1969 (VI-2.1)
(2) Shevchenko, (VI-2.2)
(3) Kolmogorov, (VI-2.3)
(4) Anisiforov, (VI-2.4)
(5) Shveikin, (VI-2.5)
(6) Gulyaev, (VI-2.6)
[7] & [8] Test results (ref. 15)

VII

TEST RESULTS

Test Results

The test results are presented in tables (VII-1)-(VII-4) which contain all the recorded data concerning each test. The results are classified according to the test phase and type of pass as follows:-

1) tests 1 to 60 are phase one i.e,unguided sinking,of the Round-to-Oval pass type,
2) tests 61 to 67 are phase one of the Oval-to-Oval pass type.
3) tests 68 to 74 are phase two, i.e, guided sinking, of the R-O pass type
4) tests 75 to 84 are phase two of the O-O pass type,
5) tests 85 to 109 are phase three, i.e, stretch reducing of the R-O pass type, and,
6) tests 110 to 123 are phase three of the O-O pass type.

The dimensions of the test pieces before and after rolling together with the percentage reduction of area and the gap setting are included in table (VII-1).This table includes the tube dimensions measured directly from the test pieces at the root of the groove besides the mean tube dimensions measured as described in chapter IV.

Table(VII-2) "Deformation" contains the following quantities:

$\bar{\epsilon}_m$ the generalised strain,

$\bar{\sigma_y}$ (N/mm^2) the mean yield stress in uniaxial compression of the tube material,

δ_r (mm) the absolute draft at the root of the groove

δ (mm) mean draft

δ_t/δ is the ratio between the change in wall thickness δ_t and the change in diameter δ .

δ_{tr}/δ_r as above but from direct measurements at the root of the groove.

d_o/t_o tube diameter to thickness ratio before rolling

L_m (mm) measured mean length of the arc of contact corrected only for the finite width of the pin but not for torque sharing.

U_o, U_1 (mm/s) tube velocities upon entering and leaving the deformation zone respectively.

Table(VII-3) "Loads" contains the recorded loads during the rolling trials as listed below:-

1) RSF (KN) Roll separating Force

F Front loadcell reading

B Back loadcell reading

2) Torque (Nm) the rolling torque

T_u top torquemeter reading

T_1 bottom torquemeter reading

T_t total torque = $T_u + T_1$

3) Roll Pressure (N/mm^2):

p_1 recorded pressure from pin loadcell number 1

p_2 recorded pressure from pin loadcell number 2

p_3 recorded pressure from pin loadcell number 3

p_4 recorded pressure from pin loadcell number 4

p_m mean pressure = $(p_1 + p_2 + p_3 + p_4)/4$

Finally, table(VII-4) contains values of the applied front and back tensions for phase three tests , i.e, stretch reducing, both R-O and O-O passes.

A list of the relevant constants is included below:

R_r radius of roll at the root of the groove
$= 94.60$ mm

R_s radius of roll at the shroud
$= 113.45$ mm

R_m effective roll radius
$= 99.92$ mm

r_g radius of the groove
$= 23.39$ mm

h_g height of the groove (see fig.(11)on page 51)
$= 18.9$ mm

N roll speed in RPM
$= 1.590$ RPM

ω roll angular velocity
$= 0.16653\ s^{-1}$

Table (VII-1.1)

Test Results

R-0 passes

Dimensions

Unguided Sinking

Test No.	Gap setting	r %	Dimensions (mm)							
			mean values				at root of groove			
			d_o	t_o	d_1	t_1	d_{or}	t_{or}	d_{1r}	t_{1r}
1	III	0.56	43.9	2.87	42.5	2.96	44.4	2.89	40.3	3.00
2	III	2.35	43.9	2.87	42.3	2.92	44.4	2.89	40.3	2.89
3	III	0.61	43.9	2.87	42.4	2.98	44.4	2.89	40.0	3.00
4	III	2.8	43.9	6.09	42.2	6.21	44.5	6.20	40.0	6.12
5	III	3.13	43.9	6.09	42.3	6.17	44.5	6.20	40.6	6.13
6	III	3.7	43.9	6.09	42.2	6.15	44.5	6.20	40.3	6.16
7	III	3.14	43.8	9.20	42.4	9.32	44.0	9.19	40.6	9.15
8	III	3.5	43.8	9.20	42.2	9.37	44.0	9.19	40.3	9.22
9	III	3.5	43.8	9.20	42.4	9.27	44.0	9.19	40.3	9.15
10	II	3.2	43.9	2.90	41.9	2.95	43.5	2.86	39.0	2.90
11	II	3.6	43.9	2.90	41.8	2.95	43.5	2.86	38.7	2.86
12	II	4.15	43.9	2.90	41.8	2.93	43.5	2.86	38.7	2.90
13	II	3.2	43.9	2.90	41.9	2.95	44.0	2.82	38.8	2.92
14	II	4.1	43.9	2.87	41.5	2.93	44.3	2.79	39.1	2.88
15	II	3.5	43.9	2.87	41.5	2.94	44.3	2.79	39.1	3.00
16	II	4.2	43.9	2.87	41.4	2.93	44.3	2.79	39.1	2.62
17	II	3.58	43.9	6.06	42.0	6.20	44.0	6.13	39.5	6.16
18	II	3.07	43.9	6.06	41.9	6.25	44.0	6.13	39.4	6.13
19	II	3.28	43.9	6.06	41.8	6.24	44.0	6.13	39.4	6.29
20	II	4.95	44.0	6.14	41.5	6.29	44.3	6.31	38.8	6.31

Table(VII-1.1) (contd.)

Test Results

R-O passes

Dimensions

Unguided Sinking

Test No.	Gap setting	r %	Dimensions (mm)							
			mean values				at root of groove			
			d_o	t_o	d_1	t_1	d_{or}	t_{or}	d_{1r}	t_{1r}
21	II	4.85	44.0	6.14	41.4	6.30	44.3	6.31	39.1	6.38
22	II	5.3	44.0	6.14	41.4	6.27	44.3	6.31	39.1	6.27
23	II	3.4	43.8	6.38	41.5	6.61	43.6	6.41	39.4	6.48
24	II	4.1	43.8	6.38	41.5	6.55	43.6	6.41	39.4	6.48
25	II	3.6	44.0	6.60	41.7	6.82	44.2	6.54	38.8	6.56
26	II	3.6	44.0	6.60	41.7	6.82	44.2	6.54	38.8	6.56
27	II	3.6	44.0	6.60	41.7	6.82	44.2	6.54	38.8	6.56
28	II	3.58	43.9	6.06	42.0	6.20	44.0	6.04	39.5	6.06
29	II	5.68	43.9	9.21	41.7	9.31	43.5	9.03	39.1	9.12
30	II	4.93	43.9	9.21	42.0	9.30	43.5	9.03	39.7	9.35
31	II	5.96	43.9	9.21	41.7	9.28	43.5	9.03	39.0	9.03
32	II	5.6	43.8	9.22	41.5	9.37	44.0	9.23	38.8	9.31
33	II	6.5	43.8	9.22	41.2	9.35	44.0	9.23	38.5	9.00
34	II	6.5	43.8	9.22	41.2	9.33	44.0	9.23	38.8	8.85
35	I	4.8	43.9	2.92	40.9	3.02	43.7	2.73	37.9	2.98
36	I	7.03	43.9	2.93	40.6	2.95	43.7	2.73	38.2	2.96
37	I	5.32	43.9	2.92	41.1	2.97	43.7	2.73	38.0	2.88
38	I	5.32	43.9	2.92	41.1	2.97	43.7	2.73	38.0	2.88
39	I	6.06	44.0	2.90	41.0	2.95	44.0	2.82	38.2	2.85
40	I	6.77	43.9	2.90	40.8	2.87	44.0	2.82	37.5	2.85

Table(VII-1.1) (contd.)

Test Results

R-O passes

Dimensions

Unguided Sinking

Test No.	Gap setting	r %	Dimensions (mm)							
			mean values				at root of groove			
			d_o	t_o	d_1	t_1	d_{or}	t_{or}	d_{1r}	t_{1r}
41	I	4.8	43.9	2. 92	40.9	3.02	44.0	2.82	39.5	3.00
42	I	4.8	43.9	2.92	40.9	3.02	44.0	2.82	39.5	3.00
43	I	6.76	44.0	6.15	40.9	6.26	44.3	6.31	39.0	6.33
44	I	6.76	44.0	6.15	40.9	6.26	44.0	6.15	38.3	6.18
45	I	5.6	43.9	6.51	40.9	6.73	44.0	6.50	37.5	6.54
46	I	7.3	43.9	6.51	40.8	6.60	44.0	6.50	37.7	6.50
47	I	5.5	43.9	6.10	40.8	6.33	44.2	6.15	37.5	6.15
48	I	5.5	43.9	6.10	40.8	6.33	44.2	6.15	37.5	6.18
49	I	5.5	43.9	6.10	40.8	6.33	44.2	6.15	37.7	6.19
50	I	6.76	44.0	6.15	40.9	6.26	44.0	6.04	37.5	6.06
51	I	6.57	44.0	6.15	40.9	6.26	44.0	6.04	38.2	6.15
52	I	6.4	43.6	6.15	40.9	6.27	44.0	6.04	37.7	6.05
53	I	6.4	43.6	6.15	40.9	6.27	44.0	6.04	38.2	6.15
54	I	6.76	44.0	6.15	40.9	6.26	44.0	6.04	37.5	6.06
55	I	7.2	43.8	9.13	40.8	9.33	43.3	8.94	37.8	8.85
56	I	7.7	43.8	9.20	40.8	9.33	44.0	9.08	38.2	9.08
57	I	8.0	43.8	9.20	40.8	9.28	44.0	9.08	37.8	8.92
58	I	7.6	43.8	9.20	40.9	9.33	44.0	9.08	37.8	8.96
59	I	6.04	43.5	9.09	40.8	9.30	44.0	9.08	37.8	8.96
60	I	6.6	43.7	9.05	40.8	9.29	43.3	8.94	37.8	8.85

Table(VII-1.2)

Test Results

0-0 passes

Dimensions

Unguided Sinking

Test No.	Gap setting	r %	Dimensions (mm)							
			mean values				at root of groove			
			d_o	t_o	d_1	t_1	d_{or}	t_{or}	d_{1r}	t_{1r}
61	II	1.9	41.5	6.61	40.3	6.73	43.6	6.41	38.2	6.67
62	II	0.63	41.7	6.52	40.5	6.75	38.8	6.56	38.0	6.60
63	I	2.4	40.9	6.27	39.7	6.38	37.7	6.05	37.2	6.12
64	I	2.3	40.9	6.26	39.7	6.38	37.7	6.05	37.2	6.12
65	II	1.98	41.8	6.24	40.6	6.34	39.4	6.29	38.8	6.46
66	I	3.9	40.8	9.29	39.2	9.46	37.8	8.85	37.5	8.92
67	II	3.5	41.2	9.33	39.9	9.42	43.5	9.03	38.5	9.55

Table(VII-1.3)

Test Results

R-0 passes

Dimensions

Guided Sinking

Test No.	Gap setting	r %	Dimensions (mm)							
			mean values				at root of groove			
			d_o	t_o	d_1	t_1	d_{or}	t_{or}	d_{1r}	t_{1r}
68	II	5.14	44.0	6.13	41.38	6.28	44.0	6.15	39.4	6.16
69	II	5.14	44.0	6.13	41.38	6.29	44.0	6.15	39.4	6.16
70	II	5.14	44.0	6.13	41.38	6.29	44.0	6.15	39.4	6.16
71	I	4.48	43.65	2.88	40.8	2.96	44.0	2.82	39.5	3.00
72	I	3.78	43.7	2.88	40.8	2.99	44.6	2.90	37.8	2.95
73	I	3.78	43.7	2.88	40.8	2.99	44.6	2.90	37.8	2.95
74	I	7.78	43.8	9.25	40.8	9.36	44.3	9.23	37.9	9.25

Table(VII-1.4)

Test Results

0-0 passes

Dimensions

Guided Sinking

Test No.	Gap setting	r %	Dimensions (mm)							
			mean values				at root of groove			
			d_o	t_o	d_1	t_1	d_{or}	t_{or}	d_{1r}	t_{1r}
75	I	2.92	41.9	6.36	40.4	6.46	39.1	6.15	36.9	6.46
76	I	2.92	41.9	6.36	40.4	6.46	39.1	6.15	36.9	6.46
77	I	3.24	41.7	9.35	40.5	9.43	40.5	8.92	37.2	8.96
78	I	3.24	41.7	9.35	40.5	9.43	40.5	8.92	37.2	8.96
79	I	2.79	40.82	9.36	39.7	9.49	40.8	9.08	37.5	9.09
80	I	2.79	40.82	9.36	39.7	9.49	40.8	9.08	37.5	9.09
81	I	1.51	39.7	9.49	39.1	9.56	39.7	9.09	38.2	9.11
82	I	1.51	39.7	9.49	39.1	9.56	39.7	9.09	38.2	9.11
83	I	0.22	39.1	9.56	38.8	9.66	39.1	9.08	38.2	9.11
84	I	0.22	39.1	9.56	38.8	9.66	39.1	9.08	38.2	9.11

Table(VII-1.5)

Test Results

R-O passes

Dimensions

Stretch-Reducing

Test No.	Gap setting	r %	Dimensions (mm)							
			mean values				at root of groove			
			d_o	t_o	d_1	t_1	d_{or}	t_{or}	d_{1r}	t_{1r}
85	II	4.71	43.9	2.92	44.4	2.97	44.0	2.82	38.8	2.92
86	II	4.71	43.9	2.92	44.4	2.97	44.0	2.82	38.8	2.92
87	II	5.3	44.0	6.13	41.9	6.16	44.0	6.15	39.1	6.15
88	II	5.3	44.0	6.13	41.9	6.16	44.0	6.15	39.1	6.15
89	II	5.26	43.8	9.20	41.6	9.35	44.0	9.13	39.1	9.00
90	II	5.26	43.8	9.20	41.6	9.35	44.0	9.13	39.1	9.00
91	II	5.26	43.8	9.20	41.7	9.31	44.0	9.13	39.4	9.23
92	II	5.0	43.8	9.20	41.7	9.35	44.0	9.13	39.0	8.92
93	II	5.0	43.8	9.20	41.7	9.35	44.0	9.13	39.0	8.92
94	II	5.0	43.8	9.20	41.7	9.35	44.0	9.13	39.0	8.92
95	I	6.94	43.9	2.92	40.9	2.94	44.0	2.82	38.14	2.92
96	I	7.0	43.9	2.98	40.9	2.99	43.4	2.88	38.14	2.92
97	I	7.0	43.9	2.98	40.9	2.99	43.4	2.88	38.14	2.92
98	I	6.46	43.9	2.98	40.8	3.02	44.0	2.82	37.8	3.08
99	I	6.46	43.9	2.98	40.8	3.02	44.0	2.82	37.8	3.08
100	I	7.97	43.9	2.92	40.8	2.91	44.0	2.82	37.5	2.88
101	I	7.97	43.9	2.92	40.8	2.91	44.0	2.82	37.5	2.88
102	I	7.97	43.9	2.92	40.8	2.91	44.0	2.82	37.5	2.88
103	I	7.97	43.9	2.92	40.8	2.91	44.0	2.82	37.5	2.88
104	I	7.5	44.0	6.13	40.9	6.19	44.0	6.15	38.1	6.16

Table(VII-1.5) (contd.)

Test Results

R-O passes

Dimensions

Stretch-Reducing

Test No.	Gap setting	r %	Dimensions (mm)							
			mean values				at root of groove			
			d_o	t_o	d_1	t_1	d_{or}	t_{or}	d_{1r}	t_{1r}
105	I	7.5	44.0	6.13	40.9	6.19	44.0	6.15	38.14	6.16
106	I	6.23	43.8	6.13	40.9	6.26	44.0	3.00	38.2	6.23
107	I	6.23	43.8	6.13	40.9	6.26	44.0	3.00	38.2	6.23
108	I	10.29	43.8	9.20	40.2	9.20	44.0	9.39	38.2	9.15
109	I	10.29	43.8	9.20	40.2	9.20	44.0	9.39	38.2	9.15

Table(VII-1.6)

Test Results

0-0 passes

Dimensions — Stretch-Reducing

Test No.	Gap setting	r %	Dimensions (mm)							
			mean values				at root of groove			
			d_o	t_o	d_1	t_1	d_{or}	t_{or}	d_{1r}	t_{1r}
110	II	2.33	41.9	6.16	40.5	6.27	41.89	6.15	38.5	6.18
111	II	2.33	41.9	6.16	40.5	6.27	41.89	6.15	38.5	6.18
112	II	2.33	41.9	6.16	40.5	6.27	41.89	6.15	38.5	6.18
113	II	2.33	41.9	6.16	40.5	6.27	41.89	6.15	38.5	6.18
114	II	2.96	41.9	9.39	41.1	9.33	41.88	9.0	38.8	9.13
115	II	2.96	41.9	9.39	41.1	9.33	41.88	9.0	38.8	9.13
116	I	2.24	40.8	2.90	40.33	2.87	40.79	3.08	36.6	3.00
117	I	2.24	40.8	2.90	40.3	2.87	40.79	3.08	36.6	3.00
118	I	1.85	40.4	6.46	40.4	6.32	40.44	6.46	39.1	6.48
119	I	1.85	40.4	6.46	40.4	6.32	40.44	6.46	39.1	6.48
120	I	0.99	40.9	6.26	40.3	6.33	40.89	6.23	38.2	6.69
121	I	0.99	40.9	6.26	40.3	6.33	40.89	6.23	38.2	6.69
122	I	3.32	40.5	9.43	39.4	9.44	40.45	8.96	37.2	9.15
123	I	3.32	40.5	9.43	39.4	9.44	40.45	8.96	37.2	9.15

Test Results

R-0 passes

Deformation — Unguided Sinking

Test No.	$\bar{\epsilon}_m$	σ_y (N/mm^2)	δ_r (mm)	δ (mm)	$\frac{\delta_t}{\delta}$	$\frac{\delta_{tr}}{\delta_r}$	$\frac{d_o}{t_o}$	L_m (mm)	Velocities (mm/s) U_o	Velocities (mm/s) U_1
1	0.040	11.72	4.10	1.40	0.065	0.027	15.4	11.9	16.4	16.8
2	0.041	11.76	4.10	1.60	0.030	0.00	15.4	14.2	16.1	16.8
3	0.045	11.89	4.10	1.56	0.067	0.027	15.4	14.6	16.5	16.8
4	0.048	11.98	4.50	1.63	0.070	0.018	7.2	10.2	16.3	17.0
5	0.046	11.92	3.90	1.55	0.049	0.021	7.2	9.8	16.2	17.0
6	0.047	11.95	4.25	1.68	0.036	0.009	7.2	11.0	16.2	17.0
7	0.046	11.92	3.40	1.40	0.085	0.012	4.8	11.9	16.2	16.7
8	0.054	12.15	3.70	1.62	0.100	0.008	4.8	12.9	16.2	16.7
9	0.046	11.92	3.70	1.40	0.049	0.011	4.8	11.8	16.2	16.7
10	0.052	12.10	4.50	2.03	0.025	0.009	15.2	14.6	16.5	17.0
11	0.056	12.21	4.80	2.13	0.025	0.00	15.2	16.0	16.5	17.0
12	0.057	12.23	4.80	2.11	0.016	0.008	15.2	15.5	16.5	17.0
13	0.052	12.10	5.20	2.00	0.025	0.019	15.1	14.8	16.5	—
14	0.063	12.38	5.20	2.41	0.025	0.017	15.3	18.1	16.3	17.3
15	0.062	12.36	5.20	2.39	0.029	0.040	15.3	18.3	16.3	17.2
16	0.066	12.45	5.20	2.51	0.024	0.033	15.3	17.8	16.3	17.2
17	0.058	12.26	4.50	1.96	0.073	0.007	7.3	15.9	16.4	17.0
18	0.061	12.33	4.60	2.06	0.091	0.00	7.3	13.7	16.4	17.0
19	0.063	12.38	4.60	2.13	0.086	0.035	7.3	13.4	16.4	17.0
20	0.076	12.66	5.50	2.57	0.057	0.00	7.2	17.2	16.2	17.1

Table(VII-2.1) (contd.)

Test Results

R-O passes

Deformation — Unguided Sinking

Test No.	$\bar{\epsilon}_m$	σ_y (N/mm^2)	δ_r (mm)	δ (mm)	$\frac{\delta_t}{\delta}$	$\frac{\delta_{tr}}{\delta_r}$	$\frac{d_o}{t_o}$	L_m (mm)	Velocities (mm/s)	
									U_o	U_1
21	0.077	12.68	5.20	2.60	0.063	0.013	7.2	15.5	16.2	17.1
22	0.078	12.70	5.20	2.63	0.051	0.008	7.2	16.2	16.2	17.1
23	0.072	12.57	4.20	2.30	0.100	0.017	6.9	14.3	16.4	—
24	0.07	12.54	4.20	2.32	0.074	0.017	6.9	13.7	16.2	—
25	0.08	12.73	5.40	2.33	0.096	0.004	6.7	14.0	16.5	—
26	0.07	12.54	5.40	2.31	0.096	0.004	6.7	12.5	16.3	—
27	0.07	12.54	5.40	2.31	0.096	0.004	6.7	11.8	15.8	—
28	0.061	12.33	4.50	2.03	0.074	0.004	7.2	15.9	16.4	17.0
29	0.074	12.62	4.4	2.22	0.046	0.02	4.8	12.1	16.0	17.0
30	0.065	12.43	3.8	1.94	0.048	0.084	4.8	12.1	16.0	17.0
31	0.076	12.66	4.50	2.24	0.031	0.0	4.8	11.3	16.0	17.0
32	0.078	12.70	5.20	2.30	0.07	0.015	4.8	14.3	16.1	17.3
33	0.087	12.87	5.50	2.56	0.05	0.042	4.8	14.4	16.1	17.3
34	0.085	12.83	5.20	2.51	0.043	0.073	4.8	13.6	16.1	17.3
35	0.081	12.76	5.80	3.07	0.033	0.043	15.0	19.3	16.0	—
36	0.092	12.96	5.50	3.33	0.009	0.044	15.0	18.5	16.3	—
37	0.076	12.66	5.70	2.82	0.018	0.026	15.0	18.1	16.3	—
38	0.076	12.66	5.70	2.82	0.018	0.026	15.0	19.4	16.5	—
39	0.082	12.78	5.80	3.00	0.017	0.005	15.2	18.5	16.2	—
40	0.084	12.81	6.50	2.95	0.01	0.005	15.1	18.2	—	—

Table(VII-2.1) (contd.)

Test Results

R-O passes

Deformation — Unguided Sinking

Test No.	$\bar{\epsilon}_m$	$\bar{\sigma}_y$ (N/mm²)	δ_r (mm)	δ (mm)	$\frac{\delta_t}{\delta}$	$\frac{\delta_{tr}}{\delta_r}$	$\frac{d_o}{t_o}$	L_m (mm)	Velocities (mm/s)	
									U_o	U_1
41	0.081	12.76	4.50	3.00	0.033	0.040	15.0	18.8	15.8	—
42	0.081	12.76	4.50	3.00	0.033	0.040	15.0	18.8	15.8	—
43	0.093	12.97	5.30	3.10	0.035	0.004	7.2	18.1	16.0	—
44	0.094	12.99	5.70	3.11	0.035	0.005	7.2	16.8	15.9	—
45	0.092	12.96	6.50	3.03	0.073	0.006	6.7	16.3	16.15	—
46	0.096	13.02	6.30	3.10	0.029	0.00	6.7	16.1	16.2	—
47	0.080	12.74	6.70	3.12	0.074	0.00	7.2	16.0	16.1	—
48	0.080	12.74	6.70	3.12	0.074	0.004	7.2	15.6	16.0	—
49	0.080	12.74	6.50	3.12	0.074	0.006	7.2	16.7	16.1	—
50	0.093	12.97	5.80	3.03	0.039	0.019	7.1	18.1	16.2	17.2
51	0.091	12.94	5.80	3.03	0.039	0.019	7.1	18.1	16.2	17.2
52	0.090	12.92	6.30	2.99	0.047	0.002	7.1	16.8	16.2	17.2
53	0.090	12.92	6.30	2.99	0.047	0.002	7.1	16.8	16.2	17.2
54	0.093	12.97	6.50	3.10	0.035	0.003	7.2	19.6	15.6	—
55	0.101	13.10	5.50	3.00	0.067	0.016	4.8	16.4	15.9	16.8
56	0.102	13.12	5.80	2.98	0.043	0.0	4.8	16.3	15.9	—
57	0.102	13.12	6.20	2.97	0.021	0.026	4.8	16.3	15.9	—
58	0.100	13.09	6.20	2.93	0.043	0.019	4.8	17.8	16.0	—
59	0.091	12.94	6.20	2.69	0.078	0.01	4.8	17.8	16.0	—
60	0.098	13.05	5.50	2.9	0.083	0.016	4.8	16.5	15.9	—

Table(VII-2.2)

Test Results

0-0 passes

Deformation — Unguided Sinking

Test No.	$\bar{\epsilon}_m$	σ_y (N/mm^2)	δ_r (mm)	δ (mm)	$\frac{\delta_t}{\delta}$	$\frac{\delta_{tr}}{\delta_r}$	$\frac{d_o}{t_o}$	L_m (mm)	Velocities (mm/s)	
									U_o	U_1
61	0.037	11.61	5.40	1.13	0.100	0.048	6.3	16.9	-	-
62	0.044	11.86	0.80	1.18	0.192	0.050	6.4	17.2	16.2	-
63	0.041	11.76	0.50	1.28	0.087	1.740	6.5	13.1	15.4	-
64	0.041	11.76	5.80	1.20	0.100	0.016	6.5	11.2	15.5	-
65	0.060	11.58	0.60	1.17	0.085	0.283	6.7	10.4	15.8	-
66	0.060	12.31	0.30	1.61	0.106	0.233	4.4	14.9	15.7	-
67	0.048	11.98	5.0	1.34	0.070	0.102	4.4	15.2	15.5	-

Table(VII-2.3)

Test Results

R-O passes

Deformation — Guided Sinking

Test No.	$\bar{\epsilon}_m$	σ_y (N/mm^2)	δ_r (mm)	δ (mm)	$\frac{\delta_t}{\delta}$	$\frac{\delta_{tr}}{\delta_r}$	$\frac{d_o}{t_o}$	L_m (mm)	Velocities (mm/s)	
									U_o	U_1
68	0.078	12.70	4.60	2.62	0.057	0.002	7.2	13.36	16.09	17.06
69	0.078	12.70	4.60	2.62	0.057	0.002	7.2	13.84	16.09	17.06
70	0.078	12.70	4.60	2.62	0.057	0.002	7.2	14.16	16.09	17.06
71	0.075	12.64	4.50	2.83	0.028	0.040	15.2	20.8	14.3	-
72	0.073	12.60	6.80	2.85	0.038	0.007	15.2	18.9	16.08	16.83
73	0.073	12.60	6.80	2.85	0.038	0.007	15.2	20.1	16.08	16.83
74	0.101	13.10	6.40	2.96	0.037	0.003	4.7	16.8	—	17.30

Table(VII-2.4)

Test Results

0-0 passes

Deformation — Guided Sinking

Test No.	$\bar{\epsilon}_m$	$\bar{\sigma_y}$ (N/mm^2)	δ_r (mm)	δ (mm)	$\frac{\delta_t}{\delta}$	$\frac{\delta_{tr}}{\delta_r}$	$\frac{d_o}{t_o}$	L_m (mm)	Velocities (mm/s) U_o	U_1
75	0.045	11.89	2.18	1.45	0.069	0.142	6.6	9.49	16.06	16.37
76	0.045	11.89	2.18	1.45	0.069	0.142	6.6	10.55	16.06	16.37
77	0.044	11.89	3.30	1.23	0.065	0.012	4.5	13.96	16.17	16.69
78	0.044	11.89	3.30	1.23	0.065	0.012	4.5	11.66	16.17	16.69
79	0.043	11.83	3.30	1.16	0.112	0.003	4.4	13.03	16.8	17.15
80	0.043	11.83	3.30	1.16	0.112	0.003	4.4	14.86	16.8	17.15
81	0.023	10.97	1.50	0.60	0.117	0.013	4.2	12.30	15.9	16.29
82	0.023	10.97	1.50	0.60	0.117	0.013	4.2	11.92	15.9	16.29
83	0.014	10.34	0.90	0.27	0.370	0.033	4.10	9.10	16.1	16.36
84	0.014	10.34	0.90	0.27	0.370	0.033	4.10	9.55	16.1	16.36

Table(VII-2.5)

Test Results

R-O passes

Deformation — Stretch-Reducing

Test No.	$\bar{\epsilon}_m$	σ_y (N/mm^2)	δ_r (mm)	δ (mm)	$\frac{\delta_t}{\delta}$	$\frac{\delta_{tr}}{\delta_r}$	$\frac{d_o}{t_o}$	L_m (mm)	Velocities (mm/s) U_o	Velocities (mm/s) U_1
85	0.067	12.47	5.20	2.5	0.02	0.019	15.0	16.11	15.5	16.57
86	0.067	12.47	5.20	2.51	0.02	0.019	15.0	13.45	15.5	16.57
87	0.065	12.43	4.90	2.11	0.014	0.0	7.2	13.68	15.52	16.64
88	0.065	12.43	4.90	2.11	0.014	0.0	7.2	13.24	15.52	16.64
89	0.073	12.60	4.90	2.18	0.069	0.03	4.8	14.39	15.63	-
90	0.073	12.60	4.90	2.18	0.069	0.03	4.8	13.58	15.63	-
91	0.070	12.54	4.60	2.08	0.053	0.02	4.8	14.64	16.52	-
92	0.070	12.54	5.00	2.10	0.071	0.042	4.8	13.64	15.40	17.15
93	0.070	12.54	5.00	2.10	0.071	0.042	4.8	12.81	15.40	17.15
94	0.070	12.54	5.00	2.10	0.071	0.042	4.8	13.20	15.40	17.15
95	0.086	12.85	6.50	3.03	0.007	0.005	15.0	18.3	-	18.1
96	0.086	12.85	5.30	3.01	.003	0.008	14.7	18.3	17.1	17.9
97	0.086	12.85	5.30	3.01	0.003	0.008	14.7	19.1	17.1	17.9
98	0.085	12.83	6.20	3.09	0.013	0.042	14.7	17.8	-	17.8
99	0.085	12.83	6.20	3.09	0.013	0.042	14.7	15.8	-	17.8
100	0.094	12.99	6.50	3.15	0.003	0.009	15.0	19.6	-	-
101	0.094	12.99	6.50	3.15	0.003	0.009	15.0	16.4	-	-
102	0.094	12.99	6.50	3.15	0.003	0.009	15.0	15.2	-	-
103	0.094	12.99	6.50	3.16	0.003	0.009	15.0	16.8	-	-
104	0.096	13.02	5.90	3.12	0.019	0.002	7.2	17.3	16.2	-

Table(VII-2.5) (contd.)

Test Results

R-O passes

Deformation — Stretch-Reducing

Test No.	$\bar{\epsilon}_m$	σ_y (N/mm^2)	δ_r (mm)	δ (mm)	$\frac{\delta_t}{\delta}$	$\frac{\delta_{tr}}{\delta_r}$	$\frac{d_o}{t_o}$	L_m (mm)	Velocities (mm/s)	
									U_o	U_1
105	0.096	13.02	5.90	3.12	0.019	0.002	7.2	16.40	16.2	-
106	0.089	12.90	5.80	2.95	0.044	0.014	14.8	13.26	17.06	-
107	0.089	12.90	5.80	2.95	0.044	0.014	14.8	17.51	17.06	-
108	0.125	13.44	5.80	3.55	0.00	0.041	4.8	16.48	17.01	18.3
109	0.125	13.44	5.80	3.55	0.00	0.041	4.8	18.36	17.01	18.3

Table(VII-2.6)

Test Results

0-0 passes

Deformation — Stretch-Reducing

Test No.	$\bar{\epsilon}_m$	σ_y (N/mm^2)	δ_r (mm)	δ (mm)	$\frac{\delta_t}{\delta}$	$\frac{\delta_{tr}}{\delta_r}$	$\frac{d_o}{t_o}$	L_m (mm)	Velocities (mm/s)	
									U_o	U_1
110	0.042	11.79	3.39	1.345	0.08	0.009	6.8	17.29	-	-
111	0.042	11.79	3.39	1.345	0.08	0.009	6.8	15.37	-	-
112	0.042	11.79	3.39	1.345	0.08	0.009	6.8	16.40	-	-
113	0.042	11.79	3.39	1.345	0.08	0.009	6.8	14.86	-	-
114	0.032	11.41	3.08	0.83	0.072	0.042	4.5	13.5	14.93	16.83
115	0.032	11.41	3.08	0.83	0.072	0.04	4.5	13.13	14.93	16.83
116	0.023	10.95	4.19	0.446	0.067	0.02	14.1	11.66	16.54	17.02
117	0.023	10.95	4.19	0.446	0.07	0.02	14.1	9.68	16.54	17.02
118	0.024	11.03	1.34	0.015	9.33	0.015	6.3	11.47	16.1	16.26
119	0.024	11.03	1.34	0.015	9.33	0.015	6.3	11.47	16.1	16.26
120	0.020	10.79	2.69	0.63	0.011	0.171	6.5	11.86	-	-
121	0.020	10.79	2.69	0.63	0.011	0.171	6.5	12.68	-	-
122	0.039	11.69	3.25	1.05	0.010	0.058	4.3	13.64	15.46	-
123	0.039	11.69	3.25	1.05	0.010	0.058	4.3	13.58	15.46	-

Table(VII-3.1)

Test Results

R-0 passes

Loads

Unguided Sinking

Test No.	RSF (kN)			Torque (Nm)			Roll Pressure (N/ mm^2)				
	F	B	Tot.	T_u	T_1	T_t	p_1	p_2	p_3	p_4	p_m
1	1.15	1.11	2.25	26.0	40.7	66.7	4.33	3.87	4.65	5.54	4.60
2	1.19	1.03	2.22	19.2	43.5	62.7	4.62	3.10	5.81	5.87	4.85
3	1.19	1.03	2.22	31.6	37.3	68.9	3.88	3.94	5.87	5.32	4.75
4	2.61	2.72	5.33	66.7	80.2	146.9	5.31	5.05	8.96	4.99	6.07
5	2.76	2.72	5.48	65.5	83.6	149.1	4.57	5.60	7.46	4.37	5.50
6	2.65	2.65	5.30	74.6	67.8	142.4	5.21	4.29	7.42	8.18	6.27
7	5.07	4.86	9.93	132.2	121.5	253.7	6.80	9.12	12.41	2.72	9.44
8	4.91	4.71	9.62	100	155.4	255.4	7.38	9.53	12.53	NC	9.81
9	4.76	4.57	9.33	85.9	157.1	24.3	8.32	10.3	13.65	NC	10.76
10	1.38	1.25	2.63	32.8	48.0	80.8	3.84	3.96	5.54	5.7	4.76
11	1.50	1.36	2.86	38.9	49.7	88.7	3.79	4.43	5.29	5.19	4.67
12	1.46	1.44	2.90	40.7	49.2	89.9	4.99	4.27	5.21	4.03	4.62
13	1.32	1.21	2.52	39.0	35.6	74.6	4.90	3.97	5.28	6.72	5.22
14	1.77	1.62	3.39	45.2	59.9	105.1	5.27	4.55	5.43	4.67	4.98
15	1.81	1.69	3.50	51.4	58.8	110.2	5.01	4.29	4.79	3.52	4.40
16	1.81	1.69	3.50	51.4	57.1	108.5	5.05	4.52	4.87	3.77	4.55
17	3.53	3.46	6.99	98.3	101.7	200	6.35	NC	7.59	8.15	7.36
18	3.61	3.50	7.11	90.4	110.7	201	5.95	7.12	7.99	9.02	7.52
19	3.53	3.39	6.92	92.1	101.7	194	5.45	7.09	7.90	8.64	7.27
20	4.03	3.87	8.90	103	130	233	6.38	6.07	9.09	6.21	6.94

Table(VII-3.1) (contd.)

Test Results

R-0 passes

Loads

Unguided Sinking

Test No.	RSF (kN)			Torque (Nm)			Roll Pressure (N/ mm^2)				
	F	B	Tot.	T_u	T_l	T_t	p_1	p_2	p_3	p_4	p_m
21	4.07	3.75	7.82	77.9	153.7	231.7	6.20	7.92	8.60	8.87	7.89
22	4.03	3.87	7.90	90.4	143.0	233.4	5.30	6.52	8.68	8.40	7.22
23	2.46	3.23	5.69	77.4	105.3	182.7	5.01	4.94	8.18	7.72	6.46
24	2.49	2.76	5.25	71.8	93.2	165.0	4.71	4.42	6.19	9.10	6.11
25	2.55	2.82	5.37	58.8	98.3	157.1	5.32	5.01	7.91	8.98	6.81
26	2.49	2.76	5.25	68.9	87.6	156.5	5.32	5.75	7.74	8.21	6.76
27	2.88	2.65	5.53	61.6	88.1	149.7	5.95	6.40	9.72	5.60	6.92
28	3.11	3.42	6.53	92.1	118.7	210.8	4.83	4.24	5.72	6.79	5.40
29	5.60	4.78	10.4	85.9	210.2	296.1	7.13	9.24	12.5	6.92	8.95
30	5.53	4.93	10.5	106	177.4	284	7.61	8.24	11.2	2.83	9.02
31	5.53	5.01	10.5	106	191.9	298.1	6.95	8.81	12.2	4.14	9.32
32	6.03	5.52	11.6	106	228.5	338.7	6.63	9.23	11.75	12.7	10.07
33	5.91	5.71	11.6	137.3	191.9	329	6.58	9.17	11.7	12.6	10.01
34	5.60	5.97	11.6	143.5	191.9	335.4	6.43	9.29	11.2	8.40	8.89
35	1.77	1.73	3.50	63.3	41.8	105.1	5.03	4.00	5.53	6.37	5.23
36	1.88	1.84	3.72	63.9	66.7	130.6	4.08	3.93	5.40	6.59	5.00
37	2.03	1.99	4.02	58.5	81.6	140.1	4.19	3.17	5.34	4.81	4.38
38	1.94	1.82	3.76	50.5	80.5	131.0	4.76	4.34	4.60	4.01	4.45
39	2.17	1.84	4.01	50.9	73.5	124.4	5.07	4.23	5.27	5.58	5.04
40	2.18	1.85	4.03	55.4	66.1	121.5	5.30	4.13	5.29	5.79	5.14

Table(VII-3.1) (contd.)

Test Results

R-0 passes

Loads

Unguided Sinking

Test No.	RSF (kN)			Torque (Nm)			Roll Pressure (N/ mm^2)				
	F	B	Tot.	T_u	T_l	T_t	p_1	p_2	p_3	p_4	p_m
41	1.85	1.79	3.64	53.1	59.3	112.4	4.91	3.96	5.50	8.52	5.72
42	1.75	1.73	3.48	50.9	56.8	107.7	5.04	4.10	5.38	6.64	5.29
43	2.94	3.56	6.50	84.8	130.0	214.8	4.86	5.58	5.31	7.17	5.73
44	3.05	3.40	6.45	98.0	117.8	215.8	5.20	4.53	6.63	11.14	6.70
45	3.40	3,63	7.03	85.9	135.6	221.5	4.63	5.15	8.43	9.41	6.91
46	3.40	3.70	7.10	84.8	152.0	236.8	5.72	4.89	8.01	10.78	7.35
47	3,87	3.58	7.45	84.8	137.6	222.4	6.33	6.29	8.05	8.89	7.39
48	3.64	3.34	6.98	78.8	124.9	203.7	6.09	6.34	8.22	8.07	7.18
49	3.90	3,67	7.57	87.2	135.6	222.8	6.00	6.30	8.54	7.41	7.06
50	4.73	4.38	9.10	124.9	139.0	263.9	6.65	6.38	8.92	9.76	7.93
51	4.51	4.23	8.74	106.2	151.4	257.6	6.65	6.23	6.96	11.49	7.83
52	4.70	4.38	9.08	104.5	159.9	264.4	6.42	7.26	8.08	9.48	7.81
53	4.72	4.36	9.08	104	160.0	270	6.40	7.28	8.05	9.51	7.81
54	4.64	4.38	9.03	129.4	160.5	289.9	6.93	6.11	8.16	5.03	6.56
55	6.90	6.67	13.6	182.5	231.2	413.7	7.43	8.96	13.01	12.17	10.39
56	6.32	6.77	13.09	176.3	190.9	367.3	6.74	8.31	14.05	11.63	10.18
57	7.03	6.67	13.70	169.7	223.8	393.5	6.70	10.8	13.40	1191	10.69
58	6,95	6.83	13.78	186.1	211.9	398.0	6.88	9.34	12.49	13.5	10.56
59	7.06	6.81	13.87	199.1	204.6	403.7	6.97	9.42	13.84	10.1	10.09
60	7.11	7.03	14.14	180.4	219.2	399.6	7.50	10.2	12.2	14.4	11.07

Table(VII-3.2)

Test Results

0-0 passes

Loads

Unguided Sinking

Test No.	RSF (kN)			Torque (Nm)			Roll Pressure (N/ mm^2)				
	F	B	Tot.	T_u	T_l	T_t	p_1	p_2	p_3	p_4	p_m
61	1.52	2.33	3.85	73.5	64.4	137.9	9.46	NC	Nc	NC	9.46
62	1.41	1.79	3.20	57.6	64.4	122.0	9.69	NC	NC	NC	9 46
63	2.63	3 02	5.65	59.3	112.4	1717	6.76	10.93	NC	NC	8 85
64	3 13	2.85	5.98	102.8	84 8	187.6	9.17	NC	NC	NC	9 17
65	2.30	2.28	4.58	48.59	78 5	127.1	7.28	9.44	NC	NC	8.36
66	6.32	5.30	11.6	184 2	187 4	372	12.16	11 0	13.3	Nc	12 18
67	6.53	4.93	11.5	172.9	195.6	368.5	13.71	10.9	11.01	8 40	11.06

Table(VII-3.3)

Test Results

R-0 passes

Loads

Guided Sinking

Test No.	RSF (kN)			Torque (Nm)			Roll Pressure (N/ mm^2)				
	F	B	Tot.	T_u	T_l	T_t	p_1	p_2	p_3	p_4	p_m
68	2.82	2.60	5.42	70.6	83 6	154.2	5.57	7.36	8 69	8.34	7 49
69	2.98	2.89	5.87	81.4	84.8	166.2	6.10	7.35	8.10	8.89	7 61
70	3.05	2.78	5.83	70.6	90.4	161.0	6.10	7.04	9.06	8 61	7.60
71	1.94	1.68	3.62	52.0	62.2	114.2	4.61	3.82	5.31	3.60	4.33
72	1.79	1.68	3.47	61.0	52.5	113.7	4.78	4.23	5.08	6 52	5.15
73	2.06	1.86	3.91	65.0	66.7	131.7	4 87	4 36	5 30	4.00	4 63
74	6.54	6 14	12.68	191.5	193.2	384.7	6.40	10.9	13.56	10 98	10 47

Table(VII-3.4)

Test Results

0-0 passes

Loads

Guided Sinking

Test No.	RSF (kN)			Torque (Nm)			Roll Pressure (N/mm^2)				
	F	B	Tot.	T_u	T_l	T_t	p_1	p_2	p_3	p_4	p_m
75	2.36	2.49	4.85	74.6	64.4	139.0	4.41	6.16	9.32	NC	6.63
76	2.49	2.63	5.12	73.5	76 8	150.3	6.43	6.04	9.83	NC	7 43
77	4 54	3.95	8.49	98.3	135.6	233.9	8.71	12.02	12.5	NC	11 06
78	4.31	3.87	8.18	104.5	115.8	220.3	7.51	11.12	7 58	NC	8 74
79	4.40	4.00	8.40	131.1	130.0	261.1	10.96	9 96	6 54	NC	9.16
80	4.40	4.00	8.4	131.1	130.0	261.1	10.10	11.33	NC	NC	10.71
81	3.51	3.14	6.65	79.7	88.1	167.8	9.65	13.65	NC	NC	11.65
82	3.51	3.14	6.65	79.7	88.1	167.8	10.43	12.16	NC	NC	11.29
83	2.86	2.39	5.25	54.2	48.0	102.2	10.11	12.27	NC	NC	11 20
84	2.86	2.39	5.25	54.2	48.0	102.2	9.80	14.22	NC	NC	12 01

Table(VII-3.5)

Test Results

R-O passes

Loads

Stretch-Reducing

Test No.	RSF (kN)			Torque (Nm)			Roll Pressure (N/ mm^2)				
	F	B	Tot.	T_u	T_1	T_t	p_1	p_2	p_3	p_4	p_m
85	1.29	1.10	2.39	39.6	40.7	80.3	4.90	4.44	5.72	6.99	5.51
86	0.84	0.73	1.57	36.2	31.6	67.8	4.79	4.54	5.52	5.56	5.10
87	3.05	2.78	5.83	85.9	85.3	171.2	5.65	6.05	8.85	7.24	6.95
88	2.59	2.05	4.64	88.7	98.3	187.0	6.07	6.95	8.12	NC	7.05
89	6.02	4.75	10.77	128.3	157.1	285.4	7.66	10.46	13.81	3.44	10.65
90	4.23	3.66	7.93	102.8	153.7	256.5	8.08	8.07	11.44	NC	9.20
91	5.41	4.75	10.16	0.0	0.0	0.0	4.45	8.40	10.27	9.96	8.27
92	5.34	4.79	10.13	120.9	120.9	241.8	7.77	10.65	13.62	4.67	9.18
93	3.96	4.06	8.02	74.6	74.6	149.2	6.74	8.09	11.69	NC	8.84
94	4.12	4.06	8.18	74.6	74.6	149.2	7.15	8.65	11.81	NC	9.20
95	1.60	1.32	2.92	0.00	-22.6	-22.6	4.86	4.13	2.99	5.63	4.41
96	2.52	1.50	4.02	59.3	54.8	114.1	4.81	3.86	4.91	4.09	4.42
97	1.91	1.76	3.67	0.00	-28.3	-28.3	3.95	4.08	4.36	3.64	4.01
98	1.98	1.90	3.88	70.1	57.1	127.2	4.42	4.28	4.25	4.28	4.31
99	0.95	1.32	3.74	74.8	60.5	135.3	4.86	4.15	4.69	5.12	4.70
100	1.91	1.83	3.74	51.4	48.0	99.4	5.64	4.81	4.94	4.45	4.96
101	↓	↓	↓	↓	↓	↓	4.87	4.24	5.58	5.18	4.97
102	↓	↓	↓	↓	↓	↓	3.43	1.87	5.86	5.32	4.12
103	0.99	1.02	2.01	163.9	183.1	347	3.16	2.43	4.88	5.90	4.09
104	4.46	4.02	8.48	148.0	114.1	262.1	5.82	6.56	8.58	8.60	7.39

increasing back tension

Table(VII-3.5)

Test Results

R-O passes

Loads

Stretch-Reducing

Test No.	RSF (kN)			Torque (Nm)			Roll Pressure (N/ mm^2)				
	F	B	Tot.	T_u	T_l	T_t	p_1	p_2	p_3	p_4	p_m
105	4.04	3.51	7.55	107.4	112.4	219.8	7.77	8.11	8.01	9.93	8.46
106	4.39	3.95	8.34	126.6	120.9	247.5	5.91	6.23	7.46	6.88	6.62
107	3.89	3.36	7.25	0.00	0.00	0.00	5.52	4.91	6.96	7.84	6.30
108	4.73	4.61	9.34	O.S.	O.S.	O.S.	6.52	8.78	9.46	2.03	8.15
109	4.73	4.61	9.34	O.S.	O.S.	O.S.	7.16	8.63	8.41	NC	8.07

Table (VII-3.6)

Test Results

0-0 passes

Loads

Stretch-Reducing

Test No.	RSF (kN)			Torque (Nm)			Roll Pressure (N/ mm^2)				
	F	B	Tot.	T_u	T_l	T_t	p_1	p_2	p_3	p_4	p_m
110	1.79	1.76	3.55	57.1	65.0	122.1	9.57	NC	NC	NC	9.57
111	1.45	1.53	2.98	65.5	83.1	148.6	6.41	NC	NC	NC	6.41
112	1.53	1.53	3.07	59.9	77.4	137.3	10.59	NC	NC	NC	10 59
113	1.29	1.32	2.61	54.8	83.6	138.4	9.19	NC	NC	NC	9.19
114	3,59	3.29	6.88	0.00	0.00	0.00	8.32	11.69	NC	NC	10.00
115	3.59	3.07	6.66	-27.1	20.9	-6.2	9,40	10.34	NC	NC	9.87
116	0.68	0.59	1.27	22.6	21.5	44.1	7.85	NC	6.05	5.64	6.52
117	0.08	0.29	0.37	-11.3	-18.1	-29.4	6.45	NC	4.65	NC	5.54
118	2.21	2.05	4.26	70.1	63.3	133.4	5.95	9.18	NC	NC	7.56
119	2.36	2.01	4.37	58.2	75.7	133.9	6.13	9.36	NC	NC	7.79
120	1.68	1.39	3 07	11.3	21.5	32.8	7.00	6.40	NC	NC	6 70
121	1.91	1.68	3.59	-19.2	-22.6	-41.8	7.74	6.84	NC	NC	7 29
122	3.89	3 87	7.76	112.4	105.1	217.5	9.38	13.69	NC	NC	11 54
123	3 51	3.00	6.51	101.7	128.3	230.0	8.17	11 71	NC	NC	9.94

Table(VII-4)

Stretch-Reducing

Applied Tensions

R-0 passes

Test No	BT (kN)	FT (kN)
85	0.00	0.00
86	3.31	2.30
87	0.00	0.00
88	3.84	2.98
89	0.00	0.00
90	3.72	3.50
91	0.00	2.98
92	0.00	0.00
93	4.77	4.69
94	4.20	4.43
95	0.00	1.37
96	0.00	0.00
97	0.00	1.37
98	0.00	0.00
99	3.31	2.34
106	0.00	0.00
107	0.00	2.16
108	2.75	8.78
109	2.75	8.78

0-0 passes

Test No	BT (kN)	FT (kN)
110	0.00	0.00
111	0.48	0.00
112	0.67	0.00
113	0.67	0.00
114	0.00	2.56
115	0.00	2.56
116	0.00	0.00
117	2.67	3.07
118	0.00	0.00
119	0.00	0.00
120	0.00	1.79
121	2.10	3.84
122	0.00	0.00
123	3.72	2.82

VIII

DISCUSSION OF RESULTS

(VIII-1) Pin Protrusions

Examination of the surface of the rolled tubes often showed that when the pin length was adjusted to be flush with the surface of the roll, a small rod of metal was pushed into the orifice thus compressing the pin. The length of the extruded rod was measured under a travelling microscope. It was found to be of the order of 25 μm. Therefore, the pin was made to protrude above the surface of the roll by this amount, so that at full load it was flush with the surface and gave a more representative indication of pressure. This feature is believed to be reliable provided that the small pin protrusions before and after the full load was reached did not affect the performance of the loadcell.

Smith et al [25] have shown that small pin protrusions of up to 25 μm had little effect on the results of the pin loadcells. This was verified by tests of the same nature carried out in this investigation.

Fig. (51) shows the results of these tests for the pin at the root of the groove. Together with the results for the other three positions, pin protrusions of between 13 μm and 25 μm had little effect on the recorded pressure distribution. At first the bottom roll was selected to accommodate the pin loadcells but it was found that even the weight of the tube under static conditions, caused the pins to respond. In particular the static pressure measured by No. 1 pin was significant but, when rolling tube, this effect was less noticeable,

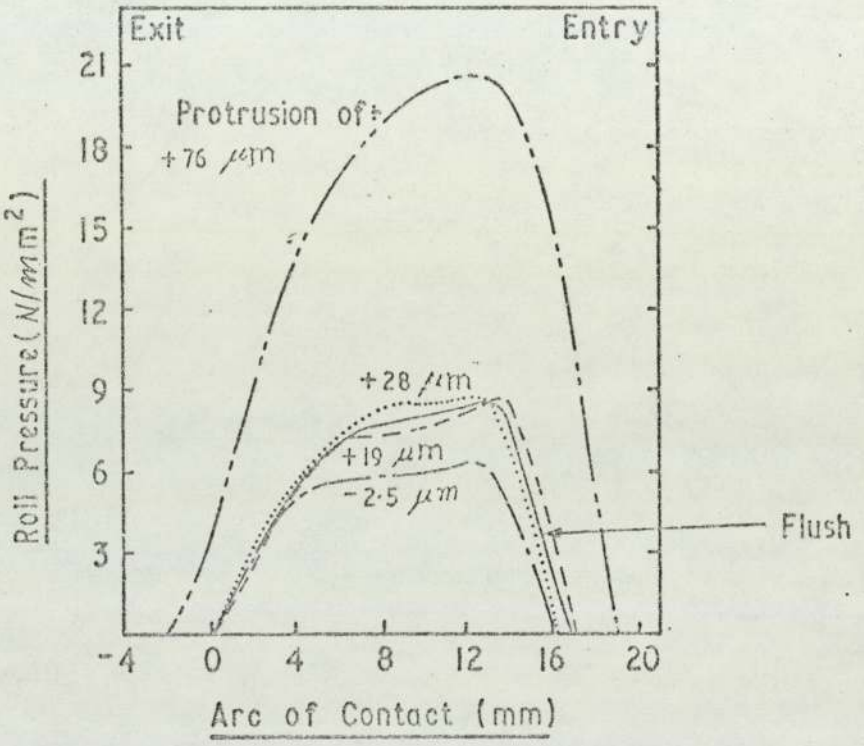

FIG. 51

THE EFFECT OF PIN PROTRUSIONS ON THE RECORDED PRESSURE FOR THE PIN AT THE ROOT OF THE GROOVE

since the weight of the tube was applied to the whole area of contact as well as to the pins. Nevertheless, to eliminate this effect, the design of the experimental mill was changed to enable the pin loadcells to be embedded in the top roll.

(VIII-2) Back Extrusion

The presence of particles of rolled metal in the annular clearance between the pin and its orifice usually results in increased frictional force between the pin and the corresponding surface causing zero drift, hysteresis and a reduction in the rate of response. Consequently, a change in the shape of the recorded pressure distribution curves takes place which varies with the amount of metal extruded between the pin and the orifice.

To investigate the extent of this problem, the pins were removed from the orifices and checked for extruded lead after one pass, 10 passes, 30 passes, and finally after more than 100 passes. Also, the pressure distribution curves for these tests of identical rolling conditions after different numbers of passes and before and after re-assembly were checked for zero drift, shape of curve and area under the curve. In so doing, allowance was made for non-uniformity of the tube wall thickness and surface conditions.

Results of this investigation showed that although lead particles were found to exist on the surfaces of the pins and in the pin orifices they did not affect the

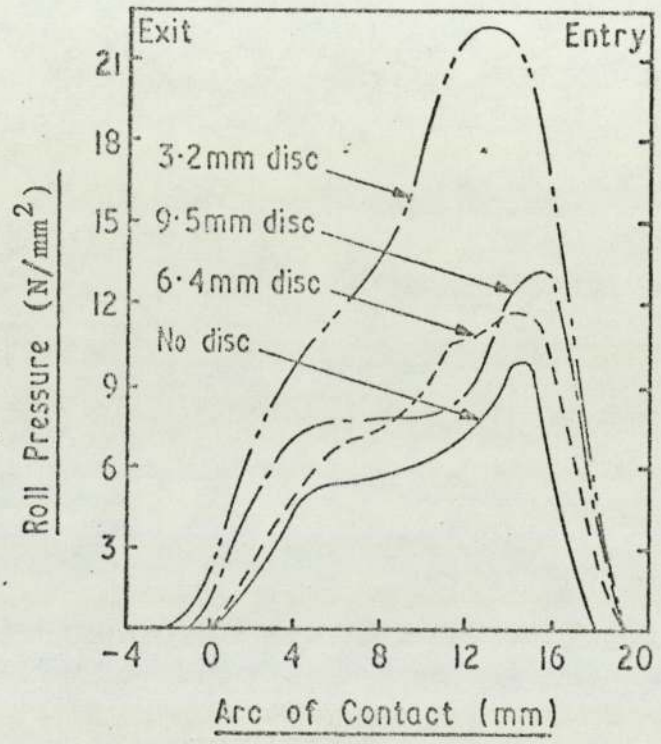

FIG.52 EFFECT OF USING PVC DISCS PIN 2 (22·5°)

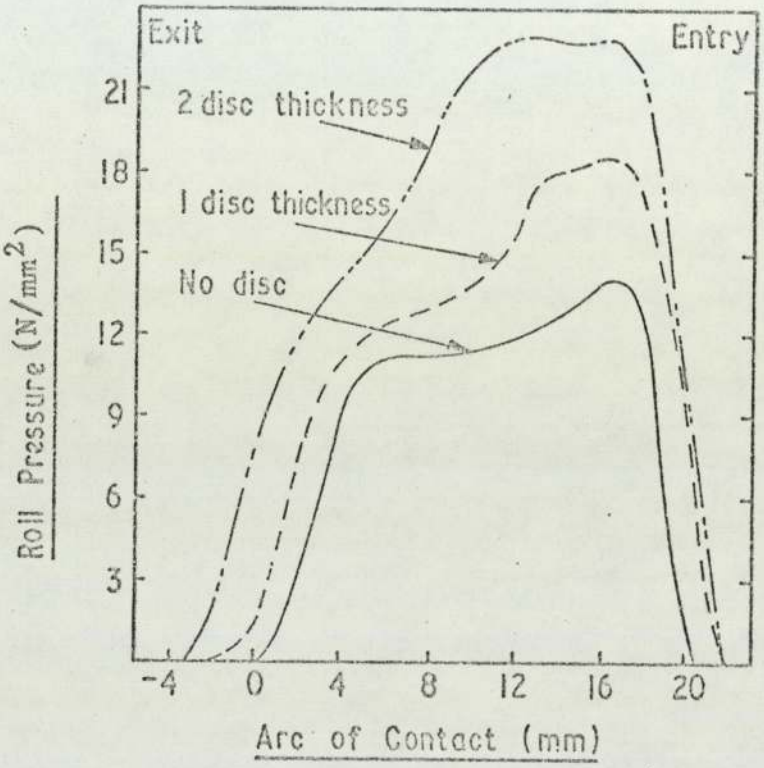

FIG. 53 EFFECT OF THICKNESS OF PVC DISCS ON THE RECORDED PRESSURE PIN 3 (45°)

performance of loadcells significantly, After more than 100 passes, the pin loadcells showed no zero drift and little change occurred in the area under the curve.The design of the pin(fig.(25)p.90) might have contributed to this.

(VIII-3) The effect of using PVC discs

To prevent the rolled metal from being extruded in to the clearance between the pin and the hole Palme and MacGregor[27] used metal washers to cover the pin tip. Also, Cole[1] suggested the use of, and employed, small PVC discs on top of the pins, i.e. as caps. In the case of Cole's tests, the pin loadcells were calibrated in situ with and without the discs and little difference was found to exist between the calibration curves for each case. However, now it is believed that, because of the use of a pin-to-pin method of calibration, the effect which the size and thickness of the discs had on the recorded pressure distribution curves, could not be irrevocably established, (see fig.(32)p.103). It was decided therefore to investigate such an effect.

A number of test-pieces was cut from the same tube and rolled through the same gap, i.e. under the same conditions, with PVC discs, of 3.2 , 6.4 and 9.5 mm diameter, cut from the same PVC tape, on top of the pins as caps. The pins were flush with the surface of the roll. The results of some of these tests are shown in fig.(52). A change in the shape of the curves and in the magnitudes of the pressures is noticed. It is also noticed that the smaller the disc the bigger the change. An explanation of this phenomenon may be that

when the diameter of the disc is large in comparison with the size of the pin, it becomes part of the surface of the roll and the increase in the recorded pressure is caused by the pressure needed to indent the 'lump' into the tube wall. But, when the disc is small in comparison with the size of the pin, it represents an extension of the pin and the increase in the recorded pressure is caused by pin protrusion as shown in fig. (51) . In both cases, the increase in recorded pressure will depend on the thickness of the disc. fig. (53) shows the effect of thickness of the disc on the recorded pressure, i.e. the effect is similar to an increase in pin protrusion.

(VIII-4) The Arc of Contact and the Free Zone:

In strip rolling, and in the absence of roll flattening, the horizontal projection of the arc of contact can be calculated simply from geometrical considerations. If R fig. (54), is the radius of the roll, and δ is the difference between the initial and final strip thicknesses, then L_g is :

$$L_g = \sqrt{R\delta} \text{ neglecting } \frac{\delta^2}{4}$$

In the strip rolling process if the value of L_g is compared with the measured value L_m , the difference is small and is due mainly to roll flattening and the elastic recovery of the strip. The effect of these two factors is to increase the measured length L_m ,i.e. the ratio L_m / L_g will be greater than unity (46) .

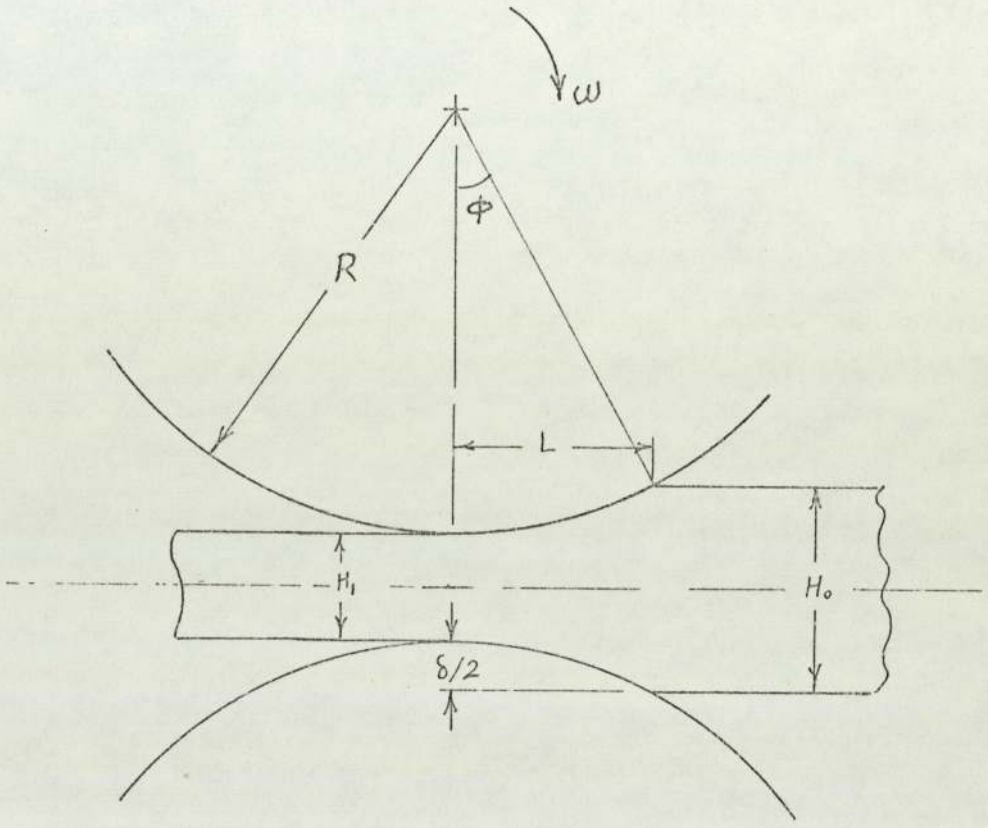

Fig. (54)

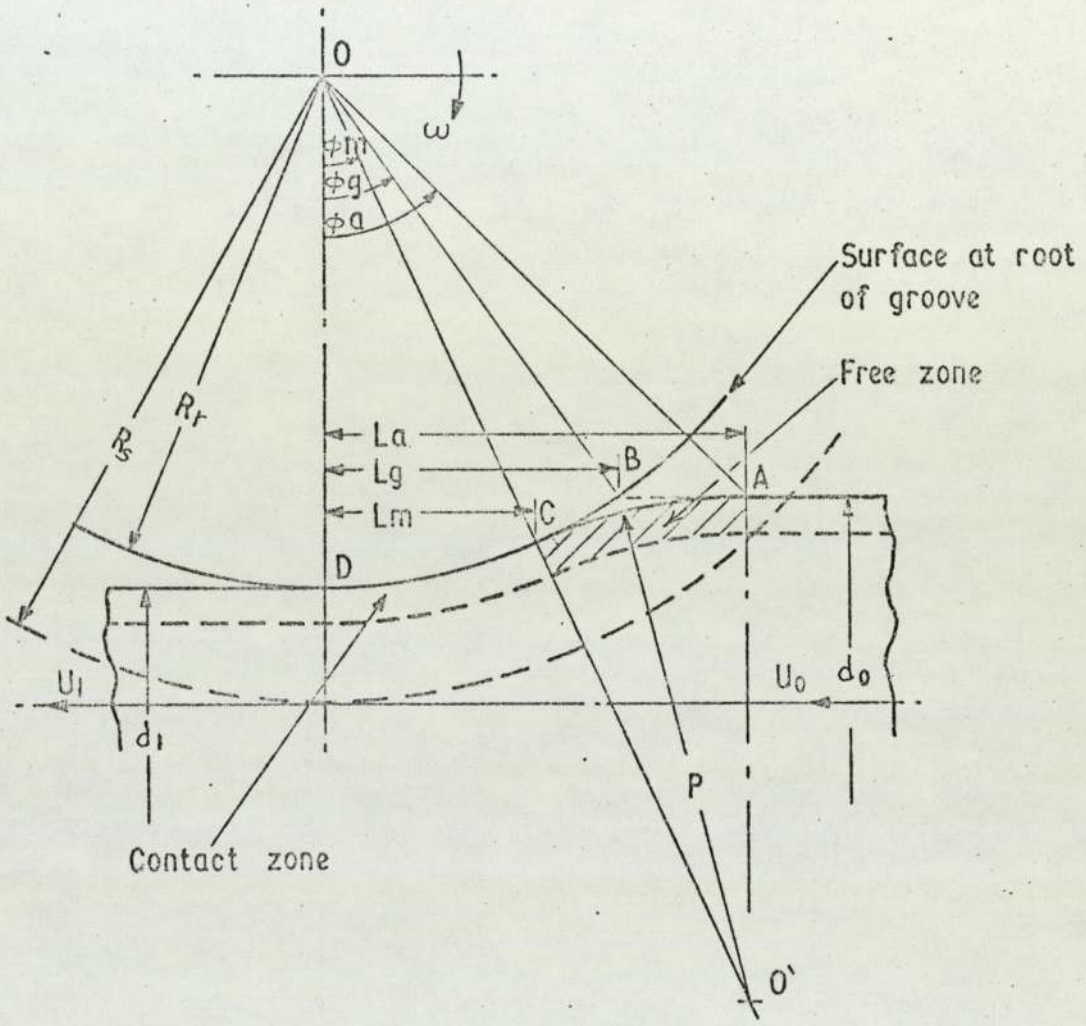

Fig. (55) EFFECT OF THE FREE ZONE ON THE ARC OF CONTACT

However, in tube rolling and sometimes in billet rolling, the measured length L_m is usually smaller than the calculated length L_g and the ratio L_m / L_g is less than unity. The reason for this is that deformation is not restricted to the geometrically reconstructed deformation zone but also occurs elsewhere, e.g. deformation starts at point A, fig. (55), instead of at point B. Due to this deformation the first point of contact between the surface of the tube and the roll is delayed to point C instead of B .

The zone of deformation between points A and C will be referred to as the "free zone", while that between points C and the exit plane D will be referred to as the "contact zone".

The measured length L_m of the arc of contact was calculated from the base length of the pressure distribution curves, allowance being made for the finite width of the pin. Fig. (56) represents the relationship between the ratio L_m / L_g and the d / t ratio for different drafs δ. It can be seen that L_m is always smaller than L_g.

Shveikin and Ivshin [47] attempted to find a theoretical solution for the problem of pre-contact plastic deformation. It was stated that this deformation unquestionably influences the process parameters, in decreasing the area of contact between the metal and the roll. It should be noted however, that the analysis was for upsetting tubes between dies the shape of which was not given.

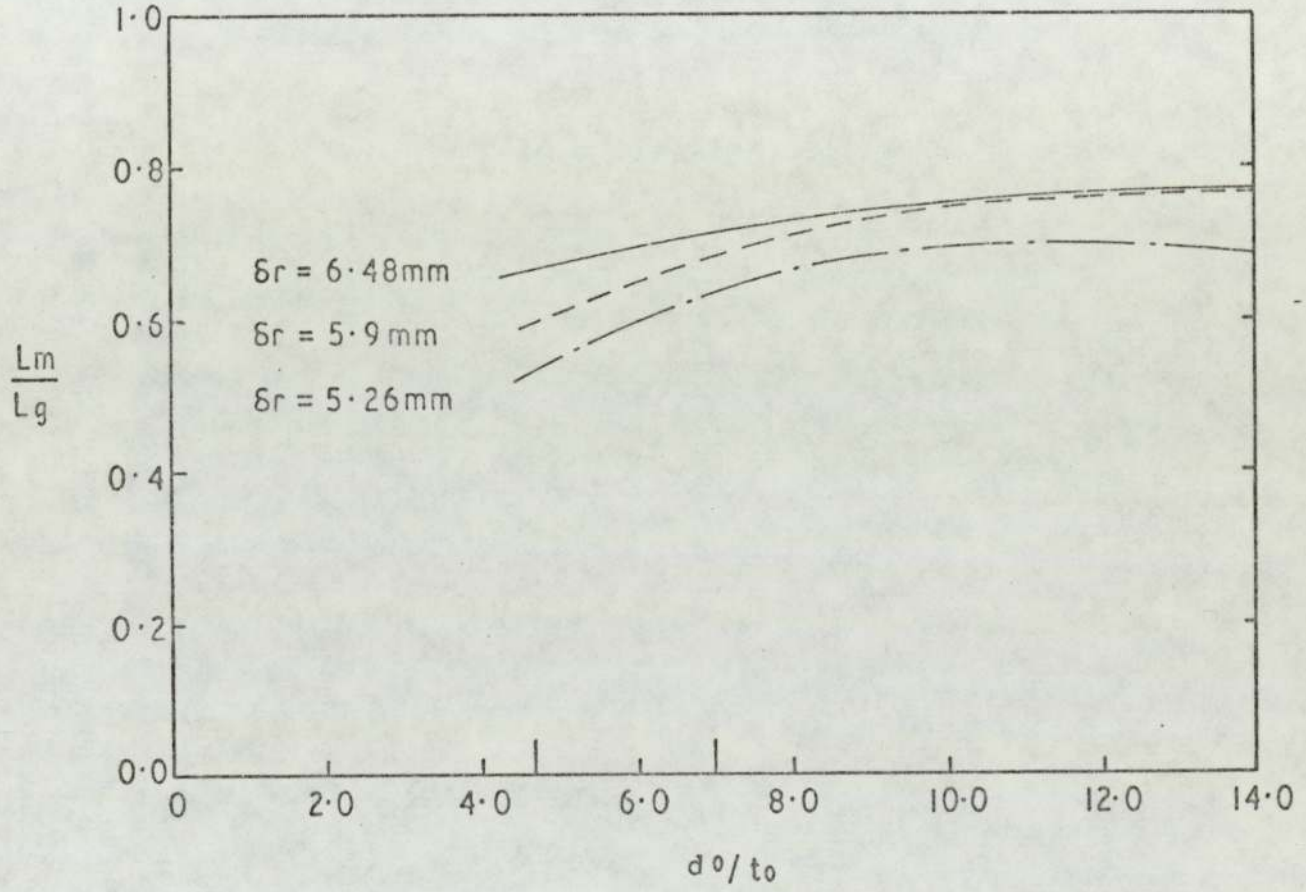

Fig. 56 VARIATION OF Lm/Lg WITH THE DRAFT δr AT THE ROOT OF THE GROOVE AND d_o/t_o

The authors assume that the generatrix of a tube varies along a parabolic curve of the form fig. (57)

$$\Delta r_x = a x^4$$

Accordingly the radial velocity of a point on the surface of the tube in the pre-contact zone is derived.

The total work of plastic deformation is assumed to be made up of three components:

- the work of the internal forces in the pre-contact zone.
- the work of the internal forces in the contact zone.
- the work of frictional forces at the contact zone .

The authors then state that tests on lead tube, have shown that the length of the pre-contact zone is independent of the length of the die, hence the differentials of the increments of plastic work at the seat of deformation with respect to the length of the pre-contact zone vanishes, Solving the given equations by computer gave the ratio of the length of the pre-contact zone (L) to the tube diameter (d) as a complex function of the tube dimensions. degree of deformation, rate of deformation and the mechanical properties of the metal. Comparison was made between calculated values of L / d and test data obtained in upsetting lead tubes. The calculated ratios L / d were lower than the values obtained in the tests and the reason given was that they only included the plastic region and did not include the elastic deformation.

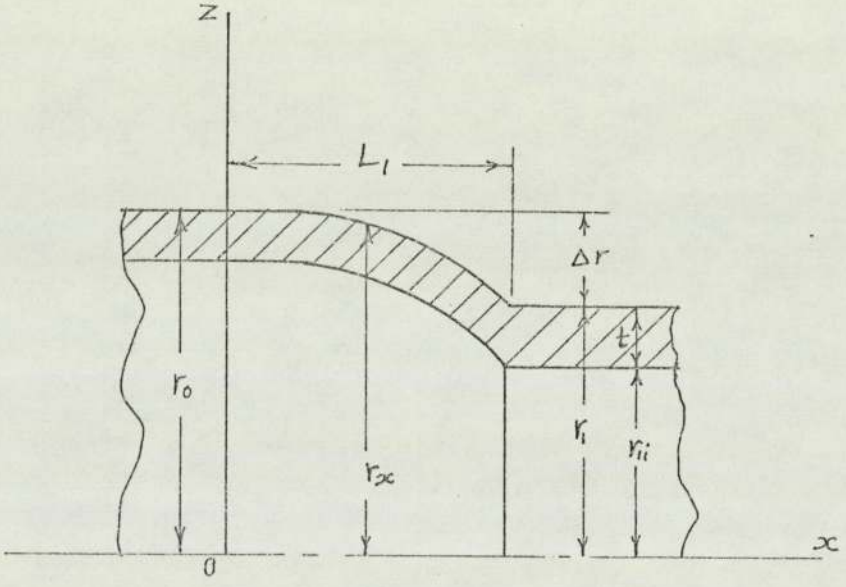

Fig. (57)

No reasons were given for the choice of the shape of the generatrix of the outer surface of the tube as a parabola.

Furthermore, the applicability of this solution to to tube rolling was not discussed although it was implied that the method of analysis applies to the actual process of tube rolling.

In another paper (48) Ivshin and Shveikin were concerned with obtaining formulae for the variation in the wall thickness of the tube and the rolling torque.

In so far as the free zone is concerned, the authors apply the solution obtained for upsetting tubes in their previous paper (47) to determine the shape and extent of the pre-contact deformation in the case of tube rolling. They divide the whole of the deformation zone into two zones fig. (58) : a pre-contact zone I and a contact zone II. As in (47) the generatrix of the outer surface of the tube in zone I is assumed to be:

$$\triangle r_x = \triangle r_1 \frac{x^4}{L_1^4}$$

and the generatrix of the roll (zone II) is given as:

$$x^2 / 2R$$

The vertical velocity of the tube outside surface v_r is written as :

$$v_{rI} = -4 \triangle r_1 \frac{x^3}{L_1^4} \cdot v$$

$$v_{rII} = - \frac{x}{R} v$$

where v is the horizontal velocity of the tube in the neutral section. At point A , the boundary of the zones,

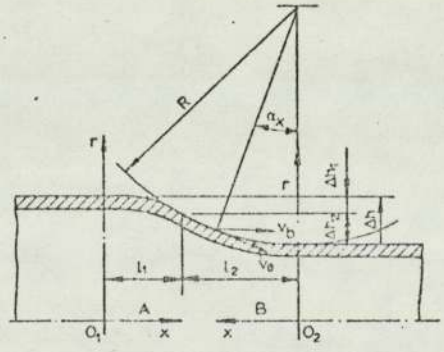

Fig. (58)

$v_{r_1} = v_{r_2}$ and the radial deflection $\Delta r_1 = \Delta r - \frac{L_2^2}{2R}$

from these equations a relationship between L_1 & L_2 is found :

$$L_1 = \frac{2R\Delta r}{L_2} - L_2$$

Later in the analysis R is called the rolling radius of the roll and is taken as the arithmetic mean of the two radii at the root of the groove and at the shroud i.e.,

$$R = \frac{R_r + R_s}{2}$$

Gulyaev et al [5] in a paper mainly concerned with the design of oval grooves base their analysis on Shveikin & Ivshin's [47] method of accounting for the pre-contact deformation. They also state that in reducing and sizing tubes the actual seat of deformation is "much" larger than the geometrical zone, consisting of the pre-contact zone and the contact zone as in [47].

In a paper by Fogg [49] on redrawing of cylindrical cups through conical dies, he takes account of the pre-contact plastic deformation which takes place in the absence of pressure sleeves.

The phenomenon is similar to that occuring in tube rolling. Fogg assumes that the path of all particles passing through the free zone is a true radius which makes the plastic work done in this zone a minimum. Elements passing through the zone undergo bending, radial drawing, and then unbending before they come in contact with the die. Thus according to the minimum

specific plastic work hypothesis, R_f the radius of the free zone, will assume a value which satisfied the condition:

$$\frac{\delta}{\delta R_f} (W_r + W_b + W_u) = 0$$

where W_r , W_b & W_u are the components of specific plastic work due to radial drawing, bending and unbending respectivily. He arrives at an expression for R_f in the form:

$$R_f = t_1 \sqrt{\frac{r_1 / t_1}{\sqrt{3}\,(1 - \cos \alpha)}} \qquad \text{(VIII.1)}$$

where ; see fig.(59)

t_1 and r_1 are the wall thickness and outer radius of the cup prior to bending, α is the die angle.

Fogg shows that the calculated value of R_f is in good agreement with the test results.

To investigate this phenomenon in the present work tubes were rolled for half of their length and, when the rolls were stationary, the gap between them was increased to allow the withdrawal of the tube. The profiles of the outer surfaces of the tubes, at the position corresponding to the root of the groove, were projected and traced. Data on the points from the projected profiles were read into a computer to establish the equation to the best fitting curve. An equation to a circle of a radius approximately equal to R_r , see fig. (55) , was found to fit the points with adequate accuracy. To confirm this, arcs of different radii were superimposed on the projected profiles. Again it was found that the

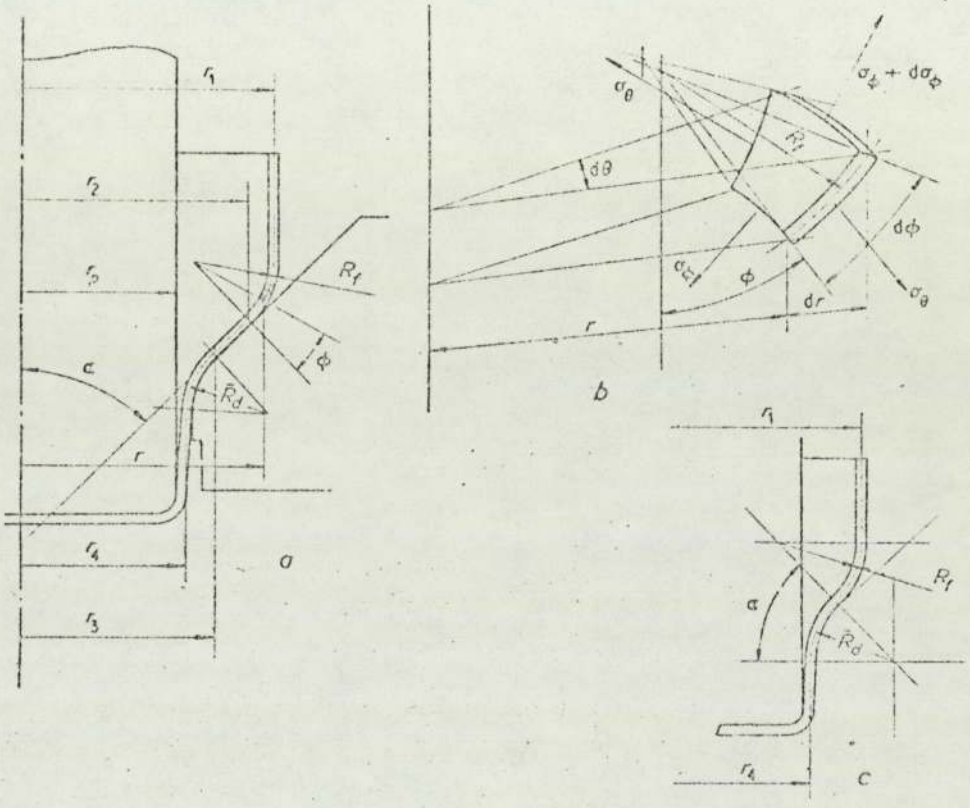

a Redrawing geometry.
b Element in free zone.
c Minimum condition.

Fig. (59) *Redrawing through a conical die*

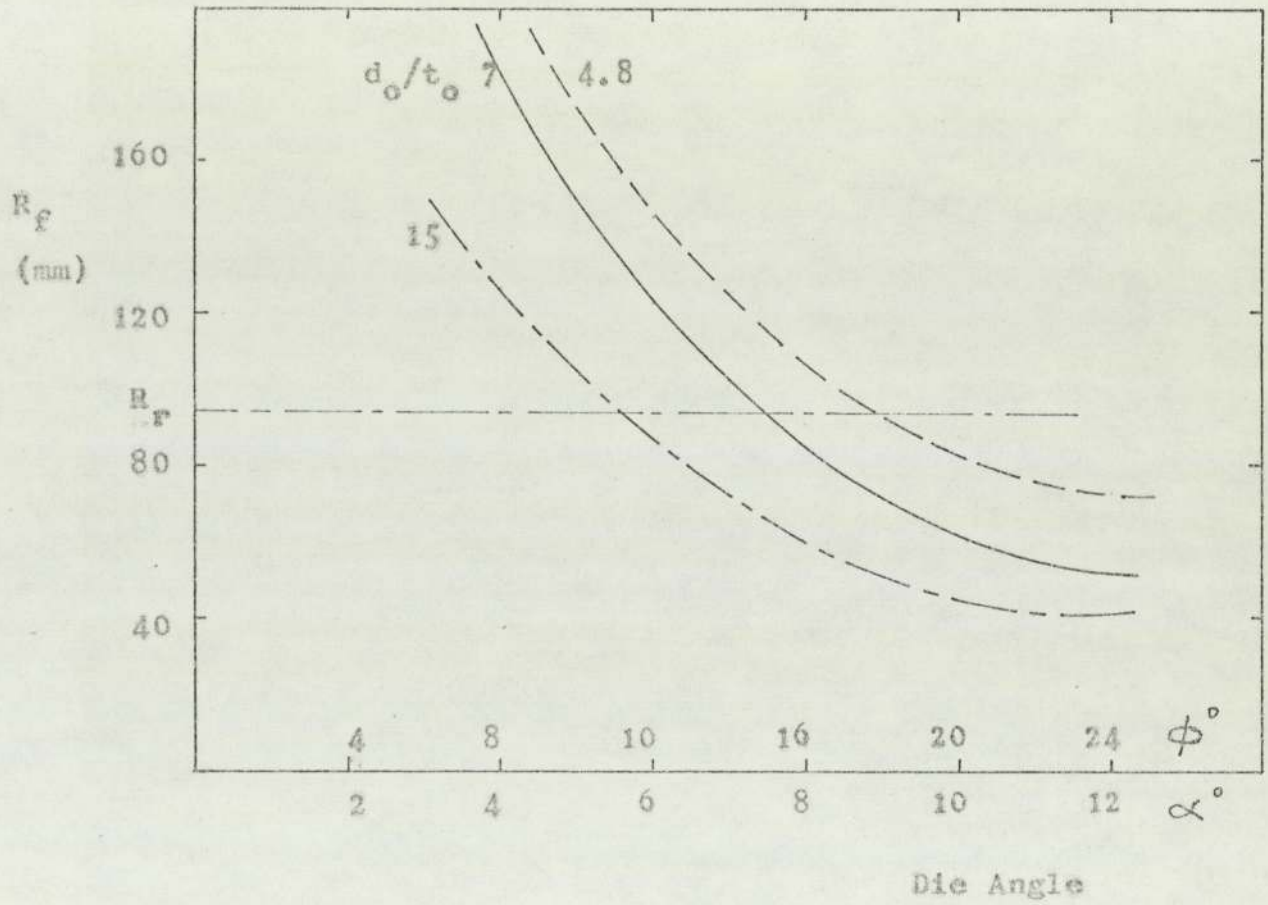
d_o/t_o 7
4.8
15
160
120
80
40
R_f
(mm)
R_r
4
8
10
16
20
24
$\phi°$
2
4
6
8
10
12
$\alpha°$
Die Angle

Fig. (60)

arc of radius equal to R_r fitted most satisfactorily. Therefore, (putting P = R_r in fig.(55)) :

$$L_m = \frac{1}{\sqrt{2}} L_g$$

Reference to fig. (56) shows that a value of L_m / L_g of 0.71 (i.e. $\frac{1}{\sqrt{2}}$) agrees satisfactorily with that from the experimental curves. Consequently, the shape of the tube at the root of the groove is confirmed as ogee in form of which both parts are arcs of circles.

If the arc of contact is replaced by a chord, then the equivalent die angle is equal to half the angle of contact . The angle of contact for the tests mentioned above was approximately 10^{o} . Applying Fogg's eqn.(VIII.1), for R_f in the case of tube rolling with d/t = 7.0 and t_1 = 6.4 mm, R_f = 147.5 mm which is an overestimate of the value of R_f found in the tests. However the calculated value of R_f from Fogg's expression compares favourably with the test result for contact angles above 14^{o} and also for thin tubes as shown in fig.(60). Also the shape of the free zone was similar to that suggested by Fogg.

(VIII-5)Torque sharing and the arc of contact:-

Ideally the total rolling torque should be equally shared between the two rolls but as table(VIII.1) shows this had not been the case. In general it seems that more than half the total rolling torque was transmitted by the bottom roll. This may be due to the tendency of the tube to bend downwards thus increasing the area

Table(VIII, 1)

Torque Sharing and the Arc of Contact

Test No.	Torque Sharing Factor γ	Lg mm	Lm mm	L_m^* mm	$\frac{Lm}{Lg}$	$\frac{L_m^*}{Lg}$	$\frac{Lm}{Lm^*}$
1	1.28	20.24	11.94	15.31	0.59	0.76	0 78
2	1.61	20 24	14.20	22.90	0.70	1.13	0.62
3	1.09	20.97	14.62	15.89	0.70	0.76	0.92
4	1.11	21.20	10.24	11.38	0.48	0.54	0.90
5	1.14	19.74	9.77	11.10	0.49	0.56	0.88
6	0.96	20.49	10.96	10.54	0.53	0.51	1.04
7	0.96	18.43	11.92	11.46	0.65	0.62	1.04
8	1.28	19.23	12.88	16.51	0.67	0.86	0.78
9	1.43	19.23	11.79	16.84	0.61	0.88	0.70
10	1.22	21.20	14.58	17.78	0.69	0.84	0.82
11	1.14	21.90	16.00	18.18	0.73	0.83	0.88
12	1.11	21.90	15.53	17.26	0.71	0.79	0.90
13	0.96	22.8	14.8	14.15	0.65	0.62	1.05
14	1.16	22.79	18.08	21.02	0.79	0.92	0.86
15	1.06	22.39	18.26	19.43	0.80	0.85	0.94
16	1.06	22.79	17.84	18.98	0.78	0.83	0.94
17	1.02	21.20	15.88	16.20	0.75	0.76	0.98
18	1.11	21.44	13.74	15.27	0.64	0.71	0.90
19	1.04	21.44	13.37	13.93	0.62	0.65	0.96
20	1.14	23.44	17.21	19.56	0.73	0.83	0.88

Table(VIII.1) (contd.) .

Torque Sharing and the Arc of Contact

Test No.	Torque Sharing Factor χ	Lg mm	Lm mm	L_m^* mm	$\frac{Lm}{Lg}$	$\frac{L_m^*}{Lg}$	$\frac{Lm}{Lm^*}$
21	1.47	22.79	15.52	22.82	0.68	1.00	0.68
22	1.28	22.79	16.12	20.67	0.71	0.91	0.78
23	1.19	20.49	14.26	16.98	0.70	0.83	0.84
24	1.16	20.5	13.65	15.87	0.67	0.77	0.86
25	1.35	23.23	13.96	18.86	0.60	0.81	0.74
26	1.14	23.23	12.52	14.23	0.54	0.61	0.88
27	1.22	23.2	11.76	14.34	0.51	0.62	0.82
28	1.14	21.2	15.9	18.20	0.75	0.86	0.87
29	1.72	20.97	12.09	20.84	0.58	0.99	0.58
30	1.35	19.49	12.08	16.32	0.62	0.84	0.74
31	1.39	21.20	11.32	15.72	0.53	0.74	0.72
32	1.56	22.79	14.25	22.27	0.63	0.98	0.64
33	1.19	23.44	14.39	17.13	0.61	0.73	0.84
34	1.16	22.79	13.60	15.81	0.60	0.69	0.86
35	0.83	24.07	19.25	16.04	0.80	0.67	1.20
36	1.02	23.44	18.46	18.84	0.79	0.80	0.98
37	1.19	23.86	18.05	21.49	0.76	0.90	0.84
38	1.28	23.9	19.44	24.92	0.81	1.05	0.78
39	1.22	24.1	18.52	22.59	0.77	0.94	0.82
40	1.09	25.5	18.2	19.96	0.71	0.78	0.91

Table (VIII.1) (contd.)

Torque Sharing and the Arc of Contact

Test No.	Torque Sharing Factor γ	Lg mm	Lm mm	L_m^* mm	$\frac{Lm}{Lg}$	$\frac{L_m^*}{Lg}$	$\frac{Lm}{Lm^*}$
41	1.06	21.2	18.8	19.90	0.89	0.94	0.94
42	1.06	21.2	18.8	19.89	0.89	0.94	0.95
43	1.28	23.0	18.1	22.92	0.79	1.00	0.79
44	1.11	23.9	16.8	18.50	0.70	0.77	0.91
45	1.28	25.48	16.25	20.83	0.64	0.82	0.78
46	1.39	25.09	16.14	22.42	0.64	0.89	0.72
47	1.32	25.87	15.95	20.99	0.62	0.81	0.76
48	1.28	25.9	15.64	20.05	0.60	0.78	0.78
49	1.28	25.5	16.68	21.38	0.65	0.84	0.78
50	1.06	25.48	17.56	18.68	0.69	0.73	0.94
51	1.22	24.07	18.09	22.06	0.75	0.92	0.82
52	1.25	25.09	16.76	20.95	0.67	0.83	0.80
53	1.25	25.09	16.76	20.95	0.67	0.83	0.80
54	1.11	25.5	19.6	21.95	0.77	0.86	0.89
55	1.14	23.4	16.4	18.59	0.70	0.79	0.88
56	1.04	24.07	16.26	16.94	0.68	0.70	0.96
57	1.16	24.89	15.42	17.93	0.62	0.72	0.86
58	1.06	24.89	17.77	18.90	0.71	0.76	0.94
59	1.02	24.28	15.85	16.17	0.65	0.67	0.98
60	1.11	23.44	16.47	18.30	0.70	0.78	0.90

Table (VIII.1)(contd.)

Torque Sharing and the Arc of Contact

Test No.	Torque Sharing Factor γ	Lg mm	Lm mm	L_m^* mm	$\frac{Lm}{Lg}$	$\frac{L_m^*}{Lg}$	$\frac{Lm}{Lm^*}$
61	0.94	23.23	16.89	15.93	0.73	0.69	1.06
62	1.06	8.9	17.2	18.30	1.93	2.05	0.94
63	1.43	7.1	13.11	18.73	1.85	2.67	0.70
64	0.91	10.9	11.2	10.2	1.03	0.93	1.10
65	1.32	7.7	10.40	13.68	1.35	1.77	0.76
66	1.00	24.07	14.91	14.91	0.62	0.62	1.00
67	1.06	22.4	15.16	16.13	0.68	0.72	0.99
68	1.09	21.4	13.36	14.59	0.62	0.68	0.92
69	1.02	21.4	13.84	14.13	0.65	0.66	0.98
70	1.14	21.4	14.16	16.15	0.66	0.75	0.88
71	1.09	21.2	20.8	22.84	0.98	1.08	0.91
72	0.93	26.1	18.86	17.55	0.72	0.67	1.07
73	1.02	26.1	20.07	20.33	0.77	0.78	0.99
74	0.75	25.3	16.81	12.50	0.66	0.49	1.35
75	0.93	14.8	9.49	8.84	0.64	0.60	1.07
76	1.02	14.8	10.55	10.79	0.71	0.73	0.98
77	1.19	18.2	13.96	16.61	0.77	0.91	0.84
78	1.06	18.2	11.66	12.29	0.64	0.68	0.95
79	1.00	18.2	13.03	12.98	0.72	0.71	1.00
80	1.00	18.2	14.86	14.80	0.82	0.81	1.00

Table (VIII.1)(contd.)

Torque Sharing and the Arc of Contact

Test No.	Torque Sharing Factor γ	Lg mm	Lm mm	L_m^* mm	$\frac{Lm}{Lg}$	$\frac{L_m^*}{Lg}$	$\frac{Lm}{Lm^*}$
81	1.06	12.2	12.30	12.95	1.01	1.06	0.95
82	1.06	12.2	11.92	12.55	0.98	1.03	0.95
83	0.94	9.5	9.10	8.58	0.96	0.90	1.06
84	0.94	9.5	9.55	9.00	1.01	0.95	1.06

of contact between the bottom roll and the tube and reducing the area of contact between the top roll, which carries the pin loadcells, and the tube. The torque is directly proportional to the area of contact as can be seen from the relationship:

$$T_{/\text{per roll}} = R \cdot A_c \cdot \tau \qquad \text{(VIII.2)}$$

Therefore if the area of contact between the tube and both rolls were not equal, then the torque transmitted by both rolls cannot be equal.

Equation(VIII.2) above also shows that if the frictional stress τ was not the same in each roll, then the torque sharing will be affected. As explained in the experimental procedure, great care was taken in cleaning and degreasing the tubes and rolls to ensure identical conditions on both rolls as far as possible. It is therefore more likely that the difference in torque sharing between the two rolls has resulted largely due to the change in the areas of contact. And since the area of contact is proportional to the length of the arc of contact, the difference in torque sharing indicates a difference in the length of the arc of contact between the two rolls and the rolled tube.

Hence the arc of contact measured from the pressure distribution curves represents the length of the arc of contact on the top roll only (Lu) i.e. $L_m = L_u$.
To determine the average arc of contact for the two rolls a correction factor, which is a function of the torque sharing factor, should be applied. Therefore the length of the arc of contact corrected for torque sharing-

$\overset{*}{L}_m$ is equal to :-

$$\overset{*}{L}_m = L_m \cdot \gamma \qquad \text{(VIII.3)}$$

where

γ is the torque sharing factor = $\dfrac{\text{Total torque}}{2 \times \text{torque of top roll}}$

Values of $\overset{*}{L}_m$ are listed in table (VIII.1) and comparisons between $\overset{*}{L}_m$ and L_g and L_m are also listed in the table.

It can be seen from this table that $\overset{*}{L}_m$ is greater than L_m but they are both still smaller than L_g. The average values of the ratios L_m/L_g and $\overset{*}{L}_m / L_g$ from table are as follows:

$$L_m/L_g = 0.66 \qquad \text{(VIII.4)}$$

$$\overset{*}{L}_m/L_g = 0.78 \qquad \text{(VIII.5)}$$

The foregoing discussion shows that when using the pin loadcells traces to determine the arc of contact then a correction factor, due to the variation in torque sharing between the two rolls, should be applied.

To demonstrate the relationship between torque sharing and the measured length of the arc of contact two tests were carried out. The first was a normal test with the tube free from external influence while in the second test the end of the tube was lifted up to increase the area of contact on the top roll which carried the pin loadcells. The results of these two tests are summarised in table (VIII.2).

It can be seen from this table that as a result of increasing the area of contact (i.e.the length of arc of

contact(L_m) on the top roll, torque sharing was significantly influenced. The corrected length of the arc of contact $L_m^* = \chi L_m$ for the two tests is practically the same .

Table(VIII.2)

Measured quantity	Normal test	Influenced test
RSF (kN)	5.0	6.1
T_t (Nm)	162.7	182.5
T_u / T_t	0.48	0.85
χ	1.04	0.59
L_m (mm)	13.16	21.45
L_m^* (mm)	13.71	12.66

(VIII-6) The Pressure Peak and the Neutral Zone

Fig. (61) shows typical pressure distribution curves for the three d /t ratios used throughout the investigation. Other curves are shown in appendix(C). It can be seen that the points of maximum pressure for the first three pins 1,2 , and 3, lie near the entry plane while for pin no. 4 the point of maximum pressure lies near the exit plane. This is partly due to the presence of the free zone. To bend the tube wall along the arc AC, fig.(55) , a moment is required. This moment is supplied by forces acting radially at point C. It is averred that the effect of such forces, in addition to the rolling pressure, increases the pressure on the roll, that is on the pin loadcells, at this plane.

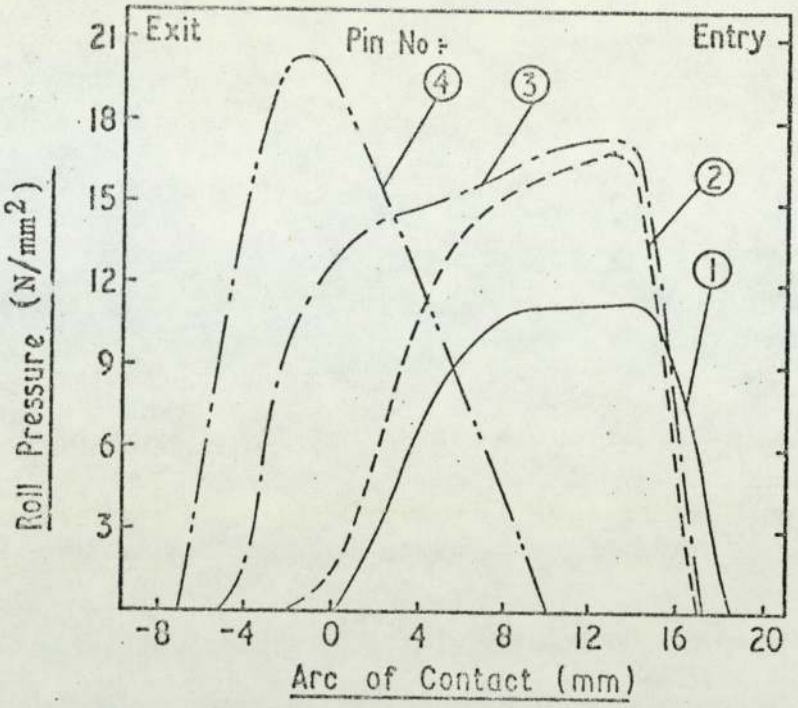

FIG. 61-c PRESSURE DISTRIBUTION CURVES FOR TUBE WITH d / t = 4.7

FIG. 61

TYPICAL PRESSURE DISTRIBUTION CURVES

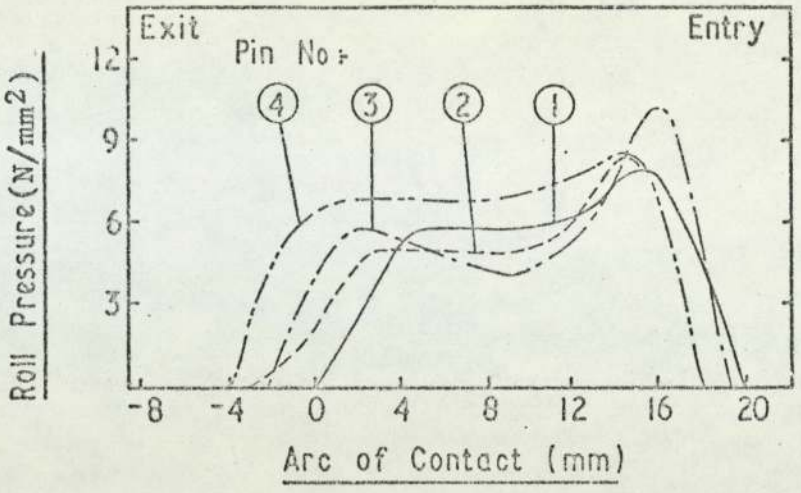

FIG6.1a PRESSURE DISTRIBUTION CURVES

FOR TUBE OF d / t = 15.0

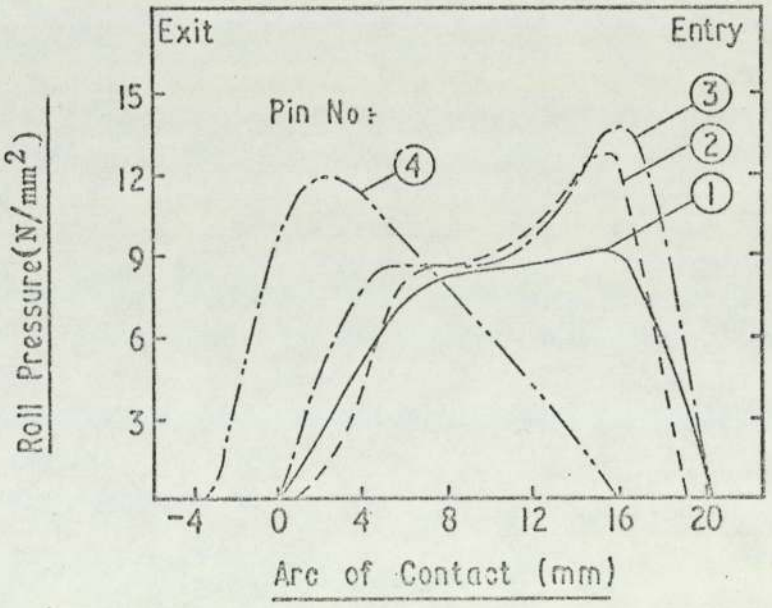

FIG.6.1b PRESSURE DISTRIBUTION CURVES

FOR TUBE WITH d / t = 7.0

Due to the ovality of the groove, the radial draft δ_r at the root of the groove varies with the groove angle θ, see fig.(62) and (63) . The magnitudes of the forces causing the bending of the tube wall depend on δ_r and on the d/t ratio. The draft δ_r has a maximum value at $\theta = 0$, i.e. where pin 1 is situated and a minimum value near the edges, i.e. where pin 4 is situated. It would follow, therefore, that the free zone would have a maximum effect on pin 1, resulting in a high pressure peak at entry, and minimum effect on pin 4 , while pins 2 and 3 are affected by differing amounts depending on the draft δ_r at the corresponding groove angles. For a high d/t ratio, i.e. a thin-walled tube, the tube is most readily deformed and pin 4 is likely to be affected to some extent by the free zone, fig.(61-a).

Pin 1 however, does not produce such pronounced peaks, and the following explanation is offered for this phenomenon. As the tube enters the gap, it first contacts the groove at a point between the root and the shroud . In which case, the angle θ of the point of first contact will depend on the ovality of the groove and the dimensions of the tube and the groove. This results in a relative movement between the groove surface and the tube which can be resolved into two components, namely a horizontal component in the axial direction, and a tangential component. The effect of the first component will be discussed later. The tangential component results in a surface stress in the tangential(tube hoop) direction produced by the roll on the workpiece acting in the direction of increasing θ. The effect of these stresses

at the root of the groove is to decrease the normal pressure i.e. radial pressure of the tube on the roll especially at entry. Therefore the increase of pressure at entry for pin 1 due to the free zone is counteracted by a decrease due to the surface hoop tensions. The complete shape of the curves connecting the undeformed to the deformed tubes corresponds to that necessary for least total work.

To corroborate this qualitative analysis experimentally, foils of steel and copper, 25 μm thick and (50 x 100) mm, fig.(64), were held on the surface of the tube during its passage through the groove. The frictional conditions between the rolls and the sheets were of course different from those between the rolls and the lead tubes, but the foils were so weak by comparison with the lead that they were found to demonstrate the effects discussed.

The rolled sheets were examined and the results proved to be very informative. As can be seen from fig. (64) the ends of the sheets corresponding to the root of the groove in the entry zone failed under hoop tension whereas the sides failed under axial tension.

In addition to the effects of the free zone and the surface tractions on the behaviour of the pin load-cells, it is necessary to consider the effect of the variation of the relative velocity between the rolls and the tube with variations in the angle θ. Analysis of this effect is based on the assumption that the mean tube velocity in the direction of rolling is constant in any plane normal to the tube axis.

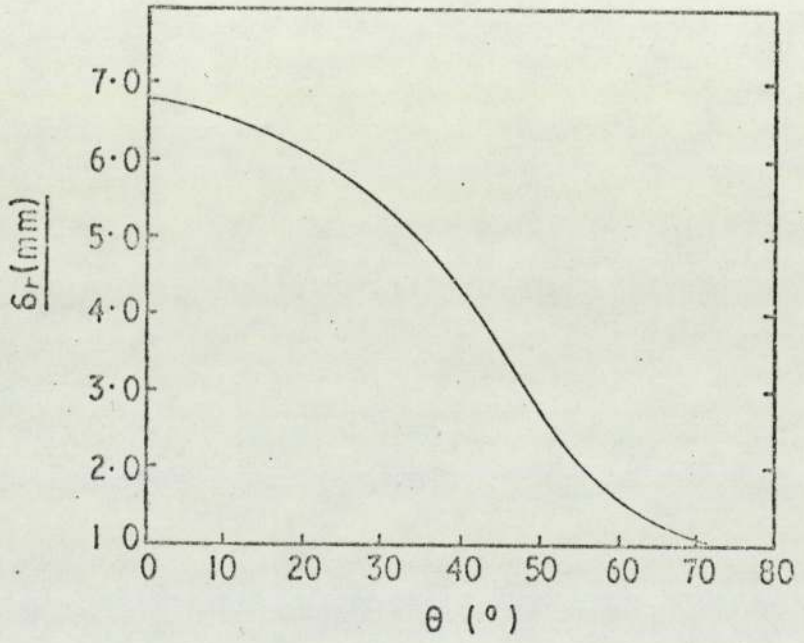

FIG. 62 VARIATION OF THE RADIAL DRAFT δ_r WITH THE GROOVE ANGLE θ

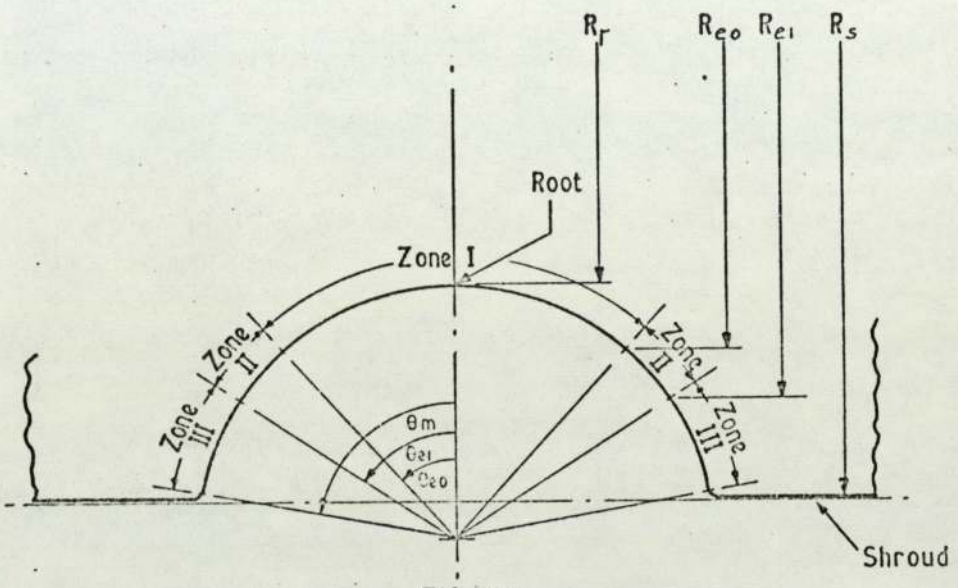

FIG 63-a

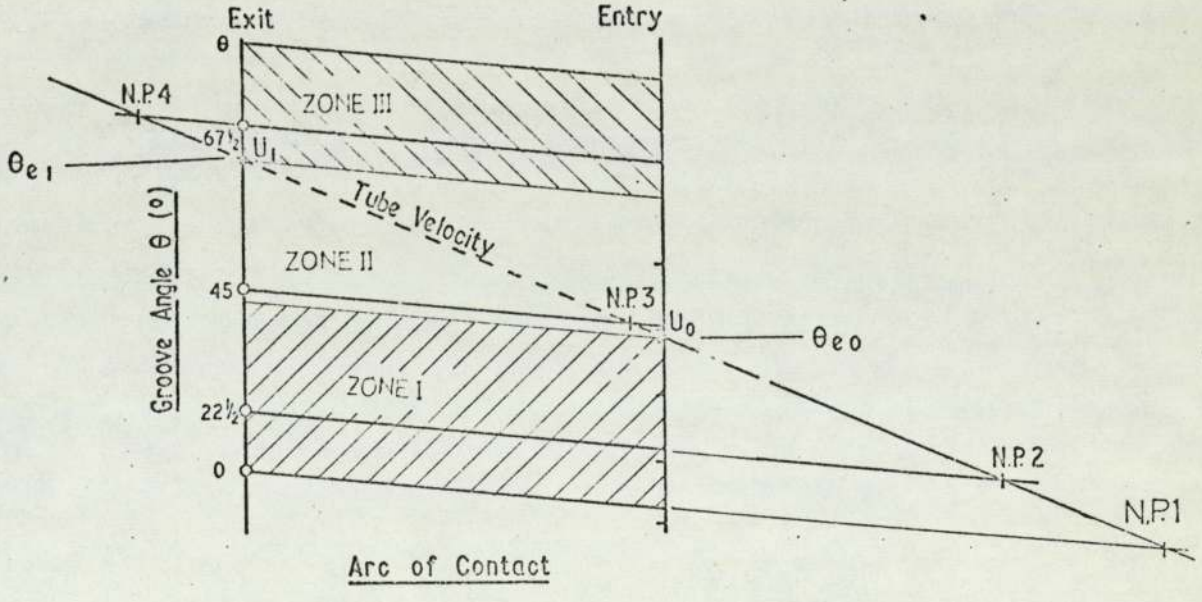

FIG 63-b

Fig. (63) POSITIONS OF NEUTRAL POINTS AND ZONES OF DEFORMATION

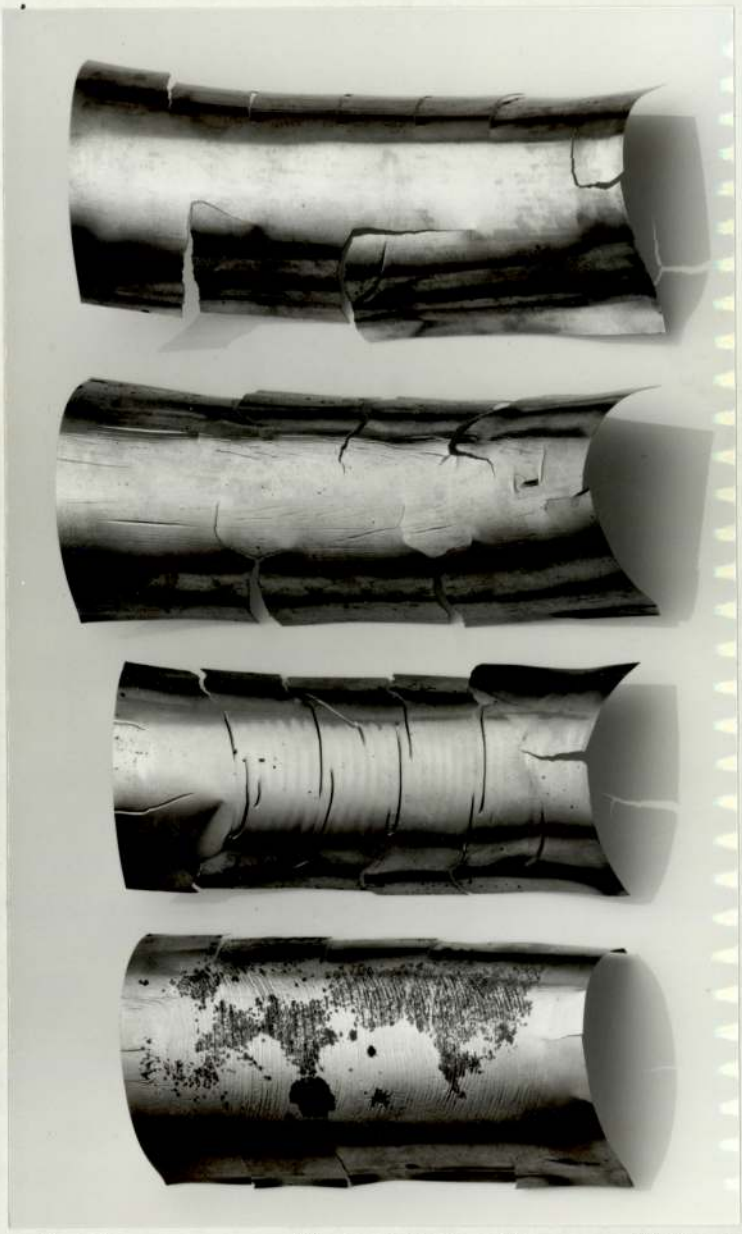

Fig. (64)

Fractured sheets after rolling

The relative velocity v_r is the difference between the horizontal projection of the peripheral velocity of the roll v_h at any point on the groove surface, and the mean tube velocity at the corresponding plane. The velocity of the entering tube U_o is constant across the entry plane. The horizontal projection of the peripheral velocity of the roll v_h however, varies with the roll radius R which in turn varies with θ, fig.(63-a). The minimum value of v_h will occur at the root of the groove where $R = R_r$ is a minimum. As U_o is assumed constant, only at a single value for the roll radius R at the plane of entry will v_h equal the tube velocity U_o This radius will be termed "the effective roll radius" at the entry plane R_{eo}.

$$\omega R_{eo} \cos \phi_m = U_o \qquad \text{(VIII.6)}$$

$$\text{Thus, } R_{eo} = \frac{U_o}{\omega \cos \phi_m} \qquad \text{(VIII.7)}$$

From fig.(63-a), the corresponding groove angle θ is:

$$\theta_{eo} = \cos^{-1} \left(1 - \frac{R_{eo} - R_r}{r_g}\right) \qquad \text{(VIII.8)}$$

Similarly, at the exit plane, where $\phi = 0$

$$\omega R_{e1} = U_1 \qquad \text{(VIII.9)}$$

where: R_{e1} = the effective roll radius at the exit plane,

U_1 = the outgoing tube velocity

$$R_{e1} = \frac{U_1}{\omega} \qquad \text{(VIII.10)}$$

But from the continuity condition,

$$U_o A = U_1 a = \text{constant} \qquad \text{(VIII.11)}$$

A and a are the cross-sectional areas of the tube at entry and exit respectively.

$$U_1 = U_o \frac{A}{a} \qquad \text{(VIII.12)}$$

If r is the reduction in area per pass, then:

$$r = \frac{A-a}{A} \qquad \text{(VIII.13)}$$

and $$U_1 = \frac{U_o}{1-r} \qquad \text{(VIII.14)}$$

hence :

$$R_{e1} = \frac{U_o}{\omega(1-r)} \qquad \text{(VIII.15)}$$

and the corresponding groove angle θ_{e1} is :

$$\theta_{e1} = \cos^{-1}\left(1 - \frac{R_{e1} - R_r}{r_g}\right) \qquad \text{(VIII.16)}$$

Accordingly, the deformation zone could be divided into three zones with respect to the groove angle θ, fig.(63)

Zone I $\quad \theta = 0$ to $\theta = \theta_{eo}$

There the relative velocity v_r is negative at every point along the arc of contact within this zone, that is, the velocity of the tube exceeds the velocity of the roll. Consequently, the frictional forces are unidirectional and correspond to the exit side of the deformation zone in flat rolling.

Zone II $\quad \theta = \theta_{eo}$ to θ_{e1}

where v_r equals zero at some point along the arc of contact, depending on the value of θ. This point moves

from the entry plane for $\theta = \theta_{eo}$ to the exit plane for $\theta = \theta_{e1}$. This zone, therefore, corresponds to the whole of the deformation zone in flat rolling for every angle θ within it.

Zone III $\theta = \theta_{eo}$ to θ_m

where v_r is always positive and the frictional forces are unidirectional. This zone corresponds to the entry side in flat rolling.

For most round-to-oval passes, the value of θ_{eo} was about 30° whereas θ_{e1} was about 50°. Bearing in mind that the groove angles for the four pin loadcells, fig.(25a), were : $\theta_1 = 0^\circ$, $\theta_2 = 22.5^\circ$, $\theta_3 = 45^\circ$ and $\theta_4 = 67.5^\circ$, pins 1 and 2 will almost certainly fall inside zone I giving an exit side type of pressure distribution with neutral points outside the deformation zone, i.e. imaginary.

Generally, pin 4 falls inside zone III giving an 'entry side' type of pressure distribution, while pin 3 falls inside zone II giving a neutral zone inside the contact zone. Fig. (63) represents the relationship between the tube mean velocity and the horizontal component of the roll speed at different positions round the groove. The continuous lines postulate v_h at different groove angles. The intersections of the dotted line, with the four lines representing v_h at groove angles corresponding to the positions of the four pin loadcells, give the position of the neutral point(N.P.), for each pin loadcell with respect to the entry and exit planes.

Comparison between the predicted position of the neutral points, fig. (63), and the measured values, fig.(61), show that the trend is the same in both cases.

It appears that the effect of the free zone, which is to increase the pressure on pin 3 at entry, is higher than the pressure peak due to friction.

So far, only the direct effect of the variation of the tangential velocity of the roll with the groove angle θ has been discussed. The contribution of this effect to the understanding of the behaviour of the pin load-cells has also been explained.

Let us now consider the indirect effect of this variation on the behaviour of the pin loadcells. If the tube is considered to be assembled from radial elements of hoop thickness, $rd\theta$ then because v_h increases with θ until at $\theta = \theta_{e1}$, it exceeds the mean tube velocity at all points along the arc of contact, the radial elements inside zone III tend, under the effect of unidirectional friction forces, to move faster than those elements in zones I and II. This tendency increases as θ increases. For elements within zone I the reverse situation applies and the mean velocity of the tube is higher than v_h. Thus the opposing unidirectional frictional forces will tend to slow down the elements within this zone. This tendency increases as θ decreases. The overall result is the creation of longitudinal stresses between the elements. Thus elements of the tube in zone I will be subjected to an equivalent front tendion which increases as θ decreases, and elements of zone III will be subjected to an equivalent back tension which increases with the angle θ.

It is known that the effect of the front tension on the contact pressure in flat rolling is to decrease the

area under the pressure distribution curve and to shift the neutral point towards the entry plane. The back tension also decreases the area under the curve and moves the neutral point towards the exit plane.

Reference to the pressure distribution curves of fig. (61) and appendix (C) show that this argument is in accord with the observations. Also, examination of the ends of the rolled tubes showed that the metal in the vicinity of the shrouds of the rolls led that rolled by the root of the groove. Consequently, these observations support the above qualitative analysis.

Cole [1] also observed the occurrence of the pressure peak near the entry plane, as can be seen from fig. (65), reproduced from his work. However the pronounced peaks in fig. (65) were observed more in the present work for thin tubes, as can be seen from the pressure distribution curves in Appendix (C).

SINKING. Tube No. 51/1. Superimposed Pin Loadcell Measurements.

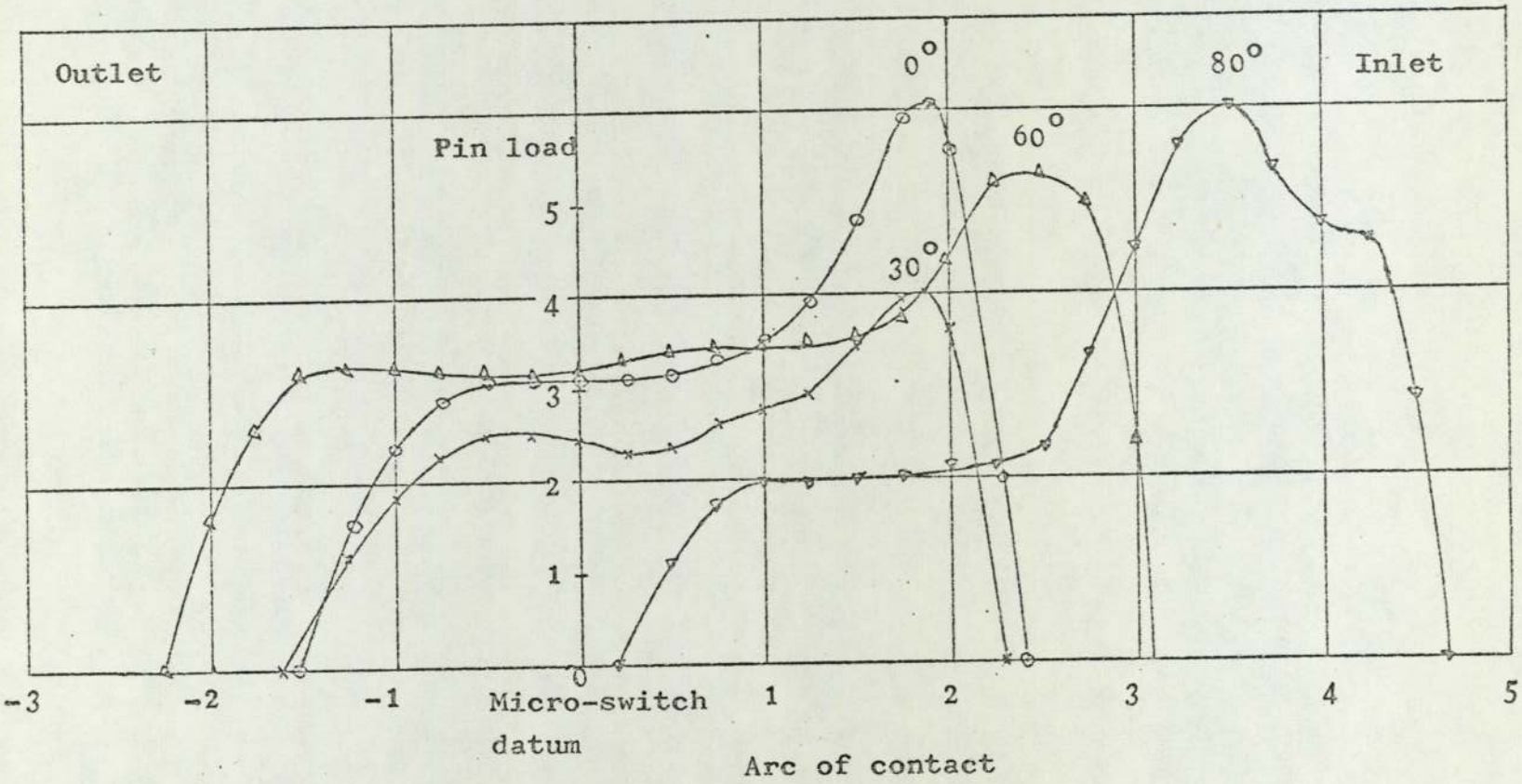

Fig. (65)

Pressure Distribution from Cole's Work[1]

(VIII-7) Roll Pressure

A selection of tracings of actual pressure distribution curves for various rolling conditions is shown in Appendix (C). The shape of these curves has been discussed in section (6) of this chapter. Figs(66) and (67) show the distribution of roll pressure around the groove for different gap settings, d_o/t_o ratios, and pass type. These figures show the tendency of the pressure to increase with the groove angle θ from a low value at the root of the groove to a maximum value somewhere around 45^o to 65^o for gap setting I i.e, condition of complete filling of the groove. When complete filling of the groove does not take place, viz., gap settings II and III, then the maximum occurs at 45^o and the pressure decreases for values of θ greater than 45^o. For gap setting III pin no.4 did not make contact with the thick tube as can be seen from tables (VIII.3)and(VII.3)for tests7,8 and 9.On the other hand for the thin and medium thickness tubes contact was maintained for all the pins because for relatively thin tubes, the tube is most readily deformed.

One observes from table (VIII.3)that for the R-O passes, mean value of the pressure lies between the readings of pin 2 and 3 being closer to pin 2 in most cases. In other words the mean roll pressure occurs at a groove angle of between 25 and 40 degrees.

For O-O passes, fig.(66) show that the distribution of the pressure around the groove is different as might be expected. For unguided sinking, fig. (67-a) only pin 1 made contact with the tube. As reported in chapter(IV) difficulty

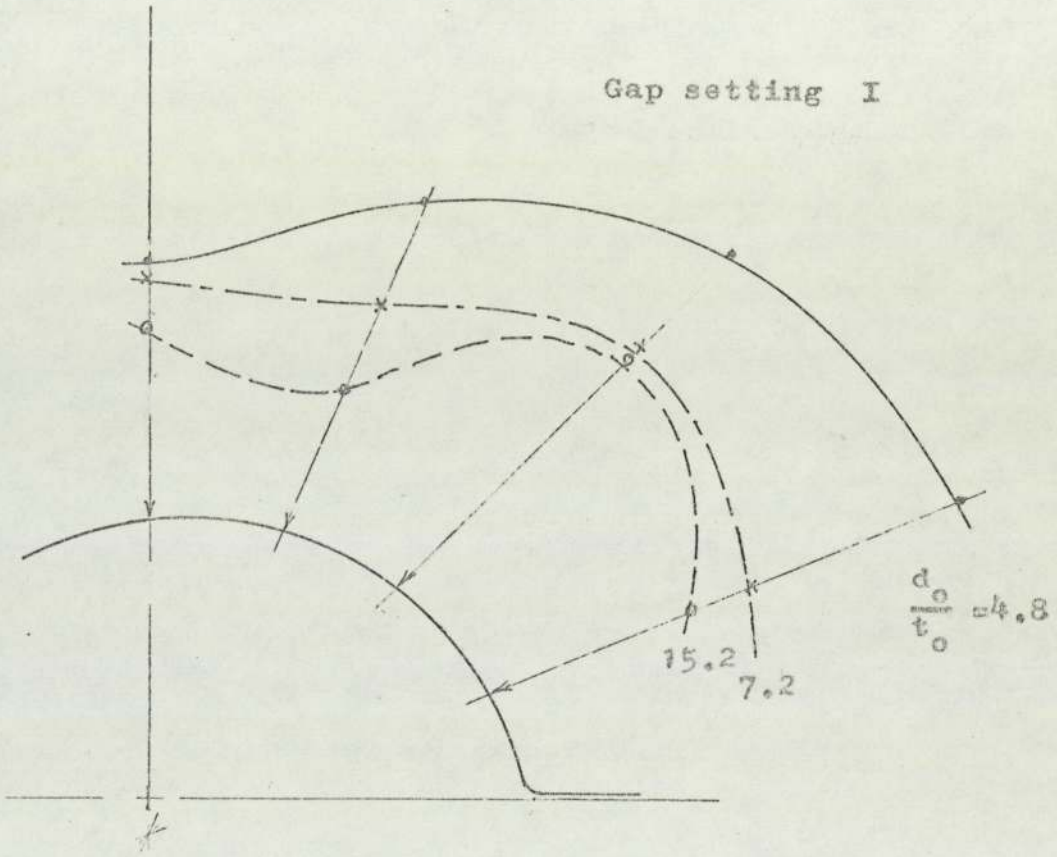

Fig.(66-a)

Distribution of the roll pressure round the groove

phase I, R-O pass

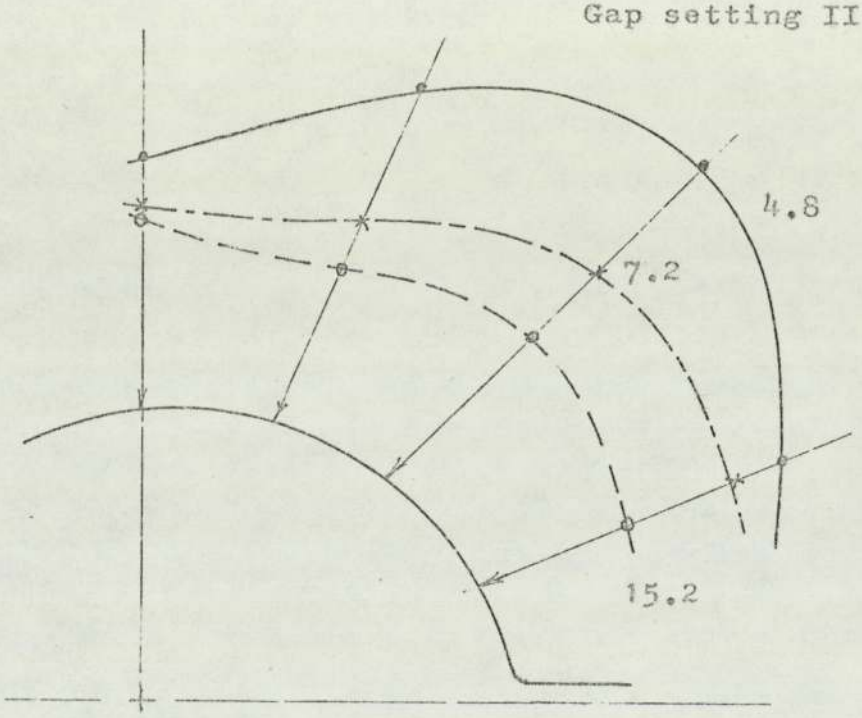

Fig. (66-b)

Distribution of the roll pressure round the groove

phase I, R-O pass

Gap setting III

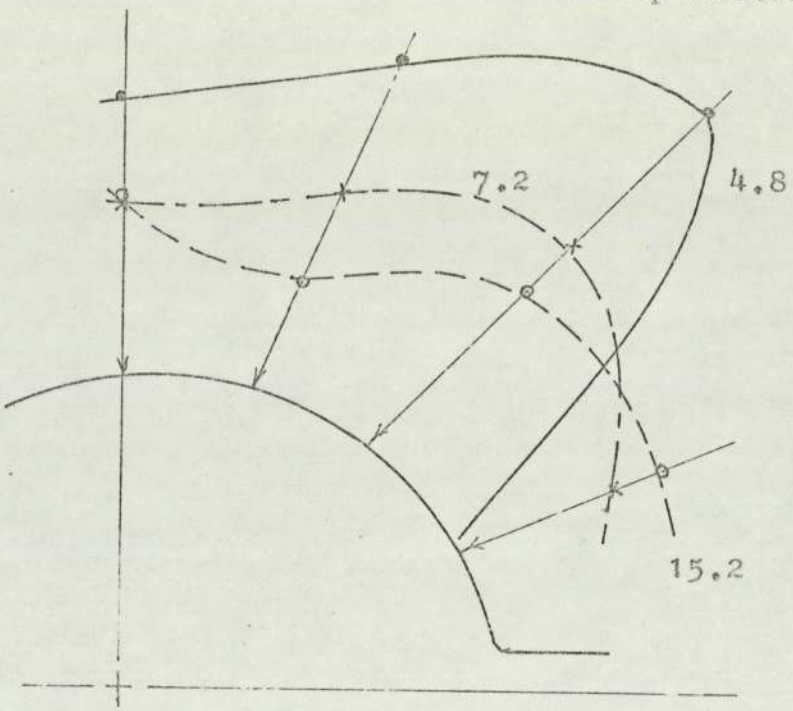

Fig. (66-c)

Distribution of the roll pressure round the groove

phase I, R-O pass

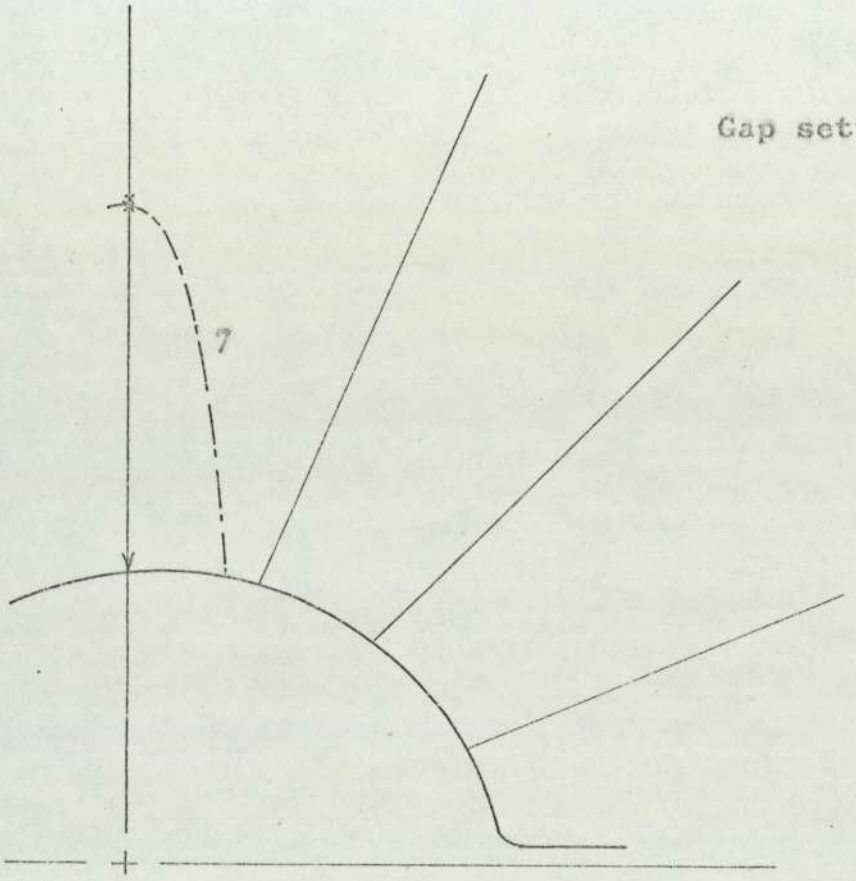

Fig. (67-a)

Distribution of the roll pressure
round the groove
(Oval-to-Oval pass)

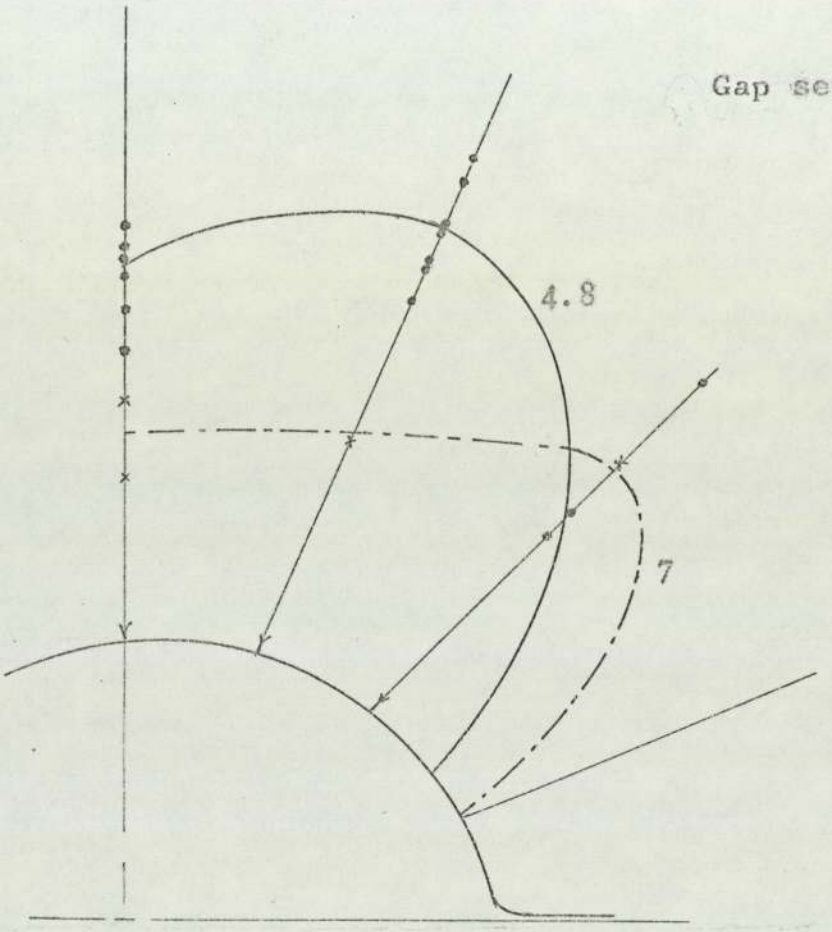

Fig. (67-b)

Distribution of the roll pressure
round the groove
(Oval-to-Oval pass)

was encountered in preventing the tube from rotating round its axis in this type of pass. By comparison with the guided sinking 0-0 case, fig.(67-b), where contact with other pins took place, the use of the pin loadcell results for the unguided sinking(0-0 passes only) is restricted. It is believed that the guided sinking case is a more representative one of the true state of stress between the tube and the rolls. For this reason the unguided sinking 0-0 tests are not included in the comparison between test results and theoretical predictions shown in table (VIII.3). When using the Russian theories, the following points were borne in mind:

a) the coefficient of friction for Vatkin's and Kirichenko's theory was taken to be 0.25 as recommended by Vatkin (33).

b) L in equations VI.4 and VI.8 was replaced in the calculations by L_m^* 'the measured length of the arc of contact corrected for torque sharing and the finite width of the pin.

c) mean tube dimensions were used in all the theories.

d) t, the wall thickness of the tube, in Vatkin's and Kirichenko's expressions, which was assumed by the authors to remain constant, was replaced by t_o .

e) in the case of Kirichenko's expression, a point at the root of the groove (i.e, $\theta = 0$) in the middle of the contact zone (i.e, $x = L/2$) was considered. Therefore Kirichenko's predictions of the roll pressure should be compared with the reading of pin 1.

f) ϕ the angle of contact has been calculated from the expression:

$$\phi = L_m^* / R_r .$$

In the case of the proposed theory (Energy method) the following points were considered in the calculations:-

a) θ_c , the maximum groove angle of contact for the R-O passes was calculated according to equation (IV.2), chapter (IV). As for O-O passes of phase II, the number of pins in contact with the tube was taken to determine θ_c. A value of 60° was used in the calculation. It should be noted that small variations in θ_c have little effect on the calculated roll pressure.

b) ϕ_m, the maximum angle of contact was calculated from

$$\phi_m = L_m^*/R_r$$

c) the frictional stresses in zones 1 and 2 were assumed the same, hence the shear factors m_1 and m_2 were assumed equal, i.e, $m_1 = m_2 = m$.

The shear factor m when set to zero, i.e, frictionless condition, should result in a lower bound solution. This is the upper value for each test in the last column of table VIII.3.On the other hand, setting m to 1.0 gives the condition of complete sticking between tube and rolls which should represent an upper bound solution. This is the lower value in the last column (Energy method) of table(VIII.3).

The actual pressure should ideally lie between these two limits.

Table (VIII.3) and fig.(68-a-b-c) show the comparison made between test results and the theoretical predictions. All the theoretical predictions should be compared with the mean roll pressure p_m with the exception of Kirichenko's which has been calculated for the position corresponding to pin 1

and should therefore be compared with p_1.

It can be seen from fig. (68) that p_m falls inside the two limits of the Energy method with the exception of a few cases, particularly for thick tubes($d_o/t_o \simeq 4.8$). This in fact means that if the shear factor m is set at the right value between zero and unity, the proposed theory would predict the actual mean pressure satisfactorily. It has been observed that setting $m = 0.5-0.75$ gives good correlation with the majority of the test results. Although it may be possible to measure the frictional stress with some degree of accuracy it may be sufficient for practical applications to calculate the lower and upper limits of the mean pressure. If this is so, then the Energy method can prove useful for estimating the pressure, since by comparison with the other three theories its predictions are more accurate. The table shows that the predictions of the three Russian theories are close to the predicted lower bound of the proposed theory.

For thin tubes, the three theories seriously underestimate the roll pressure while the correlation improves for the medium thickness and thick tubes but remains an underestimate for all cases. Cole[1] noted that these three theories gave poor correlation with his test results (see chapter(VI). section 4), the theoretical predictions being lower than the test results.

When tested against Cole's results, the Energy method gives a lower bound similar to the predictions of the other three theories and an upper bound which varies between about 1.5-3 times the lower bound, depending on the reduction in

area. For the high reduction tests the upper bound is some 1.5 times the lower bound, while for the low reduction tests the upper bound increases in relation to the lower bound. Cole's results indicate that the recorded pressures for the low reduction tests were higher than those for the high reduction tests. The Energy method indicates that friction contribution to the total roll pressure is greater for low reductions and also for thin tubes than it is for high reductions and relatively thick tubes. The test results of the present investigation show that there is little change in the recorded pressure for the three gap settings and fig. (74) shows that for the thin tube there is hardly any change in pressure with r% . An explanation for this phenomenon is readily supplied by the Energy method, viz., friction contribution is high for small reduction of area. This result is not surprising since for very light reductions, as in the final few stands of a tube rolling mill, most of the pressure exerted by the tube on the rolls would be due to friction

In brief, the comparison between the test results and the predictions of the available theories shows that the Energy approach proposed here represents a suitable alternative to the equilibrium approach in the case of a complex problem like tube rolling.

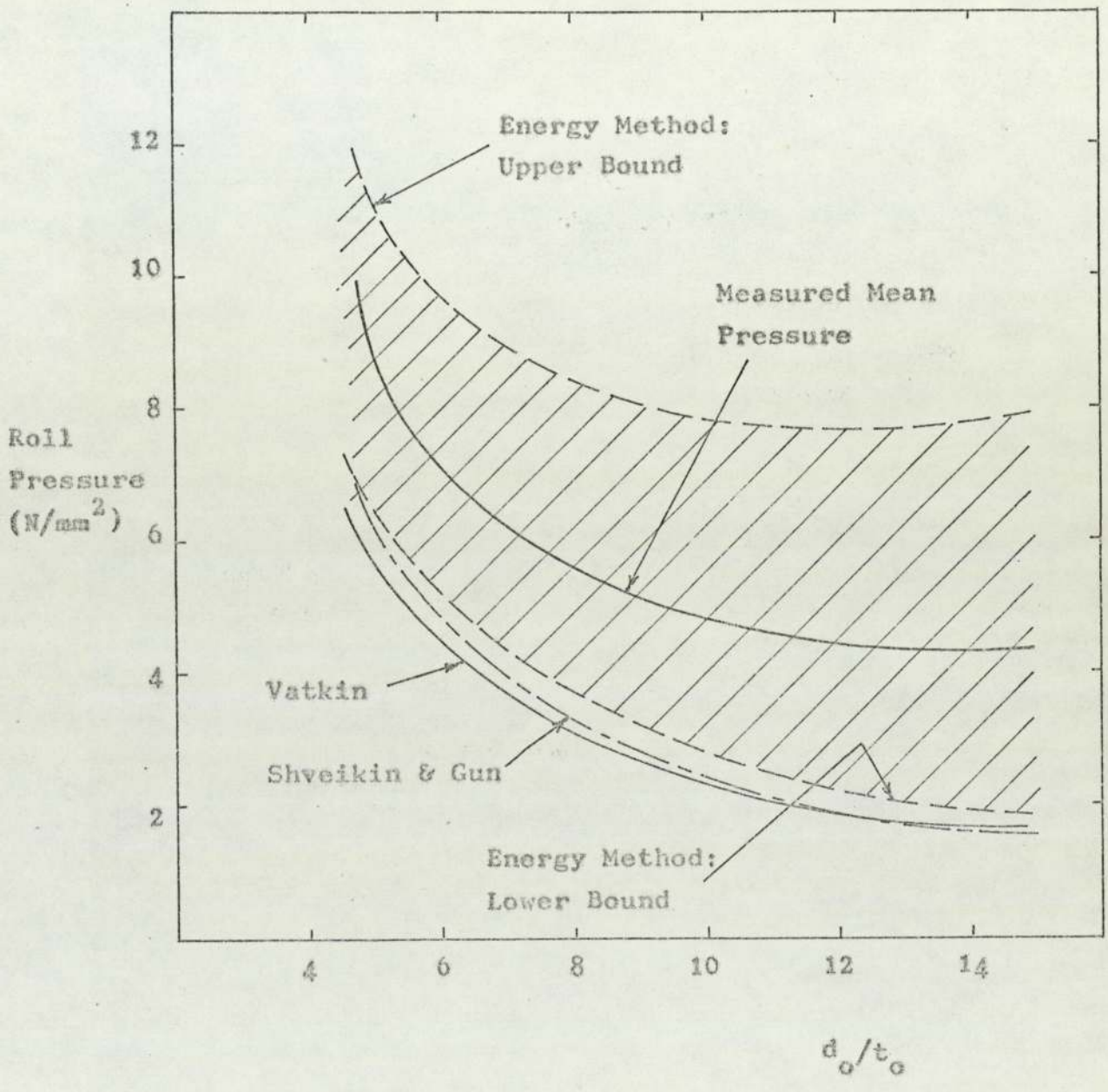

Fig. (68-a)

Comparison between Measured and Calculated

Roll Pressure

(gap setting III, R-O pass)

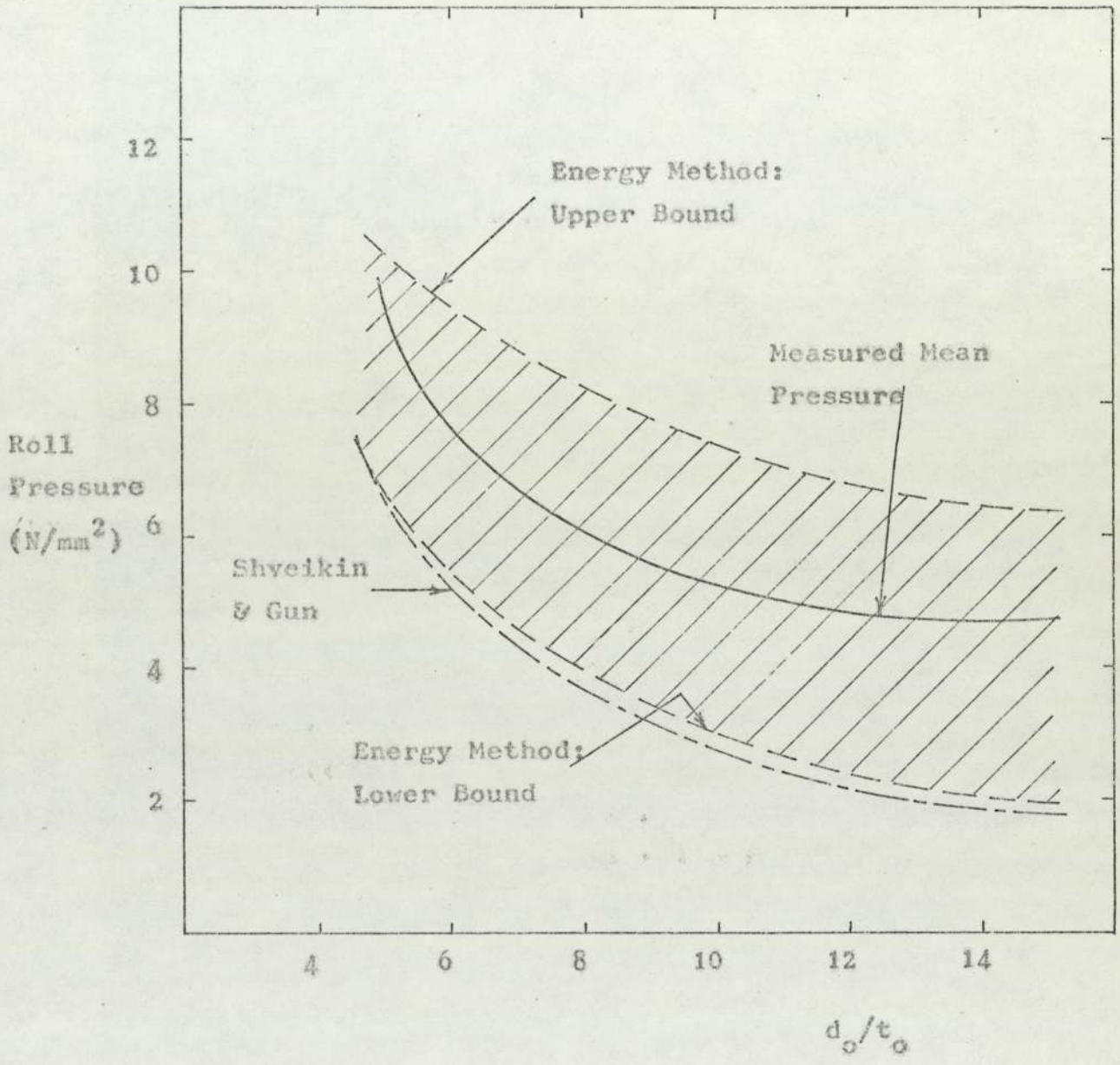

Fig. (68-b)

Comparison between Measured and Calculated

Roll Pressure

(gap setting II, R-O pass)

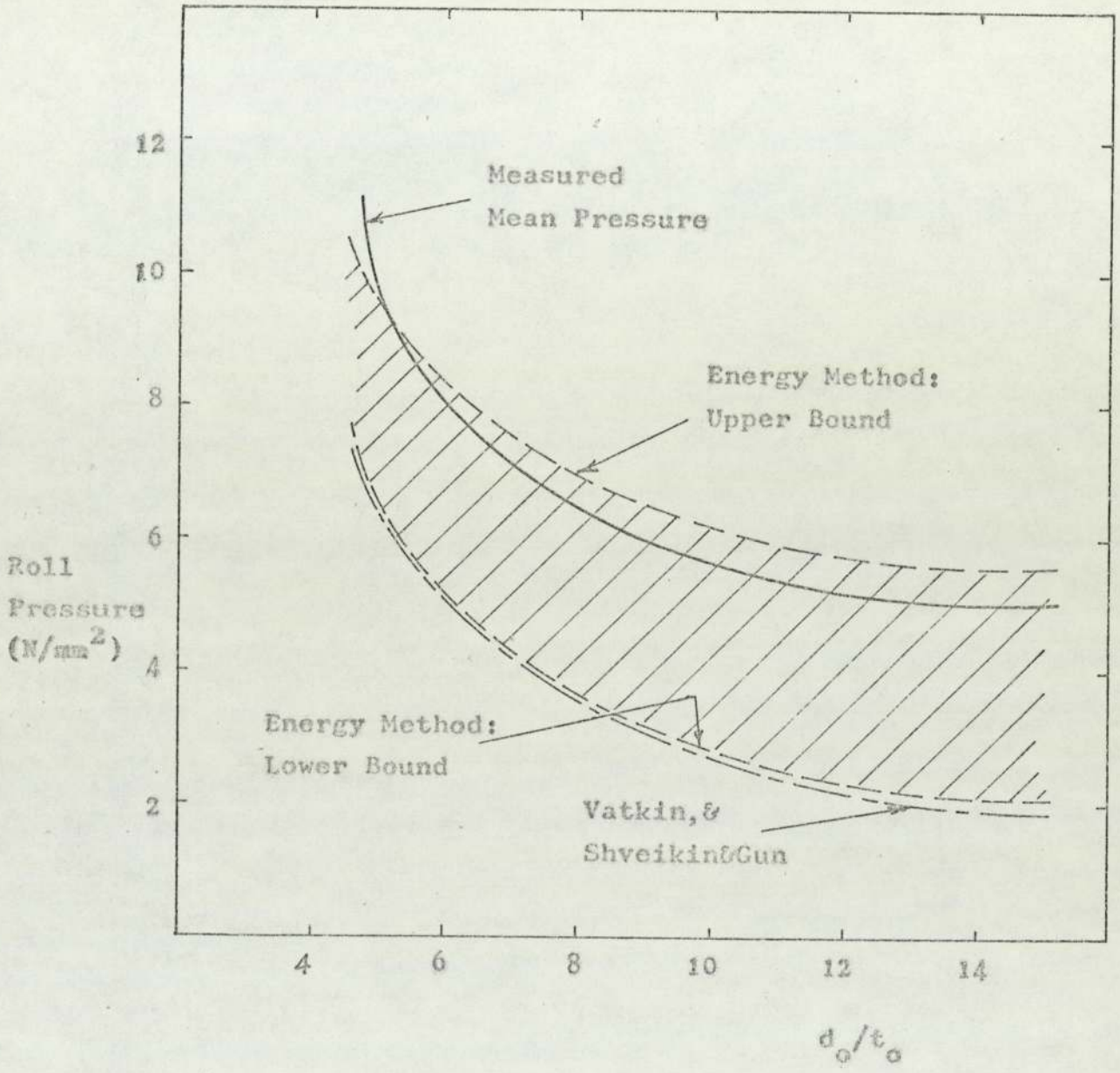

Fig.(68-c)

Comparison between Measured and Calculated

Roll Pressure

(gap setting I , R-0 pass)

Table(VIII.3)

Roll Pressure

Comparison between Test Results and Theoretical Predictions

Test No.	Measured Pressure (N/mm^2)					Theoretical Predictions (N/mm^2)			
	p_1	p_2	p_3	p_4	p_m	Shveik. & Gun	Vatkin	Kinch-enko	Energy Method
1	4.33	3.87	4.65	5.54	4.60	1.70	-1.79	1.60	2.14* 8.52**
2	4.62	3.10	5.81	5.87	4.85	1.69	-1.88	1.45	1.92 6.95
3	3.88	3.94	5.87	5.32	4.75	1.73	-1.82	1.62	2.19 8.29
4	5.31	5.05	8.96	4.99	6.07	4.00	-3.79	3.95	4.40 9.23
5	4.57	5.60	7.46	4.37	5.50	3.96	-3.77	3.93	4.41 9.16
6	5.21	4.29	7.42	8.18	6.27	3.96	-3.76	3.97	4.17 8.44
7	6.80	9.12	12.41	2.72	9.44	6.53	-5.76	6.46	6.76 11.74
8	7.38	9.53	12.53	NC	9.81	6.70	-6.09	6.26	6.99 11.51
9	8.32	10.3	13.65	NC	10.76	6.51	-6.00	6.07	6.76 11.53
10	3.84	3.96	5.54	5.7	4.76	1.77	-1.89	1.65	1.89 6.67
11	3.79	4.43	5.29	5.19	4.67	1.79	-1.91	1.66	1.96 6.47
12	4.99	4.27	5.21	4.03	4.62	1.79	-1.90	1.68	2.02 6.29
13	4.90	3.97	5.28	6.72	5.22	1.77	-1.84	1.72	1.92 6.73
14	5.27	4.55	5.43	4.67	4.98	1.81	-1.94	1.61	1.96 6.03
15	5.01	4.29	4.79	3.52	4.40	1.81	-1.92	1.64	1.94 6.30
16	5.05	4.52	4.87	3.77	4.55	1.82	-1.92	1.67	1.98 5.95
17	6.35	NC	7.59	8.15	7.36	4.09	-3.98	3.85	4.27 9.00
18	5.95	7.12	7.99	9.02	7.52	4.14	-3.98	3.93	4.30 9.20
19	5.45	7.09	7.90	8.64	7.27	4.15	-3.95	4.01	4.31 9.04
20	6.38	6.07	9.09	6.21	6.94	4.32	-4.24	3.90	4.47 8.11
21	6.20	7.92	8.60	8.87	7.89	4.33	-4.34	3.70	4.48 8.16

* Lower bound solution

** Upper bound solution

Table (VIII. 3) (contd.)

Roll Pressure

Comparison between Test Results and Theoretical Predictions

Test No.	Measured Pressure (N/mm^2)					Theoretical Predictions (N/mm^2)			
	p_1	p_2	p_3	p_4	p_m	Shveik. & Gun	Vatkin	Kinch-enko	Energy Method
22	5.30	6.52	8.68	8.40	7.22	4.33	-4.28	3.85	4.49 7.95
23	5.01	4.94	8.18	7.72	6.46	4.53	-4.31	4.21	4.82 9.40
24	4.71	4.42	6.19	9.10	6.11	4.49	-4.26	4.25	4.63 8.84
25	5.32	5.01	7.91	8.98	6.81	4.74	-4.58	4.29	5.54 10.05
26	5.32	5.75	7.74	8.21	6.76	4.66	-4.36	4.49	4.81 9.26
27	5.95	6.40	9.72	5.60	6.92	4.66	-4.36	4.48	4.81 9.26
28	4.83	4.24	5.72	6.79	5.40	4.11	-4.07	3.77	4.36 9.04
29	7.13	9.24	12.51	6.92	8.95	6.98	-6.50	6.16	6.90 10.45
30	7.61	8.24	11.19	2.83	9.01	6.83	-6.20	6.40	6.82 10.96
31	6.95	8.81	12.19	4.14	9.32	6.99	-6.26	6.70	7.04 10.46
32	6.63	9.23	11.75	12.7	10.07	7.09	-6.62	6.07	7.05 10.60
33	6.58	9.17	11.72	12.58	10.01	7.21	-6.41	6.78	7.15 10.15
34	6.43	9.29	11.2	8.40	8.89	7.18	-6.32	6.89	7.11 10.13
35	5.03	4.00	5.53	6.37	5.23	1.93	-1.96	1.83	1.99 5.82
36	4.08	3.93	5.40	6.59	5.00	1.94	-2.02	1.81	2.11 4.93
37	4.19	3.17	5.34	4.81	4.38	1.89	-2.02	1.68	2.02 5.76
38	4.70	4.34	4.70	4.01	4.45	1.89	-2.07	1.58	2.02 5.76
39	5.07	4.23	5.27	5.58	5.04	1.89	-2.03	1.65	2.05 5.38
40	5.30	4.13	5.29	5.79	5.13	1.88	-2.00	1.74	2.16 5.22
41	4.91	3.96	5.50	8.52	5.72	1.93	-2.01	1.74	2.03 5.91
42	5.04	4.10	5.38	6.64	5.29	1.93	-2.01	1.74	2.03 5.91

Table(VIII.3) (contd.)

Roll Pressure

Comparison between Test Results and Theoretical Predictions

Test No.	Measured Pressure (N/mm^2)					Theoretical Predictions (N/mm^2)			
	p_1	p_2	p_3	p_4	p_m	Shveik. & Gun	Vatkin	Kinch-enko	Energy Method
43	4.80	5.58	5.31	7.17	5.73	4.45	-4.43	3.83	4.46 7.50
44	5.20	4.53	6.03	11.14	6.70	4.46	-4.29	4.14	4.50 7.57
45	4.63	5.15	8.43	9.41	6.91	4.81	-4.02	4.25	4.73 8.30
46	5.72	4.89	8.01	10.78	7.35	4.78	-4.09	4.16	4.83 7.66
47	6.33	6.29	8.05	8.89	7.39	4.40	-4.25	3.87	3.72 7.22
48	6.09	6.34	8.22	8.07	7.18	4.40	-4.23	3.93	3.72 7.22
49	6.00	6.30	8.54	7.41	7.06	4.40	-4.27	3.85	3.72 7.22
50	6.65	6.38	8.92	9.76	7.93	4.45	-4.29	4.12	4.51 7,56
51	6.65	6.23	6.96	11.49	7.83	4.43	-4.38	3.88	4.46 7.59
52	6.42	7.26	8.08	9.48	7.81	4.46	-4.37	3.96	4.46 7.70
53	6.40	7.28	8.05	9.51	7.81	4.46	-4.37	3.96	4.46 7.70
54	6.93	6.11	8.16	5.03	6.56	4.45	-4.40	3.90	4.46 7.50
55	7.43	8.96	13.01	12.17	10.39	7.33	-6.50	6.74	6.89 9.82
56	6.74	8.31	14.05	11.63	10.18	7.38	-6.47	6.99	7.05 9.77
57	6.70	10.80	13.40	11.91	10.69	7.35	-6.52	6.89	7.07 9.67
58	6.88	9.34	12.49	13.50	10.56	7.35	-6.57	6.74	7.01 9.80
59	6.97	9.42	13,84	10.10	10.09	7.24	-6.30	6.87	6.87 9.74
60	7.50	10.20	12.20	14.40	11.07	7.26	-6.41	6.67	6.82 10.05
68	5.57	7.36	8.69	8.34	7.49	4.33	-4.09	4.19	4.50 8.04
69	6.10	7.35	8.10	8.89	7.61	4.33	-4.08	4.21	4.50 8.04
70	6.10	7.04	9.06	8.61	7.60	4.33	-4.14	4.11	4.50 8.04

Table(VIII.3) (contd.)

Roll Pressure

Comparison between Test Results and Theoretical Predictions

Test No.	Measured Pressure (N/mm^2)					Theoretical Predictions (N/mm^2)			
	p_1	p_2	p_3	p_4	p_m	Shveik. & Gun	Vatkin	Kinch-enko	Energy Method
71	4.61	3.82	5.31	3.60	4.33	1.88	-2.01	1.62	1.94 6.03
72	4.78	4.23	5.08	6.52	5.15	1.89	-1.93	1.76	1.87 6.24
73	4.87	4.36	5.30	4.00	4.63	1.89	-1.96	1.69	1.87 6.24
74	6.40	10.90	13.56	10.98	10.47	7.41	-6.27	7.44	7.05 9.74
75	4.41	6.16	9.32	NC	6.63	4.39	-3.88	4.43	5.35 8.56
76	6.43	6.04	9.83	NC	7.43	4.39	-3.94	4.37	5.35 8.56
77	8.71	12.02	12.50	NC	11.06	7.03	-6.12	6.54	8.23 11.51
78	7.51	11.12	7.58	NC	8.74	7.03	-5.91	6.91	8.23 11.51
79	10.96	9.96	6.54	NC	9.16	7.23	-5.95	7.02	8.28 11.93
80	10.10	11.33	NC	NC	10.71	7.23	-6.04	6.87	8.28 11.93
81	9.65	13.65	NC	NC	11.65	7.00	-5.66	6.77	7.73 13.49
82	10.43	12.16	NC	NC	11.29	7.00	-5.66	6.77	7.73 13.49
83	10.11	12.27	NC	NC	11.20	6.77	-5.21	6.76	9.71 19.27
84	9.80	14.22	NC	NC	12.01	6.77	-5.22	6.74	9.71 19.27

Tests 75-84 are phase II, 0-0 pass NC = No Contact

(VIII-8) Effect of d_o/t_o and r% on the loads

Figs. (69) , (70) and (71) show the variation of torque, RSF and pressure with the d_o/t_o ratio for the three gap settings used in the tests. Figs. (69) and (70) show that as the ratio d_o/t_o decreases the torque and RSF increase rapidly which is to be expected as the conditions approach those of the rolling of a solid bar. However the variation of the mean pressure with d_o/t_o is less steep for small values of d_o/t_o. Ideally the variation of the mean pressure should be similar to that of the RSF particularly since the area of contact varies little with d_o/t_o. This difference in behaviour between the RSF and mean pressure curves could be attributed partly to some lack of response on the part of the pin loadcells for high values of pressure. This phenomenon has also been observed when comparing the measured RSF with that calculated from the mean pressure and the area of contact as will be discussed later. It could also be responsible for the low values of torque calculated using the lever arm concept for the thick tubes also discussed later.

Figs. (72) , (73) and (74) show the variation of torque, RSF and mean pressure with the percentage reduction of area for the various d_o/t_o ratios.

The variation of loads for the thin tube with r% is small compared with that for the thick tube.

It can be seen from these graphs and figs. (69), (70) and (71) that d_o/t_o is a more significant parameter and its influence on the rolling loads is more pronounced than that of r% .

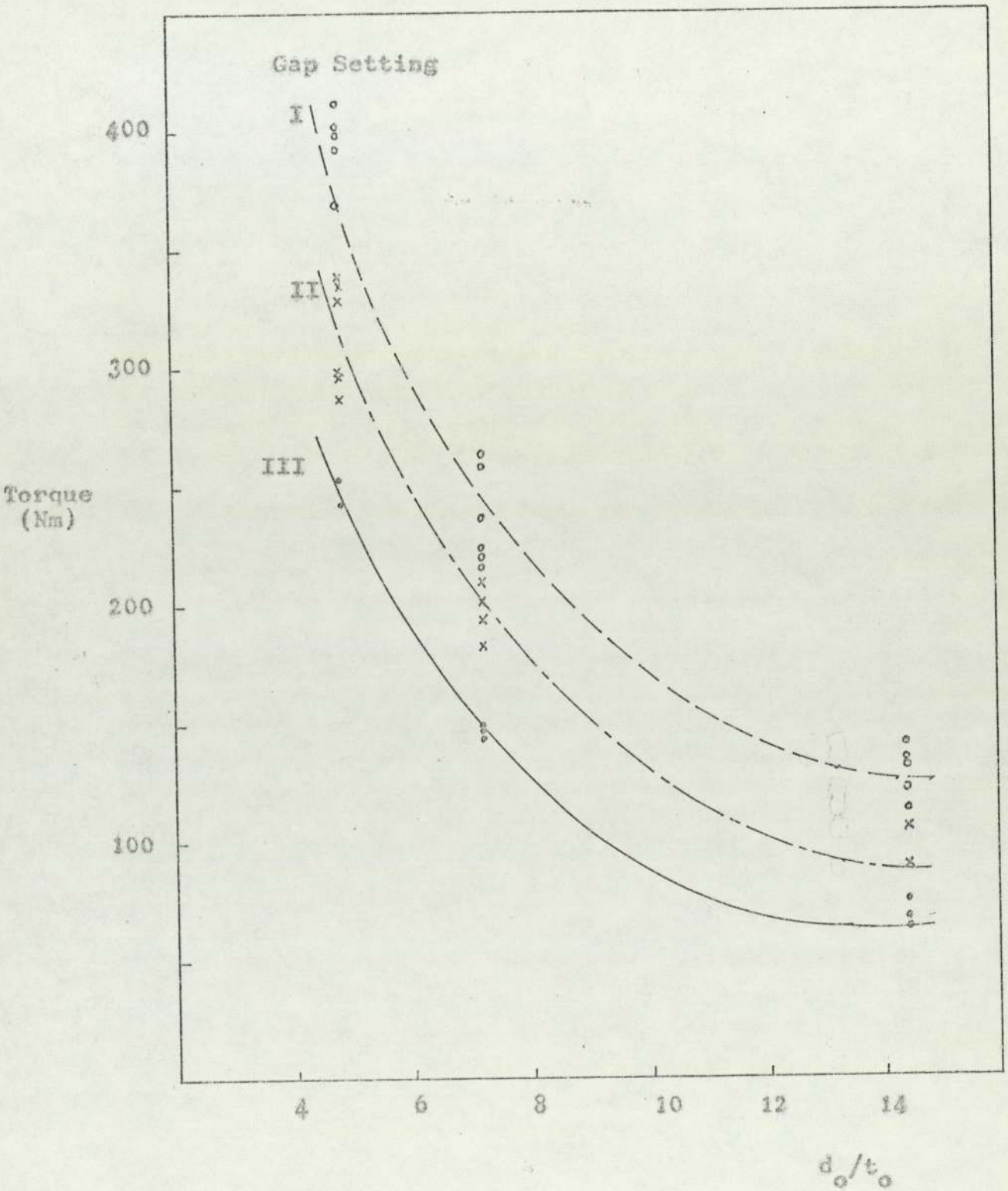

Fig. (69)

Variation of Torque with d_o/t_o

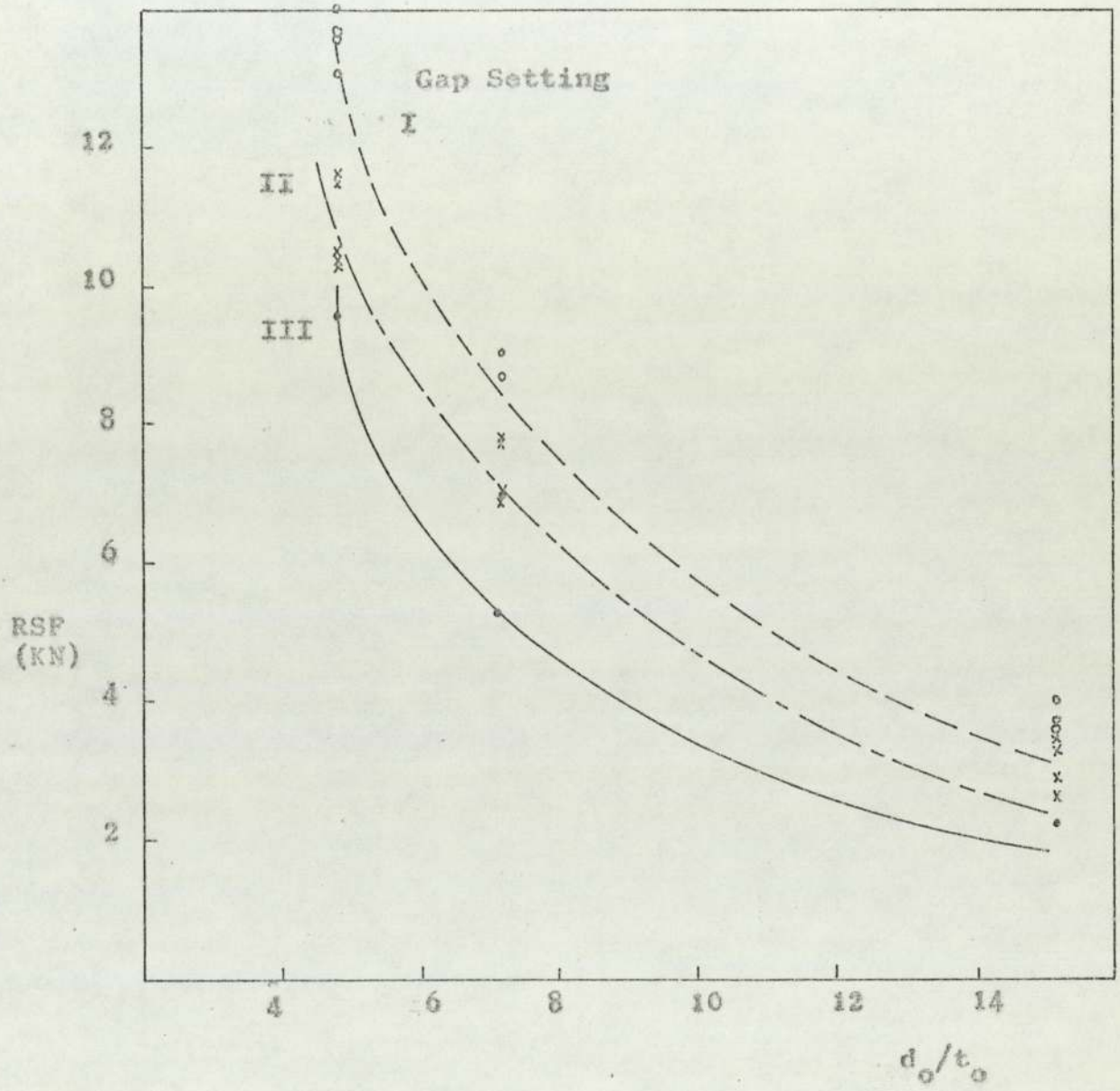

Fig (70)

Variation of RSF with d_o/t_o

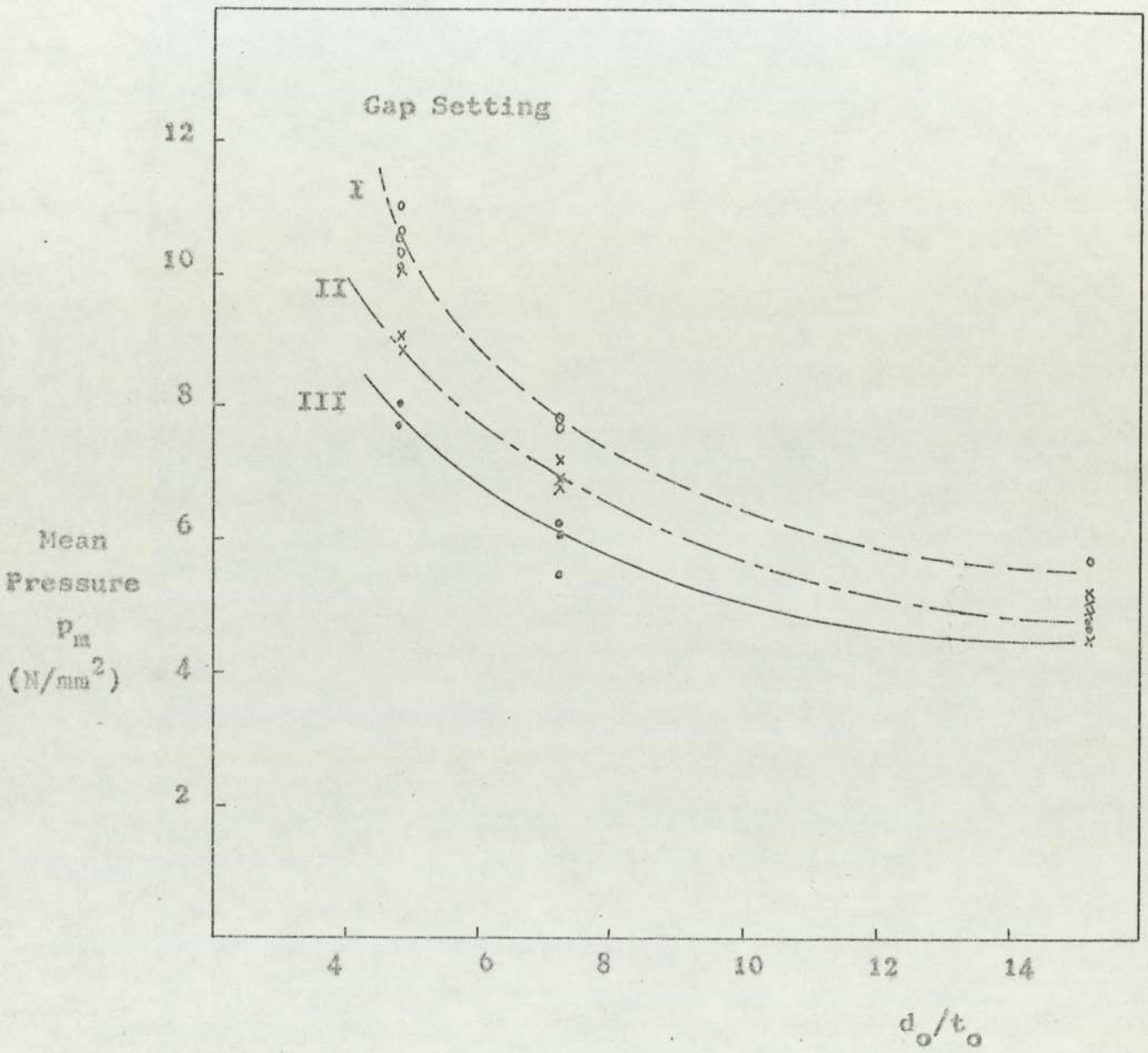

Fig. (71)

Variation of p_m with d_o/t_o

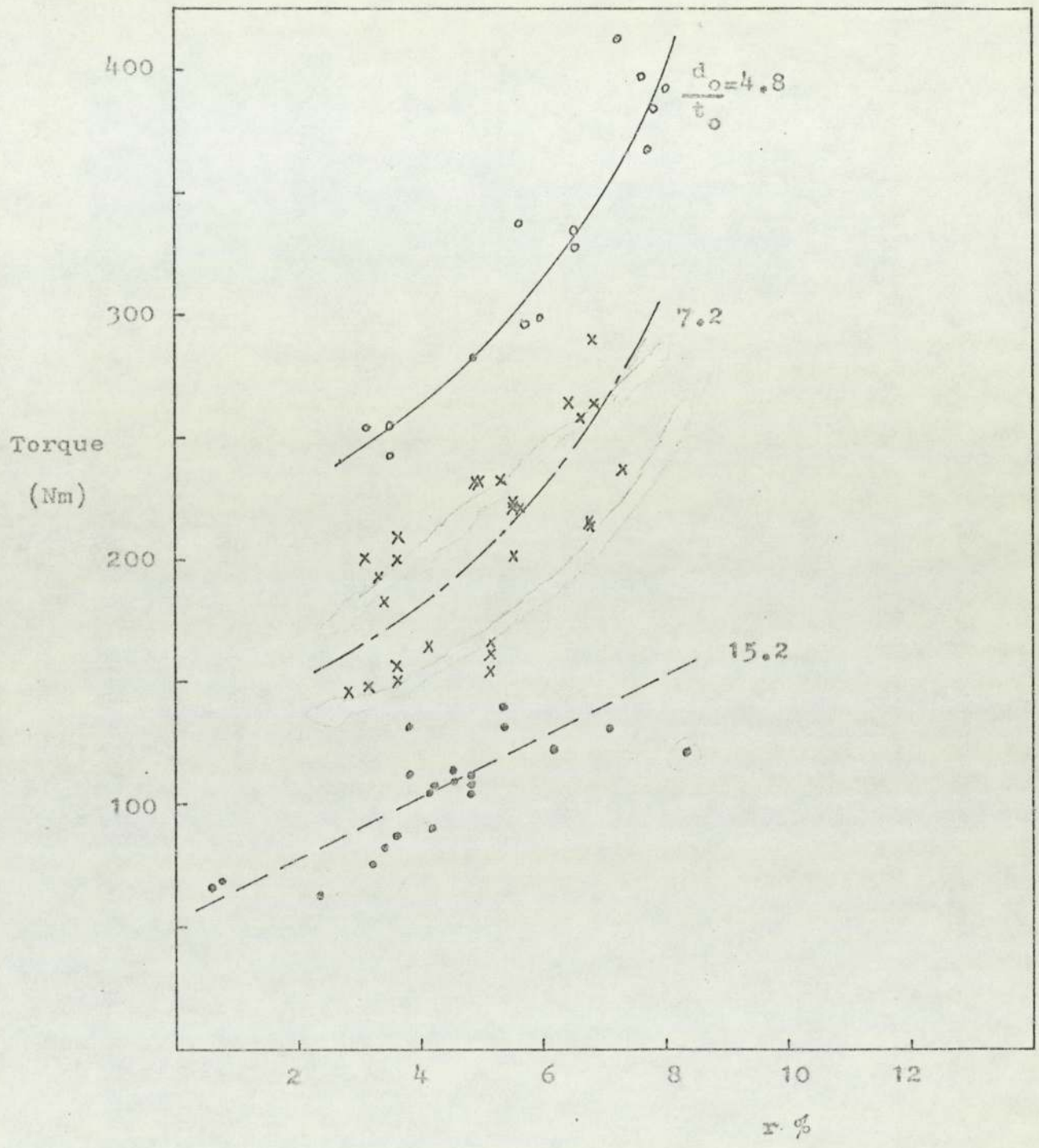

Fig (72)

Variation of Torque with r%

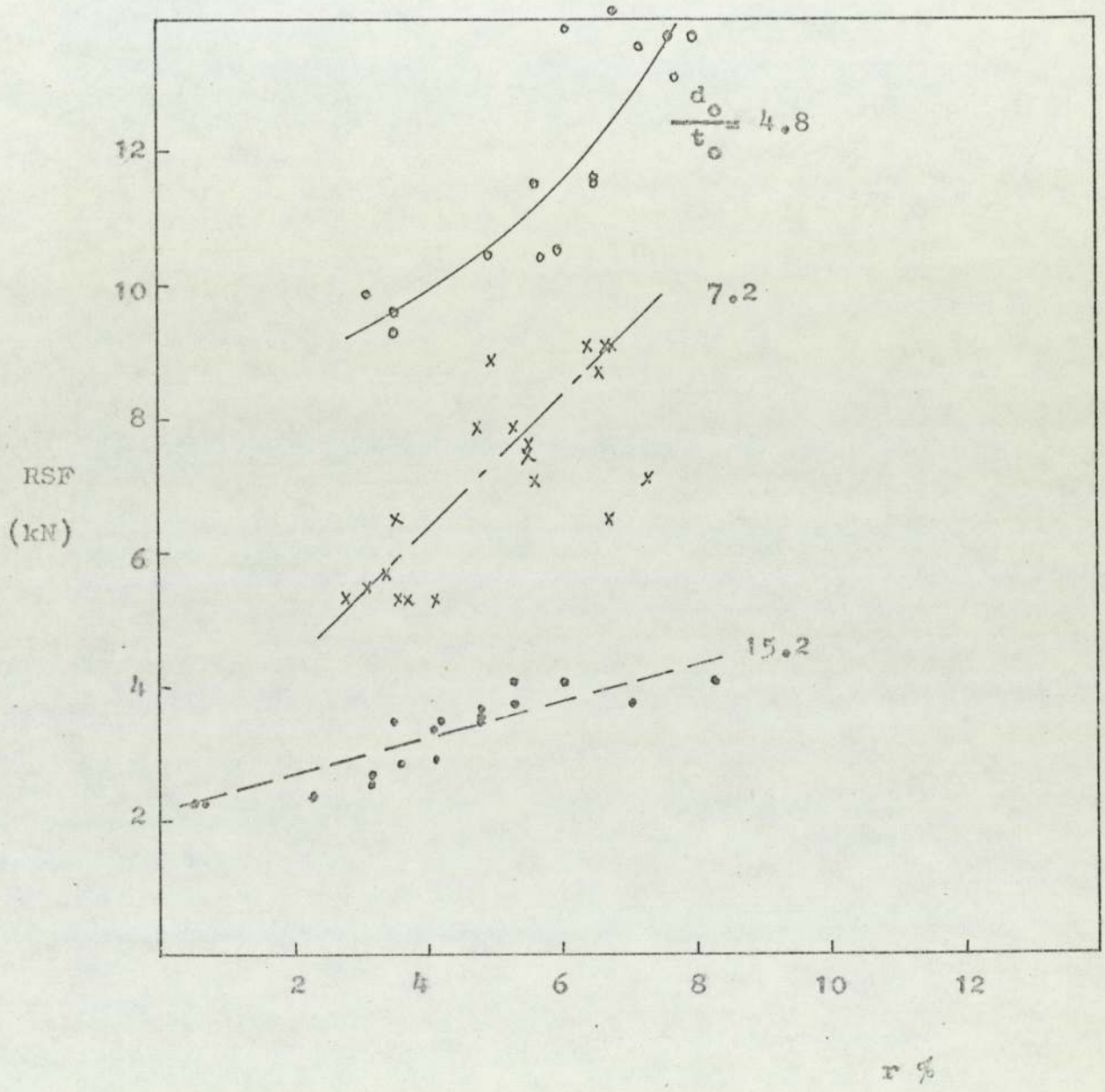

Fig (73)

Variation of RSF with r %

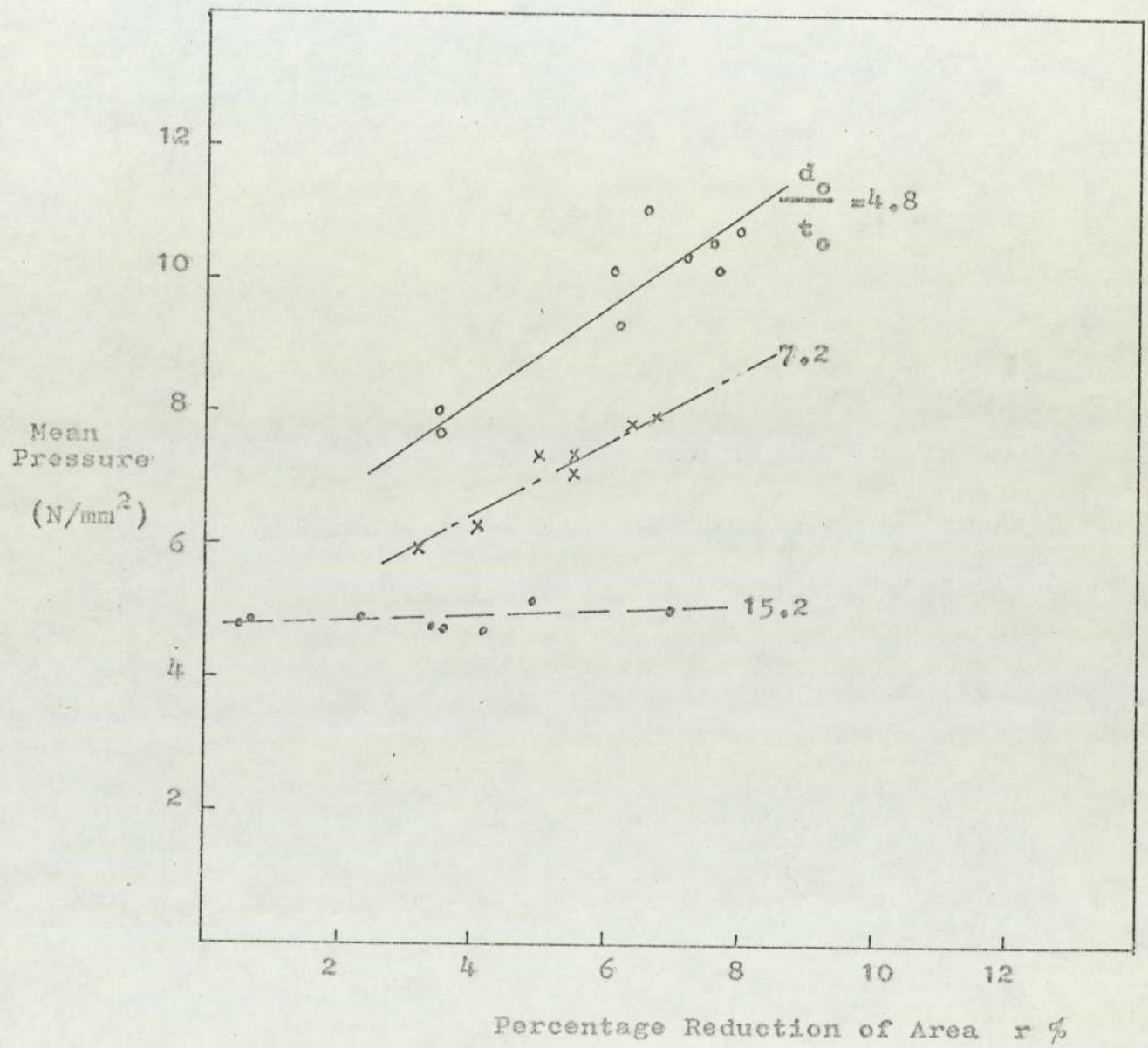

Fig (74)

Variation of Mean Pressure with r %

(VIII-9) The Rolling Torque

A simple method of estimating the rolling torque is that based on the concept of the lever arm as used in flat rolling. In this method the roll separating force P is assumed to be acting at a distance(a) from the roll centre as in fig. (75). The torque per roll therefore is:

$$T/roll = P.a \qquad \text{.....(VIII.17)}$$

and for a two roll stand, the total torque becomes:

$$T_t = 2P.a \qquad \text{.....(VIII.18)}$$

the distance(a) is known as the lever arm and is usually expressed as a ratio of the arc of contact.

Thus

$$a = (a/L).L$$

$$= \lambda .L \qquad \text{.....(VIII.19)}$$

substituting for(a) from (VIII.19) into (VIII.18) we get:-

$$T_t = 2P\lambda L \qquad \text{.....(VIII.20)}$$

λ is normally assumed to be equal to 0.5 in hot flat rolling.

This method only gives an approximate value of the torque and its accuracy depends on λ which will obviously depend on the rolling conditions.

Due to the simplicity and common use of this method, λ has been calculated for the present tests from equation (VIII.20) from measurements of torque, arc of contact and the roll separating force as shown in table (VIII.4).

The table gives three values of λ for each test i.e, λ_g, λ_m and λ_m^*.

These three values correspond to the three lengths of arc of contact L_g, L_m and L_m^* in the expression :-

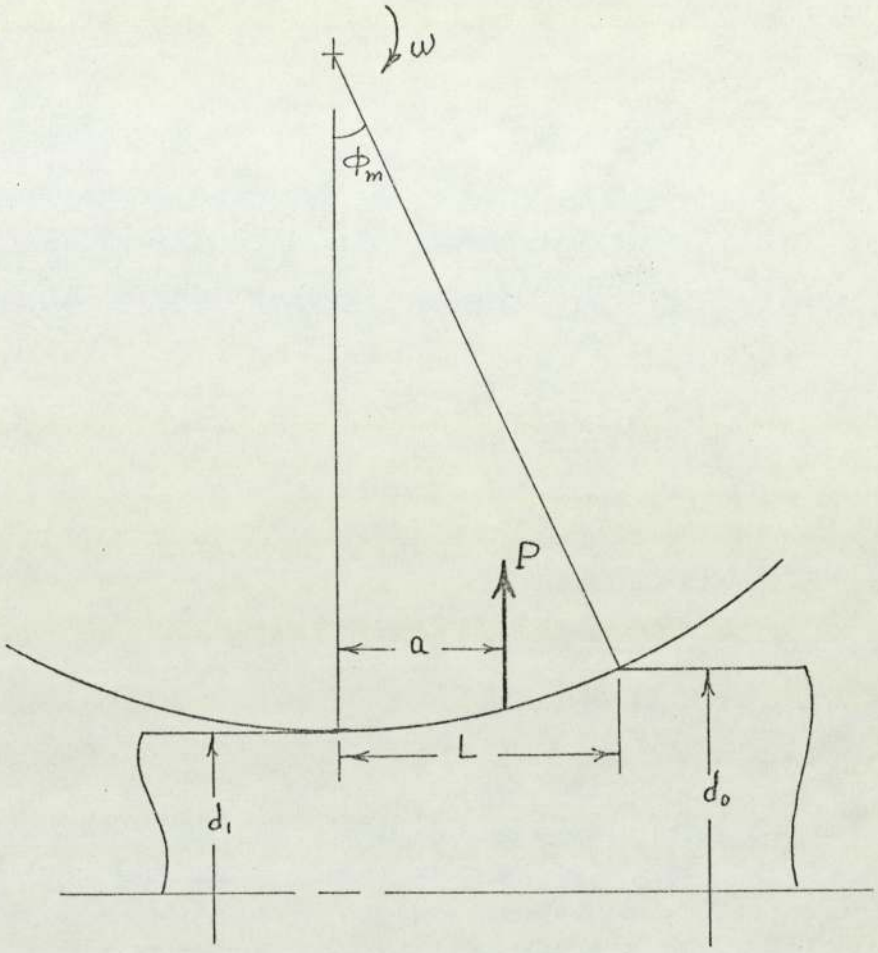

Fig. (75)

$$\lambda = T_t/2PL$$

i.e,

$$\lambda_g = T_t/2PL_g \quad , \qquad \text{.....(VIII.21)}$$

$$\lambda_m = T_t/2PL_m \quad , \qquad \text{.....(VIII.22)}$$

and

$$\lambda^*_m = T_t/2PL^*_m \qquad \text{.....(VIII.23)}$$

The reason for including the three values of λ is to stress the importance of considering the arc of contact carefully before chasing a value of λ. It can also be seen from the table that λ_m is nearly equal to one which indicates that the pressure peak at entry observed in the tests and discussed earlier is characteristic of tube rolling.

Now to calculate the torque from knowledge of the mean roll pressure we must first calculate the roll separating force and its vertical component from the pressure.

$$dP = p_m \cdot \cos\theta \, R_r d\phi \, r_g \, d\theta \cdot \cos \qquad \text{.....(VIII.24)}$$

where $R_r \, d\phi \cdot r_g d\theta$ is the elemental surface area.

$$\therefore \quad P = \int_0^{\phi_m} 2 \cdot \int_0^{\theta_c} p_m \, R_r \, r_g \cos\phi \cos\theta \, d\theta \, d\phi \qquad \text{.....(VIII.25)}$$

$$P = 2 \, p_m \, R_r \, r_g \sin\phi_m \sin\theta_c \qquad \text{.....(VIII.26)}$$

Hence the total rolling torque is

$$T_t = 4 \, p_m \, R_r \, r_g \sin\phi_m \sin\theta_c \cdot \lambda L \qquad \text{.....(VIII.27)}$$

Since in practice it is easier to calculate the length of the arc of contact from geometrical considerations i.e., L_g, this value will be used in equation (VIII.27) above, together with the mean value of λ_g from table (VIII.4).

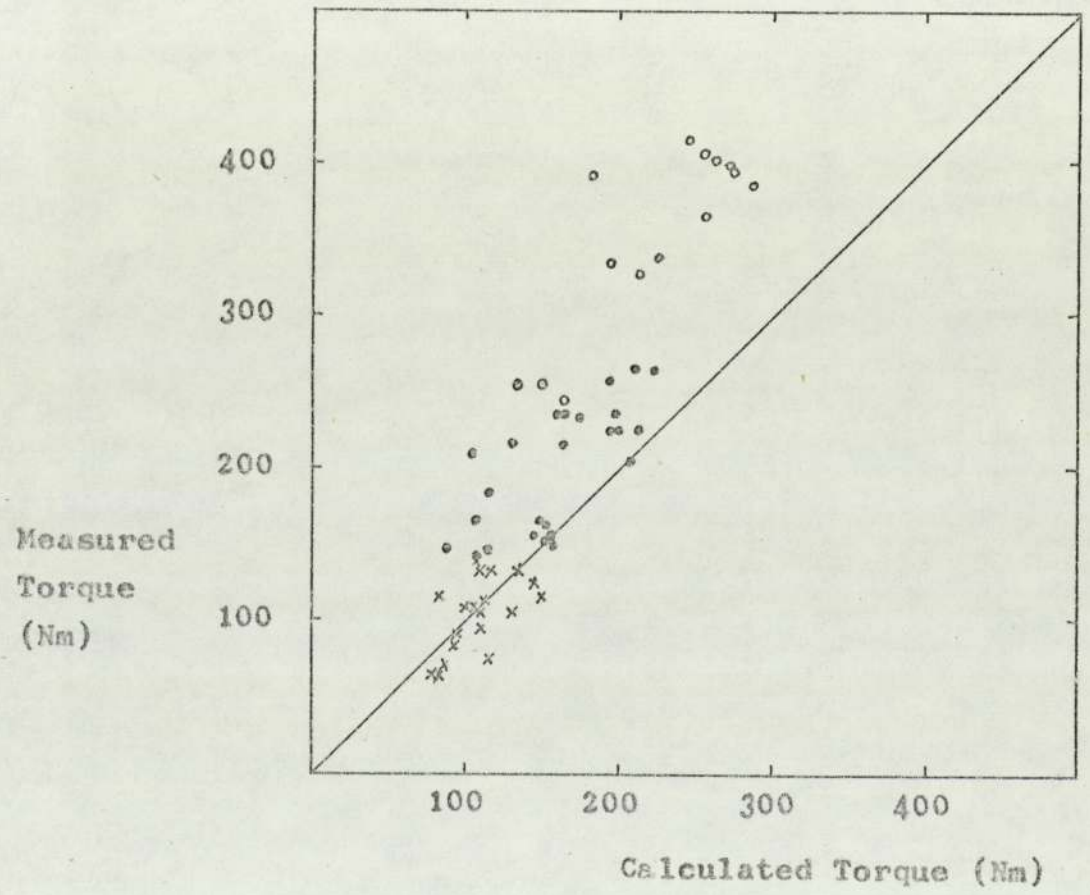

Fig. (76)

Comparison between Measured & Calculated Rolling Torque for R-O passes (phase I)

× d_o/t_o = 14

• = 7

○ = 4.8

$$T_t = 4p_m R_r r_g \sin\phi_m \sin\theta_c \lambda_g \cdot L_g \quad \ldots\ldots\ldots (VIII.28)$$

Fig. (76) shows the results of this equation against measured values of T_t.

For the round to oval passes from phases I and II the mean value of λ_g is 0.66 with a standard deviation of 0.06 .

The approximate nature of this method of calculating the rolling torque is clearly shown in fig. (76) which compares the measured and calculated rolling torque. The correlation seems to vary between good and poor. The agreement is reasonable for the thin tubes ($d_o/t_o = 14$) and also for the medium thickness tubes ($d_o/t_o = 7$) but is poor for the thick tubes ($d_o/t_o = 5$).

On the basis of these calculations and comparisons it can be concluded that the lever arm concept gives only an approximate estimate of the torque and should only be used for light reductions and relatively thin tubes ($d_o/t_o > 5.0$).

The lever arm for O-O tests (75-84) is higher than for R-O passes as can be seen from the table.

Table (VIII.4)

The Lever Arm

Test No.	Torque (Nm)	RSF (kN)	λ_g	λ_m	λ_m^*
1	66.7	2.25	0.73	1.24	0.97
2	62.7	2.22	0.70	0.99	0.62
3	68.9	2.22	0.74	1.06	0.98
4	146.9	5.33	0.65	1.35	1.21
5	149.1	5.48	0.69	1.39	1.23
6	142.4	5.30	0.66	1.23	1.27
7	253.7	9.93	0.69	1.07	1.11
8	255.4	9.62	0.69	1.13	0.79
9	224.3	9.33	0.63	1.02	0.71
10	80.8	2.63	0.72	1.05	0.86
11	88.7	2.86	0.71	0.97	0.85
12	89.9	2.90	0.71	1.00	0.90
13	74.6	2.52	0.65	1.00	1.05
14	105.1	3.39	0.68	0.86	0.74
15	110.2	3.50	0.70	0.86	0.81
16	108.5	3.50	0.68	0.87	0.82
17	200.0	6.99	0.67	0.90	0.88
18	201.0	7.11	0.66	1.03	0.93
19	194.0	6.92	0.65	1.05	1.01
20	233.0	8.90	0.56	0.76	0.67

Table (VIII.4) (contd.)

The Lever Arm

Test No.	Torque (Nm)	RSF (kN)	λ_g	λ_m	λ_m^*
21	231.7	7.82	0.65	0.95	0.65
22	233.4	7.90	0.65	0.92	0.71
23	182.7	5.69	0.78	1.13	0.95
24	165.0	5.25	0.77	1.15	0.99
25	157.1	5.37	0.63	1.05	0.78
26	156.5	5.25	0.64	1.19	1.05
27	149.7	5.53	0.58	1.15	0.94
28	210.8	6.53	0.76	1.02	0.89
29	296.1	10.40	0.68	1.18	0.68
30	284.0	10.50	0.69	1.12	0.83
31	298.1	10.50	0.67	1.25	0.90
32	338.7	11.60	0.64	1.02	0.66
33	329.2	11.60	0.61	0.99	0.83
34	335.4	11.60	0.63	1.06	0.91
35	105.1	3.50	0.62	0.78	0.94
36	130.6	3.72	0.75	0.95	0.93
37	140.1	4.02	0.73	0.97	0.81
38	131.0	3.76	0.73	0.90	0.70
39	124.4	4.01	0.64	0.84	0.69
40	121.5	4.03	0.59	0.83	0.76

Table (VIII.4) (contd.)

The Lever Arm

Test No.	Torque (Nm)	RSF (kN)	λ_g	λ_m	λ_m^*
41	112.4	3.64	0.73	0.82	0.78
42	107.7	3.48	0.73	0.82	0.78
43	214.8	6.50	0.72	0.91	0.72
44	215.8	6.45	0.70	1.00	0.90
45	221.5	7.03	0.62	0.97	0.76
46	236.8	7.10	0.66	1.03	0.74
47	222.4	7.45	0.58	0.94	0.71
48	203.7	6.98	0.56	0.93	0.73
49	222.8	7.57	0.58	0.88	0.69
50	263.9	9.10	0.57	0.83	0.78
51	257.6	8.74	0.61	0.81	0.67
52	264.4	9.08	0.58	0.87	0.69
53	270.0	9.08	0.59	0.89	0.71
54	289.9	9.03	0.63	0.82	0.73
55	413.7	13.60	0.65	0.93	0.82
56	367.3	13.90	0.55	0.81	0.78
57	393.5	13.70	0.58	0.93	0.80
58	398.0	13.78	0.58	0.81	0.76
59	403.7	13.87	0.60	0.92	0.90
60	399.6	14.14	0.60	0.86	0.77

Table (VIII.4) (contd.)

The Lever Arm

Test No.	Torque (Nm)	RSF (kN)	λ_g	λ_m	λ_m^*
68	154.2	5.42	0.66	1.06	0.97
69	166.2	5.87	0.66	1.02	1.00
70	161.0	5.83	0.65	0.98	0.85
71	114.2	3.62	0.74	0.76	0.69
72	113.7	3.47	0.63	0.87	0.93
73	131.7	3.91	0.65	0.84	0.83
74	384.7	12.68	0.60	0.90	1.21
	The following are 0-0 pass type				
75	139.0	4.85	0.97	1.51	1.62
76	150.3	5.12	0.99	1.39	1.36
77	233.9	8.49	0.76	0.99	0.83
78	220.3	8.18	0.74	1.15	1.10
79	261.1	8.40	0.85	1.19	1.20
80	261.1	8.40	0.85	1.05	1.05
81	167.8	6.65	1.03	1.03	0.97
82	167.8	6.65	1.03	1.06	1.01
83	102.2	5.25	1.02	1.07	1.13
84	102.2	5.25	1.02	1.02	1.08

(VIII-10) Comparison between Measured and Calculated RSF:-

Fig. (77)shows the comparison between measured and calculated RSF on the basis of equation (VIII.26):

$$P = 2\, p_m\, R_r\, r_g \sin\phi_m \sin\theta_c \qquad \ldots\ldots\ldots (VIII.26)$$

The comparison is made for two cases with respect to the value of the angle of contact ϕ_m :-

a) using L_m^* to calculate ϕ_m from the relationship $\phi_m = \frac{L_m^*}{R_r}$

b) using L_g to calculate ϕ_m , i.e $\phi_m = \frac{L_g}{R_r}$

The reason for introducing the second case into the comparison was to establish whether it would be possible to use L_g to calculate ϕ_m , hence the roll separating force P because it is an easier parameter to determine than L_m^* from a practical point of view.

In making the comparisons, the appropriate value of θ_c , the maximum groove angle of contact, was used.

Fig. (77)shows that:-

1) using L_m^* to calculate ϕ_m gives better agreement with measured RSF than using L_g which seems to over estimate the value of RSF .

2) there seems to be a tendency to underestimate the value of RSF in the case of tubes with d/t of 4.8 and gap setting I. This may be attributed to some lack of response on the part of the pin loadcells when rolling relatively thick tubes with high reductions. This observation was made in section (8) of this chapter.

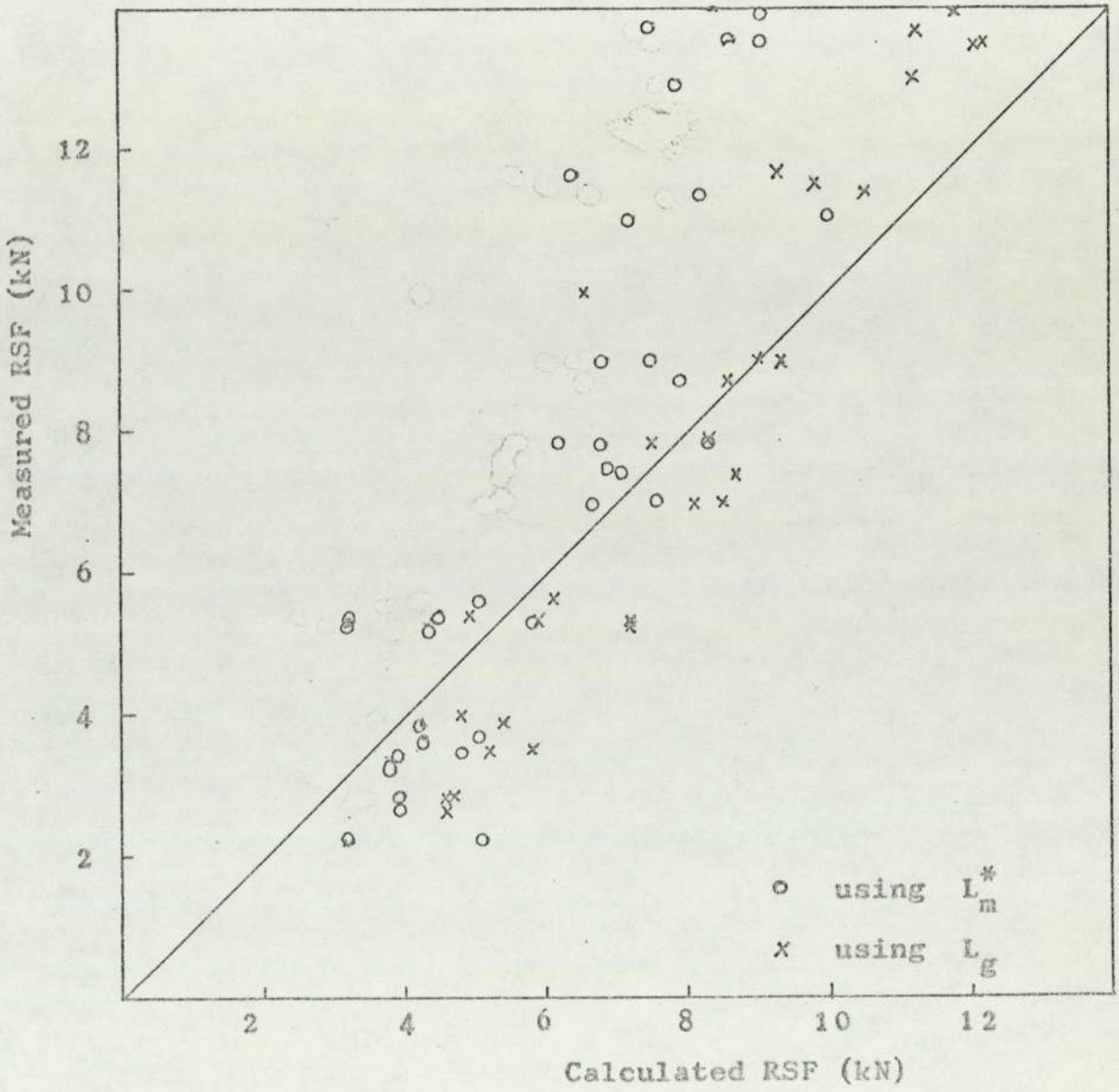

Fig. (77)

Comparison between Measured and Calculated Roll Separating Force (RSF)

(VIII.11) Effect of the Groove Shape on the Arc of Contact

The variation of the length of the arc of contact, with the groove angle θ, for the three d/t ratios used in the present investigation is shown in figs. (78-a-b-c) for gap settings I, II, & III.

Metal flow in the deformation zone is related, amongst other factors, to the d/t ratio of the tube. For thick tubes, the degree of flow seems to be primarily radial. Hence the tendency of thick tubes to have polygonized bores. Where the deformation is primarily radial, the differences in the length of the arc of contact across the groove become important in the formation of the polygonized bore. Therefore, to inhibit the formation of polygoniztion, particularly for thick tubes, it is necessary to minimize the differences in the length of the arc of contact [14]. This can be achieved by choosing a suitable groove shape.

A cross section of some of the rolled tubes is shown in photo. (6) for R-O and O-O passes and gap settings I and II.

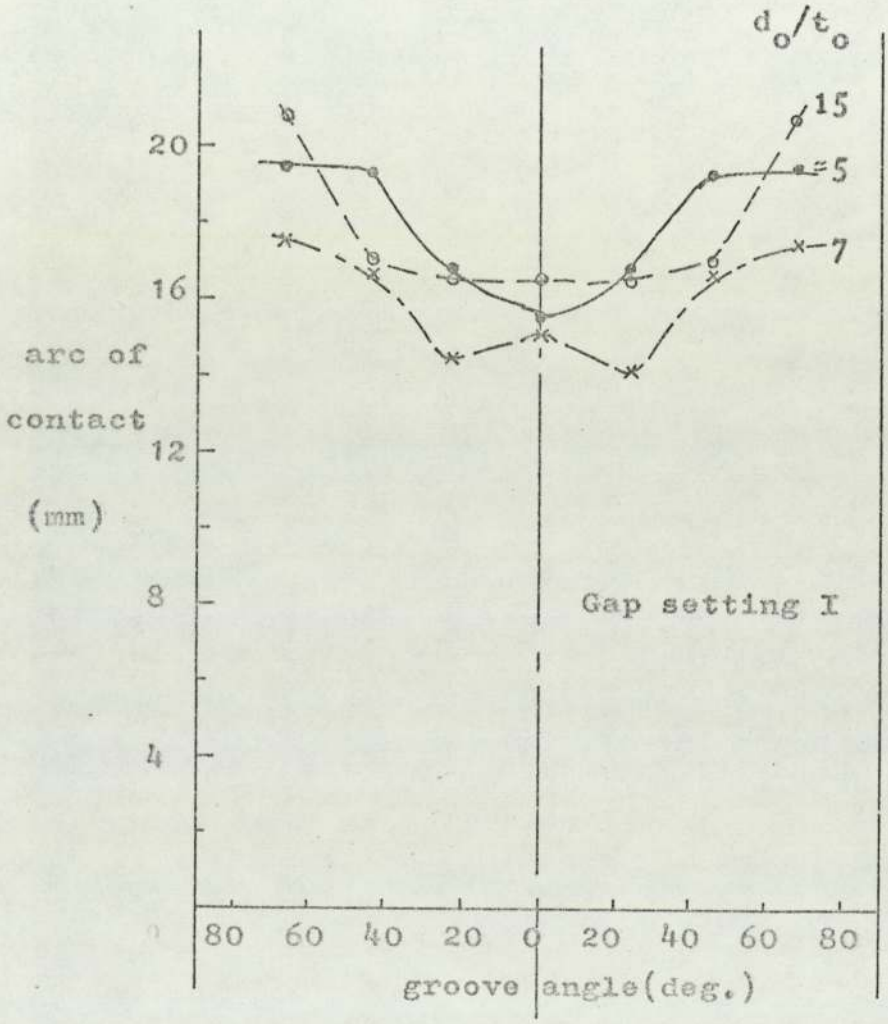

Fig.(78-a)

Variation of the length of the arc of contact with the groove angle.

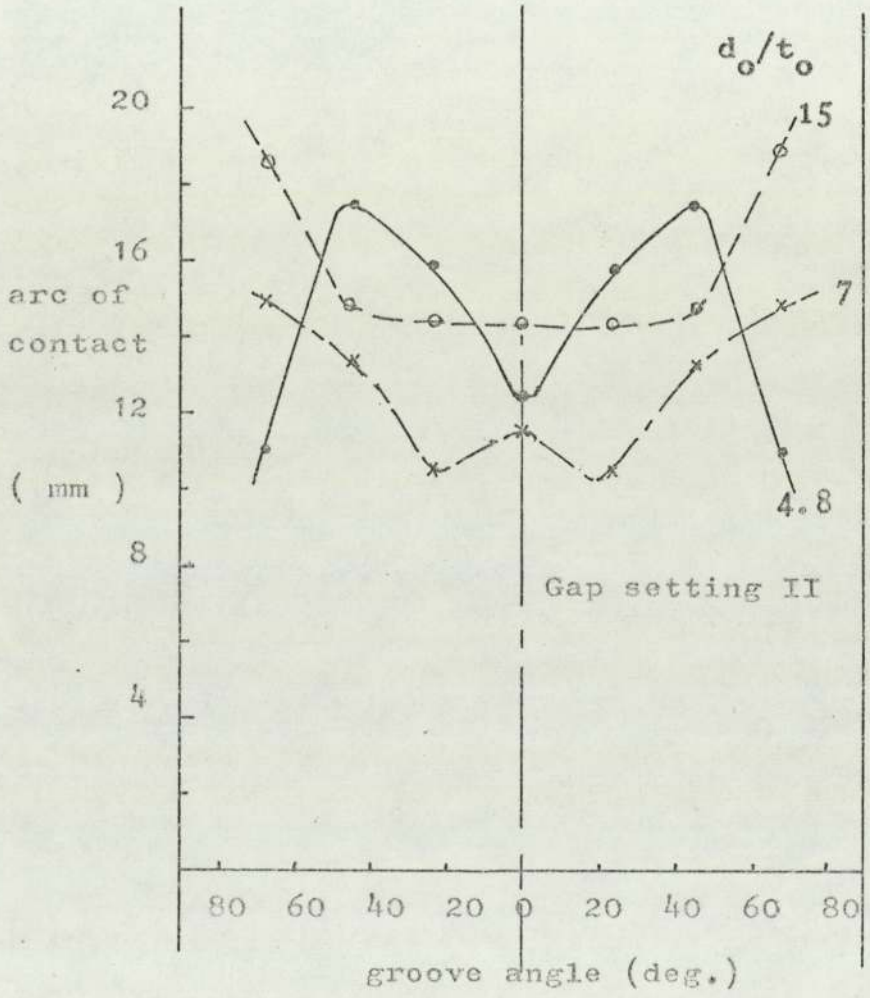

Fig.(78 -b)

Variation of the length of the arc of contact with the groove angle.

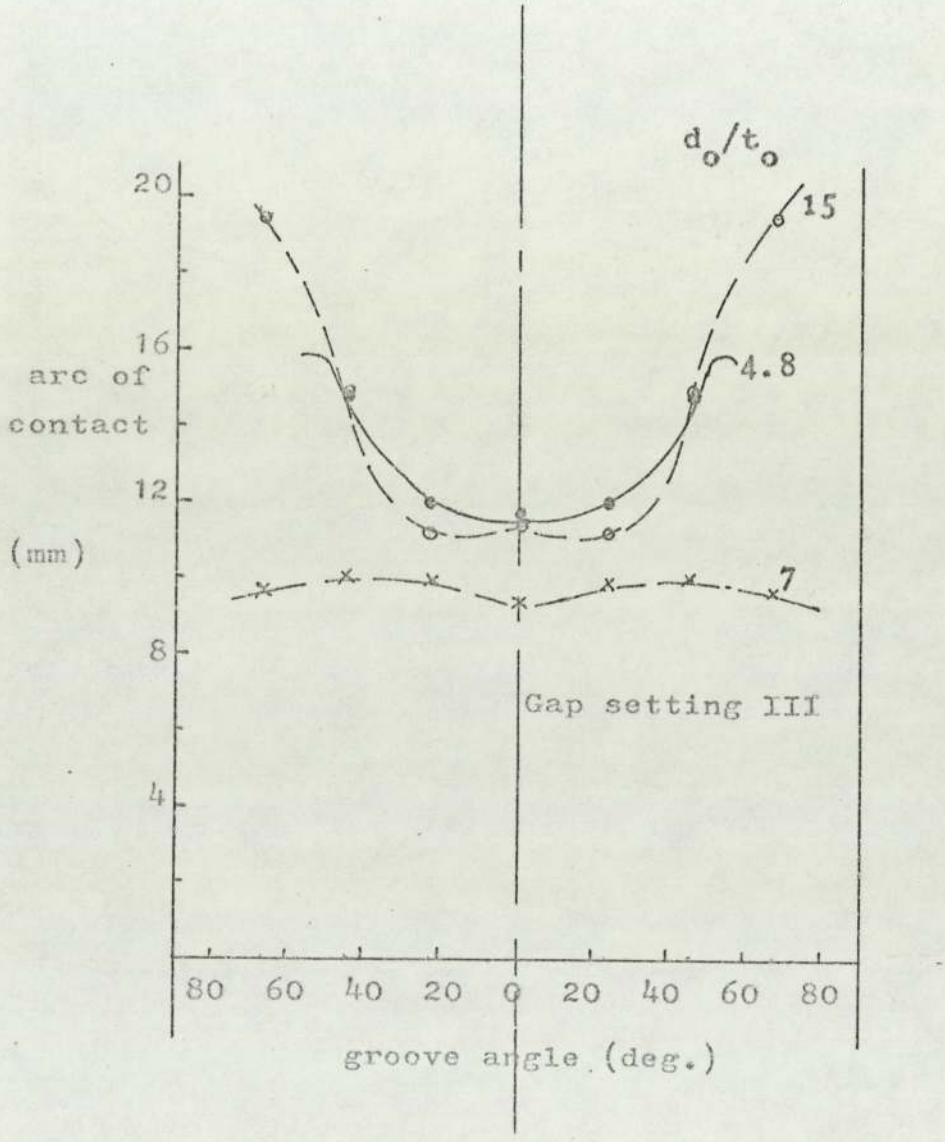

Fig. (78-c)

Variation of the length of the arc of contact with the groove angle.

Photo. (6)

Cross Section of Some of the

Rolled Tubes.

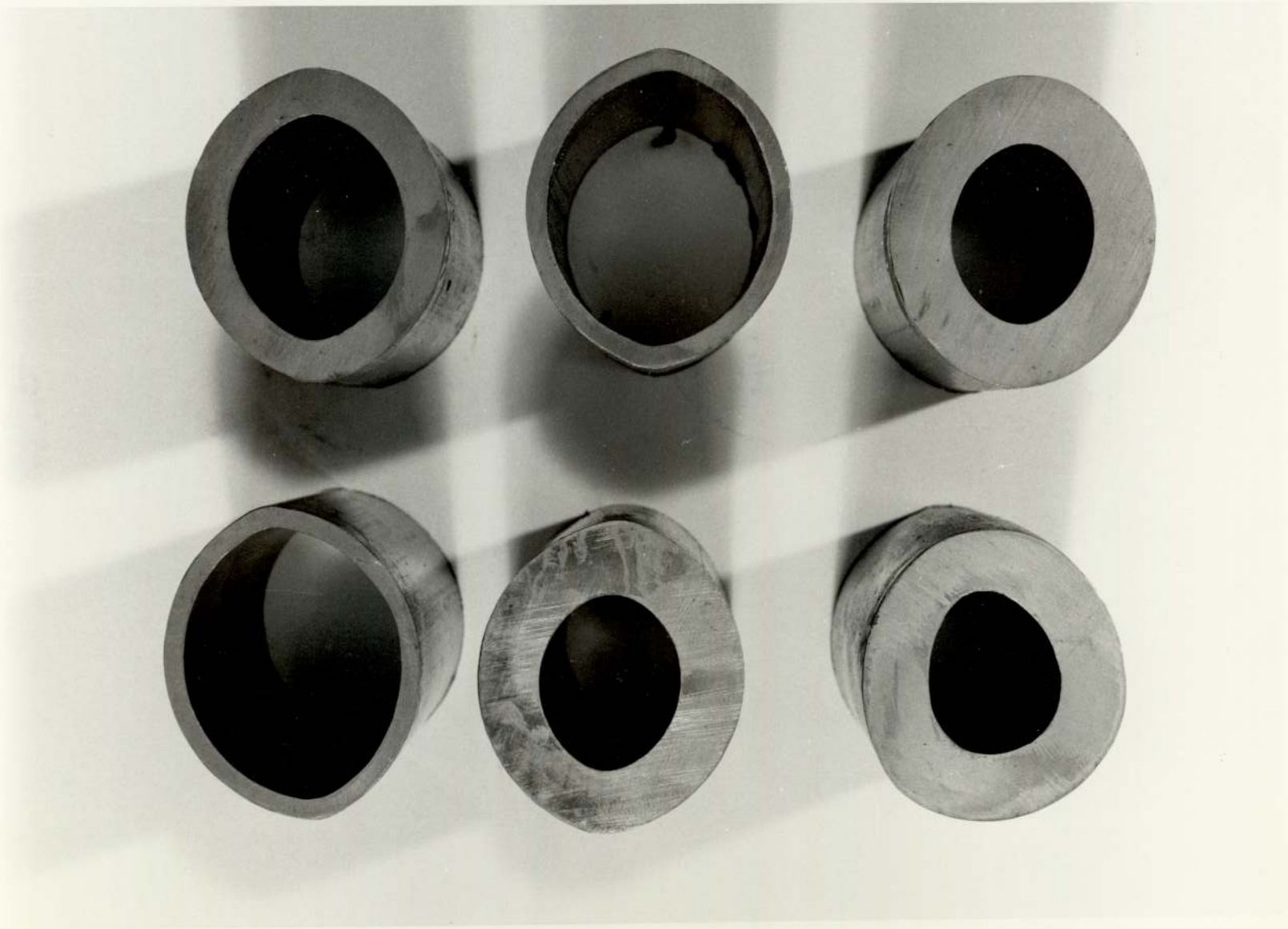

(VIII.12) Effect of Applied Tensions:-

The expected effects of the applied tensions on the rolling torque, RSF, and roll pressure have been observed. These effects can be seen by reference to table(VII-3.5)of the test results. The applied tensions seem to have a greater effect on the rolling torque than on other parameters. The RSF also is proportionally affected by stretching the tube while the effect on the roll pressure seem to be less noticeable. As an example, tests 100 to 103 were carried out on one length of tube under an increasing back tension. The torque, RSF, and pressure were recorded at different stages during the test. By reference to the table it can be seen that the effect of the increasing back tension is greatest for the torque and smallest for the pressure. Also tests 92 to 94 had front and back tensions applied to the tube and the effect on the loads, as discussed above, can be seen.

The apparent small effect on the mean pressure seems to be due to redistribution of the load around the groove, rather than a lack of effect. For although the mean pressure for tests 100 to 103 seems to be little affected by the increasing back tension, the pressure on pins 1 and 2 has steadily decreased while the pressure on pin 4 has increased.

Thus it is possible to explain the apparent lack of effect of the applied tensions on the roll pressure by the phenomenon of redistribution of load across the groove.

(VIII-13) Variation in Wall Thickness

The test results (table(VII-1)show that in general the change in wall thickness measured at the root of the groove is lower than the mean values. It can also be seen from table VII-2 that δ_{tr}/δ_r at the root of the groove is lower than δ_t/δ i.e.. mean value. This difference between δ_{tr}/δ_r and δ_t/δ is not surprising since δ_r is a maximum at the root of the groove as shown in fig.(62) . There is however a certain degree of uncertainty in the measurements of δ_{tr} due mainly to non-uniformity of the wall thickness of the tube round its circumference. Therefore the above comparisons between mean values and measurements at the root of the groove must be viewed in the light of this uncertainty . However the general conclusion that measurements at the root of the groove are lower than the mean values is acceptable. Wall thickness variation at the root of the groove should only be used as a measure of the variation at that plane. Methods of calculations employing an energy approach are best used in conjunction with the mean variation in wall thickness and mean tube dimensions in general.

The comparison which Cole [1] made between his test results and two of the equations in chapter (VI) showed that the predicted wall thickness variation was greater than the measured one. If the groove was oval in shape,then this would be expected since the equations give the mean value of the variation while the measurements were made at the root, but for circular grooves and tubes the difference should be small.

The test results of the present work seem to show that

the change in wall thickness is a function of the reduction in diameter and the ratio t_o/d_o . The shape of the curve in fig.(79) shows the tendency of δ_t/δ to decrease for values of $t_o/d_o > 0.20$ in conformity with the curves in fig. (50). Table (VIII-5) shows the comparison made between the test results and theoretical predictions of δ_t/δ for the formulae reviewed in chapter (VI) . By considering fig.(50) with the table one can see that the predictions of all the formulae are very similar with the exception of the proposed formula (VI.61)which seems to correlate well with the test results. Also Gun's first formula (Gun-1 in the table) gives lower predictions than the rest of the formulae for the thin tubes i.e, with d_o/t_o of 15, and, Kolmogorov's and Shveikin's predictions are high for relatively thick tubes ($d_o/t_o = 4.8$).

The negative values of Gun's second and Anisiforov's eqs. indicate thickening of the wall and are function of the way the formulae are written.

Gun's second formula and Gulyaev's give identical predictions as can be seen from table (VIII.5) and fig.(50). Gun's formula is distinguished by a great degree of simplicity of structure. When it comes to simplicity of structure however, Kolmogorov's formula must be one of the simplest for tube sinking.

The correlation between the test results and the various theoretical predictions seem to vary between good and poor.. This may be a reflection on the accuracy of the formulae which prompted Gulyaev [15], after reviewing them, to develop a new formula which he claimed was more accurate. It can also be the result of some inaccuracy in the measurements of the tube dimensions.

It is difficult to pinpoint the exact source of the randomness of the correlation in view of the difficulty encountered in measuring the tube dimensions. On the other hand the predictions of the proposed formula, which is based on the method of measurement , and the care taken in making these measurements, seem to indicate that the lack of correlation in most cases is caused by the inaccuracy of the formulae rather than by inaccuracies in the measurements.

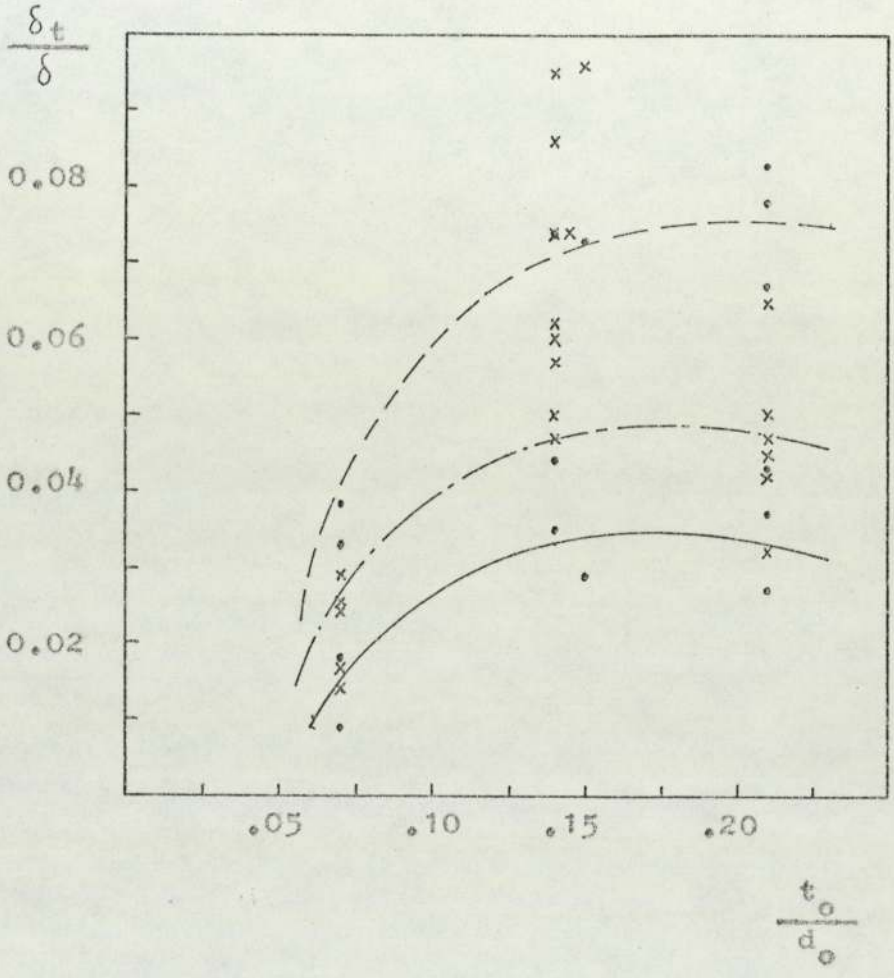

Fig.(79)

Change in Wall Thickness

(R-O passes only)

Table (VIII.5)

Wall Thickness Variation

Comparison between Test Results and Theoretical Predictions

Test No.	$\frac{d_o}{t_o}$	$\frac{\delta_t}{\delta}$	Theoretical Predictions of δ_t/δ							
			Gun-1	Gun-2	Shevchenko	Kolmogorov	Ansiforov	Shveikin	Gulyaev	Present Work
1	15.4	0.065	0.020	-0.032	0.029	0.033	-0.031	0.036	0.032	0 061
2	15.4	0.030	0.020	-0.032	0.031	0.033	-0.031	0.036	0.032	0.029
3	15.4	0.067	0.020	-0.032	0.029	0.033	-0.031	0.036	0.032	0 060
4	7.2	0.070	0.043	-0.063	0.052	0.069	-0.063	0 073	0 063	0 064
5	7.2	0.049	0.043	-0.063	0.053	0.069	-0.062	0 073	0.063	0.044
6	7.2	0.036	0.043	-0.063	0.054	0.069	-0.062	0.073	0.063	0.030
7	4.8	0.085	0.064	-0.077	0.054	0.105	-0.087	0.096	0 077	0 062
8	4.8	0.100	0.65	-0.077	0.053	0.105	-0.087	0.096	0 077	0 068
9	4.8	0.049	0.064	-0.077	0.056	0.105	-0.087	0.096	0.077	0 037
10	15.2	0.025	0.020	-0.032	0.031	0.033	-0.032	0.036	0 032	0 027
11	15.2	0.025	0.020	-0.032	0.031	0.033	-0.032	0.036	0.032	0.022
12	15.2	0.016	0.020	-0.032	0.032	0.033	-0.032	0.036	0 032	0 014

Table (VIII.5) (contd.)

Wall Thickness Variation

Comparison between Test Results and Theoretical Predictions

Test No.	$\frac{d_o}{t_o}$	$\frac{\delta_t}{\delta}$	Theoretical Predictions δ_t/δ							
			Gun-1	Gun-2	Shevchenko	Kolmogorov	Ansiforov	Shveikin	Gulyaev	Present Work
13	15.1	0.025	0.020	-0.032	0.032	0.033	-0.032	0.036	0.032	0 .026
14	15.3	0.025	0.020	-0.032	0.031	0.033	-0.032	0.036	0 032	0.022
15	15.3	0.029	0.020	-0.032	0.031	0.033	-0.032	0.036	0.032	0.030
16	15.3	0.024	0.020	-0.032	0.031	0.033	-0.032	0.036	0 032	0.023
17	7.3	0.073	0.043	-0.063	0.052	0.069	-0.062	0.073	0 063	0.048
18	7.3	0.091	0.043	-0.063	0.051	0.069	-0.062	0.073	0.063	0 071
19	7.3	0.086	0.043	-0.063	0.051	0.069	-0.062	0.073	0.063	0 069
20	7.2	0.057	0.043	-0.063	0.053	0.070	-0.063	0.074	0.063	0 043
21	7.2	0.063	0.044	-0.063	0.053	0.070	-0.063	0.074	0.063	0 051
22	7.2	0.051	0.044	-0.063	0.054	0.070	-0.063	0.074	0.063	0.040
23	6.9	0.100	0.045	-0.065	0.052	0.073	-0.065	0.076	0.065	0.081
24	6.9	0.074	0.045	-0.065	0.054	0.074	-0.065	0.076	0 065	0 060

Table (VIII.5) (contd.)

Wall Thickness Variation

Comparison between Test Results and Theoretical Predictions

Test No.	$\frac{d_o}{t_o}$	$\frac{\delta_t}{\delta}$	Theoretical Predictions δ_t/δ							
			Gun-1	Gun-2	Shevchenko	Kolmogorov	Ansiforov	Shveikin	Gulyaev	Present Work
25	6.7	0.096	0.047	-0.067	0.053	0.075	-0.067	0.078	0.067	0 078
26	6.7	0.096	0.047	-0.067	0.053	0.075	-0.067	0.078	0.067	0 078
27	6.7	0.096	0.047	-0.067	0.053	0.075	-0.067	0.078	0.067	0 078
28	7.2	0.074	0.043	-0.063	0.052	0.069	-0.062	0.073	0.063	0.048
29	4.8	0.046	0.065	-0.077	0.056	0.105	-0.088	0.096	0.077	0.030
30	4.8	0.048	0.065	-0.077	0.056	0.105	-0.087	0.096	0.077	0 029
31	4.8	0.031	0.065	-0.077	0.057	0.105	-0.088	0.096	0 077	0 017
32	4.8	0.07	0.065	-0.077	0.055	0.105	-0.088	0.096	0 077	0.045
33	4.8	0.050	0.066	-0.077	0.056	0.105	-0.089	0.096	0.077	0 039
34	4.8	0.043	0.066	-0.077	0.056	0.105	-0.089	0.096	0.077	0 039
35	15.0	0.033	0.021	-0.033	0.032	0.033	-0.032	0.037	0.033	0.026
36	15.0	0.009	0.021	-0.033	0.033	0.033	-0.033	0.037	0 033	0 010

Table (VIII.5) (contd.)

Wall Thickness Variation

Comparison between Test Results and Theoretical Predictions

Test No.	$\frac{d_o}{t_o}$	$\frac{\delta_t}{\delta}$	Theoretical Predictions δ_t/δ							
			Gun-1	Gun-2	Shevchenko	Kolmogorov	Ansiforov	Shveikin	Gulyaev	Present Work
37	15.0	0.018	0.021	-0.033	0.032	0.033	-0.032	0 037	0 033	0 017
38	15.0	0.018	0.021	-0.033	0.032	0.033	-0.032	0.037	0 033	0 017
39	15.2	0.017	0.021	-0.030	0.032	0.033	-0.032	0 036	0 032	0 013
40	15.2	0.010	0.021	-0.032	0.033	0.033	-0.032	0.036	0 032	0 007
41	15.0	0.033	0.021	-0.033	0.032	0.033	-0.032	0.037	0 033	0 026
42	15.0	0.033	0.021	-0.033	0.032	0.033	-0.032	0.037	0 033	0 026
43	7.2	0.035	0.044	-0.063	0.055	0.070	-0.064	0 074	0 063	0 031
44	7.2	0.035	0.044	-0.063	0.055	0.070	-0.064	0 074	0 063	0 031
45	6.7	0.073	0.047	-0 066	0.054	0.074	-0 067	0 077	0 066	0 057
46	6.7	0.029	0.047	-0.066	0 057	0.074	-0 067	0.077	0.066	0.023
47	7.2	0 074	0 044	-0.063	0.053	0.069	-0.063	0 073	0 063	0 058
48	7.2	0 074	0 044	-0.063	0 053	0.069	-0 063	0 073	0 063	0 058

Table (VIII.5) (contd.)

Wall Thickness Variation

Comparison between Test Results and Theoretical Predictions

Test No.	$\frac{d_o}{t_o}$	$\frac{\delta_t}{\delta}$	Theoretical Predictions δ_t/δ							
			Gun-1	Gun-2	Shevchenko	Kolmogorov	Ansiforov	Shveikin	Gulyaev	Present Work
49	7.2	0.074	0.044	-0.063	0.053	0.069	-0.063	0.073	0 063	0 058
50	7.1	0.039	0.044	-0.063	0.055	0.070	-0.064	0.074	0 063	0 031
51	7.1	0.039	0.044	-0.063	0.055	0.070	-0.064	0.074	0 063	0 035
52	7.1	0.047	0.044	-0.064	0.055	0.071	-0.064	0.074	0 064	0 020
53	7.1	0.047	0.044	-0.064	0.055	0.071	-0.064	0.074	0.064	0 020
54	7.2	0.035	0.044	-0.063	0.055	0.070	-0.064	0 074	0 063	0 031
55	4.8	0.067	0.065	-0.077	0.055	0.104	-0.088	0 096	0 077	0 048
56	4.8	0.043	0.066	-0.077	0.056	0.105	-0 089	0 096	0 077	0 033
57	4.8	0 021	0.066	-0.077	0 057	0.105	-0.089	0 096	0 077	0 023
58	4.8	0.043	0.066	-0.077	0.056	0.105	-0.089	0 096	0 077	0 027
59	4.8	0.078	0.065	-0.077	0.055	0.104	-0 088	0 096	0 077	0 066
60	4.8	0.083	0.065	-0.077	0.055	0.104	-0.088	0 095	0 077	0 060

Table (VIII.5) (contd.)

Wall Thickness Variation

Comparison between Test Results and Theoretical Predictions

Test No.	$\frac{d_o}{t_o}$	$\frac{\delta_t}{\delta}$	Theoretical Predictions δ_t/δ							
			Gun-1	Gun-2	Shevchenko	Kolmogorov	Ansiforov	Shveikin	Gulyaev	Present Work
61	6.3	0.100	0.049	-0.070	0.053	0.080	-0 069	0 082	0 070	0 088
62	6.4	0.192	0.048	-0.069	0.049	0.078	-0.068	0 081	0 069	0 156
63	6.5	0.087	0.047	-0 069	0.053	0.077	-0 067	0 080	0 068	0 058
64	6.5	0.100	0.047	-0.069	0.053	0.077	-0.067	0.080	0 068	0 063
65	6.7	0.085	0.046	-0.067	0.053	0.075	-0 066	0 078	0 067	0 075
66	4.4	0.106	0.070	-0.076	0.050	0.114	-0.093	0.098	0.076	0.072
67	4.4	0.070	0.069	-0.076	0.052	0.113	-0.092	0.098	0.077	0.043

Table (VIII.5) (contd.)

Wall Thickness Variation

Comparison between Test Results and Theoretical Predictions

Test No.	$\frac{d_o}{t_o}$	$\frac{\delta_t}{\delta}$	Theoretical Predictions δ_t/δ							
			Gun-1	Gun-2	Shevchenko	Kolmogorov	Ansiforov	Shveikin	Gulyaev	Present Work
68	7.2	0.057	0.043	-0.063	0.053	0.070	-0.063	0.074	0.063	0 045
69	7.2	0.057	0.043	-0.063	0.053	0.070	-0.063	0.074	0 063	0.045
70	7.2	0.057	0.043	-0.063	0.053	0.070	-0.063	0.074	0.063	0.045
71	15.2	0.028	0.021	-0.032	0.033	0.033	-0.032	0 036	0 032	0 027
72	15 2	0.038	0.021	-0.032	0.031	0.033	-0.032	0.036	0.032	0.036
73	15.2	0.038	0.021	-0.032	0.031	0.033	-0.032	0 036	0.032	0.036
74	4 7	0.037	0.066	-0 077	0 057	0.106	-0 089	0.096	0.077	0.030

IX

CONCLUSIONS

Conclusions

From this investigation of the longitudinal rolling of tubes through two grooved rolls the following conclusions can be drawn:

A) Regarding Deformation:

1) It has been shown that the deformation zone can be divided into three zones with respect to the groove angle θ and that there are regions in contact with the roll surface where the neutral point lies outside the deformation zone.

2) The deformation zone has been shown experimentally to consist of two axial zones: a free zone where plastic deformation takes place prior to the tube contacting the rolls, and a contact zone.

3) The presence of the free zone, which is inevitable in the absence of a mandrel, decreases the length of the arc of contact. The actual arc of contact was found to be about $1/\sqrt{2}$ of the calculated value in the absence of the free zone. However, this ratio increases slightly when the measured arc of contact is corrected for the difference in torque sharing between the two rolls. The effects of the free zone on other process parameters have been discussed.

B) Roll Pressure Measurement:

1) A new design of the pin loadcell assembly was developed enabling the easy removal of the whole assembly for periodic inspection of the pins and orifices for back-extruded metal fragments. The design also enabled the adjustment of the heights of the pins with respect to the surface of the groove.

2) The presence of small lead fragments between the pin and its orifice did not disturb the performance of the loadcells due mainly to the modified design of the pin.

3) Pin protrusions of up to 25 μm enable reliable data to be obtained, whereas pin recession below the surface yields an incorrect representation of the pressure distribution. The modified design of the pin loadcells made it possible to study the effects of the various factors on the behaviour of the loadcells.

4) The occurrence of a pressure peak at or near the entry plane and the shape of the pressure distribution curves in general have been discussed.

C) Theoretical Solution:

1)A new theoretical approach based on the strain energy of deformation and the concept of apparent strain has been developed which compares favourably with the test results. It has been shown that this approach is an improvement on the equilibrium approach used by the Russian workers.

2) The solution contains a shear factor which when set to zero, representing the frictionless condition, yields a lower bound estimate of the pressure and when set to unity, representing the condition of complete sticking, yields an upper bound estimate. Thus it is possible with this concept of a shear factor to apply the theory to tube rolling under varying friction conditions by choosing the appropriate value of the shear factor.

D) Wall Thickness Variation:

1) Seven existing theories for the prediction of the change in wall thickness have been presented and compared

with the test results. It has been shown that the predictions of all the theories do not differ greatly up to t_o/d_o ratio of 0.20 .

2) A simple method of calculating the change in wall thickness based on the method of measurement of the tube dimensions and the condition of volume constancy has been presented and compared with the test results. The predictions of this method are in good agreement with the test results but need further checking against other test results based on measurement of the mean tube dimensions.

3) For oval grooves the change in wall thickness in particular, and tube diameter should be based on the measured mean values and not on measurements made at a particular point on the surface of the tube. However, for truly circular grooves and tubes this requirement is not critical.

E) General

1) Calculation of the rolling torque using the lever arm concept has been shown to be of an approximate nature and should not be relied upon to provide accurate estimates of the actual torque.

2) The effect of the difference in the torque sharing between the two rolls on the length of the arc of contact and other parameters has been studied and proved experimentally.

3) Test results are now available for the rolling of oval tubes through oval grooves, a condition which is relevant to the tube rolling practice. These results have been used in the analysis in this work and should prove useful for future investigations.

Thus, the findings of this investigation provide a contribution to the understanding of the mechanics of longitudinal rolling of tubes for both industrial and research engineers.

X

SUGGESTIONS FOR FURTHER WORK

Suggestions for Further Work:

1) The mandrel rolling process has not been studied in this investigation and it appears from the available literature that further work in this field,particularly regarding deformation,is still required.

2) Knowledge of the frictional stresses in the direction of the tube hoop may prove useful in the full understanding of the mechanics of the tube rolling process and may assist in the design of the groove shape. This type of friction represents a basic difference between tube rolling and flat rolling and should therefore be considered in the study of the former.

In this connection the design of the pin loadcell assembly employed in the present investigation can be used after some modifications.

3) The design of the groove and the size of the rolls which ensure maximum efficiency of the process should be investigated in some detail. This is an important aspect of the tube rolling practice which has not received enough attention in research work.

4) If lead is used again in rolling tests which involve measuring the roll pressure and wall thickness variation,then the test pieces should be adequately prepared before testing so that the surface is free from irregularities and the wall thickness is uniform to eliminate the need for repeated testing.

5) The method of measuring the tube dimensions in general and the wall thickness in particular,should be improved, perhaps by using electronic scanning techniques.

XI

AKNOWLEDGEMENTS

Acknowledgements

The author is deeply indebted to Professor D.H.Sansome for his continued help and encouragement in making this work possible.

The author wishes to express his sincere gratitude to Dr.I.M.Cole, his supervisor, for his generous help and assistance in various fields.

Thanks are due to the University of Aston in Birmingham, to the department of Mechanical Engineering and to the late Professor A.J.Ede former head of the department, for providing the financial support which made this project and its continuation possible.

Thanks are also due to the technical staff of the departments of Mechanical and Production Engineering and to all who contributed in any way to this work.

Last, but not least, thanks to my wife and family for their interest, encouragement and patience.

XII

BIBLIOGRAPHY

(1) COLE, I.M. "An Investigation of the Rolling of Cylindrical Tube by Grooved Rolls." Ph.D. Thesis, 1969, The University of Aston in Birmingham.

(2) FAZAN, B.
BLAIN, P. "Le Laminage des Tubes sur Laminoirs Rèducteurs-Ètireurs" (Tube Rolling in Stretch-Reducing Mills.) Revue de Mètallurgie, March 1967. pp. 209-225

(3) NEUHOFF, V.K.
PFEIFFER, G. "Deformation-Technological Knowledge Obtained During the Operation of a Continuous Tube Rolling Mill" Stahl und Eisen 1970, 90, April, pp. 405-412

(4) TSELIKOV, A.I.
GULYAEV, G.I.
SEIFULIN, G.K.
DANILOV, F.A.
NODEV, E.O.
MARKOV, V.P. "Development of the Continuous Rolling of Tubes in the USSR." Steel in the USSR, March 1970, pp. 235-237

(5) GULYAEV, G.I.
IVSHIN, P.N.
EROKHIN, I.N.
KURILENKO, V.Kh. "Metal Spread and Ovalization of the Passes in the Reduction and Sizing of Tubes" Steel in the USSR, September 1971, pp. 734-736

(6) VATKIN, Ya.L.
DANCHENKO, V.N.
LEBED, G.SH.
"Parameter of Longitudinal Stress in Tube Reduction"
Steel in the USSR, January 1971, pp. 56-57

(7) VASHKIN, Ya.L.
CHERNYAVASKII, A.A.
BRODSKII, I.I.
"Force Parameters when Rolling Tubes on an Automatic Mill".
Izvest.V.U.Z. Chern. Met., 1971, (3), pp. 85-88.

(8)
"Research at Works Laboratories and Institutes at Urals Scientific Research Institute for the Tube Industry".
Stal', 1971, (10), pp. 931-933.

(9) VATER, M.
"Influence of the Flow Condition on the Consumption of Power and Work as well as the Material Flow in Plastic Forming."
Bänder Bleche Rohre, 12(1971), Nr. 5, pp. 191-194.

(10) JELOMEK, H.
"Rolling of Reheated Tubes in Reducing Mills."
Problemy Projektowe Hutn. (Poland), August 1971, pp. 257-263 .

(11) OKAMOTO,T. "The Theory of Deformation and Stress of Tubes by Deformation Factor." The Sumitomo Search No 5, May 1971, pp. 62-72 .

(12) OKAMOTO,T. NAYASHI,C. "Theory of Plastcity on Mandrel Rolling" Proc. Int. Conf. Sc. Technol. Iron Steel, Tokyo (Japan), 1971, vol.11, pp. 655-658.

(13) POTAPKIN,V.F. ZHURAVLEV,A.S. BOBUKH,I.A. "Effect of External Zones on the Distribution of Specific Pressures in Rolling." Steel in the USSR, January 1972, pp. 49-50.

(14) PROCTOR,J.S. JUBB,C. "The Stretch Mill" Journal of the Iron and Steel Institute, February 1973, pp. 115-122.

(15) GULYAEV,G.I. IVSHIN,P.N. "An Evaluation of the Accuracy of Formulae for Calculating the Change in Wall Thickness During Tube Reduction" Staî, 32(1) 1973, pp. 55-58.

(16) TAMANO,T.
TAKADA,N.
YANAGIMOTO,S.
"Determination of Coefficient of Friction for Various Rolling Conditions". Proceedings Int. Conf. Sc. Technol. Iron Steel, Tokyo(Japan),Sept.1970, part (11), pp.669-673.

(17) SHIDA,S.
"Resistance of Metals to Compression and Rolling Loads". Hitachi Hyoron(Japan),1965, 47-9 pp. 57-62.

(18) GULYAEV,G.I.
KUZNETSOV,E.D.
EROKHIN,I.N.
KORSHAKOV,A.N.
YANOVICH,V.K.
"Effect of Deformation on Transverse Wall-Thickness Variation in the Hot Reduction and Cold Rolling of Tubes." Steel in the USSR, January 1974, pp. 64-67 .

(19) LOMACHENKO,A.N.
BLINOV,Yu.I.
et al.
"Transverse Variations in Wall Thickness of Tubes with Reduction in Two- and Four-Roll Stands." Stal' , 1973,(10), pp. 927-928 .

(20) NEUMANN,F.W.
HANKE,D.
"Verformungstheoretiche Betrachtungen zum Rohrreduzierverfahren". Stahl und Eisen,1955,75,No.22, pp. 1452-1460 .

(21) UNITED STEEL COMPANIES LTD. "Roll Pass Design" U.S.C., 1960 .

(22) HUBER,K. Z.Ange. Math. Mech., 9(1929), pp. 454-465

(23) SIEBEL,E. LUEG,W. "Investigations into the Distribution of Pressure at the Surface of the Material in Contact with the Rolls." Mitt. K.W. Inst. Eisenf., 1933, 15, p.1

(24) OROWAN,E. SCOTT,F.H. SMITH,G.L. "A Photoelastic Dynamometer for Rapidly Varying Forces." Jnl. of Scientific Instruments, vol.27, May 1950, pp. 118-122

(25) SMITH,C.L. SCOTT,F.H. SYLWESTROWICZ,W. "Pressure Distribution Between Stock and Rolls in Hot and Cold Flat Rolling" Journal of The Iron and Steel Institute, April 1952, pp. 347-359

(26) PARISH,G.J. "Measurement of the Pressure Distribution between Rollers in Contact". British Journal of Applied Physics, vol.6, 1955, pp.256-261

(27) MacGREGOR, C.W.
PALME, R.B.
"The Distribution of Contact Pressure in the Rolling of Metals."
Trans. ASME, Jnl. of Basic Eng.
1959, December,
pp. 669-680

(28) MUZALEVSKII, O.G.
GRISHKOV, A.I.
"Methods for the Combined Investigation of Metal Flow and Distribution of Forces in the Deformation Zone in Rolling."
Izvest. V.U.Z. Mashinostroenie,
1959, (11),
pp. 82-90

(29) OSADCHII, V.Ya.
GLEIBERG, A.Z.
"Distribution of Specific Stress in the Deformation Zone during Piercing."
Stal in English, 1959 August,
pp. 609-610

(30) FRISCH, J.
"Contribution to the Knowledge of Pressure Measurements During Metal Deformation"
Transactions of the ASME, May 1955
pp. 509-513

(31) NORITSYN, I.A.
GOLOVIN, V.A.
BAZYK, A.S.
"The Measurement of Normal Stress by the use of Measuring Pins".
Kuznechno-Shtampovochnoe Proizvodstvo
1964, No. 2 pp. 6-9

(32) SHVEIKIN, V.V.
GUN, G.Ya.
"Specific Pressure for Tube Rolling without a Mandrel."
Nauchnye Doklady Vysshei Shkoly, Mettallurgiya, 1958, No.2, pp. 167-169

(33) VATKIN, Ya.L.
"The Pressure of the Workpiece on the Rolls for the Rolling of Tubes without a Mandrel."
Obrabotka Metallov Davleniem, Sbornik III, 1954, Moscow

(34) KIRICHENKO, A.N.
"The Distribution of Stress and Specific Pressure in the Deformation Zone for the Reducing of Tubes."
Proizvodstvo Trub, Vypusk 13, Ukrainskii Nauchno-Issledovatel'skii Trubnyi Institute, 1964, Moscow, pp. 37-44

(35) KIRICHENKO, A.N.
"Torque and Power Requirement for the Rolling of Solid Billets and Unsupported Tubes in Grooves."
Proizvodstvo Trub, Vypusk 12, Ukrainskii Nauchno-Issledovatel'skii Trubnyi Institute, 1964, Moscow, pp. 24-29

(36) THOMPSON, P.J.
SANSOME, D.H.
"Apparent Strain Method for Analysis of Steady-State Metal-Working Operations." Metals Technology, November 1976, pp. 497-502.

(37) AVITZUR, B.
"Metal Forming Processes and Analysis". McGraw-Hill. 1968.

(38) BLAND, D.R.
FORD, H.
"The calculation of Roll Force and Torque in Cold Strip Rolling with Tension."
Proc. Inst. Mech. Engrs. 159, 1948, pp. 144-163.

(39) SHVEIKIN, V.V.
GUN, G.Ya.
"A Study of the Change in Tube Wall-Thickness during Rolling."
Nauchnye Doklady Sshei Shkoly. Metallurgiya. 1958, No. 1.
pp. 140-145

(40) GUN, G.Ya.
"Plastic Forming of Metals"
Moscow, Metallurgiya, 1968,
p. 162.

(41) SHEVCHENKO, A.A.
YUREGELENAS, V.A.
"Trud. nauchno-tekh. konf. po nepreryvnoi prokotke (KNP; Ukraine Branch of Ferrous Met. NTO, 13)."
Dnepropetrovsk. 1959.
pp. 77-86.

(42) TARNOVSKII, I.Ya., etal. "Theory of Metal Treatment by Pressure-Forming." Moscow, Metallurgizdat, 1963. pp. 641-646

(43) ANISIFOROV, V.P., etal "Reduction Mills." Moscow, Metallurgiya 1970. pp. 8-10

(44) SHEIKIN, V. IVSHIN, P.N. "New Solutions in the Theory of Metal Treatment by Pressure." collected works. (no. 142). Moscow, Metallurgiya, 1965, pp. 64-73.

(45) FEODOS'EV, V.I. "Resistance of Metals." Nauka, 1970, p. 280

(46) KOBASA, D., SCHULTZ, R.A. "Experimental Determination of the Length of the Arc of contact in Cold Rolling." Iron and Steel Engineer, April 1968, Vol. 45, pp. 97-102

(47) SHVEIKIN, V.V., IVSHIN, P.N. "Pre-Seat Deformation during Tube Reduction without a Mandrel."

Izv. V.U.Z. Chern. Metallurgiya, 8, 1964, pp. 66-71

(48) IVSHIN, P.N., SHVEIKIN, V.V. "Power Requirements for Rolling and Drawing Tubes for Reduction." Tr. Ural. Politekh. Inst., 1965, (192) pp. 64-73

(49) FOGG, B. "Theoretical Analysis for the Redrawing of Cylindrical Cups Through Conical Dies without Pressure Sleeves." Journal Mechanical Engineering Science vol. 10, No. 2, 1968, pp. 141-152 .

(50) GULYAEV, G.I. YURGELENAS, V.A. "The Change in the Mean Wall Thickness of Tubes During Continuous Reduction, without Internal Support and without Tension, on Mills with Individual Drives." Stal , Sbornik Statei, 1961, pp. 373-384 .

(51) LEVANOV, A.N. TARNOVSKII, I.Ya. SPASSKII, Yu.I. "Investigation of the Contact Stresses during Rolling in an Oval Pass." Izvest. V.U.Z. Chern. Met., 1971, (9), pp. 70-74

(52) SACHS,G. "Stress Analysis of Tube-Sinking"
BALDWIN,W.M. Trans. ASME, 1946 August,
pp. 655-661

APPENDICES

En 24

1½ PER CENT NICKEL-CHROMIUM-MOLYBDENUM STEEL

BARS AND BILLETS FOR FORGING
FORGINGS AND DROP-FORGINGS
BARS FOR MACHINING
BRIGHT BARS

Suitable for tensile ranges of 50/60 (S), 55/65 (T), 60/70 (U), 65/75 (V), 70/80 (W), 75/85 (X), 80/90 (Y), and 100 (Z) tons/sq. in. according to the ruling section of the part. The purchaser should state on the order the condition, S, T, U, V, W, X, Y or Z, for which the material is ultimately required.

Chemical composition. The steel shall contain :

Element	Per cent	
	min.	max.
Carbon	0·35	0·45
Silicon	0·10	0·35
Manganese	0·45	0·70
Nickel	1·30	1·80
Chromium	0·90	1·40
Molybdenum	0·20	0·35
Sulphur	—	0·050
Phosphorus	—	0·050

Condition of material on delivery. *a.* Bars and billets for forging shall be delivered as rolled or forged, unless the order states otherwise.

b. Forgings and drop-forgings shall be delivered in the finally heat treated condition, unless the order states otherwise.

c. Bars for machining shall be delivered in the softened condition, unless the order states otherwise.

d. Bright bars shall be delivered in the finally heat treated condition, heat treatment being given either before or after any cold work at the option of the manufacturer, unless the order states otherwise.

Mechanical properties. The mechanical properties obtained from the test pieces selected and prepared as stated in the appropriate general clauses shall be as follows :—

Property	Hardened and tempered condition							
	S	T	U	V	W	X	Y	Z
Limiting ruling section, in.	6	6	4	2½	1⅛	1⅛	1⅛	1⅛
Tensile strength, tons/sq. in., min.	50	55	60	65	70	75	80	100
Yield stress, tons/sq. in., min.	*33*	*44*	*48*	*52*	*58*	*63*	*68*	*85*
Elongation, per cent, min.	20	18	17	16	15	14	14	8
Izod impact value, ft. lb., min.	40	40	35	35	30	25	22	8
Brinell hardness numbers	*223/ 277*	*248/ 302*	*269/ 321*	*293/ 341*	*311/ 375*	*341/ 388*	*363/ 415*	*444 min.*

When supplied in the softened condition the material shall have a Brinell hardness number not exceeding 277.

NOTE. When proof stress tests are specifically requested in the enquiry and order, the values shall be as follows :—

Property	Hardened and tempered condition							
	S	T	U	V	W	X	Y	Z
Proof stress (0·2 per cent), tons/sq. in., min.	36	41	46	50	55	59	64	80

2½ PER CENT NICKEL-CHROMIUM-MOLYBDENUM STEEL (HIGH CARBON)

BARS AND BILLETS FOR FORGING
FORGINGS AND DROP-FORGINGS
BARS FOR MACHINING
BRIGHT BARS

Suitable for tensile ranges of 60/70 (U), 65/75 (V), 70/80 (W), 75/85 (X), 80/90 (Y) and 100 (Z) tons/sq. in. according to the ruling section of the part. The purchaser should state on the order the condition, U, V, W, X, Y or Z, for which the material is ultimately required.

Chemical composition. The steel shall contain :

Element	Per cent	
	min.	max.
Carbon	0·36	0·44
Silicon	0·10	0·35
Manganese	0·50	0·70
Nickel	2·30	2·80
Chromium	0·50	0·80
Molybdenum	0·40	0·70
Sulphur	—	0·050
Phosphorus	—	0·050

Condition of material on delivery. *a.* Bars and billets for forging shall be delivered as rolled or forged, unless the order states otherwise.

b. Forgings and drop-forgings shall be delivered in the finally heat treated condition, unless the order states otherwise.

c. Bars for machining shall be delivered in the softened condition, unless the order states otherwise.

d. Bright bars shall be delivered in the finally heat treated condition, heat treatment being given either before or after any cold work at the option of the manufacturer, unless the order states otherwise.

Heat treatment. The heat treatment to be given to the test bars, selected as stated in Clause 7, and to material supplied in the finally heat treated condition, shall be as follows :—

Harden in oil from a temperature of 820/850°C.
Temper at a suitable temperature not exceeding 660°C.

Mechanical properties. The mechanical properties obtained from the test pieces selected and prepared as stated in the appropriate general clauses shall be as follows :—

Property	Hardened and tempered condition									
	U	V		W		X		Y		Z
Limiting ruling section, in.	6	6	4	6	4	6	4	6	4	4
Tensile strength, tons/sq. in., min.	60	65	65	70	70	75	75	80	80	100
Yield stress, tons/sq. in., min.	*48*	*52*	*52*	*58*	*58*	*63*	*63*	*68*	*68*	*85*
Elongation, per cent, min.	17	14	16	13	15	12	14	12	14	10
Izod impact value, ft. lb., min.	35	35	35	30	30	25	25	25	25	10
Brinell hardness number	*269/321*	*293/341*	*293/341*	*311/375*	*311/375*	*341/388*	*341/388*	*363/415*	*363/415*	*444 min.*

When supplied in the softened condition the material shall have a Brinell hardness number not exceeding 277.

NOTE. When proof stress tests are specifically requested in the enquiry and order, the values shall be as follows :—

Property	Hardened and tempered condition					
	U	V	W	X	Y	Z
Proof stress (0·2 per cent), tons/sq. in., min.	46	50	55	59	64	80

Appendix(B)

Table B1

Values of voltage supply and natural frequencies of galvanometers used with loadcells.

Loadcell		dc voltage supply. volts	Galvo. Natural Frequency. Hz
RSF	Front	12.00	20
	Back	12.00	20
Torque	Top	12.00	40
	Bottom	7.56	40
Tension	Front	7.50	60
	Back	7.50	60
Roll pressure	Pin 1	7.48	60
	Pin 2	7.48	60
	Pin 3	7.48	60
	Pin 4	7.48	60
Velocity	In	-	100
	Out	-	150
Marker		-	60

Appendix C

Pressure Distribution Curves

The curves on pages (a) to (j) of this appendix are traces of actual pressure distribution curves for a number of tests. Each page contains a number of sets of curves which show a certain effect, viz, effect of d_o/t_o, gap setting, and the variation in the pressure for tests of identical conditions.

Key to the curves:

The horizontal axis represents the arc of contact and is divided into units of length each representing 2 mm of the arc of contact. The vertical axis represents the galvanometer deflection for the pin loadcells and is divided in units of length of 20 mm each.

The pin loadcell records are identified as follows:-

———— pin No. 1 — — — — pin No. 2

—·—·— pin No. 3 —··—·· pin No. 4

Test identification:-

Example:

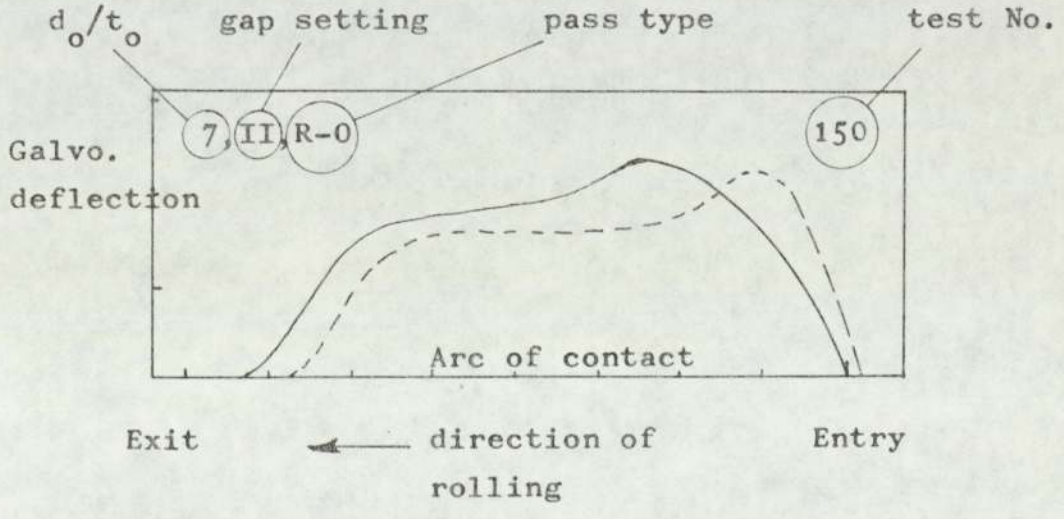

Effect of d_o/t_o:-

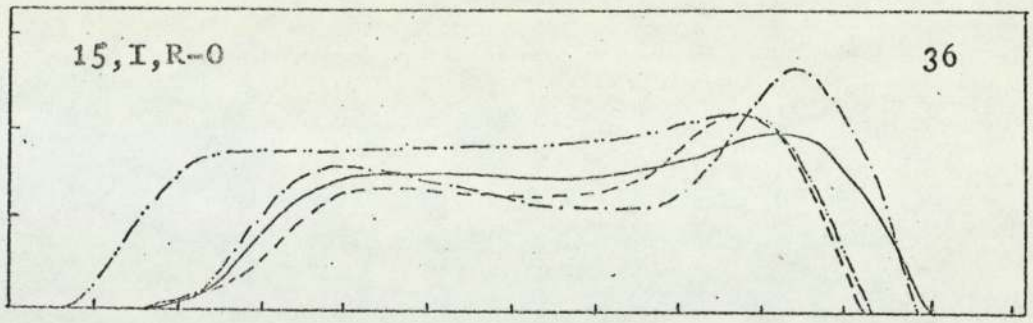

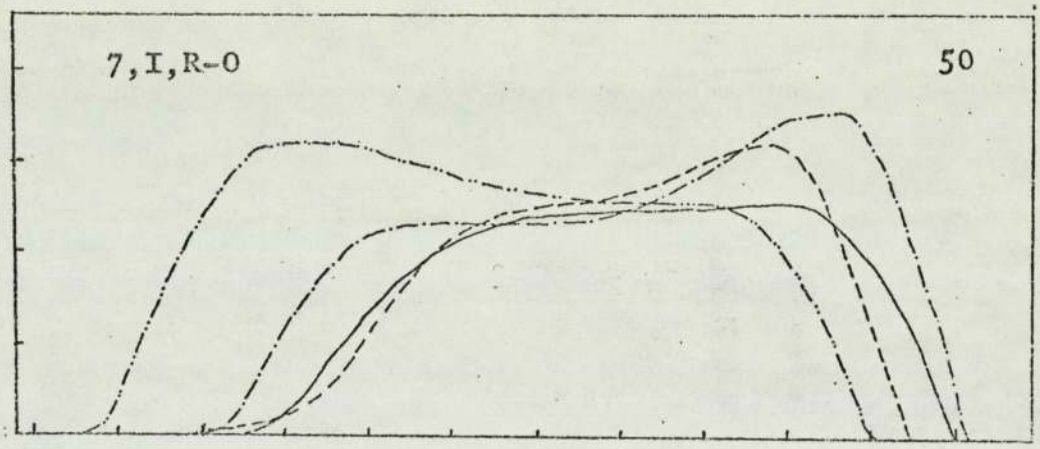

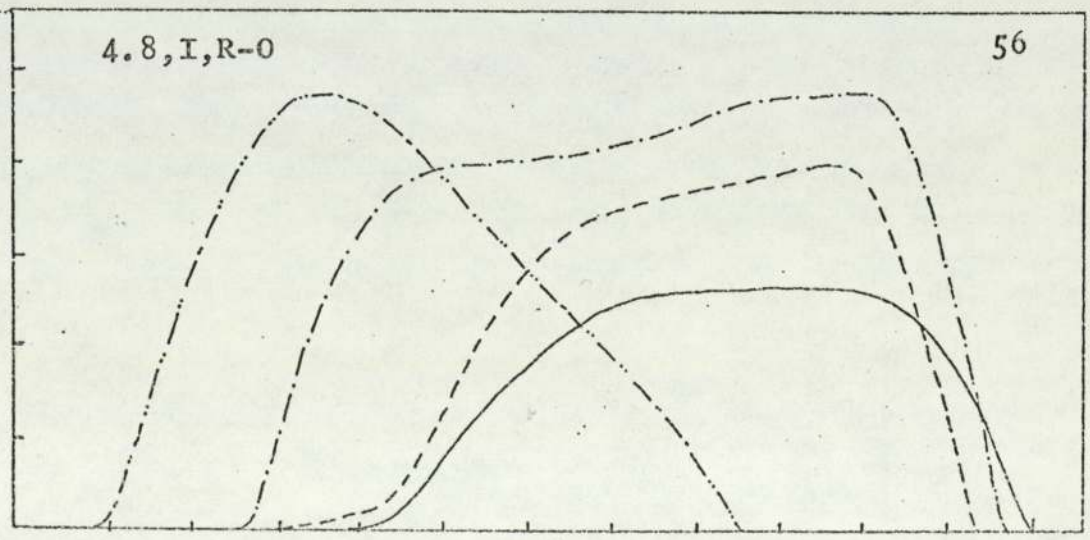

Effect of d_o/t_o :-

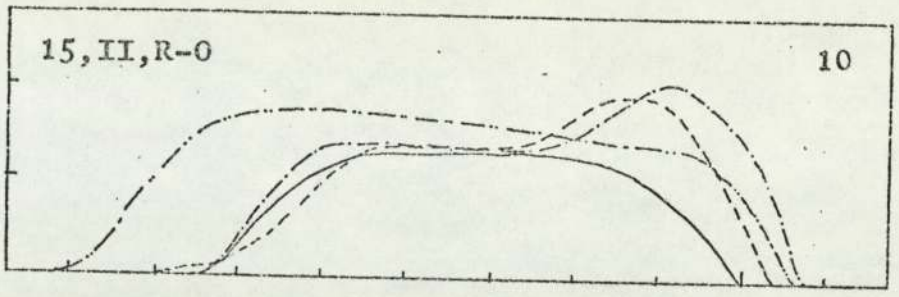

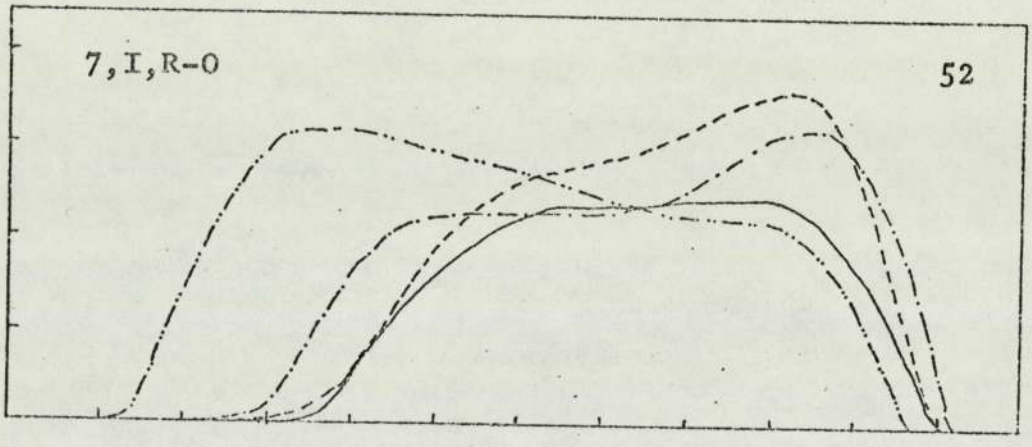

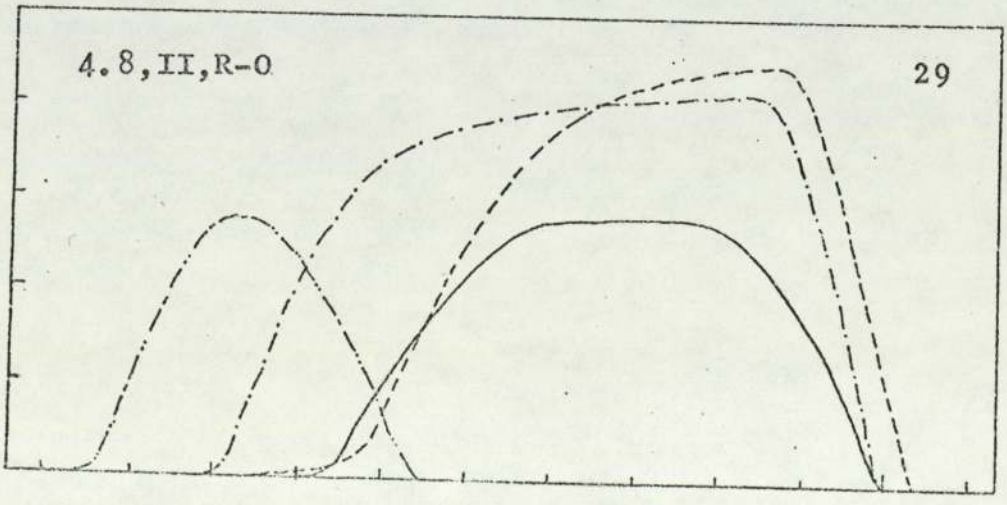

Effect of gap setting (i.e., r%):-

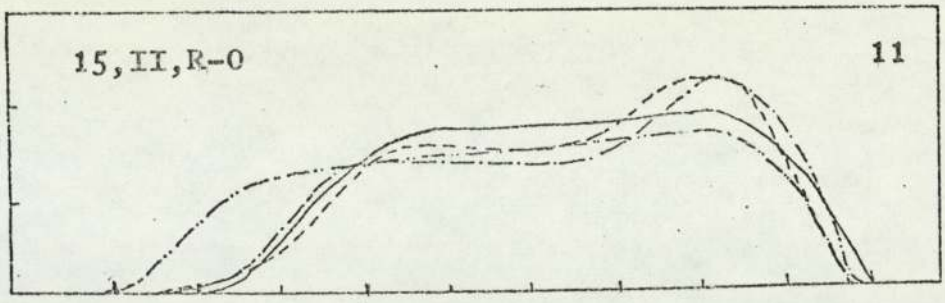

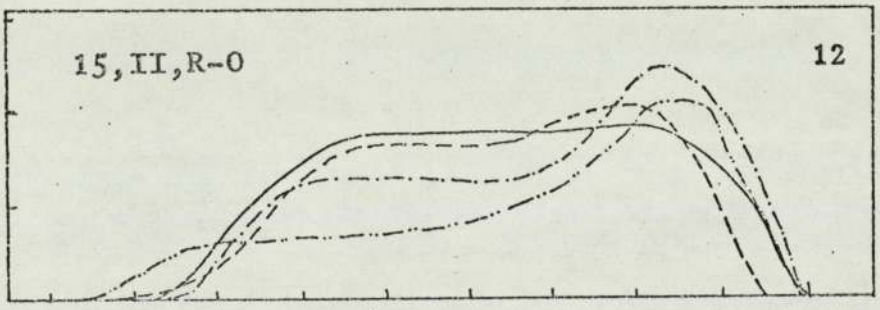

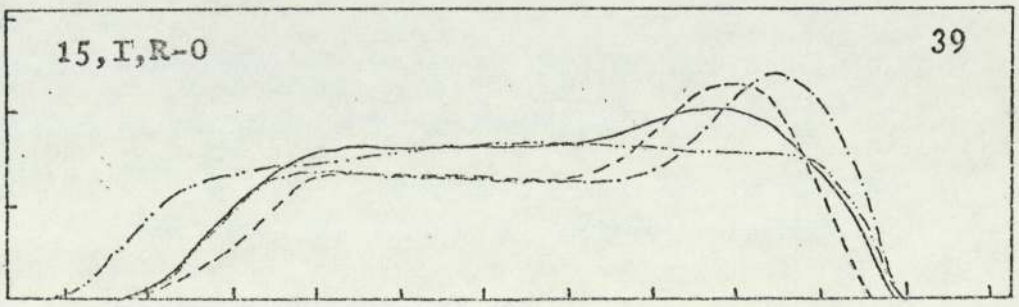

Effect of gap setting (i.e. r%):-

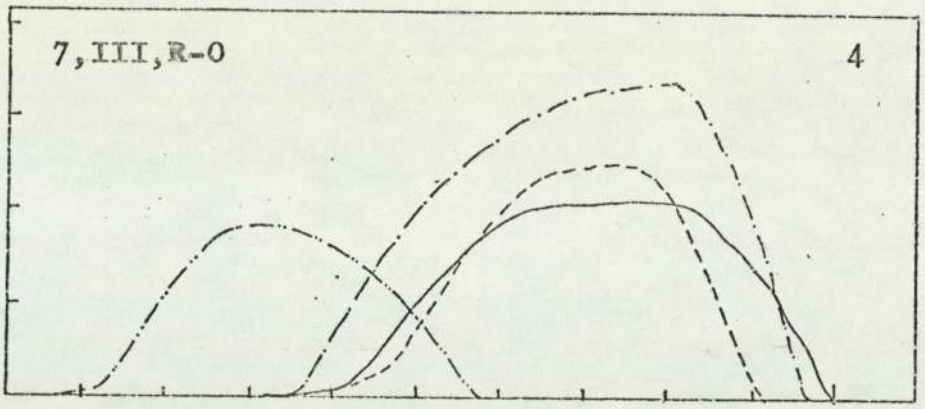

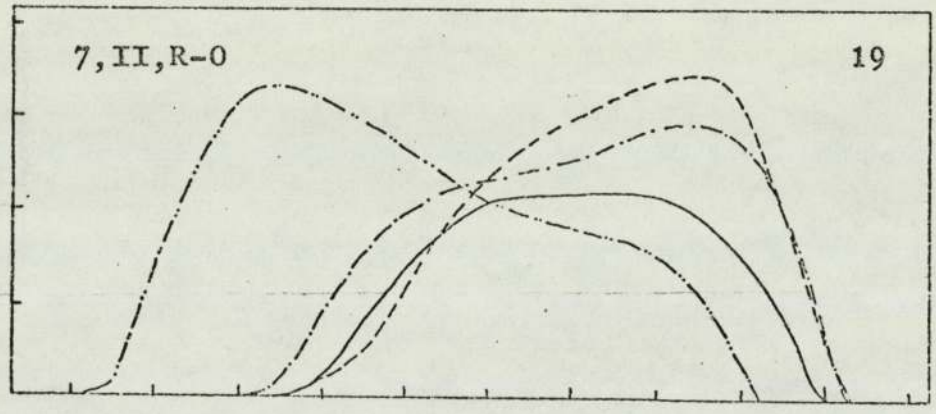

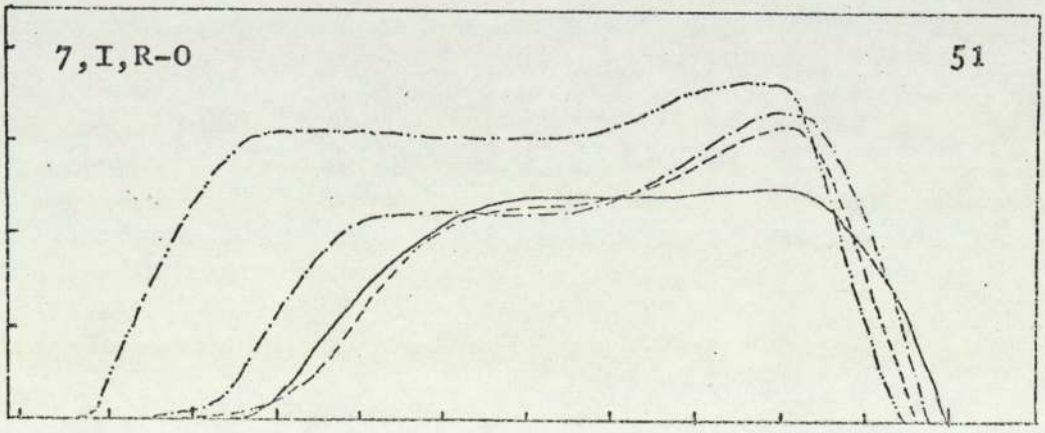

Effect of gap setting (i.e., r%):-

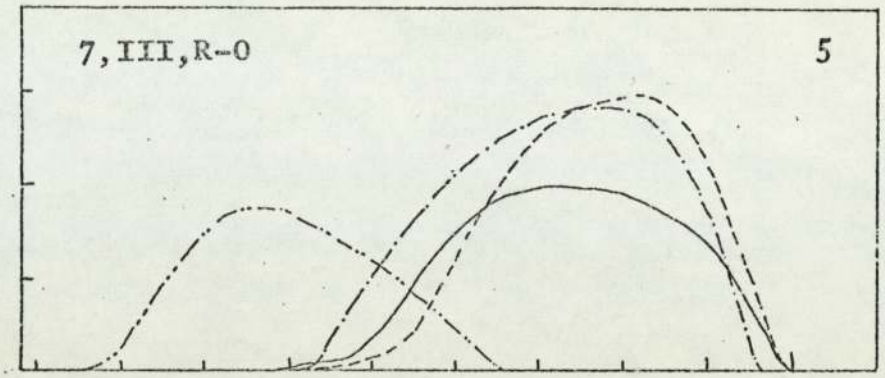

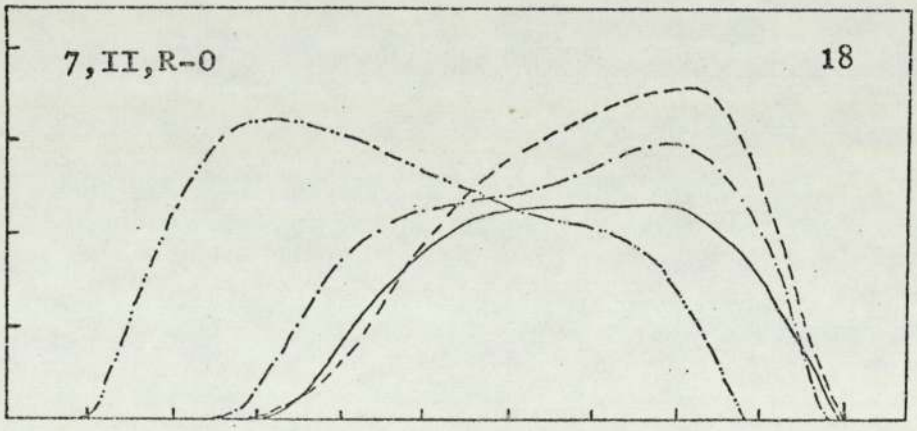

Effect of gap setting (i.e., r%):-

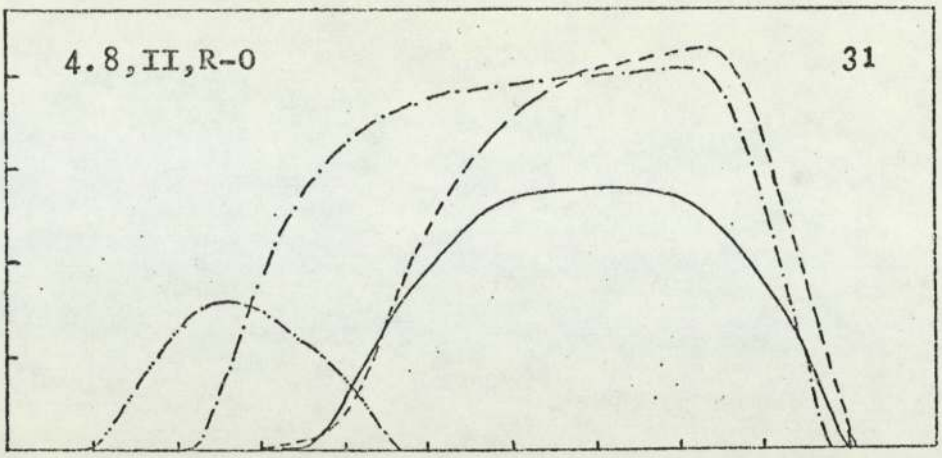

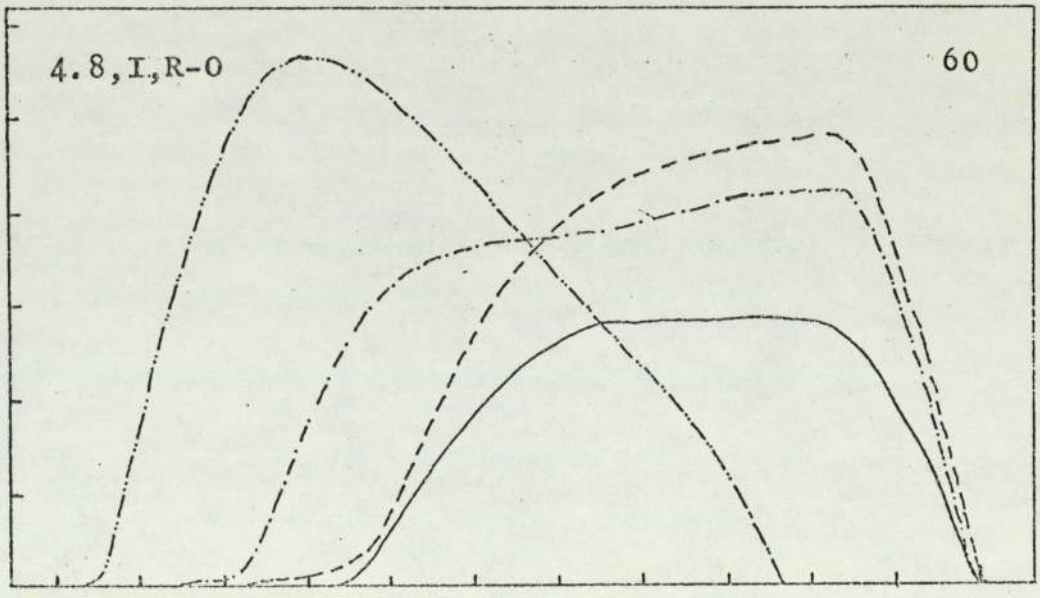

Variation in shape of curves for same d_o/t_o and gap.

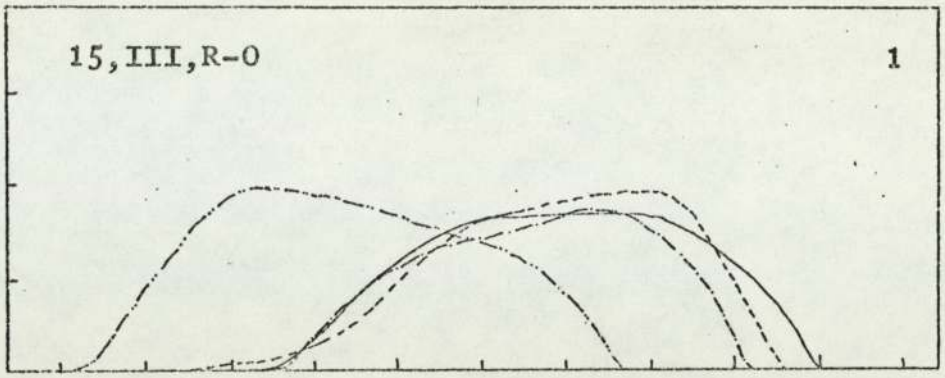

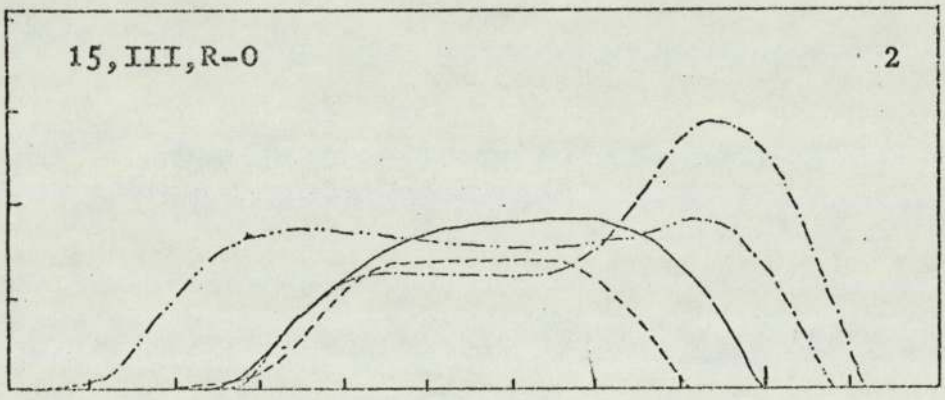

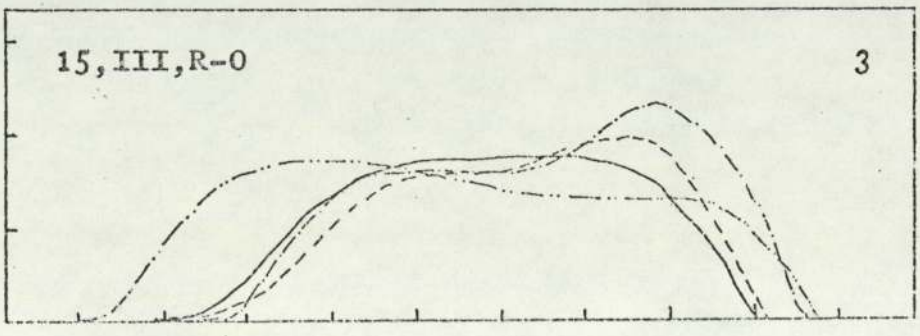

Variation in shape of curves for same d_o/t_o and gap.

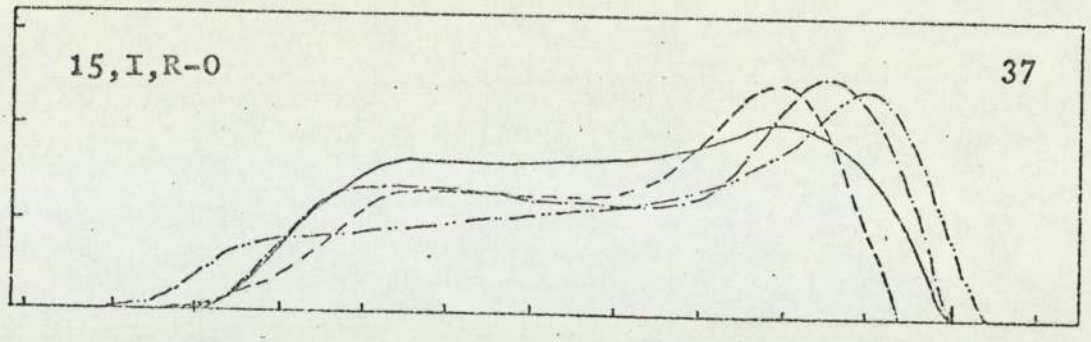

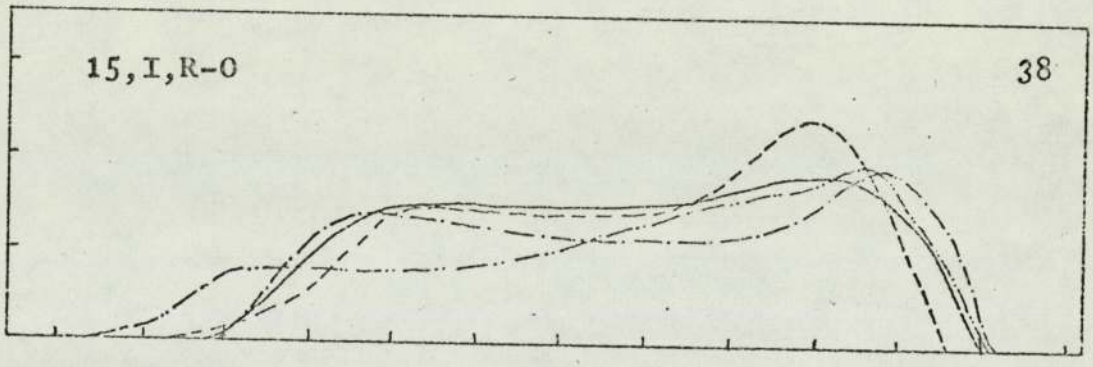

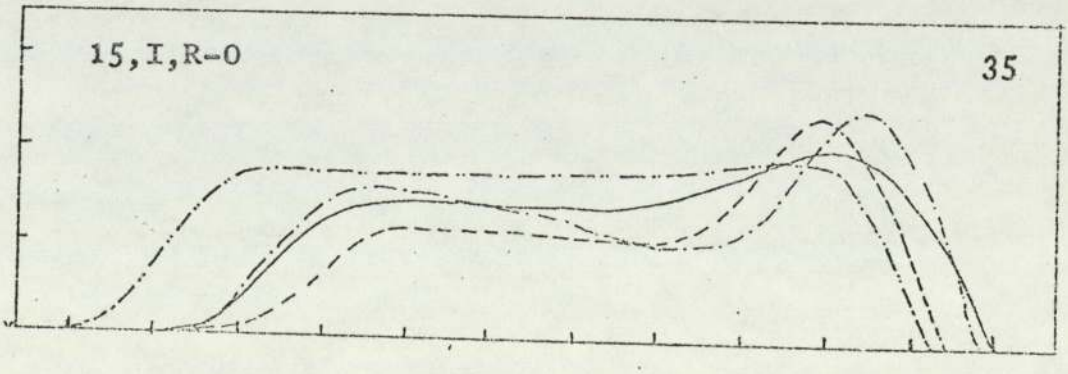

Variation in shape of curves for same d_o/t_o and gap.

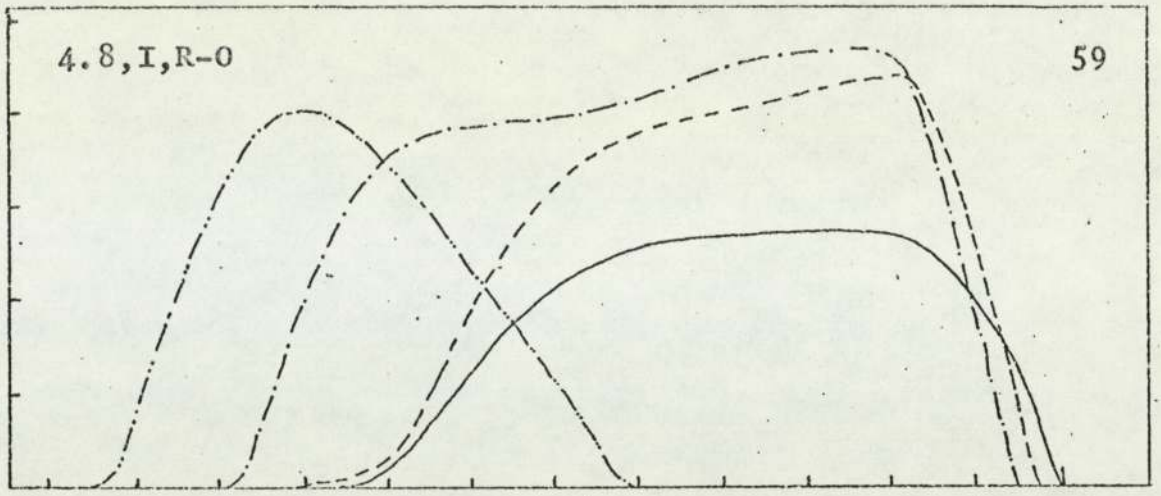

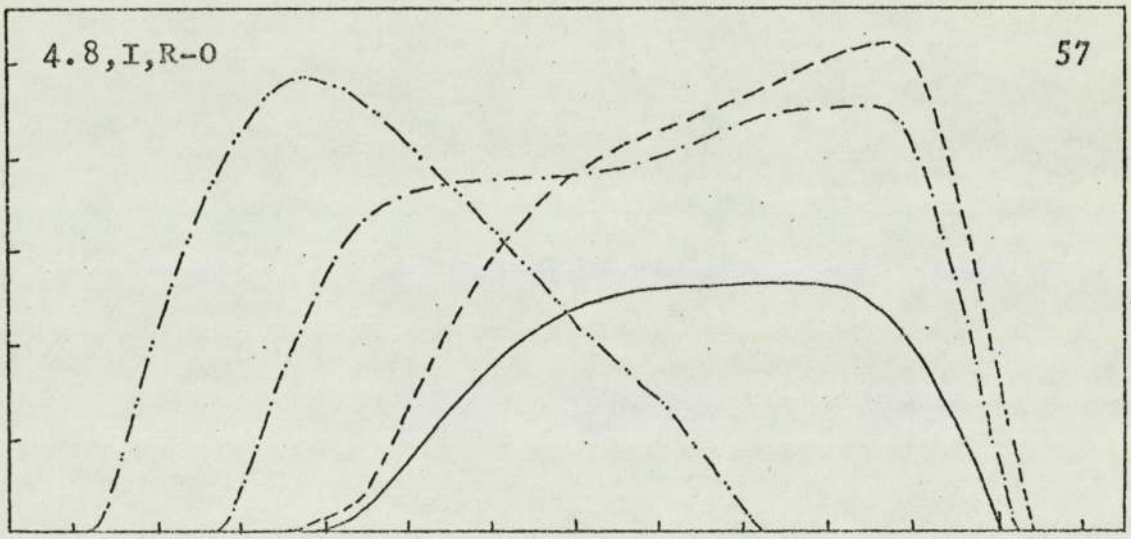

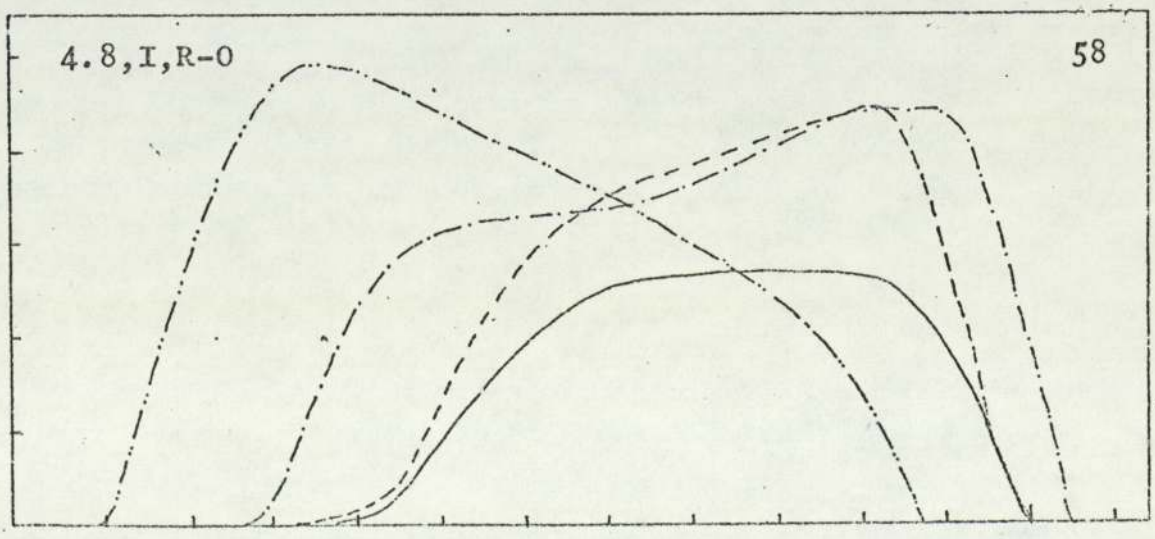

0-0 passes:-